

AD-A078 673

DOUGLAS AIRCRAFT CO LONG BEACH CA

F/G 1/3

EVALUATION OF AIRCRAFT WINDSHEILD MATERIALS IN A SIMULATED SUPE--ETC(U)

JUN 79 J B HOFFMAN

F33615-75-C-3105

UNCLASSIFIED

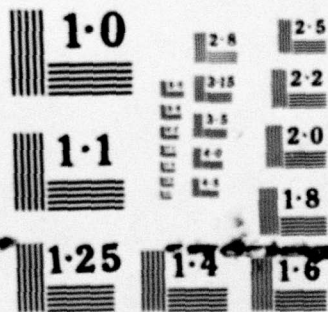
MDC-J7186

AFFDL-TR-79-3058

NL

1 OF 3
AD-A078673





NATIONAL BUREAU OF STANDARDS
MICROCOPY RESOLUTION TEST CHART

ADA 078673

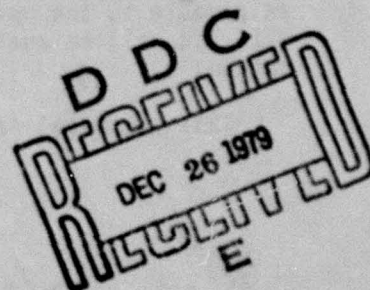
AFFDL-TR-79-3058

LEVEL *IV*

(2)

**EVALUATION OF AIRCRAFT WINDSHIELD MATERIALS
IN A SIMULATED SUPERSONIC FLIGHT ENVIRONMENT**

J.B. HOFFMAN
Douglas Aircraft Company
McDonnell Douglas Corporation
3855 Lakewood Boulevard
Long Beach, California 90846



JUNE 1979

TECHNICAL REPORT AFFDL-TR-79-3058

Final Report May 1978-March 1979

Approved for public release; distribution unlimited.

AIR FORCE FLIGHT DYNAMICS LABORATORY
AIR FORCE WRIGHT AERONAUTICAL LABORATORIES
AIR FORCE SYSTEMS COMMAND
WRIGHT-PATTERSON AIR FORCE BASE, OHIO 45433

DDC FILE COPY

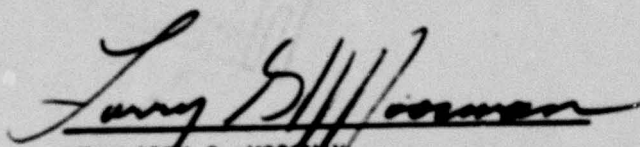
79 12 18 151

NOTICE

When Government drawings, specifications, or other data are used for any purpose other than in connection with a definitely related Government procurement operation, the United States Government thereby incurs no responsibility, nor any obligation whatsoever; and the fact that the Government may have formulated, furnished, or in any way supplied the said drawings, specifications, or other data, is not to be regarded by implication or otherwise as in any manner licensing the holder or any other person or corporation, or conveying any rights or permission to manufacture, use, or sell any patented invention that may in any way be related thereto.

This report has been reviewed by the Information Office (OI) and is releasable to the National Technical Information Service (NTIS). At NTIS, it will be available to the general public, including foreign nations.

This technical report has been reviewed and is approved for publication.

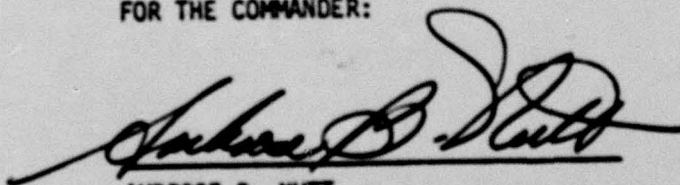


LT. LARRY G. MOOSHAY
Project Manager
Improved Windshield Protection ADPO
Vehicle Equipment Division



ROBERT E. WITTMAN
Program Manager
Improved Windshield Protection ADPO
Vehicle Equipment Division

FOR THE COMMANDER:



AMBROSE B. NUTT
Director
Vehicle Equipment Division

Copies of this report should not be returned unless return is required by security considerations, contractual obligations, or notice on a specific document.

UNCLASSIFIED

SECURITY CLASSIFICATION OF THIS PAGE (When Data Entered)

19 REPORT DOCUMENTATION PAGE		READ INSTRUCTIONS BEFORE COMPLETING FORM																
1. REPORT NUMBER AFFDL TR-79-3058	2. GOVT ACCESSION NO.	3. RECIPIENT'S CATALOG NUMBER																
4. TITLE (and Subtitle) EVALUATION OF AIRCRAFT WINDSHIELD MATERIALS IN A SIMULATED SUPERSONIC FLIGHT ENVIRONMENT		5. TYPE OF REPORT & PERIOD COVERED FINAL REPORT May 1978 - March 1979																
7. AUTHOR(s) J. B. Hoffman		6. PERFORMING ORG. REPORT NUMBER MDC-J7186																
9. PERFORMING ORGANIZATION NAME AND ADDRESS Douglas Aircraft Company McDonnell Douglas Corporation Long Beach, California 90846		8. CONTRACT OR GRANT NUMBER(s) F33615-75-C-3105																
11. CONTROLLING OFFICE NAME AND ADDRESS Air Force Flight Dynamics Laboratories (AFFDL/FFW) Air Force Wright Aeronautical Laboratories Air Force Systems Command Wright-Patterson Air Force Base, Ohio 45433		10. PROGRAM ELEMENT, PROJECT, TASK AREA & WORK UNIT NUMBERS 2202-01 1102																
14. MONITORING AGENCY NAME & ADDRESS (if different from Controlling Office)		12. REPORT DATE June 1979																
		13. NUMBER OF PAGES 200 12203																
		15. SECURITY CLASS. (of this report) Unclassified																
		15a. DECLASSIFICATION/DOWNGRADING SCHEDULE																
16. DISTRIBUTION STATEMENT (of this Report) Approved for public release, distribution unlimited.																		
17. DISTRIBUTION STATEMENT (of the abstract entered in Block 20, if different from Report)																		
18. SUPPLEMENTARY NOTES																		
19. KEY WORDS (Continue on reverse side if necessary and identify by block number) <table border="0"> <tr> <td>Acrylic</td> <td>Interlayer</td> <td>Polycarbonate</td> </tr> <tr> <td>Aerodynamic heating</td> <td>Laminated transparencies</td> <td>Silicone</td> </tr> <tr> <td>Aircraft transparencies</td> <td>Monolithic transparencies</td> <td>Supersonic flow</td> </tr> <tr> <td>Aircraft windshields</td> <td>Optics</td> <td>Transparent materials</td> </tr> <tr> <td>Glass</td> <td>Plastic materials</td> <td>Urethane</td> </tr> </table>				Acrylic	Interlayer	Polycarbonate	Aerodynamic heating	Laminated transparencies	Silicone	Aircraft transparencies	Monolithic transparencies	Supersonic flow	Aircraft windshields	Optics	Transparent materials	Glass	Plastic materials	Urethane
Acrylic	Interlayer	Polycarbonate																
Aerodynamic heating	Laminated transparencies	Silicone																
Aircraft transparencies	Monolithic transparencies	Supersonic flow																
Aircraft windshields	Optics	Transparent materials																
Glass	Plastic materials	Urethane																
20. ABSTRACT (Continue on reverse side if necessary and identify by block number) A series of wind tunnel tests were conducted at Mach 2.4, 2.6 and 3.0 to determine material survivability and optical clarity for a variety of small, flat laminated and monolithic specimens of acrylic, urethane, glass, silicone and polycarbonate materials for potential use in the design of Mach 3.0 aircraft windshields. Twenty-seven specimens were tested to determine the material limitations and capabilities, which included an investigation of specific edge designs and the effect of edge structure on temperature distribution.																		

DD FORM 1 JAN 73 1473 EDITION OF 1 NOV 65 IS OBSOLETE

UNCLASSIFIED

SECURITY CLASSIFICATION OF THIS PAGE (When Data Entered)

116 400

JOB

UNCLASSIFIED

SECURITY CLASSIFICATION OF THIS PAGE (When Data Entered)

19. KEY WORDS (continued)

Wind tunnel tests

20. ABSTRACT (continued)

The tests were conducted in a Mach 6 wind tunnel which utilized a shock generator to reduce the air stream to the desired flow across the outer surface of the specimens. The specimens were individually mounted in a pressurized box to provide a simulated cabin environment on their inner surface. Grid line photography was used to delineate inflight and permanent optical distortion. Material damage was evaluated and thermal gradients were documented.

Prior to this test program, the aerodynamic effect of a Mach 2.4 through Mach 3.0 flight environment on transparent plastic and interlayer materials was unknown. The survival of these specimens demonstrated that laminated configurations consisting of acrylic/silicone/polycarbonate or urethane/urethane/polycarbonate, as well as glass/silicone/polycarbonate are viable candidates for aircraft windshields that would be exposed to a Mach 3.0 flight environment for short exposures. The limits for these materials are still unknown and further testing is recommended at longer exposures and higher velocities to define their maximum capabilities.

This effort supplements a previous test program conducted at Mach 1.6 through Mach 2.2.

Accession For	
NTIS GRA&I	
DDC TAB	
Unannounced	
Justification	
By	
Distribution/	
Availability Codes	
Dist	Avail and/or special
A	

UNCLASSIFIED

SECURITY CLASSIFICATION OF THIS PAGE (When Data Entered)

FOREWORD

This report is one of a series of reports that describes work performed by Douglas Aircraft Company, McDonnell Douglas Corporation, 3855 Lakewood Blvd., Long Beach, California 90846, under the Windshield Technology Demonstrator Program. This work was sponsored by the Improved Windshield Protection ADPO (FEW) of the United States Air Force Flight Dynamics Laboratory, Wright-Patterson Air Force Base, under Contract F33615-75-C-3105, Project 2202/02/01.

Lieutenant L. Moosman (AFFDL/FEW) was the Air Force Project Manager who monitored the program.

Mr. J. H. Lawrence, Jr., was Program Director for the Douglas Aircraft Company.

Mr. J. B. Hoffman was the principal investigator and author of this report, and a Douglas Test Representative at the Arnold Engineering Development Center (AEDC).

Mr. L. P. Koegeboehn was a Douglas Test Representative at the Arnold Engineering Development Center (AEDC) and was responsible for the heat transfer computer program referred to in Section VII of this report.

8032 4211
Mr. D. B. Carver of the ARO, Inc., was the Test Director of the Hypersonic Wind Tunnel (B) of the Von Karman Gas Dynamics Facility (VKF) located at the Arnold Engineering Development Center (AEDC), Tennessee. Photographs were supplied by the ARO, Inc. (AEDC Division) for this report. AEDC-TSR-78-V33, Aerothermodynamic Evaluation of Windshield Materials at Simulated Flight Speeds of Mach 2.4 to 3.0 was the final report prepared by the ARO, Inc., for this program.

This report was submitted by the author to the Air Force in April 1979 and covers work performed during the period of May 1978 through March 1979.

TABLE OF CONTENTS

SECTION		PAGE
I	INTRODUCTION	1
II	TEST PLAN	3
	TEST OBJECTIVES.	3
	TEST FACILITY DESCRIPTION	4
	RESPONSIBILITIES	6
	TEST SPECIMEN DESCRIPTION	6
	TEST HARDWARE.	19
	TEST DESCRIPTION	23
	TEST CONDITIONS	28
	TEST PROCEDURE	39
	DOCUMENTATION AND DATA REDUCTION	42
III	TEST OPERATION	45
	PRE-TEST ACTIVITIES	45
	TEST OPERATION	45
	SUMMARY.	53
IV	TEST ENVIRONMENT	55
	TUNNEL CONDITIONS	55
	PRESSURE DISTRIBUTION	57
	HEAT TRANSFER RATE DISTRIBUTION	61
	SHADOWGRAPH PHOTOS	61
	SUMMARY.	67
V	MATERIALS EVALUATION	69
	LAMINATED - ACRYLIC FACE PLY, NO EDGE ATTACHMENTS.	71
	LAMINATED - ACRYLIC FACE PLY CUT BACK, EDGE ATTACHMENTS.	74
	LAMINATED - ACRYLIC FACE PLY, RABBETED AND DRILLED.	78
	LAMINATED - ACRYLIC FACE PLY, DRILLED	80
	LAMINATED - URETHANE FACE PLY, NO EDGE ATTACHMENTS	83
	LAMINATED - GLASS FACE PLY, EDGE ATTACHMENTS	85
	MONOLITHIC POLYCARBONATE - NO EDGE ATTACHMENTS	89
	SUMMARY.	91
VI	OPTICS EVALUATION	93
	OPTICAL DISTORTION	93
	LIGHT TRANSMISSION AND HAZE	138
	SUMMARY.	140
VII	THERMAL EVALUATION	145
	INSTRUMENTATION	145

TABLE OF CONTENTS (Continued)

SECTION	PAGE
TEMPERATURE/TIME HISTORY	146
EXTERIOR SURFACE TEMPERATURES	160
INTERIOR SURFACE TEMPERATURES	162
THERMAL RESISTANCE OF FACE PLY/INTERLAYER	
MATERIAL	165
EFFECT OF EDGE STRUCTURE	170
HEAT CONDUCTION BY EDGE FASTENERS	171
PLASTIC VERSUS ALUMINUM BUSHINGS	173
THERMAL PAINT	173
SUMMARY	179
VIII CONCLUSIONS AND RECOMMENDATIONS.	183
TEST PLAN	183
TEST OPERATION	184
TEST ENVIRONMENT	184
MATERIAL EVALUATION	185
OPTICS EVALUATION	187
THERMAL EVALUATION	188
REFERENCES.	189

LIST OF ILLUSTRATIONS

FIGURE		PAGE
1	Wind Tunnel at AEDC	4
2	Schematic of Wind Tunnel	5
3	Sierracin Specimen SK05 and SK06	9
4	Goodyear Test Specimens GY01 Through GY05	10
5	Sierracin Specimens SK21 Through SK23A	11
6	Sierracin Test Specimens SK21 Through SK23A (Section B-B, Figure 5)	12
7	Swedlow Test Specimens	13
8	Swedlow Test Specimen (Section B-B, Figure 7)	14
9	PPG Test Specimens.	15
10	PPG Test Specimens (Section B-B, Figure 9)	16
11	Goodyear Test Specimens GY21 Through GY26	17
12	Goodyear Test Specimens GY21 Through GY26 (Section B-B, Figure 11).	18
13	Cabin Simulator	19
14	View Through Quartz Window in Cabin Simulator	20
15	Cabin Simulator in Tunnel	21
16	Wedge and Instrumented Panel (IP)	22
17	Test Setup (Angles are for Mach 3.0 Simulation)	25
18	Windshield Flight Environment at Mach 3.0	29
19	Specimen Test Environment at Mach 3.0	31
20	Locations Where Light Transmission and Haze to be Measured	35
21	Camera Arrangement for Pre-Test/Post-Test Viewing	37
22	Camera Arrangement for Tunnel Grid Viewing	38
23	Pressure Distribution at Mach 2.4	58
24	Pressure Distribution at Mach 2.6	59
25	Pressure Distribution at Mach 3.0	60
26	Instrumented Panel Showing Orifice and Gage Locations	62
27	Heat Transfer Distribution at Mach 2.4.	63
28	Heat Transfer Distribution at Mach 2.6	64
29	Heat Transfer Distribution at Mach 3.0	65

LIST OF ILLUSTRATIONS (Continued)

FIGURE		PAGE
30	Typical Shadowgraphs	66
31	Post-Test Photo of Specimen SK05	73
32	Post-Test Photo of Specimen GY01	73
33	Post-Test Photo of Specimen SK21	75
34	Post-Test Photo of Specimen SK22	76
35	Post-Test Photo of Specimen SWU21.	77
36	Post-Test Photo of Specimen SWU22.	77
37	Post-Test Photo of Specimen GY21	79
38	Post-Test Photo of Specimen GY22	79
39	Post-Test Photo of Specimen GY23	80
40	Post-Test Photo of Specimen GY24	81
41	Post-Test Photo of Specimen GY25	82
42	Post-Test Photo of Specimen GY02	84
43	Post-Test Photo of Specimen GY02, Aft Edge	85
44	Post-Test Photo of Specimen SK23	87
45	Post-Test Photo of Specimen PPG22A	88
46	Post-Test Photo of Specimen PPG21	88
47	Post-Test Photo of Specimen TEX21	90
48	Post-Test Photo of Specimen TEX21A	91
49	Grid Board Photos for Specimen SK05.	96
50	Grid Board Photos for Specimen SK06.	97
51	Grid Board Photos for Specimen SK21.	98
52	Grid Board Photos for Specimen SK22.	99
53	Grid Board Photos for Specimen SWU21	100
54	Tunnel Photos for Specimens SK05, SK21 and SWU21 at Mach 2.4 (10-Minute Injection).	101
55	Overlays of Tunnel Photos for Specimens SK05, SK21 and SWU21 at Mach 2.4 (10-Minute Injection)	102
56	Tunnel Photos for Specimens SK06, SK21, SK22 and SWU21 at Mach 2.6 (10-Minute Injection).	103
57	Overlays of Tunnel Photos for Specimens SK06, SK21, SK22 and SWU21 at Mach 2.6 (10-Minute Injection)	104

LIST OF ILLUSTRATIONS (Continued)

FIGURE		PAGE
58	Tunnel Photos for Specimens SK05, SK21, SK22 and SWU21 at Mach 3.0 (3-Minute Injection)	105
59	Overlay of Tunnel Photos for Specimens SK05, SK22 and SWU21 at Mach 3.0 (3-Minute Injection)	106
60	Grid Board Photos for Specimen GY01	109
61	Grid Board Photos for Specimen GY02	110
62	Grid Board Photos for Specimen GY03	111
63	Grid Board Photos for Specimen GY04	112
64	Grid Board Photos for Specimen GY05	113
65	Tunnel Photos for Specimens GY03, GY04 and GY05 at Mach 2.4 (10-Minute Injection)	114
66	Overlays of Tunnel Photos for Specimens GY03, GY04 and GY05 at Mach 2.4 (10-Minute Injection)	115
67	Tunnel Photos for Specimens GY01, GY02 and GY03 at Mach 2.6	116
68	Overlay of Tunnel Photos for Specimen GY01, GY02 and GY03 at Mach 2.6	117
69	Tunnel Photos for Specimens GY04 and GY05 at Mach 3.0 (3-Minute Injection)	118
70	Tunnel Photo Overlays for Specimens GY04 and GY05 at Mach 3.0 (3-Minute Injection)	118
71	Pre-Test Grid Board Photos for Specimens GY24, GY25 and GY26	120
72	Post-Test Grid Board Photos for Specimens GY24, GY25, and GY26	121
73	Tunnel Photos for Specimens GY24, GY25 and GY26 at Mach 2.4 (5-Minute Injection)	122
74	Overlays of Tunnel Photos for Specimens GY24, GY25 and GY26 at Mach 2.4 (5-Minute Injection)	123
75	Pre-Test Grid Board Photos for Specimens GY21, GY22 and GY23	125
76	Post-Test Grid Board Photos for Specimens GY21, GY22 and GY23	126
77	Tunnel Photos for Specimens GY21, GY22 and GY23	127
78	Grid Board Photos for Specimen PPG21	130
79	Grid Board Photos for Specimen PPG21A	130

LIST OF ILLUSTRATIONS (Continued)

FIGURE		PAGE
80	Grid Board Photos for Specimen PPG22	131
81	Grid Board Photos for Specimen PPG22A	131
82	Grid Board Photos for Specimen SK23	132
83	Tunnel Photo for Specimen PPG21 at Mach 2.4 (Injection 24, 10 Minutes)	133
84	Tunnel Photo for Specimen PPG22A at Mach 2.6 (Injection 66, 2.5 Minutes)	133
85	Tunnel Photo and Overlay for Specimen PPG22 at Mach 2.4 (Injection 35, 5 Minutes)	133
86	Tunnel Photo and Overlay for Specimens SK23 at Mach 2.6 (Injection 56, 10 Minutes)	134
87	Tunnel Photo and Overlay for SK23 at Mach 3.0 (Injection 78, 3 Minutes)	134
88	Grid Board Photos for Specimen TEX21A	136
89	Tunnel Photo and Overlay for Specimen TEX21 at Mach 2.4 (Injection 28, 10 Minutes)	137
90	Tunnel Photo for Specimen TEX21A at Mach 2.6 (Injection 65, 5 Minutes)	137
91	Temperature/Time History at Mach 2.4 for 5 Minute Injection of GY Specimens	151
92	Temperature/Time History at Mach 2.4 for Specimens SK05, SK21 and SWU21	152
93	Temperature/Time History at Mach 2.4 for 10-Minute Injections of Specimens GY03, GY04 and GY05	153
94	Temperature/Time History at Mach 2.4 for 10-Minute Injections of Specimens GY24, GY25 and GY26	154
95	Temperature/Time History at Mach 2.6 for 5-Minute Injections of SK and GY Specimens	155
96	Temperature/Time History at Mach 2.6 for GY01, GY02 and GY03	156
97	Temperature/Time History at Mach 2.6 for SK and SWU Specimens	157
98	Temperature/Time History at Mach 3.0 for SK05, SK21, SK22, SK23 and SWU21	158
99	Temperature/Time History at Mach 3.0 for Specimens GY04, GY05 and GY23	159

LIST OF ILLUSTRATIONS (Continued)

FIGURE		PAGE
100	Average Maximum Surface Temperature Versus Mach Number	161
101	Thermal Resistance of Face Ply and Interlayer at Mach 2.4	167
102	Thermal Resistance of Face Ply Plus Interlayer at Mach 2.6	168
103	Thermal Resistance of Face Ply Plus Interlayer at Mach 3.0	169
104	Maximum Temperature at Interlayer/Polycarbonate Interface Adjacent to Forward Inserts	174
105	Thermal Paint Injections at Mach 2.4	176
106	Thermal Paint Injections at Mach 2.6	178
107	Teflon Panel Injection at Mach 3.0	178

LIST OF TABLES

TABLE		PAGE
1	WIND TUNNEL PERFORMANCE DATA	5
2	SPECIMEN IDENTIFICATION	7
3	TEST SCHEDULE	24
4	FLIGHT AND TEST ENVIRONMENT	32
5	INJECTION SEQUENCE	46
6	SUMMARY OF INJECTIONS	47
7	SPECIMEN EXPOSURE TIMES	48
8	SUMMARY OF TEST TIMES	49
9	PLANNED INJECTIONS VERSUS ACTUAL INJECTIONS	51
10	TEHRMOCOUPLE PEEL-OFF	52
11	TEST ENVIRONMENT - ACTUAL VERSUS PREDICTED	56
12	SUMMARY OF TESTED SPECIMENS	70
13	POST-TEST SPECIMEN DESCRIPTION - ACRYLIC FACE PLY, NO EDGE ATTACHMENTS	72
14	POST-TEST SPECIMEN DESCRIPTION - ACRYLIC FACE PLY CUT BACK, EDGE ATTACHMENTS	74
15	POST-TEST SPECIMEN DESCRIPTION - ACRYLIC FACE PLY RABBETED AND DRILLED	78
16	POST-TEST DESCRIPTION - ACRYLIC FACE PLY DRILLED	81
17	POST-TEST SPECIMEN DESCRIPTION - URETHANE FACE PLY, NO EDGE ATTACHMENTS	83
18	POST-TEST SPECIMEN DESCRIPTION - GLASS FACE PLY, EDGE ATTACHMENTS	86
19	POST-TEST SPECIMEN DESCRIPTION - MONOLITHIC POLYCARBONATE, NO EDGE ATTACHMENTS	89
20	EVALUATION OF GRID LINE PHOTOGRAPHS FOR THREE-PLY LAMINATED SPECIMENS	95
21	EVALUATION OF GRID LINE PHOTOGRAPHS FOR FIVE-PLY LAMINATED SPECIMENS	108
22	EVALUATION OF GRID LINE PHOTOGRAPHS FOR SEVEN-PLY LAMINATED SPECIMENS	119
23	EVALUATION OF GRID LINE PHOTOGRAPHS FOR NINE-PLY LAMINATED SPECIMENS	124
24	EVALUATION OF GRID LINE PHOTOGRAPHS FOR LAMINATED SPECIMENS WITH GLASS FACE PLY	129

LIST OF TABLES (Continued)

TABLE		PAGE
25	EVALUATION OF GRID LINE PHOTOGRAPHS FOR MONOLITHIC SPECIMENS	135
26	LIGHT TRANSMISSION AND HAZE DATA	139
27	TEMPERATURES AT MACH 2.4	148
28	TEMPERATURES AT MACH 2.6	149
29	TEMPERATURES AT MACH 3.0	150
30	MAXIMUM EXTERIOR SURFACE TEMPERATURES	160
31	EXTERIOR SURFACE HEAT-UP RATE, INITIAL INJECTIONS (°F/SECOND)	163
32	MAXIMUM INTERIOR SURFACE TEMPERATURES	164
33	MATERIAL PROPERTIES	165
34	TEMPERATURE COMPARISON AT INTERFACE OF INTERLAYER AND POLYCARBONATE	170
35	EFFECT OF EDGE FASTENERS ON INTERNAL TEMPERATURES . . .	172
36	SURFACE HEAT UP TIME	177

SECTION I

INTRODUCTION

Military aircraft with coated polycarbonate canopies and windshields had previously encountered inflight erosion problems. These adverse experiences precipitated the development of multi-ply transparencies for potential use on high-speed aircraft. The laminated configuration selected to fulfill the current need consisted of a face ply and structural ply joined by a soft interlayer. The performance and reliability of the materials for these potential laminated transparencies were substantiated by wind tunnel tests conducted at velocities of Mach 1.6 through Mach 2.2 (References 1 and 2). The operating range of current inventory military aircraft had been considered to be within the limits of the selected test conditions.

The next generation of military aircraft will be capable of attaining velocities in the Mach 3.0 region. The temperature generated on an aircraft windshield at this speed would be much higher than experienced in the Mach 2.2 region. Hence, a need existed to define the capabilities and limitations of materials currently considered for use in multi-ply windshields for future high-speed aircraft.

To provide data for a material's evaluation, a series of wind tunnel tests were performed in the hypersonic wind tunnel of the Von Karman Gas Dynamics Facility (VKF) located at the Arnold Engineering Development Center (AEDC), Tennessee. These tests were completed in August 1978. The goals of this test program were to determine and document the survivability of selected materials and multi-ply laminates subjected to Mach 2.4 through Mach 3.0 flight conditions, evaluate the resultant effect on the laminates' optics, delineate the thermal environment, investigate the reliability of potential edge designs, and determine the edge effects on temperature distribution at these flight conditions.

These goals were achieved. Twenty-seven flat panels, 7 x 11 inches in size, were tested in a Mach 6.0 wind tunnel, using a shock generator to reduce the air stream to the desired flow conditions. The test specimens were supported in a pressurized box to simulate inflight cabin conditions. Heat transfer distribution and pressure distribution across the specimen surfaces, using an instrumented panel, were measured. Shadowgraph photos were taken to illustrate shock interactions and flow-field conditions. Temperatures were recorded on the appropriate specimen surfaces to define the thermal environment. Material degradation and survivability were evaluated. Edge effects were investigated. Grid line photography (in-tunnel photos taken of a system of grid lines through the specimens) was utilized to delineate potential inflight optical distortion. Loss of light transmission and haze growth were measured.

The report is structured in eight parts. Section II contains the test plan, while Section III discusses pre-test activities, operation of the test, and the basic test conditions achieved. Section IV compares the planned environment to the actual test environment. Section V appraises material damage and survivability. Section VI evaluates optical distortion. Section VII analyzes the thermal data. Section VIII presents conclusions and makes recommendations for further testing.

SECTION II

TEST PLAN

This section presents the test plan that had been prepared at the beginning of the program. The purpose of this plan was to guide the testing to be conducted at the Von Karman Gas Dynamics Facility (VKF) located at the Arnold Engineering Development Center (AEDC), Tennessee.

The test plan delineates the test objectives, describes the test facility, outlines responsibilities, describes the specimens and hardware, presents a brief test description, establishes the test requirements, defines the test procedure, and spells out the documentation and data reduction requirements. As with any test, the operation of the test does not always follow the written plan. Any deviations to the test plan during testing are described in Section III.

TEST OBJECTIVES

The goals of this test program are to determine material survivability and optical distortion for potential laminated windshield designs that can be used in aircraft that will operate at velocities up to Mach 3.0 and at altitudes consistent with the operating range of military aircraft. These goals will be met by evaluating damage to the transparency materials and to specific edge configurations, by appraising optical distortion, light transmission losses, and haze growth, by recording surface temperatures and thermal gradients through the laminates, and by studying the effect of the edge structure on thermal distribution. A correlation will be made to compare the test conditions and the predicted conditions.

To accomplish the goal of this program and to complete a meaningful evaluation of the various windshield materials, it is essential that a test environment be produced similar to the selected flight environment.

TEST FACILITY DESCRIPTION

These tests will be conducted in the Hypersonic Wind Tunnel (B) of the Von Karman Gas Dynamics Facility (VKF) located at the Arnold Engineering Development Center (AEDC), Tennessee. Tunnel B, Figure 1, is a continuous, closed-circuit, variable density wind tunnel with an axisymmetric contoured nozzle and a 50-inch diameter test section. The tunnel, Figure 2, can be operated at a nominal Mach number of 6 and 8, at stagnation pressures ranging from 20 PSIA to 300 PSIA and 50 PSIA to 900 PSIA, respectively, and at stagnation temperatures up to 890⁰F as noted in Table 1. The model can be injected into the tunnel for a test run and then retracted for model cooling or model changes without interrupting the tunnel flow. A complete description of the tunnel may be found in Reference 3. The tunnel will be operated at Mach 6.0 for these tests.

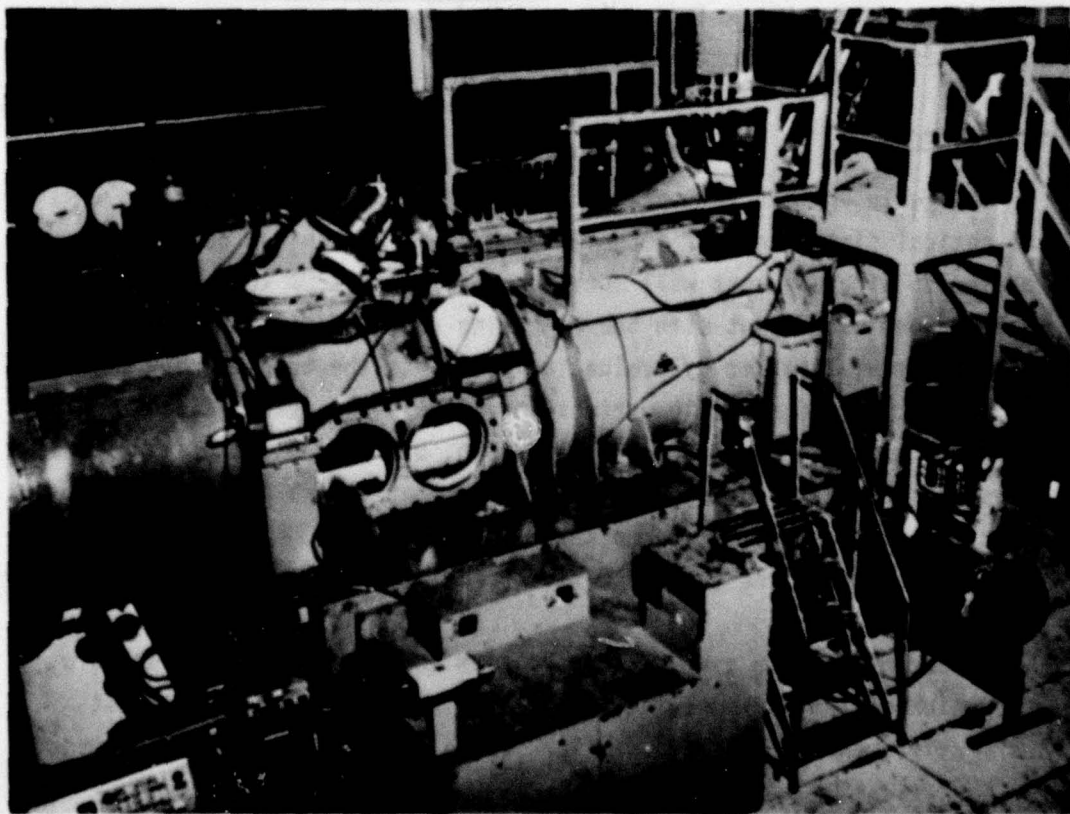


Figure 1. Wind Tunnel at AEDC.

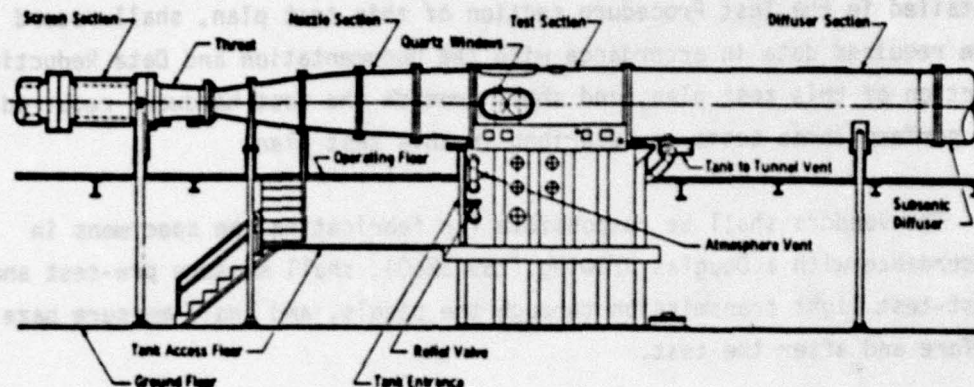


Figure 2. Schematic of Wind Tunnel.

TABLE 1. WIND TUNNEL PERFORMANCE DATA

Tunnel	Nominal Mach Number	P_0 , psia		T_0 , °F	q_∞ , psia		$Re/Ft \times 10^{-6}$	
		Min.	Max.	Max.	Min.	Max.	Min.	Max.
B	6	20	270 (1)	390 (3)	0.3	4.1	0.3	4.7
	8	50	850 (2)	890	0.3	3.8	0.3	3.7
<p> P_0 Stagnation pressure T_0 Stagnation Temperature q_∞ Free-stream dynamic pressure Re Free-stream Reynolds number </p> <p> Notes: (1) Maximum for short duration 300 psia (2) Maximum for short duration 900 psia (3) Up to 890°F can be supplied at low stagnation pressures. </p>								

RESPONSIBILITIES

The AEDC/ARO shall be responsible for the test accomplishment as detailed in the Test Procedure section of this test plan, shall record the required data in accordance with the Documentation and Data Reduction section of this test plan, and shall provide the test hardware required to perform these tests as described in this test plan.

The vendors shall be responsible for fabricating the specimens in accordance with a Douglas drawing (Z5943260), shall measure pre-test and post-test light transmission through the panels, and shall measure haze before and after the test.

Douglas Aircraft Company shall be responsible for the preparation of a test plan, a drawing of the test specimens (Z5943260), and a final report.

TEST SPECIMEN DESCRIPTION

Twenty-seven specimens, representing 19 different laminated configurations and one monolithic panel, are provided for this test program. Seven of the specimens are duplicate panels. The specimens are listed in Table 2, together with the five vendors who fabricated the parts and the materials used for construction. The specimens are flat, rectangular in shape, and 1.00 x 7.38 x 11.38 inches in size, and are shown in Figures 3 through 12.

Three general types of three-ply laminated construction are represented: as-cast acrylic/interlayer/polycarbonate, glass/interlayer/polycarbonate, and glass/interlayer/glass. Two additional groups, consisting of nine plies and seven plies, have as-cast acrylic and urethane face plies, and polycarbonate structural plies. The interlayer materials are silicone, urethane and PPG112. A coated monolithic polycarbonate configuration is also included.

Seven of the specimens are from a previous wind tunnel test that was reported in Reference 1. The seven specimens, SK05 and SK06, Figure 3,

and GY01 through GY05, Figure 4, are instrumented with three foil and wire type chromel-alumel thermocouples. The bonding agent was M-Bond 600

TABLE 2. SPECIMEN IDENTIFICATION

DACO PART NUMBER Z5943260	DACO SERIAL NUMBER	MANUFACTURER	DESCRIPTION
			AC = Acrylic SIL = Silicone Interlayer PC = Polycarbonate UR = Urethane Interlayer
-501 (1)	SK05	Sierracin	0.08 AC - 0.10 SIL - 0.62 PC
-501 (1)	SK06		0.08 AC - 0.10 SIL - 0.62 PC
-533	SK21		0.188 AC - 0.12 SIL - 0.62 PC
-533 (2)	SK21A		0.188 AC - 0.12 SIL - 0.62 PC
-535	SK22		0.188 AC - 0.12 SIL - 0.62 PC (Retainer)
-535 (2)	SK22A		0.188 AC - 0.12 SIL - 0.62 PC (Retainer)
-537	SK23		0.110 Chemcor - 0.27 SIL - 0.62 PC
-537 (2)	SK23A		0.110 Chemcor - 0.27 SIL - 0.62 PC
-529 (2)	SWU21	Swedlow	0.188 AC - 0.12 SIL - 0.62 PC
-531 (2)	SWU22		0.188 AC - 0.12 SIL - 0.62 PC (2 Bolts)
-539	PPG21	PPG	0.120 SL Glass - 0.35 PPG112 - 2 PC Plies
-539 (2)	PPG21A		0.120 SL Glass - 0.35 PPG112 - 2 PC Plies
-541	PPG22		0.120 SL Glass - 0.32 PPG112 - Glass
-541 (2)	PPG22A		0.120 SL Glass - 0.32 PPG112 - Glass
-519 (1)	GY01	Goodyear	0.10 AC - 0.04 UR - 2 PC Plies, 0.25 ea.
-521 (1)	GY02		0.10 UR - 0.04 UR - 2 PC Plies, 0.25 ea.
-523 (1)	GY03		0.10 UR - 0.04 UR - 2 PC Plies, 0.25 ea.
-525 (1)	GY04		0.10 UR - 0.10 SIL - 2 PC Plies, 0.25 ea.
-527 (1)	GY05		0.10 UR - 0.10 UR - 2 PC Plies, 0.25 ea.
-543 (2)	GY21		0.12 AC - 0.10 SIL - 3 PC Plies, 0.19 ea.
-545	GY22		0.12 AC - 0.10 UR - 3 PC Plies, 0.19 ea.
-547	GY23		0.18 AC - 0.10 SIL - 3 PC Plies, 0.19 ea.
-549	GY24		0.12 AC - 0.04 UR - 2 PC Plies, 0.19 ea.
-551	GY25		0.12 AC - 0.04 SIL - 2 PC Plies, 0.19 ea.
-553	GY26		0.18 AC - 0.04 UR - 2 PC Plies, 0.19 ea.
-555	TEX21	Texstar	Coated PC, 1.00 Thick
-555 (2)	TEX21A		Coated PC, 1.00 Thick

(1) These specimens are from previous test (Reference 1).

(2) These specimens to be coated with phase-change paint.

(3) All dimensions in inches.

adhesive manufactured by Micro-Measurements Products. Five of these specimens were previously tested.

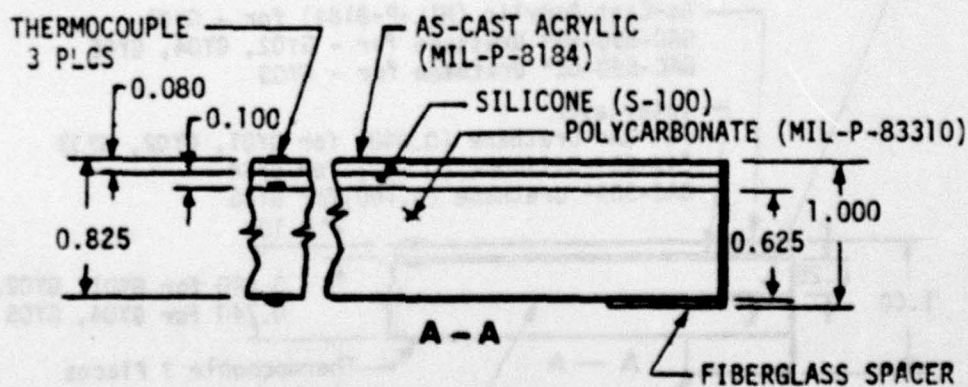
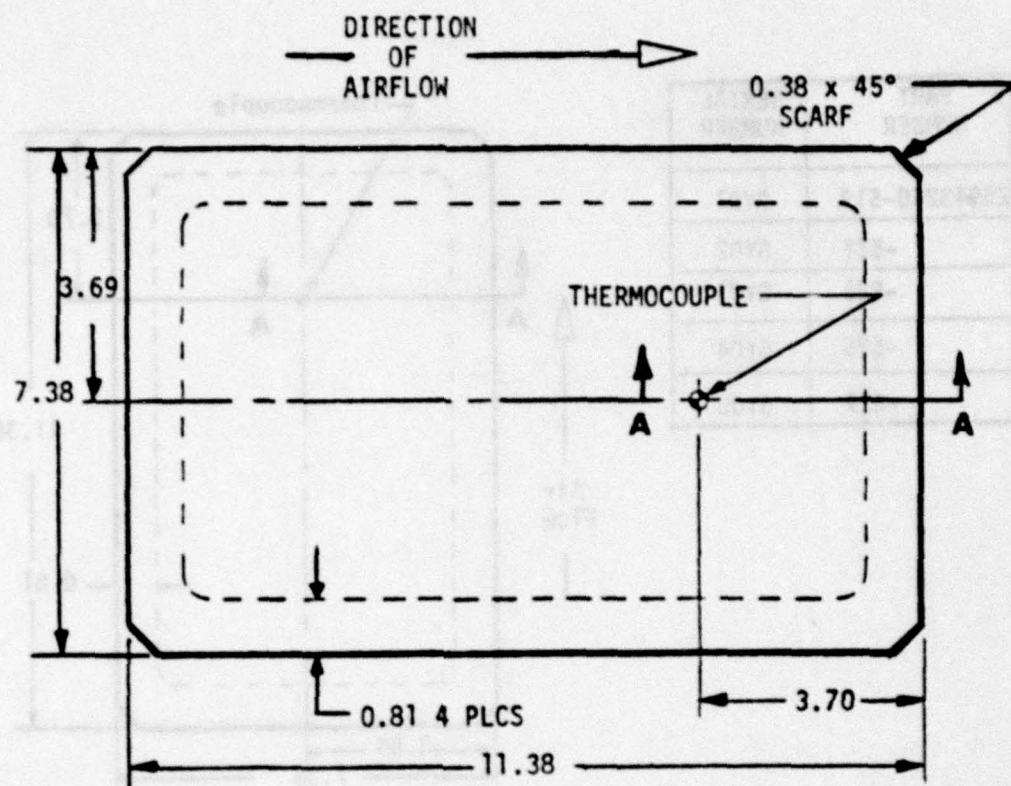
Twenty specimens were designed specifically for this test series. Eighteen of these specimens are instrumented with copper-constantan thermocouples and were designed with edges to simulate a production type installation. The remaining two specimens, fabricated by Texstar Plastics (TEX21 and TEX21A) are plain panels of coated monolithic polycarbonate.

The three Sierracin configurations (SK21, SK22 and SK23), shown in Figures 5 and 6, are instrumented with seven thermocouples. Two types of bushings are used at the edges, aluminum and plastic, and a comparison of heat conductivity into the structural ply will be made. The face plies are as-cast acrylic and glass. Three different edges are represented. Duplicate specimens, SK21A, SK22A and SK23A, are provided for thermal paint tests.

The two Swedlow specimens (SWU21 and SWU22), shown in Figures 7 and 8, are instrumented with five thermocouples. The face plies are as-cast acrylic. These configurations present two different methods of reducing heat conductivity through the attachments to the structural ply. The edges of these specimens are coated with a protective sealant.

The two PPG configurations (PPG21 and PPG22), shown in Figures 9 and 10, are instrumented with five thermocouples. The face plies are glass and the structural plies are glass and polycarbonate. Duplicate specimens (PPG21A and PPG22A) are provided for thermal paint tests. Plastic bushings are installed for the simulated edge design.

The six Goodyear configurations (GY21 through GY26), shown in Figures 11 and 12, are instrumented with five thermocouples. The face plies are as-cast acrylic. This group represents a seven-ply configuration and a nine-ply configuration. Bolts and bushings are installed to simulate a typical edge configuration.

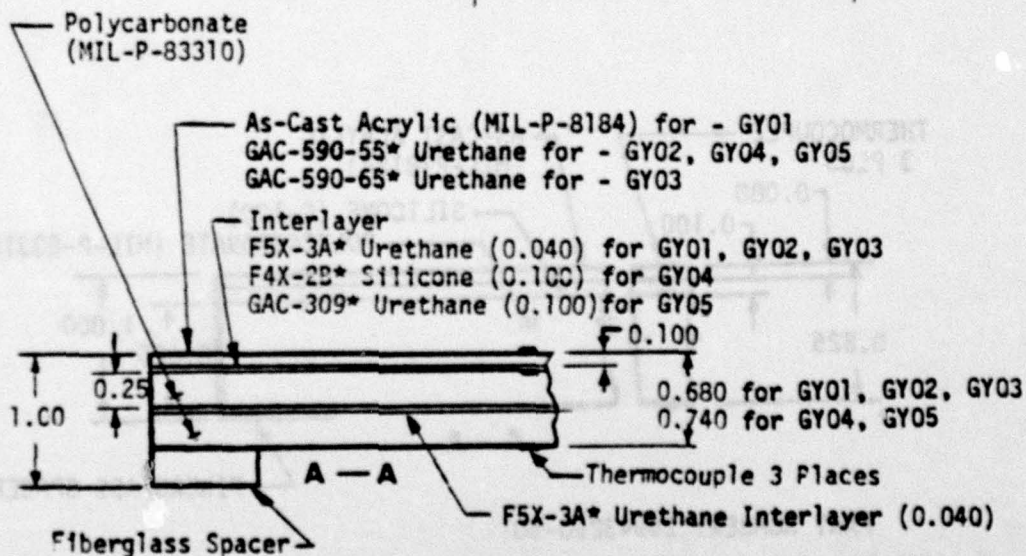
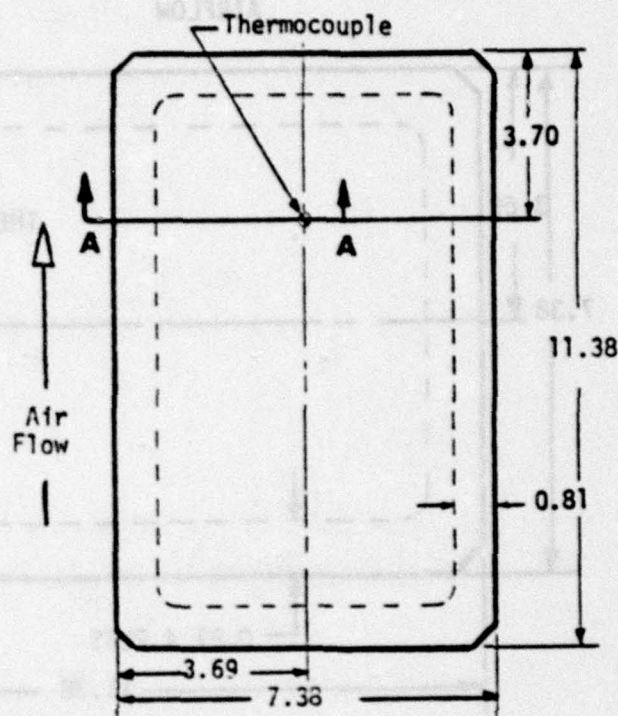


PART NUMBER: Z5943260-501

- NOTES: (1) Dimensions are nominal and in inches.
 (2) These parts were fabricated for a previous test (Reference 1) but were never tested.

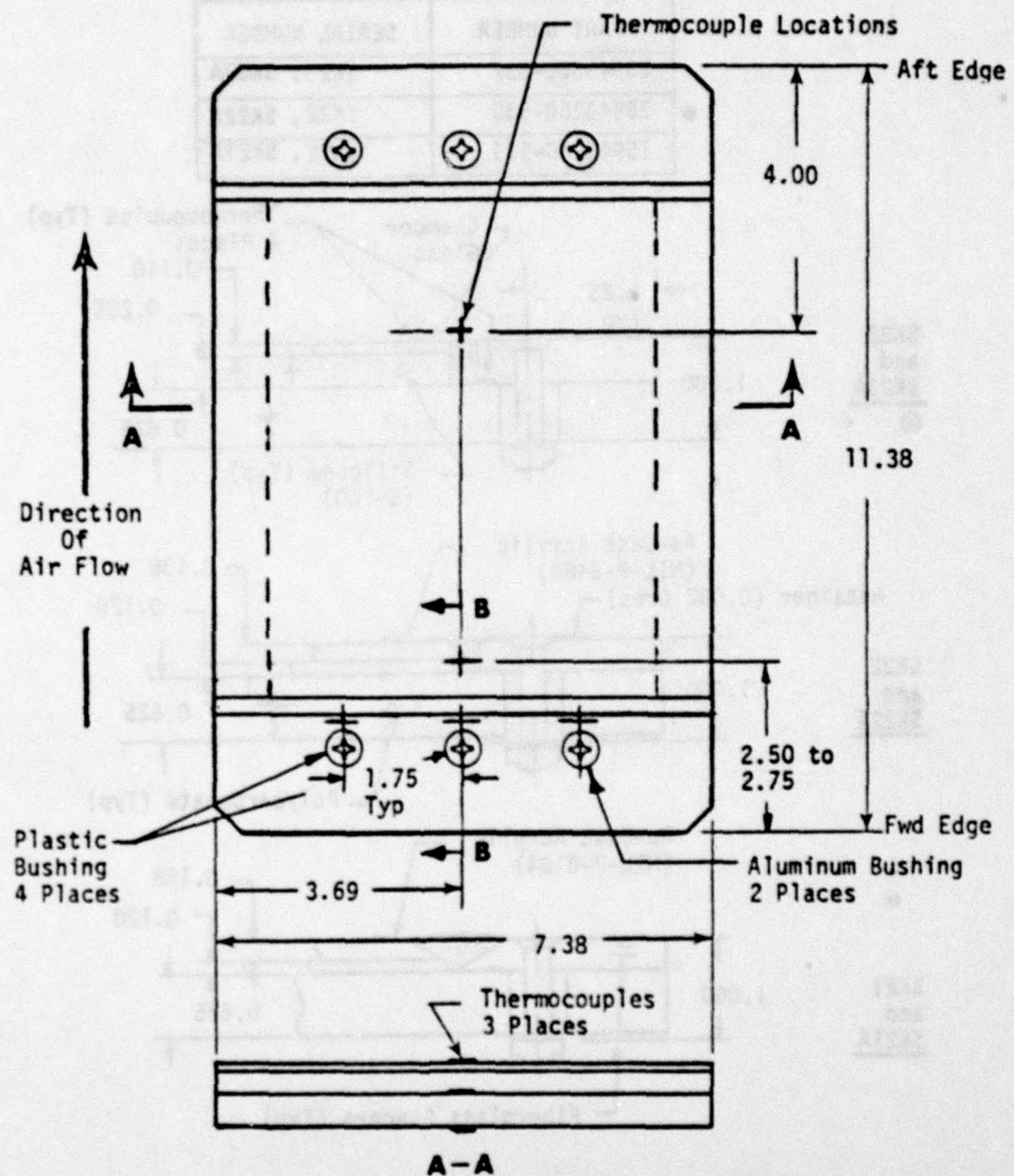
Figure 3. Sierracin Specimen SK05 and SK06.

PART NUMBER	SERIAL NUMBER
Z5943260-519	GY01
-521	GY02
-523	GY03
-525	GY04
-527	GY05



- NOTES: (1) Dimensions are nominal and in inches.
(2) These specimens were previously tested (Reference 1)
(3) * is Goodyear Aerospace (proprietary).

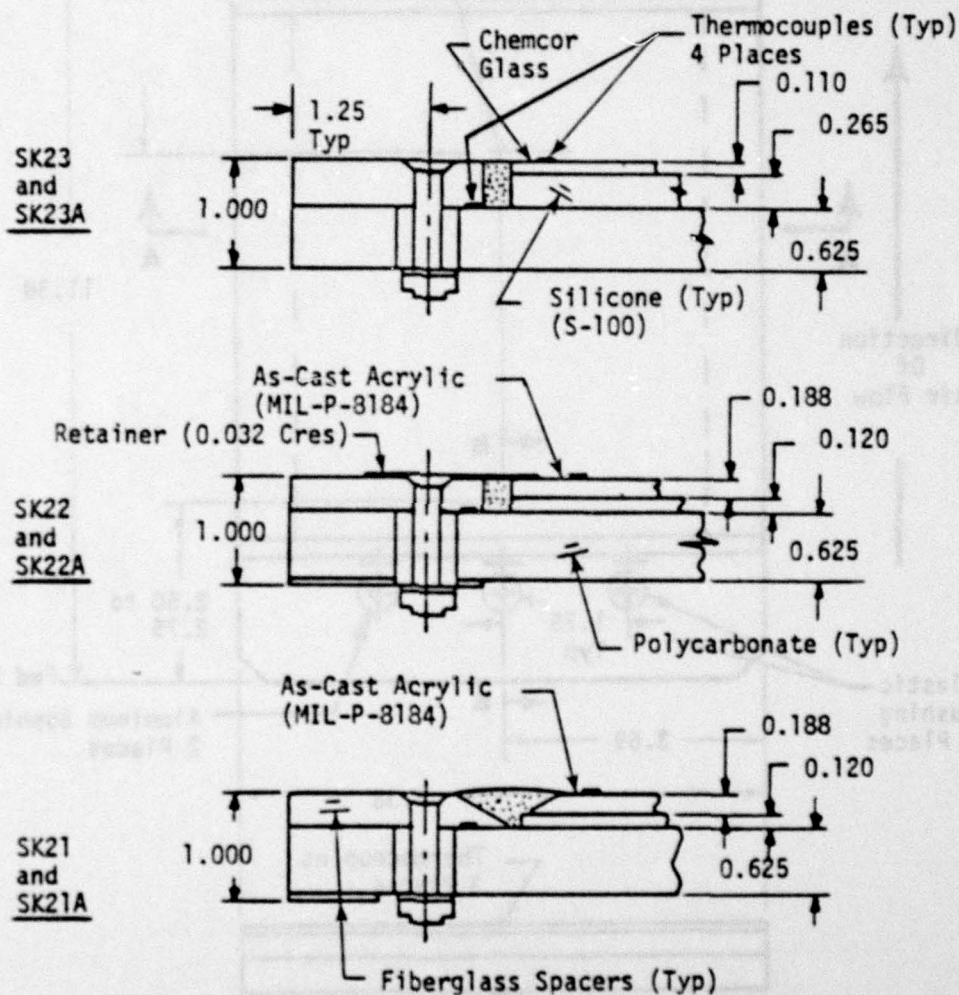
Figure 4. Goodyear Test Specimens GY01 Through GY05.



- NOTES: (1) Dimensions are in Inches.
(2) See Figure 6 for Section B-B

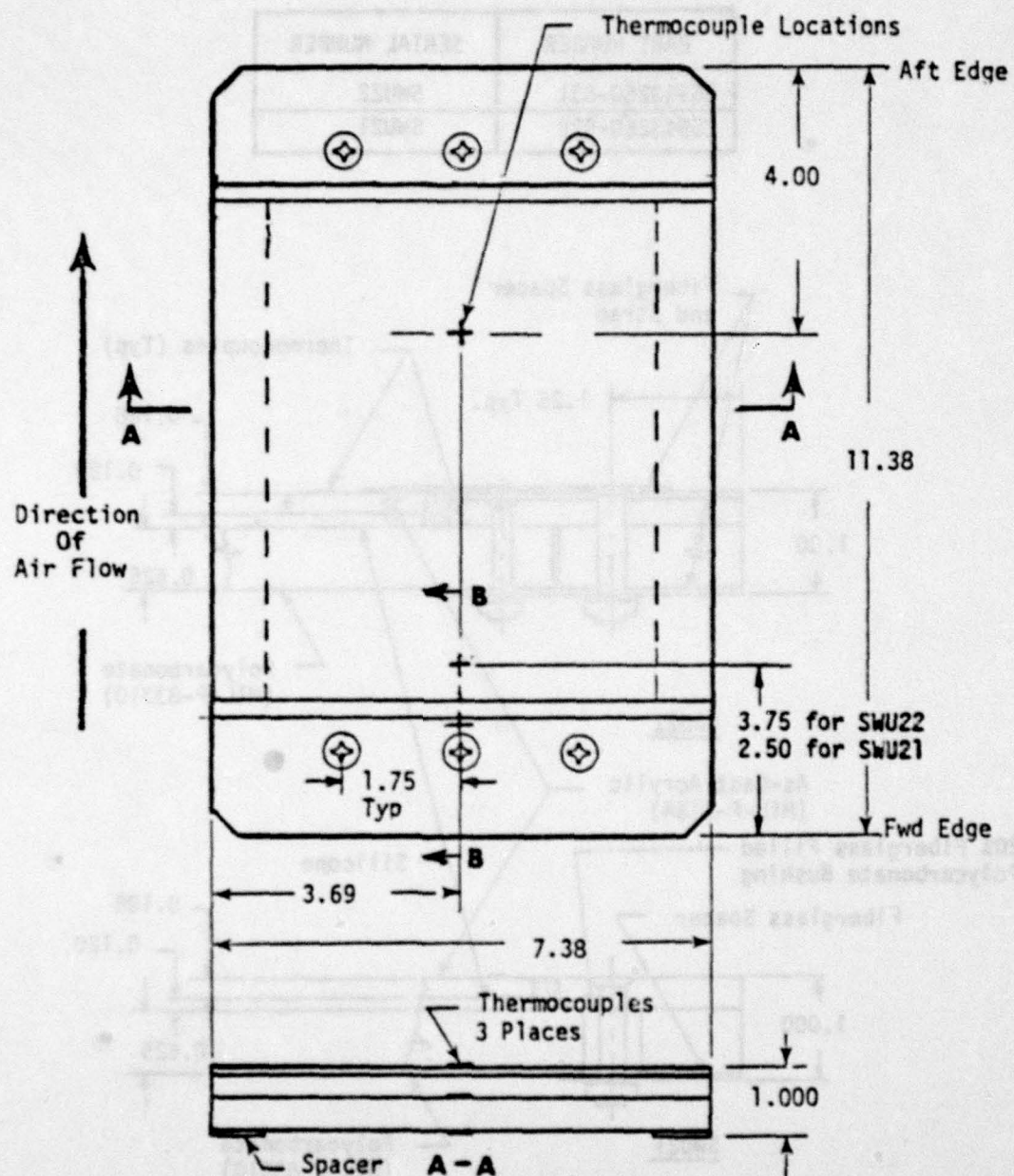
Figure 5. Sierracin Specimens SK21 Through SK23A.

PART NUMBER	SERIAL NUMBER
Z5943260-537	SK23, SK23A
Z5943260-535	SK22, SK22A
Z5943260-533	SK21, SK21A



- NOTES: (1) Dimensions are Nominal and in Inches
 (2) Bushings are 20% Fiberglass Filled Polycarbonate and Aluminum

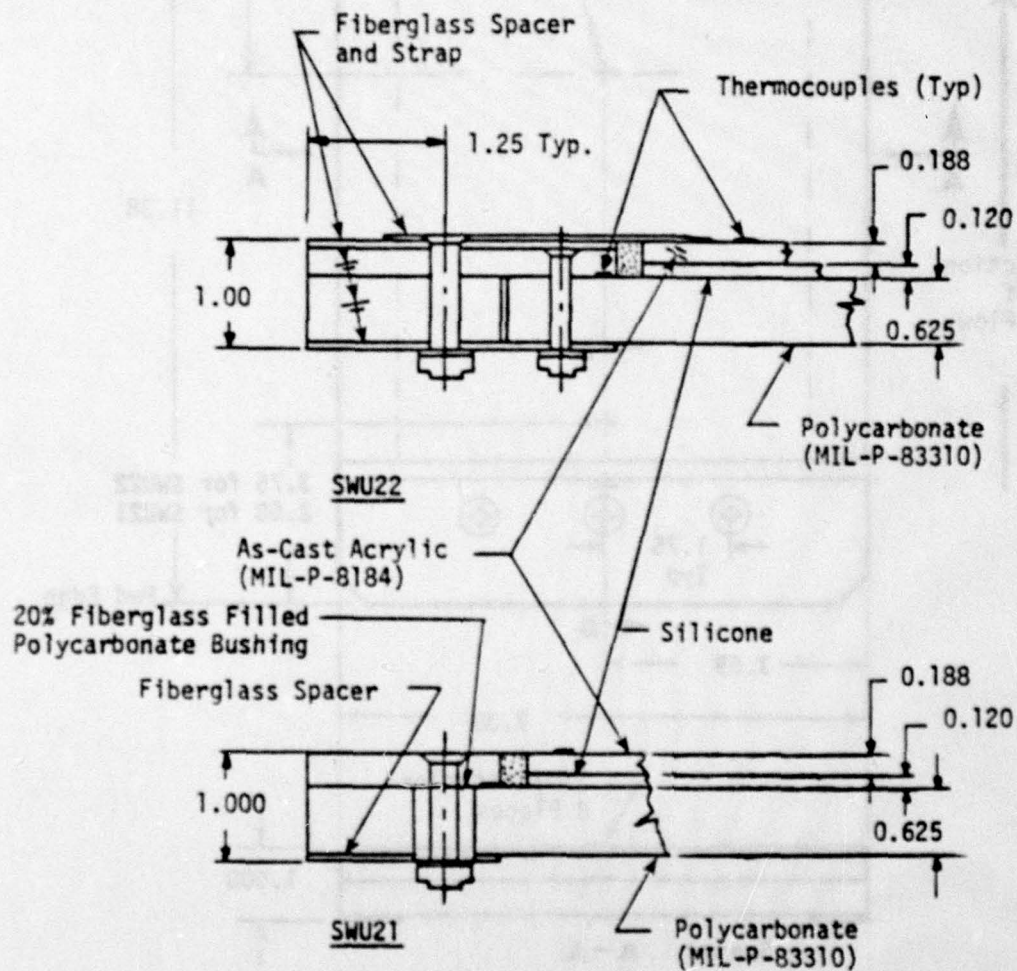
Figure 6. Sierracin Test Specimens SK21 Through SK23A (Section B-B, Figure 5).



NOTES: (1) Dimensions are in Inches.
 (2) See Figure 8 for Section B-B.

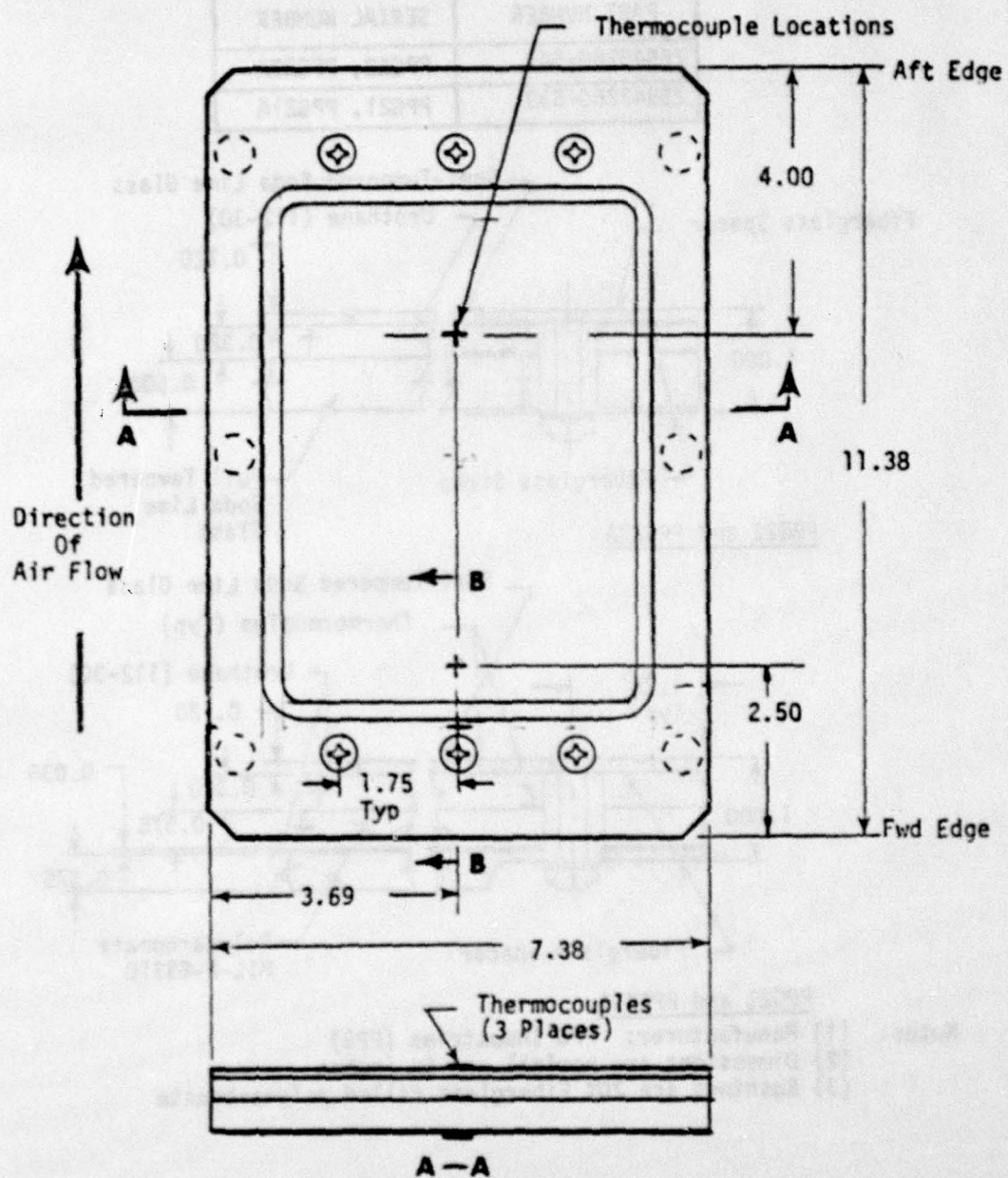
Figure 7. Swedlow Test Specimens.

PART NUMBER	SERIAL NUMBER
Z5943260-531	SWU22
Z5943260-529	SWU21



Dimensions are nominal and in inches.

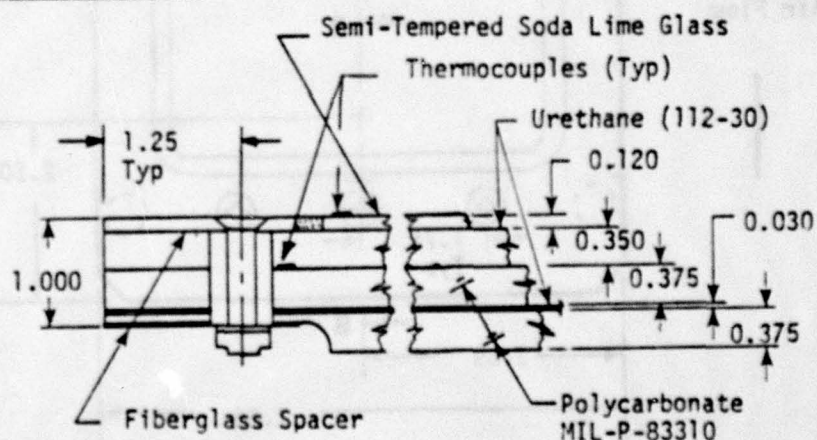
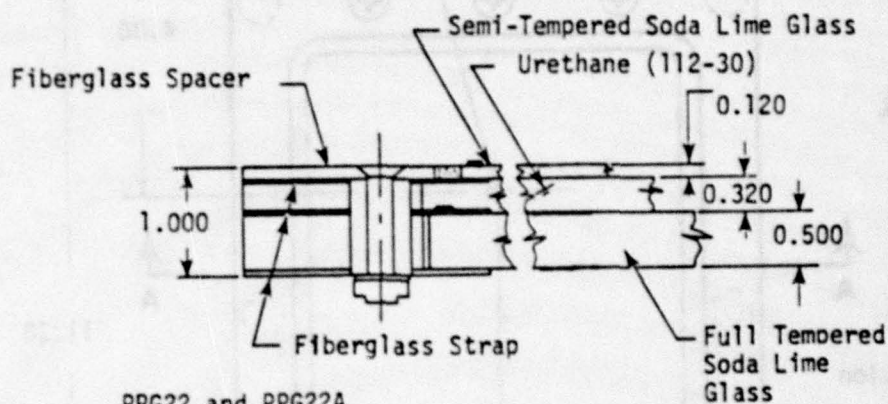
Figure 8. Swedlow Test Specimen
(Section B-B, Figure 7).



- NOTES:
- (1) Dimensions are in Inches.
 - (2) See Figure 10 for Section B-B.

Figure 9. PPG Test Specimens.

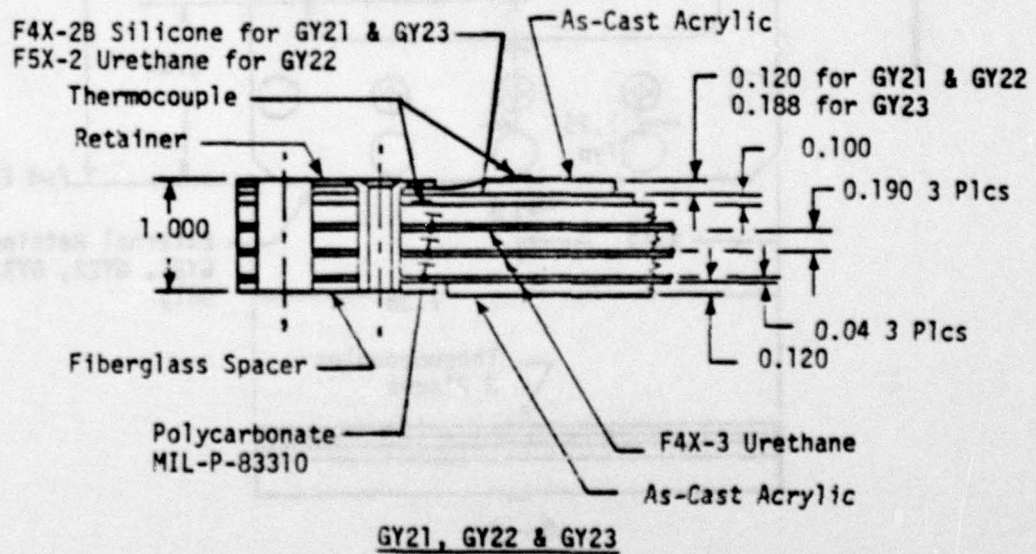
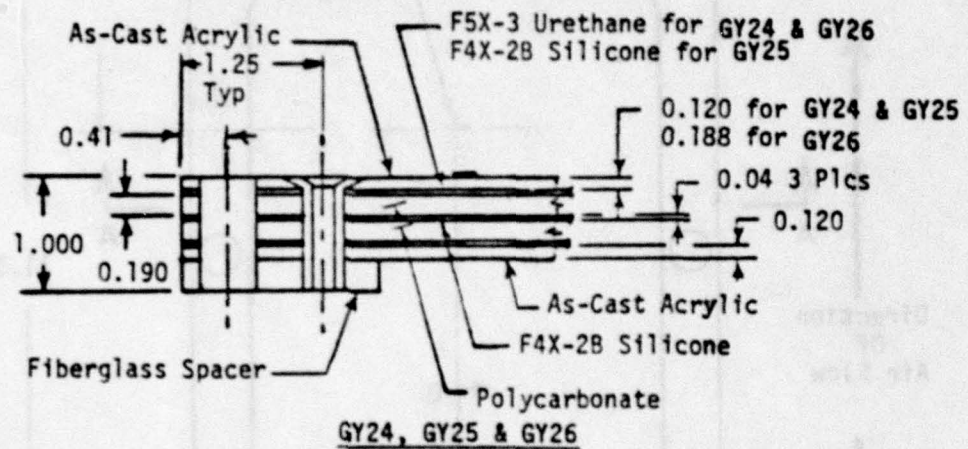
PART NUMBER	SERIAL NUMBER
Z5943260-541	PPG22, PPG22A
Z5943260-539	PPG21, PPG21A



- Notes: (1) Manufacturer: PPG Industries (PPG)
 (2) Dimensions are nominal and in inches
 (3) Bushings are 20% Fiberglass filled polycarbonate

Figure 10. PPG Test Specimens
 (Section B-B, Figure 9).

PART NUMBER	SERIAL NUMBER
Z5943260-553	GY26
Z5943260-551	GY25
Z5943260-549	GY24
Z5943260-547	GY23
Z5943260-545	GY22
Z5943260-543	GY21



Notes: (1) Bushings are 20% Fiberglass Filled Polycarbonate

Figure 12. Goodyear Test Specimens GY21 Through GY26.
(Section B-B, Figure 11.)

TEST HARDWARE

The test hardware consists of a cabin simulator, a wedge, an instrumented panel and a teflon panel. These items will be supplied by the AEDC/ARO.

Cabin Simulator

The test specimens will be mounted in an existing cabin simulator (Douglas drawing Z5943261). The purpose of the cabin simulator, Figure 13, is to provide both support for the test specimens and a simulated cabin environment on the back side of the test specimens. A specimen is installed

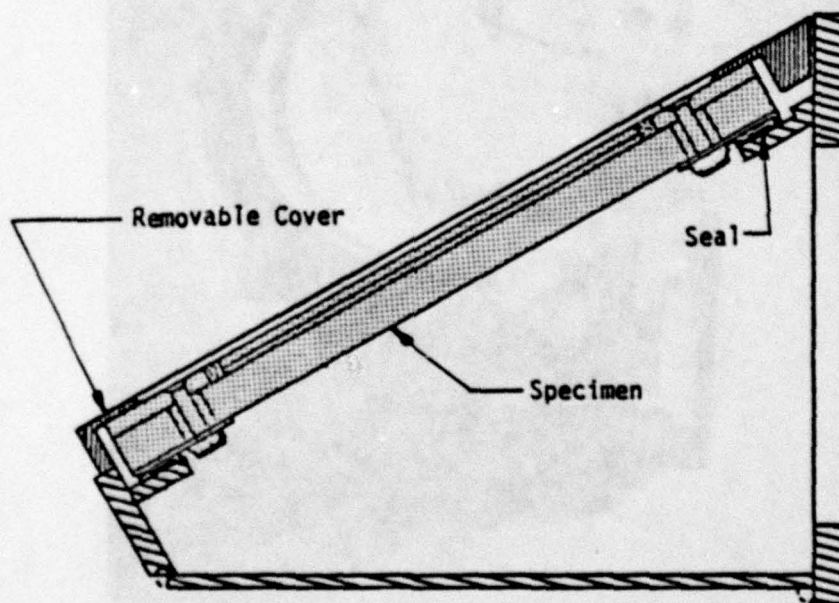


Figure 13. Cabin Simulator.

in the simulator by laying the specimen in the top of the box and installing the cover with six bolts. Regulated air at ambient temperature will be supplied to the simulator at a constant flow rate and discharged to the tunnel free-stream through vents located on the bottom of the simulator. Water coils on the simulator walls will augment air cooling. A silicone

rubber seal between the specimen and support frame will prevent air leakage and provide room for thermal expansion. A quartz port, in the rear of the simulator, Figure 14, will make it possible to photograph through the specimen during the tests. Figure 15 shows the cabin simulator in the tunnel.

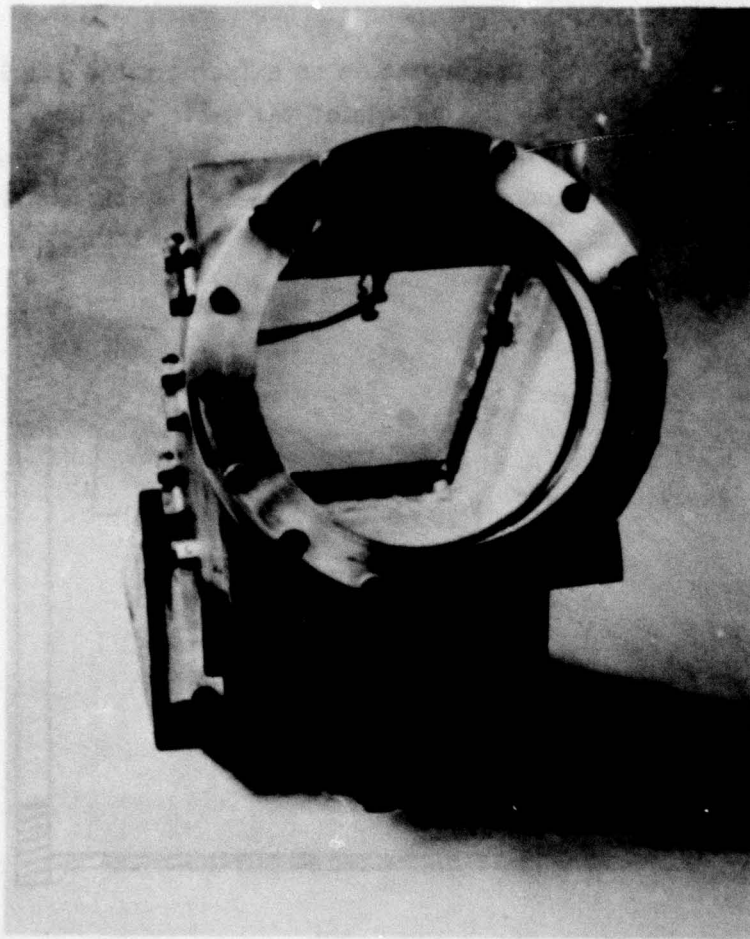


Figure 14. View Through Quartz Window in Cabin Simulator.

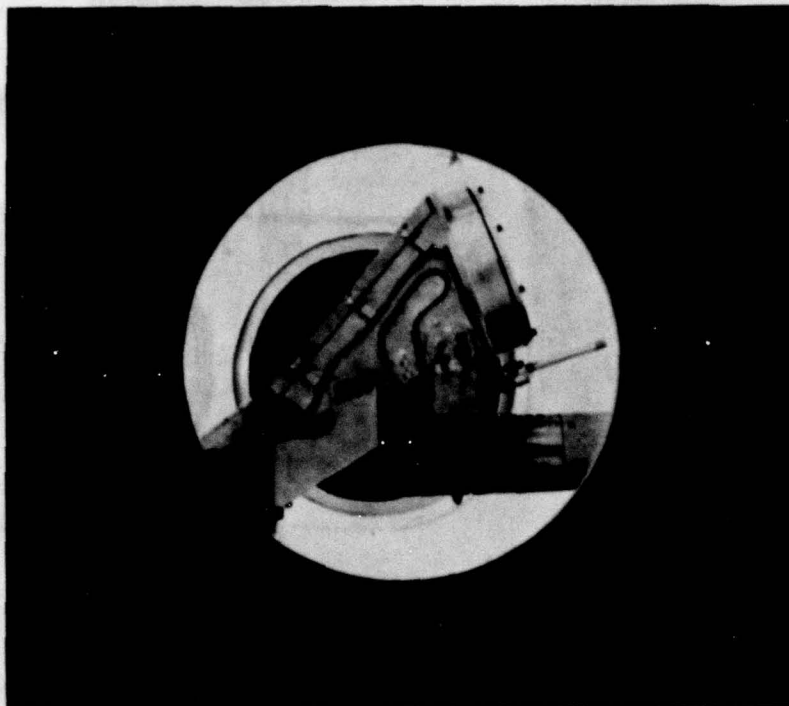


Figure 15. Cabin Simulator in Tunnel.

Wedge

The cabin simulator will be attached to a wedge, Figure 16, which serves as a shock generator. It will reduce the wind tunnel free-stream Mach number from 6 to the appropriate Mach number required across the specimen. The wedge will be mounted to the sting. The sting is the support arm, and is part of the tunnel apparatus. The slope of the front surface of the wedge will be varied to meet the Mach number requirements by manipulating the sting.

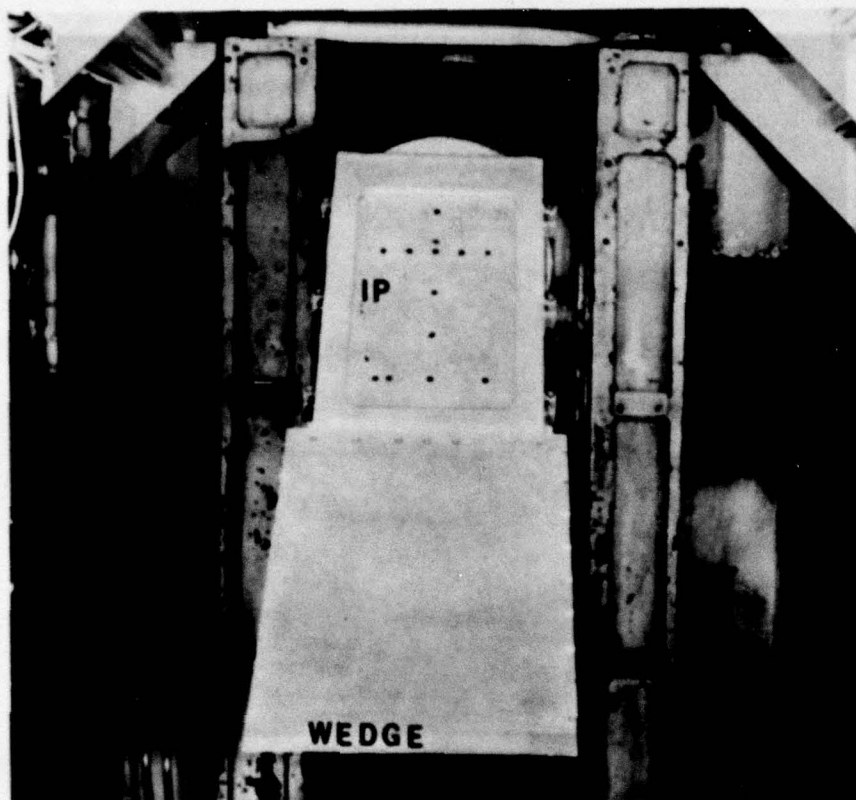


Figure 16. Wedge and Instrumented Panel (IP).

Instrumented Panel

An instrumented panel (IP), shown in Figure 16, will be used to determine the heat transfer rate and pressure distribution on the outboard surface of the test specimens. There are 15 pressure orifices and 11 heat-transfer rate gages located on the panel surface. It will be supported in the tunnel by the cabin simulator and has the same planform dimensions as the specimens.

Teflon Panel

A teflon panel will be used for phase-change paint tests. The purpose of these tests will be to obtain additional heat-transfer data and to locate possible surface "hot spots". The panel will be supported by the cabin simulator and has the same planform dimensions as the specimens.

TEST DESCRIPTION

This test series is to be completed in three nights of testing and consists of three different types of tests: obtaining pressure and heat-transfer distributions on an instrumented panel, photographing heat patterns on 9 specimens and a teflon panel that are coated with phase-change paint, and appraising thermal and optical effects of a Mach 2.4, 2.6 and 3.0 wind tunnel environment on 27 test specimens. The tests will be conducted in accordance with the test schedule shown in Table 3.

General Requirements and Setup

Prior to testing, grid board photos will be taken through each specimen by the AEDC/ARO personnel. Post-test photos will also be taken.

For in-tunnel testing the specimens will be supported by an AEDC/ARO supplied cabin simulator to provide a cockpit environment on the back of the windshield specimens. The cabin simulator will be attached to a wedge or shock generator, as shown in Figure 17. The angle between the wedge and cabin simulator will be set to 15 degrees, which represents the nose/windshield angle for a high performance aircraft. The wedge will be set at angles calculated to reduce the free stream velocity to the simulated flight conditions of Mach 2.4, 2.6 and 3.0.

A camera will be mounted outside the tunnel and aimed through a viewing port and the specimens at a system of grid lines to provide in-tunnel photography for distortion evaluation. These in-tunnel photographs will be taken at approximately 2-minute intervals. The camera will be set at an angle of approximately 20 degrees with the tunnel centerline. The angle between the camera (line of sight) and specimen (windshield) will vary from 28.2 degrees to 23.3 degrees.

Temperatures will be recorded by thermocouples installed on each specimen at intervals of approximately three readings per minute. These thermocouples are located to record the exterior surface temperature at two

TABLE 3. TEST SCHEDULE.

NIGHT 1				NIGHT 2				NIGHT 3			
SPECIMEN		MACH NO. (NOTE)	EST. TIME (HR)	SPECIMEN		MACH NO. (NOTE)	EST. TIME (HR)	SPECIMEN		MACH NO. (NOTE)	EST. TIME (HR)
PRIMARY	SECONDARY			PRIMARY	SECONDARY			PRIMARY	SECONDARY		
TP		(1)	3.0	Complete Night 1 Testing		2.4 ⁽³⁾	4.0	Complete Night 2 Testing		2.6 ⁽³⁾	7.0
TP SK21A SK22A SK23A SHU21 SHU22 PPG22A GY21 TEX21A		2.4 ⁽²⁾	2.0	TP SK21A SK22A SK23A PPG21A PPG22A TEX21A		2.6 ⁽²⁾	1.5	TP SK23A PPG21A PPG22A		3.0 ⁽²⁾	1.0
SK05 SK21 SHU21 PPG21 GY21 GY24 GY25 GY26 GY03 GY04 GY05 TEX21	SK06 SK22 SHU22 PPG21A GY22 GY01 GY02 TEX21A	2.4 ⁽³⁾	11.0 (5)	SK06 SK21 SK22 SY23 SHU21 SHU22 PPG21 PPG22 GY21 GY22 GY23 GY24 GY25 GY26 TEX21	SK22A PPG21A GY04 GY05 TEX21A	2.6 ⁽³⁾	13.5 (5)	SK21 SK22 SK23 SHU22 PPG21 PPG22 GY21 GY22 GY23 GY26	SK22A PPG21A GY25 GY24	3.0 ⁽⁴⁾	4.0

NOTES:

- (1) Injection of instrumented panel at 11:00.
- (2) Thermal mapping of teflon panel (TP) and specimens.
- (3) Injection of specimens for 5, 10 and 15 minute increments.
- (4) Injection of specimens for 1/2 and 3 minute increments.
- (5) Estimated time is based on 6 minutes between injections and 12 minutes to change a specimen.

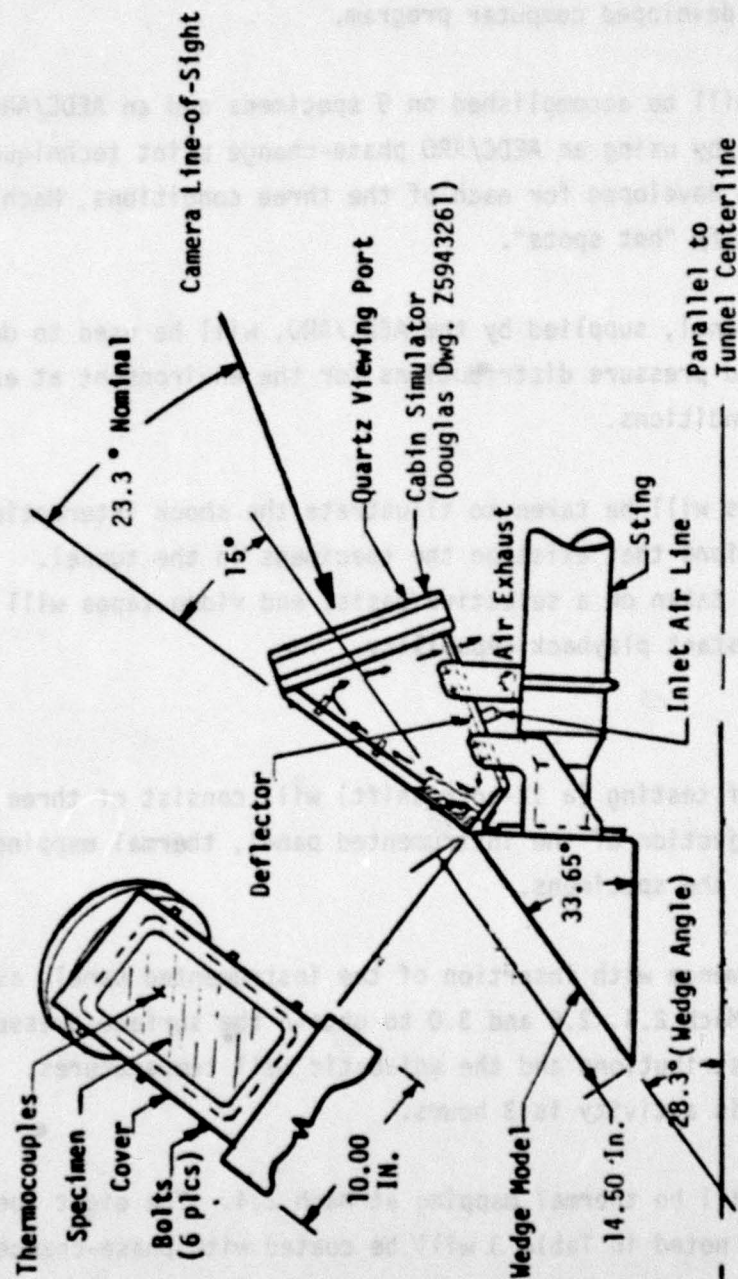


Figure 17. Test Setup. (Angles are for Mach 3.0 Simulation)

points, the interior surface temperature, the temperature of the structural ply (polycarbonate or glass), and the temperature of the structural ply adjacent to the forward bolt. These data will be compared to values calculated by a Douglas developed computer program.

Thermal mapping will be accomplished on 9 specimens and an AEDC/ARO supplied teflon panel by using an AEDC/ARO phase-change paint technique. Heat patterns will be developed for each of the three conditions, Mach 2.4, 2.6 and 3.0, to identify "hot spots".

An instrumented panel, supplied by the AEDC/ARO, will be used to determine heat-transfer and pressure distributions for the environment at each of the Mach number conditions.

Shadowgraph photos will be taken to illustrate the shock interactions and flow-field conditions that exist on the specimens in the tunnel. Direct movies will be taken on a selective basis, and video tapes will be used to provide instant playback capability.

Test Activity

The first night of testing (a 12-hour shift) will consist of three types of testing: injection of the instrumented panel, thermal mapping, and tunnel testing of the specimens.

Activity will commence with insertion of the instrumented panel, as noted in Table 3, at Mach 2.4, 2.6 and 3.0 to obtain the surface pressure, heat-transfer rate distributions and the adiabatic wall temperatures. The estimated time for this activity is 3 hours.

The second step will be thermal mapping at Mach 2.4. The eight specimens and teflon panel noted in Table 3 will be coated with phase-change paint and injected into a Mach 2.4 tunnel environment for a length of time determined by AEDC/ARO procedures. Sequence photos will be taken

to record timewise progression of paint melt lines in accordance with AEDC/ARO techniques. The estimated time for this activity is 2 hours.

Step three will consist of tunnel testing of the 12 primary specimens listed in Table 3. The specimens will be tested in a Mach 2.4 environment at time increments of 5, 10 and 15 minutes. The specimens will be cooled to 160°F between injections. A specimen failure will terminate the test for a given specimen as determined by the Douglas Test Representative. A secondary specimen may be substituted for a primary specimen. Specimens not tested will be injected the following night. The estimated time to complete these tests is 11 hours and is based on 6 minutes between injections and 12 minutes to change a specimen.

The second night of testing (a 12-hour shift) will consist of two types of testing: thermal mapping and tunnel testing of the specimens.

The activity will commence, if necessary, with the completion of the Mach 2.4 tunnel testing of specimens that were not tested on the first night. It is estimated that this activity may take up to 4 hours.

This will be followed by thermal mapping of the five specimens and teflon panel noted in Table 3 at Mach 2.6. The specimens will be coated with phase-change paint and injected into a Mach 2.6 environment for a length of time determined by the AEDC/ARO. The time estimate for this procedure is 1.5 hours.

The thermal mapping activity will be followed by tunnel testing of the 15 primary specimens listed in Table 3. The specimens will be tested in Mach 2.6 environment at time increments of 5, 10 and 15 minutes. The specimens will be cooled to 160°F between injections. A specimen failure will terminate the test as determined by the Douglas Test Representative. A secondary specimen may be substituted for a primary specimen. Specimens not tested will be injected the following night. The time estimate is 13.5 hours. It is anticipated that the test times for specimens with plastic face plies may be terminated prematurely due to material degradation.

The third night of testing will be similar to the second night and will commence, if necessary, with completion of any Mach 2.6 testing that was not completed on the previous night and may require up to 7 hours.

This activity will be followed by thermal mapping at Mach 3.0 per Table 3. The three specimens and teflon panel will be coated with paint and injected into a Mach 3.0 tunnel environment. The time estimate is one hour.

Thermal mapping will be followed by tunnel testing of the eleven specimens listed in Table 3 in a Mach 3.0 environment. Injection times will be 1/2 and 3 minutes. The specimens will be cooled to 160°F between injections. The Douglas Test Representative will be responsible for termination of a test and for substitutions. The estimated time is 4 hours.

TEST CONDITIONS

Environmental Conditions

The area of an aircraft windshield that would normally receive the highest heating, and therefore the area that would probably fail first due to overheating, is that area directly behind the aircraft nose and on its centerline. A typical supersonic aircraft nose shape with the flow environment depicted in the area of interest is shown in Figure 18. The conditions were calculated by the methods of Reference 4.

Region 1 in the figure is the free-stream environment. Region 2 represents the approach environment. The approach conditions were computed from the Region 1 conditions using inviscid cone theory. It was assumed that the aircraft nose upper surface could be approximated by a half-cone. The cone half-angle chosen for these calculations was 15 degrees. Region 3 represents the windshield environment. These conditions were calculated using inviscid wedge theory and were computed from the Region 2 conditions. A wedge angle of 15 degrees was chosen for the windshield. Region 4 represents the cabin environment.

FREE-STREAM CONDITIONS

- ① $M = 3.0$ AT 64,800 FT
 $T = -70^{\circ}\text{F}$, $P = 0.83$ PSIA
 $T_0 = 632^{\circ}\text{F}$, $P_0 = 30.6$ PSIA
- ② APPROACH CONDITIONS
 $M = 2.5$, $P = 1.74$, $T_0 = 632^{\circ}\text{F}$
- ③ WINDSHIELD CONDITIONS
 $M = 1.89$, $P = 4.24$, $T_0 = 632^{\circ}\text{F}$
- ④ CABIN CONDITION
 $T = 75^{\circ}\text{F}$, $P = 5.83$ PSIA

Where: M = Mach Number

T = Temperature

T_0 = Stagnation Temp

P = Pressure

P_0 = Stagnation Pressure

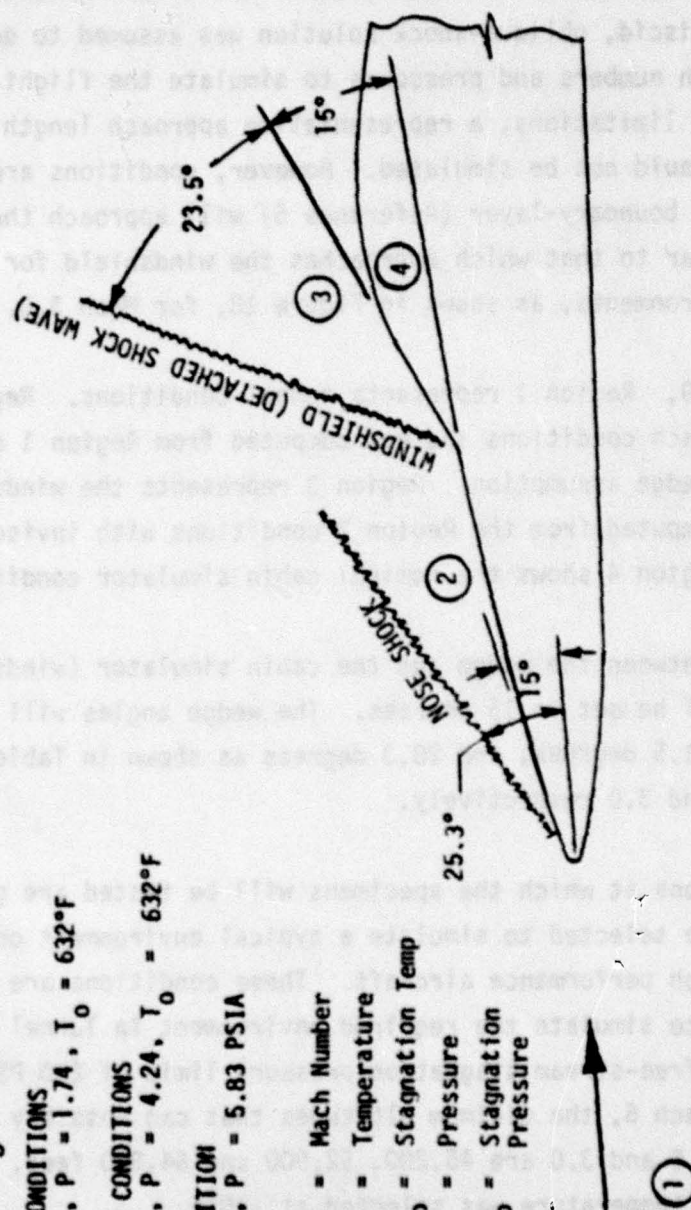


Figure 18. Windshield Flight Environment at Mach 3.0.

The specimen test environment is shown in Figure 19 for conditions at Mach 3.0. For simplicity, a two-dimensional wedge model was chosen to simulate the approach flow conditions of the aircraft nose. A two-dimensional inviscid, oblique-shock solution was assumed to determine the appropriate Mach numbers and pressures to simulate the flight environments. Because of size limitations, a representative approach length of an aircraft nose could not be simulated. However, conditions are such that fully turbulent boundary-layer (Reference 5) will approach the test specimens similar to that which approaches the windshield for each of the flight environments, as shown in Figure 18, for Mach 3.0.

In Figure 19, Region 1 represents tunnel conditions. Region 2 represents the approach conditions and was computed from Region 1 conditions with inviscid wedge assumption. Region 3 represents the windshield environment and was computed from the Region 2 conditions with inviscid wedge assumption. Region 4 shows the nominal cabin simulator conditions.

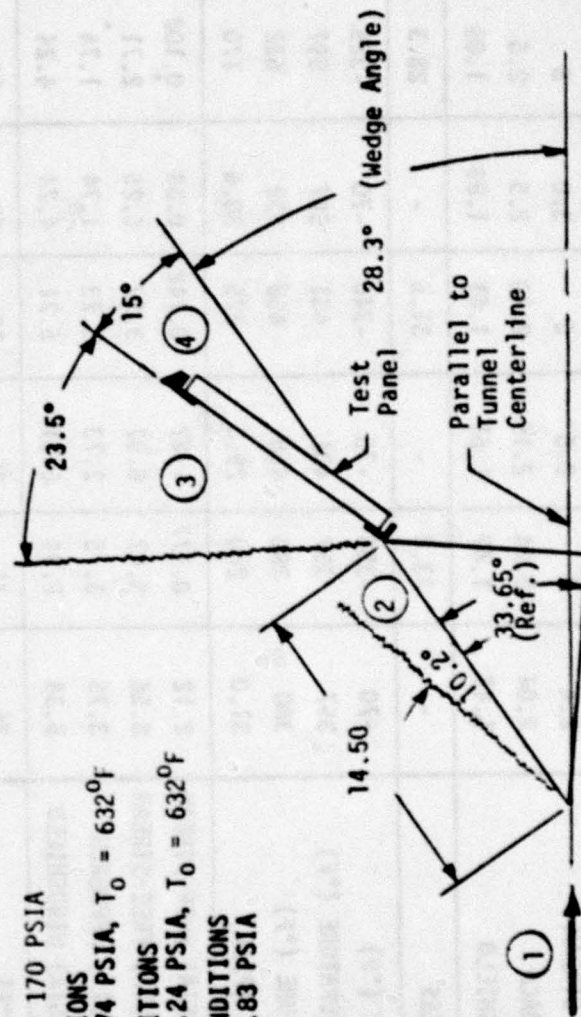
The angle between the wedge and the cabin simulator (windshield to nose angle) will be set to 15 degrees. The wedge angles will be set to 33.3 degrees, 31.5 degrees, and 28.3 degrees as shown in Table 4 for Mach 2.4, 2.6 and 3.0 respectively.

The conditions at which the specimens will be tested are given in Table 4 and were selected to simulate a typical environment on the transparency of a high performance aircraft. These conditions are limited by the ability to simulate the required environment in Tunnel B. Since Tunnel B has a free-stream stagnation pressure limit of 280 PSIA at approximately Mach 6, the minimum altitudes that can possibly be simulated for Mach 2.4, 2.6 and 3.0 are 45,200, 52,900 and 64,800 feet, respectively. The free-stream temperature was selected at -70°F .

The adiabatic wall temperature calculated for each condition is shown in Table 3 and is defined here (in degrees Rankine) by the following equation:

FREE-STREAM CONDITIONS

- 1 $M = 6$
 $T_0 = 632^\circ\text{F}$, $P_0 = 170$ PSIA
- 2 APPROACH CONDITIONS
 $M = 2.5$, $P = 1.74$ PSIA, $T_0 = 632^\circ\text{F}$
- 3 WINDSHIELD CONDITIONS
 $M = 1.89$, $P = 4.24$ PSIA, $T_0 = 632^\circ\text{F}$
- 4 INBOARD FACE CONDITIONS
 $T = 75^\circ\text{F}$, $P = 5.83$ PSIA



Where: M = Mach Number
 T = Temperature
 T_0 = Stagnation Temperature
 P = Pressure
 P_0 = Stagnation Pressure

Figure 19. Specimen Test Environment at Mach 3.0.

TABLE 4. FLIGHT AND TEST ENVIRONMENT

	MACH 2.4		MACH 2.6		MACH 3.0	
	FLIGHT	TEST	FLIGHT	TEST	FLIGHT	TEST
ALTITUDE (FEET)	45,200	-	52,900	-	64,800	-
MACH NUMBER - FREE-STREAM	2.4	6	2.6	6	3.0	6
MACH NUMBER - APPROACH	2.04	2.04	2.19	2.19	2.5	2.5
MACH NUMBER - WINDSHIELD	1.47	1.47	1.61	1.61	1.89	1.89
WEDGE ANGLE - DEGREES	-	33.2	-	31.5	-	28.3
AMBIENT TEMPERATURE (°F)	-70	-356	-70	-346	-70	-325
ADIABATIC WALL TEMPERATURE (°F)	357	357	431	431	597	597
STAGNATION TEMPERATURE (°F)	380	380	458	458	632	632
STAGNATION PRESSURE (PSIA)	31.0	280	29.3	225	30.6	170
AMBIENT PRESSURE (PSIA) FREE-STREAM	2.12	0.177	1.47	0.142	0.83	0.108
DYNAMIC PRESSURE (PSIA) FREE-STREAM	8.56	4.47	6.97	3.59	5.25	2.71
AMBIENT PRESSURE (PSIA) APPROACH	3.75	3.75	2.73	2.73	1.74	1.74
AMBIENT PRESSURE (PSIA) WINDSHIELD	8.34	8.34	6.21	6.21	4.24	4.24
CABIN TEMPERATURE (°F)	75	75	75	75	75	75
CABIN PRESSURE (PSIA)	7.12	7.12	6.47	6.47	5.83	5.83

$$T_{AW} = T_{\infty} \left(1 + r_f \frac{\gamma - 1}{2} M^2 \right)$$

where: T_{AW} is the adiabatic wall temperature in degrees Rankine
 T_{∞} is the static air temperature in degrees Rankine
 r_f is the recovery factor
 γ is the ratio of specific heat for air = 1.4
 M is the free stream Mach number.

The recovery factor to be simulated is 95 percent, which means that 95 percent of the stagnation temperature will be recovered in the adiabatic wall temperature.

That is,

$$\frac{T_{AW} - T_{\infty}}{T_0 - T_{\infty}} = 0.95$$

where T_0 is the stagnation temperature.

The pressure distribution across the specimen surface will be obtained from the instrumented panel tests and compared to calculated values.

Thermal Conditions

High temperature thermocouples are bonded to the inner and outer surfaces of each specimen by the vendors to provide temperature time histories. Foil type thermocouples are bonded to the outer surfaces with PS-18 adhesive on the as-cast acrylic face plies and with M-Bond 600 (Micro-Measurements Products) on the glass face plies. Additional thermocouples are imbedded within the specimens to measure the temperature of the structural ply and the area adjacent to the bolts. Wire and foil thermocouples are used for these imbedded thermocouples. M-Bond 600 was used for the bonding agent on the specimens procured from the previous test noted in Reference 1. Temperatures will be recorded at intervals of approximately three readings per minute.

A thermal correlation will be performed to compare test temperatures and calculated temperatures. Appropriate data, such as heat/transfer rates from the instrumented panel tests, the adiabatic wall temperatures and the material physical properties, will be inputted to a Douglas developed windshield heat/transfer computer program to perform the correlation. The material physical properties to be supplied by the vendors for use in computer program include the thermal conductivity, specific heat and density.

Thermal mapping will be accomplished in accordance with AEDC/ARO techniques through the use of phase-change paint applied to selected specimens and a teflon panel as noted in Table 3. The specimens will be injected at Mach 2.4, 2.6 and 3.0 as shown in Table 3. The specific thermally-rated paint to be used will be determined by the Douglas Test Representative after the instrumented data has been reduced. The anticipated surface temperatures, calculated by a Douglas computer program, are:

Mach 2.4: 349°F (10 minute exposure)

Mach 2.6: 419°F (10 minute exposure)

Mach 3.0: 554°F (3 minute exposure)

Time increments for specimen tunnel injections are given in Table 3 for each of the three Mach number test conditions. They are 5, 10 and 15 minutes for Mach 2.4 and Mach 2.6, and 1/2 and 3 minutes for Mach 3.0. These times are based on anticipated aircraft operating conditions and are tentative. Deterioration of the plastic materials at the high temperatures expected at the selected Mach numbers may force a reduction in the length of tunnel injection or termination of a specimens usefulness. The total estimated times would be subsequently affected. The estimated times, calculated for 6 minutes between injections and 12 minutes to change a specimen, are based on actual times from Reference 1 for a previous test.

Optical Conditions

Prior to delivery of the test specimens, each vendor will have measured and provided to Douglas the index of refraction, the light transmission values, and the haze values for each specimen. The index of refraction is to be developed per FTSM 406, Method 3022 (Reference 6). Light transmission and haze values are to be found per FTSM 406, Method 3022 (Reference 6), or ASTM D1003 (Reference 7). After the wind tunnel tests are complete, the tested specimens will be returned to the vendors and the light transmission and haze values will be measured again. Measurements will be made on each specimen at the five locations defined in Figure 20.

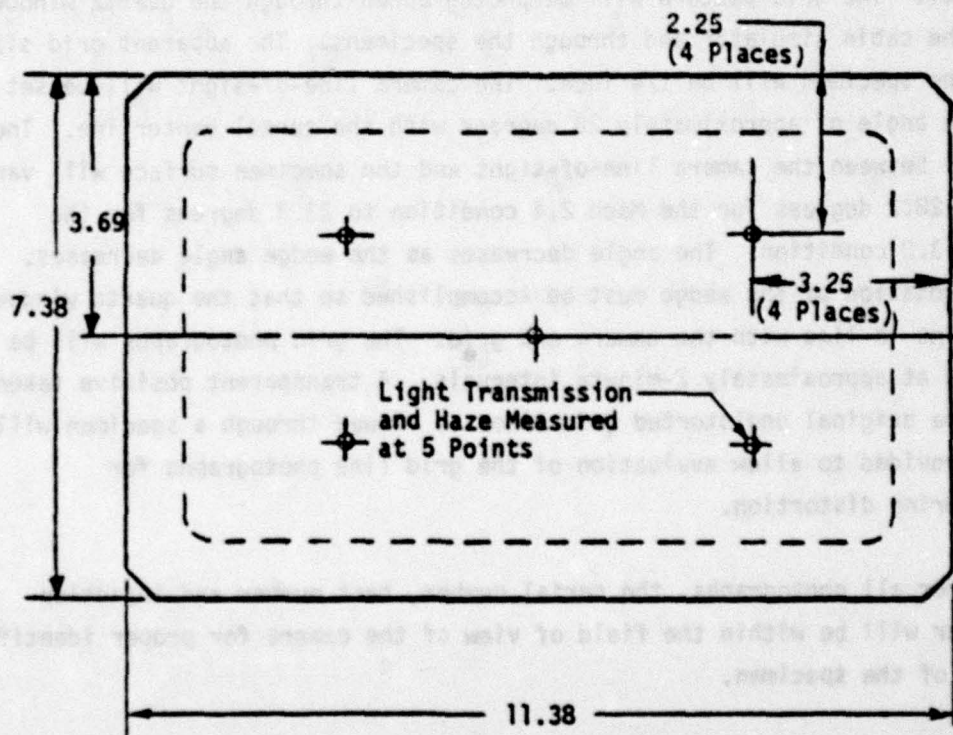


Figure 20. Locations Where Light Transmission and Haze to be Measured.

Photographic Conditions

The AEDC/ARO will use a Hasselblad camera to take pre-test and post-test photographs of a grid board as viewed through the specimens. This

arrangement is shown in Figure 21. The angle of incidence for these photos will be 60 degrees. The photographs will be used to evaluate permanent optical distortion which results from the tunnel activity. The AEDC/ARO will use a densitometer to measure light density changes on the grid photographs.

Photographs will also be used to evaluate in-tunnel optical distortion during test operations. A Hasselblad camera will be mounted outside the tunnel and aimed to look obliquely into the tunnel through a viewing port as shown in Figure 22. Prior to testing, a grid image will be projected onto the tunnel wall from the camera portal and painted on the wall of the tunnel. The grid pattern will be photographed through the quartz window in the cabin simulator and through the specimens. The apparent grid size at the specimen will be 1/4 inch. The camera line-of-sight will be set at an angle of approximately 20 degrees with the tunnel centerline. The angle between the camera line-of-sight and the specimen surface will vary from 28.2 degrees for the Mach 2.4 condition to 23.3 degrees for the Mach 3.0 condition. The angle decreases as the wedge angle decreases. The rotation of the wedge must be accomplished so that the quartz window remains in line with the camera and grid. The grid photographs will be taken at approximately 2-minute intervals. A transparent positive taken of the original undistorted grid lines as viewed through a specimen will be provided to allow evaluation of the grid line photographs for measuring distortion.

For all photographs, the serial number, test number and injection number will be within the field of view of the camera for proper identification of the specimen.

A standard refocused shadowgraph system will be installed alongside the tunnel to take Schlieren flow-field photographs.

A television camera will also be used to take general coverage color pictures for real-time monitoring and recording on videotape to provide a history of surface deteriorations.

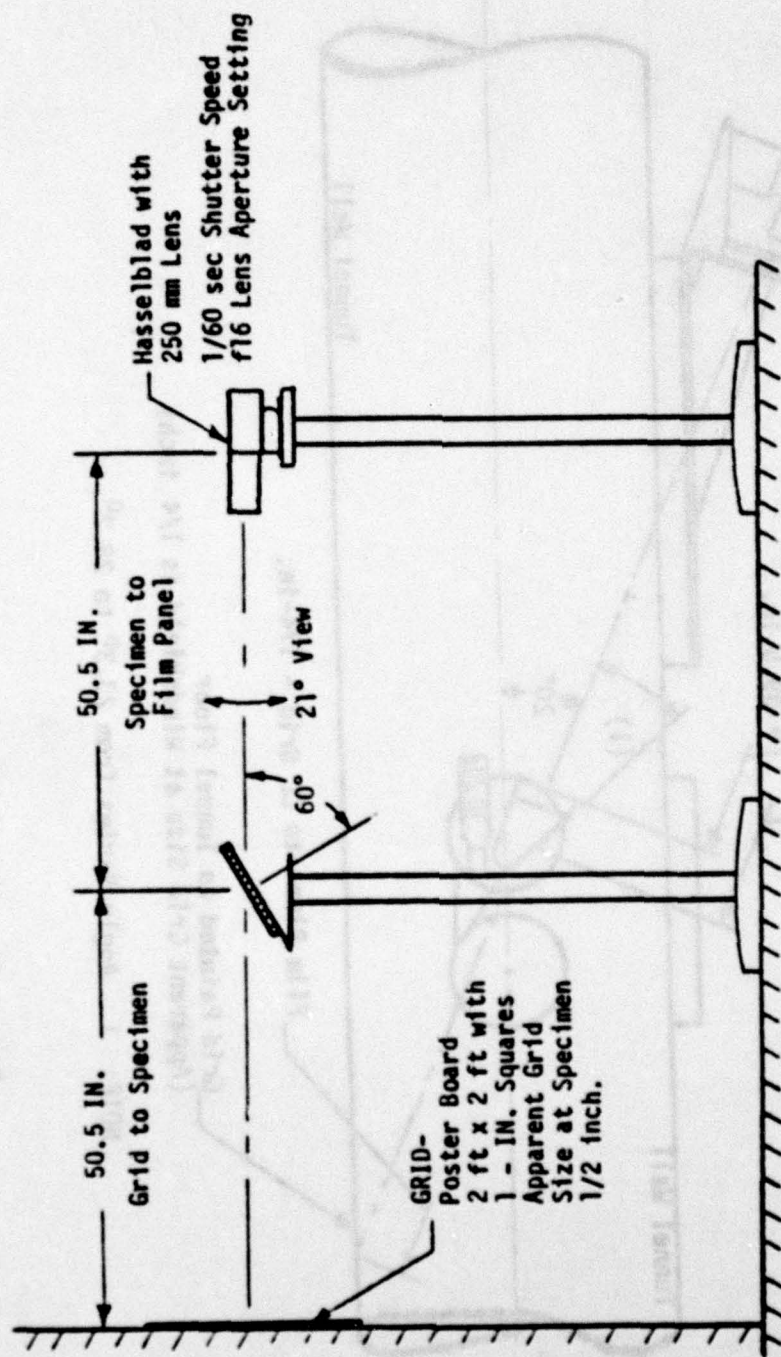


Figure 21. Camera Arrangement for Pre-Test/Post-Test Viewing.

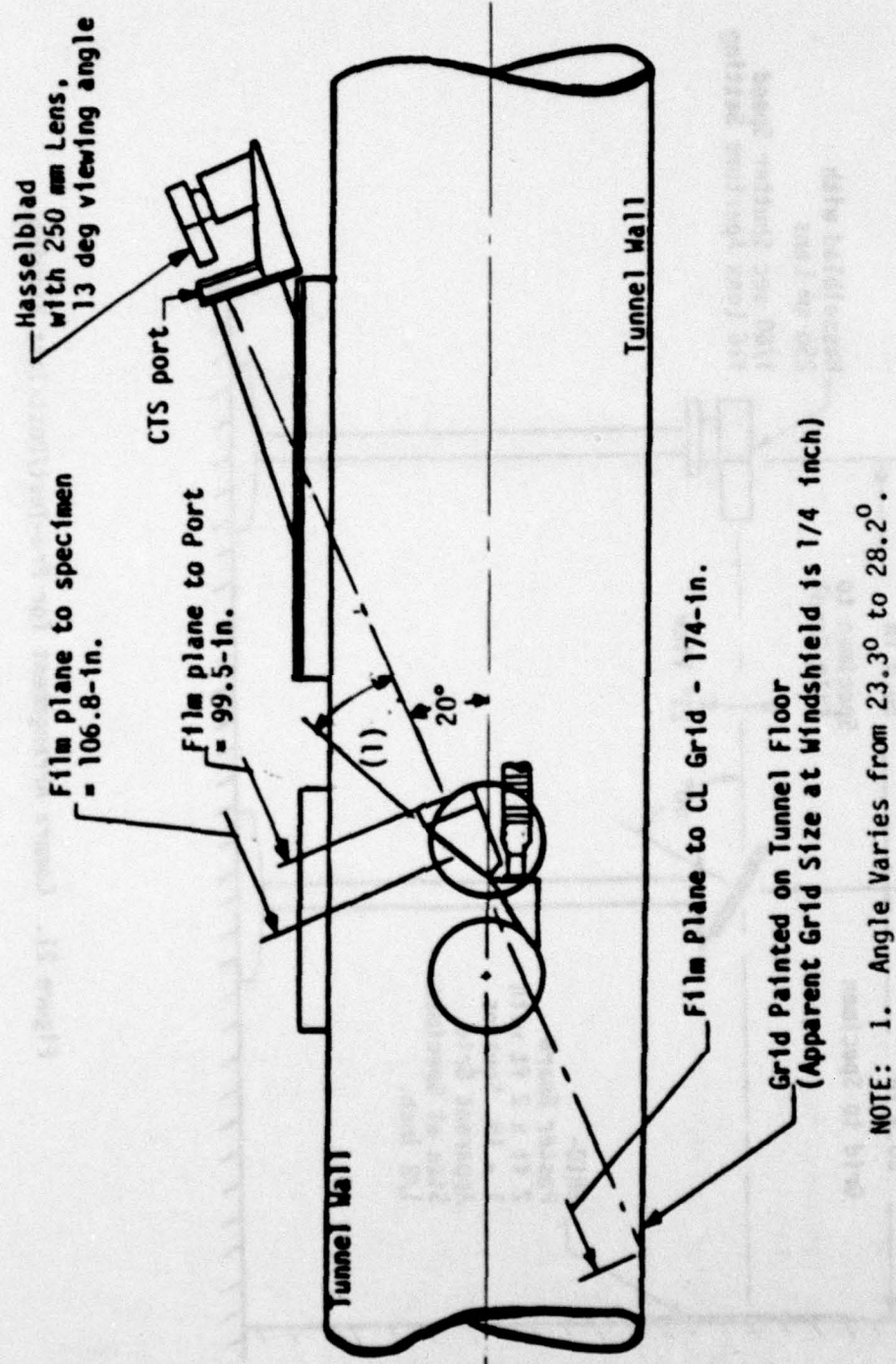


Figure 22. Camera Arrangement for Tunnel Grid Viewing.

Pre-test and post-test photographs will be taken by the AEDC/ARO of each test specimen.

Tolerances

Uncertainties of the basic tunnel parameters will be estimated from repeated calibrations of the stagnation temperature and pressure instruments by verifying repeatability and uniformity of the tunnel flow during calibration and will not exceed:

$\pm 0.5\%$ for Mach number,

± 0.5 PSI for Stagnation Pressure,

$\pm 0.5\%$ for Stagnation Temperature.

The instrumented panel surface pressure measurements will be within ± 0.5 PSI and the heat transfer coefficients within ± 6 percent. The specimen temperature measurements will be within $\pm 4^{\circ}\text{F}$. Model attitudes will be within ± 0.2 degrees. Deviations to these conditions may be approved by the on-site Douglas Test Representative.

TEST PROCEDURE

This test program will be conducted in the following sequences per the test schedule given in Table 3 and the specimen test environments given in Table 4. Each specimen will be injected into the tunnel flow for the time increment shown in Table 3 or until failure. The injection sequence or length of exposure may be altered at the discretion of the Douglas Test Representative and as necessitated by the facility capabilities. Termination of testing for a specimen or substitution of specimens will be determined by the Douglas representative. The sequence does not include provisions for completing the test over three nights and does not recognize the time constraints for each shift. The AEDC/ARO test engineer will determine how many specimens will be run each night.

1. Paint the grid pattern on the tunnel floor.
2. Obtain photographs of the specimens and grid board specimen photograph (Figure 21).
3. Install the wedge and cabin simulator to the sting and set the wedge angle to the specification of Table 4 for the Mach 2.4 condition. The angle between the wedge and cabin simulator is to be set at 15 degrees.
4. Photograph the grid panel on the tunnel wall through the quartz window in the cabin simulator prior to the test and before a specimen is installed (Figure 22).
5. Install the instrumented panel in the cabin simulator and bolt the cover securely to restrain the panel in the cabin simulator. Connect the instrumentation.
6. Inject the instrumented panel into the tunnel flow for a period of time sufficient to determine pressure distributions and heat transfer rate distributions and record the necessary information for the Mach 2.4 simulation.
7. Reset the wedge and perform the Mach 2.6 and Mach 3.0 tests.
8. Retract and remove the instrumented panel from the cabin simulator.
9. Reset the wedge for the Mach 2.4 position.
10. Prepare the appropriate specimens designated in Table 3 for the thermal paint tests by applying phase-change paint per AEDC/ARO procedures. The temperature rating of the paint will be determined by the Douglas Test Representative after initial reduction of the instrumented panel data. The specimens must be cleaned with water or isopropyl alcohol and dried with a Kaydry prior to painting.
11. Perform the thermal mapping sequence per the techniques specified by the AEDC/ARO for the Mach 2.4 test conditions.
12. Reset the wedge for the Mach 2.4 test simulation per Table 4.

13. Prepare specimens for tunnel injection. Clean the face of the specimen prior to each injection by hand rinsing with clean water and wipe dry with a Kaydry, or equivalent, paper towel. In the event that the water and hand rubbing does not properly dislodge foreign material from the face of the specimen, isopropyl alcohol may be substituted for the water.
14. Install the specimen in the cabin simulator and connect the thermocouples to the hookups.
15. Perform the Mach 2.4 testing by injecting the specimens into the tunnel for the proper time increments as noted in Table 3 and the specifications noted in Table 4.
16. Take in-tunnel grid photos at the beginning and end of each injection. Take intermediate photos at two minute intervals throughout the injection.
17. Take a Schlieren flow field photograph after the airflow has steadied.
18. Use continuous video coverage to observe the specimens during injection.
19. Record thermocouple readings at the rate of three per minute throughout the injection.
20. Retract and cool the specimen to 160°F as measured by the internal thermocouples.
21. Make a visual inspection of the specimen and record observations.
22. Re-inject or replace the specimen as noted in Table 3 or as advised by the Douglas Test Representative.
23. Repeat steps 13 through 22 and complete the Mach 2.4 test effort.
24. Take post-test photographs of the specimens and record the Mach number, specimen serial number, injection time period, and injection number.
25. The primary specimens are to be tested as shown in Table 3 during the first night of testing. Secondary specimens may be substituted

at the discretion of the Douglas Test Representative. Specimens not tested on the first night will be tested on the next night. Termination of tunnel tests for a specimen will be determined by the Douglas Test Representative.

26. Reset the wedge for the Mach 2.6 simulation.
27. Perform the Mach 2.6 thermal mapping, per Table 3 and steps 10 and 11.
28. Perform the Mach 2.6 specimen testing per Tables 3 and 4 and as described above in Steps 13 through 25.
29. Reset the wedge for the Mach 3.0 simulation.
30. Perform the Mach 3.0 thermal mapping per Table 3 and Steps 10 and 11.
31. Perform the Mach 3.0 testing per tables 3 and 4 and as described above in Steps 13 through 25.

DOCUMENTATION AND DATA REDUCTION

The following data shall be provided.

1. Tabulated and plotted longitudinal pressure distribution and lateral pressure distribution (PSIA versus inches) across the face of the instrumented panel for the Mach 2.4, 2.6 and 3.0 test conditions.
2. Tabulated and plotted longitudinal heat transfer distribution and lateral heat transfer distribution ($\text{BTU/FT}^2\text{-Sec-}^\circ\text{R}$ versus inches) across the face of the instrumented panel for the Mach 2.4, 2.6 and 3.0 test conditions.
3. The temperature/time history ($^\circ\text{F}$ versus seconds) for each specimen and injection, including test temperature, pressure and specimen injection time.
4. Schlieren shadowgraph photographs to document a comparison between the predicted shock angle and the actual test conditions.

5. Pre-test and post-test photographs, including pre-test photographic positive, of a grid viewed through the specimen at an angle of incidence of 60 degrees (30 degrees with the line-of-sight). The grid must extend beyond the edge of the specimen. The photographs of the grid will be of a quality such that distortion is clearly defined.
6. Sequential in-tunnel grid photographs with a photographic positive of the first in-tunnel photo. These photographs will allow a comparison to be made of the grid lines between the first and last photo.
7. Post-test photographs to document surface deteriorations.
8. All data will be appropriately labeled with Mach number, specimen serial number, injection period number, and injection time increment.
9. The sequence of photographs showing the time/temperature heating patterns taken during the thermal mapping testing, including heat transfer coefficients versus time frame for the teflon panel.

SECTION III

TEST OPERATION

This section describes the pre-test activities and the operation of the test. It presents the injection sequence, a summary of injections, the specimen exposure times, and a summary of times to complete specific operations. A general description of the test is presented along with a comparison of the test as performed and the test as planned.

PRE-TEST ACTIVITIES

Prior to delivery, the specimens were measured by the vendors for light transmission through the panels and, except for Sierracin, haze levels.

Douglas personnel examined the specimens when received at Douglas and prior to testing at the AEDC. Two of the specimens, GY21 and GY23, were noted as having cracked face plies. The cracks originated at the holes drilled through the face plies. Further investigation revealed that the cracks occurred during fabrication. The Texstar specimens had been marred with scratches and imperfections, and their thicknesses were not constant. The thickness varied from one corner diagonally to the other corner, 0.110 inch for TEX21 and 0.030 inch for TEX21A.

TEST OPERATION

The sequence of tunnel injection for the specimens is shown in Table 5. The first two lines of this table refer to the instrumented panel insertions (IP) and the thermal paint tests for the teflon panel (TP). The remaining data refer to specimen injections. The letter "T", such as 12T for SK21A, refers to a thermal paint insertion. The letter "F", such as 24F for PPG21, refers to a specimen that had been considered to have failed. The total number of injections, 85, does not include Number 15 (aborted early), and Numbers 58 and 59, which were inadvertently skipped. The injection numbers listed in Table 5 were assigned by the AEDC Test Director as the test progressed. A summary of the number of injections is given in Table 6.

TABLE 5. INJECTION SEQUENCE

SPECIMEN	MACH 2.4				MACH 2.6			MACH 3.0	
IP TP	(1) 10 T	11 T			(1) 44 T			(1) 37 T	88 T
SK05 SK06	15(2)	16	17	18	48	49 F		85 F	
SK21 SK21A SK22 SK22A SK23 SK23A	19 12 T 13 T 14 T	20			50 45 T 52 46 T 55 47 T	51 53 54 56		73 75 77	74 76 78
SWU21 SWU22	21 42 T	22			57 43 T	60 61 62		79 80 F	
PPG21 PPG21A PPG22 PPG22A	23 35 F	24 F						81 F	
GY01 GY02 GY03 GY04 GY05	29 31 33	30 32 34			67 69 71	68 F 70 F 72		82 83	
GY21 GY22 GY23 GY24 GY25 GY26	25 36 38 40	26 F 37 F 39 F 41 F			63	64 F		84 F	
TEX21 TEX21A	27	28			65 F			86 F	

NOTES: (1) Injection 1 through 9-instrumented panel.
 (2) Aborted at 27 seconds - no photography.
 (3) T indicates thermal paint injections.
 (4) F indicates specimen failed.

TABLE 6. SUMMARY OF INJECTIONS

	MACH 2.4	MACH 2.6	MACH 3.0	TOTAL
INSTRUMENTED PANEL INJECTIONS	3	2	4	9
THERMAL PAINT INJECTIONS	6	5	2	13
SPECIMEN INJECTIONS	26	23	14	63
TOTAL	35	30	20	85

Table 7 lists the exposure times in seconds for each specimen and the total exposure time at each Mach number in hours.

Table 8 is a summary of test times. It shows the total time to complete each of three groups of tests, instrumented panel, thermal paint, and material, as well as the actual specimen exposure time. It defines the average time required to cool a specimen to 160°F between injections, and the average time taken to replace a specimen. These figures do not include tunnel warm-up time, facility breakdown, or time lost due to other interruptions.

The tunnel test operation commenced with the installation of the instrumented panel to obtain heat transfer and pressure distributions across the panel surface and to provide definition of the test environment. These data were obtained at Mach 3.0, Mach 2.6 and Mach 2.4. Nine injections were made which consumed 3 hours, as shown in Table 8. This time period agrees with the estimated time given in Table 2.

During the first night of testing, the limitations of the facility were observed. It required maximum utilization of the available facility

TABLE 7. SPECIMEN EXPOSURE TIMES

	TIME IN SECONDS									
	MACH 2.4				MACH 2.6				MACH 3.0	
	PER INJECTION			TOTAL	PER INJECTION			TOTAL	PER INJECTION	TOTAL
SK05	314	630	888	1832	319	620		939	202	202
SK06										2034
SK21	301	602		903	320	620		940	35	203
SK21A									238	2081
SK22					301	621	920	1842	38	199
SK22A									237	2079
SK23					319	631		950	38	199
SK23A									237	1187
SWU21	321	620		942	319	621		940	198	198
SWU22					320	620		940	140	140
PPG21	321	621		942						2080
PPG21A										1080
PPG22	312			312					99	99
PPG22A					139			139		942
GY01										99
GY02										312
GY03	300	618		918	341	593		934		139
GY04	312	620		932	320	620		940		934
GY05	322	622		944	320	619		939	201	1857
									201	1133
									201	1145
GY21	319	622		941						
GY22					319	331		650		941
GY23									200	650
GY24	310	409		719					200	200
GY25	320	620		940						719
GY26	319	621		940						940
TEX21	320	622		942					54	54
TEX21A					318			318		996
										318
TOTAL IN HOURS				3.4				2.9		0.6
										6.9

capabilities to obtain and hold the required conditions for simulation of the Mach 2.6 and 3.0 flight environment. That the equipment was at its limits was evident when the morning shut down occurred early to prevent the destruction of an overheated compressor. The remainder of the testing was adversely affected by the tunnel working at its limits. Time needed to accomplish the desired testing was lost due to longer warm-up times, equipment breakdowns, and longer times to cool down and change specimens than estimated.

TABLE 8. SUMMARY OF TEST TIMES

OPERATION	TIME (NOTED)			
	MACH 2.4	MACH 2.6	MACH 3.0	TOTAL
TIME TO COMPLETE INSTRUMENTED PANEL TESTS				3 HR
TIME TO COMPLETE THERMAL PAINT TESTS	2 HR	2 HR	0.5 HR	4.5 HR
TOTAL SPECIMEN EXPOSURE TIME	3.3 HR	2.9 HR	0.6 HR	6.9 HR
TIME TO COMPLETE SPECIMEN TESTS	9 HR	7 HR	3.3 HR	19.3 HR
AVERAGE TIME TO COOL A SPECIMEN BETWEEN INJECTIONS	11 MIN	9 MIN	3 MIN	
AVERAGE TIME TO REPLACE A SPECIMEN	18 MIN	16 MIN	18 MIN	

Note: These times do not include tunnel warm-up, facility shut down or other interruptions.

Thermal mapping, using phase-change paint, was completed on five specimens at Mach 2.4 as shown in Table 5. The teflon panel was injected twice. This operation was limited to five of the nine planned specimens listed in Table 3, because observation did not indicate a significant variation in heating rates between specimens while the tests were being performed. Thermal mapping was performed at Mach 2.6 on five of the nine planned specimens. At Mach 3.0 only the teflon panel was injected. The time required to complete these operations is shown in Table 8 and agrees with the estimated time.

Table 9 is a compilation of the total test as planned and the test as performed. The number of injections required was reduced for the materials tests when it became apparent that the estimated times would not allow sufficient time to complete the tests. The reduction in available injection time was due to the longer time required to cool and replace the specimens (noted in Table 8) and the necessity to shut down the tunnel early due to an overheated compressor. The scheduled number of cycles (5, 10 and 15 minutes for Mach 2.4 and 2.6) was reduced to injections of 5 and 10 minutes. The temperature increase over the last 5 minutes did not warrant the longer injection time. At Mach 2.4, 13 specimens and 26 injections were performed against 12 specimens and 36 injections planned. Six specimens failed. An additional specimen (PPG22) with a glass face ply was tested because of the failure of PPG21.

At Mach 2.6, 12 specimens and 23 injections were performed as opposed to 15 specimens and 45 injections planned. Six specimens were considered to have failed. Six specimens originally planned for Mach 2.6 testing failed during the Mach 2.4 tests.

At Mach 3.0, 11 specimens and 14 injections were completed, compared to 11 specimens and 22 injections planned. To save time, the 1/2 minute scheduled injection was not performed. It became evident that insignificant internal heat was generated during injections of SK21, SK22 and SK23 for 1/2 minute. Five specimens failed during these tests.

To summarize, 24 of the original 27 panels were tested at Mach 2.4, 2.6 and 3.0. Seventeen failed and 7 survived. Three were subjected to thermal paint tests only.

At the beginning of each specimen injection, a shadowgraph of the flow field was taken, utilizing the facilities Schlieren System. Grid line pictures were taken at the rate of five per injection for optical evaluation. Motion pictures were taken at the beginning of each injection for approximately 1/2 to 1 minute. Video movies permitted the test personnel and Douglas representatives to monitor each injection. The

TABLE 9. PLANNED INJECTIONS VERSUS ACTUAL INJECTIONS

TYPE OF TEST	MACH 2.4		MACH 2.6		MACH 3.0	
	PLANNED INJECTIONS	ACTUAL INJECTIONS	PLANNED INJECTIONS	ACTUAL INJECTIONS	PLANNED INJECTIONS	ACTUAL INJECTIONS
INSTRUMENTED PANEL	IP	IP	IP	IP	IP	IP
THERMAL PAINT TESTS	TP SK21A SK22A SK23A SWU21 SWU22 PPG22A GY21 TEX21A	TP SK21A SK22A SK23A SWU22	TP SK21A SK22A SK23A PPG21A PPG22A TEX21A	TP SK21A SK22A SK23A SWU22	TP SK23A PPG21A PPG22A	TP
MATERIAL TESTS	(2) SK05 SK21 SWU21 PPG21 GY03 GY04 GY05 GY21 GY24 GY25 GY26 TEX21	(3) SK05 SK21 SWU21 PPG21 F PPG22 F GY03 GY04 GY05 GY21 F GY24 F GY25 F GY26 F TEX21	(2) SK06 SK21 SK22 SK23 SWU21 SWU22 PPG21 PPG22 GY21 GY22 GY23 GY24 GY25 GY26 TEX21	(4) SK06 F SK21 SK22 SK23 SWU21 SWU22 PPG22A F GY22 F GY01 F GY02 F GY03 TEX21A F	(5) SK21 SK22 SK23 SWU21 SWU22 PPG21 PPG22 GY21 GY22 GY23 GY26	(6) SK05 F SK21 SK22 SK23 SWU21 SWU22 F PPG21A F GY23 F GY04 GY05 TEX21 F
TOTAL SPECIMENS FOR MAT'L TEST	12	13	15	12	11	11

- NOTES: (1) F indicates a specimen failure.
 (2) Three injections were planned at increments of 5, 10 and 15 minutes.
 (3) Two injections were completed at increments of 5 and 10 minutes except SK05 was injected as planned.
 (4) Two injections were completed at 5 and 10 minute increments except SK22 was injected as planned.
 (5) Two injections of 1/2 and 3 minutes were planned.
 (6) One injection of 3 minutes was completed except SK21, SK22 and SK23 were injected as planned.

movie camera was activated to record any unusual reactions observed on the video systems.

Temperatures were recorded to provide temperature/time histories for the instrumented specimens. These results are shown in Section VII. Many thermocouples failed to adhere to the specimen surface. Table 10 lists the specimens that lost their thermocouples.

TALBE 10. THERMOCOUPLE PEEL-OFF

SPECIMEN	FACE PLY MATERIAL	BONDING AGENT(2)	PEEL-OFF
SK05	Acrylic	M-Bond-600	No
SK06		M-Bond 600	No
SK21		PS-18	Yes
SK22		PS-18	Yes, Aft Only
SWU21		PS-18	Yes
SWU22		PS-18	Yes, Aft Only
GY01(1)		M-Bond 600	No
GY21		PS-18	Yes
GY22		PS-18	Yes
GY23		PS-18	Yes
GY24		PS-18	Yes
GY25		PS-18	Yes
GY26		PS-18	Yes
GY02(1)	Urethane	M-Bond 600	No
GY03(1)		M-Bond 600	No
GY04(1)		M-Bond 600	No
GY05(1)		M-Bond 600	No
SK23	Glass	M-Bond 600	Yes
PPG21		M-Bond 600	Yes
PPG21A		M-Bond 600	Yes
PPG22		M-Bond 600	Yes
PPG22A		M-Bond 600	Yes

- Notes: (1) Previously tested per Reference 1.
 (2) M-Bond 600 is manufactured by Micro-Measurements Products.
 PS-18 is an acrylic based cement.

The specimens were supported in the cabin simulator. After each injection, the specimen was cooled to 160°F or less, as measured by the thermocouples, and a visual inspection was made. Cooling was accomplished on the front of the specimen by venting the ambient air into the tunnel and over the specimen. At the same time, cooling was accomplished on the back side with the cabin simulator air. The time to cool the specimens to 160°F varied from 3 to 11 minutes. The visual inspection included impact by tunnel debris, observable increase in haze, condition of the edge retainer, face ply damage, interlayer bubbling, and delamination of the face ply. Most of the failed specimens had sustained damage that could be observed through the video monitoring system during injection.

Selected specimens were returned to the vendors, after completion of the tests at AEDC, for post-test light transmission and haze measurement.

SUMMARY

A pre-test inspection revealed that the face ply on two specimens were cracked.

A total of 85 injections were made; nine were instrumented panel injections, 13 were thermal paint injections, and 63 were specimen injections.

The number of specimen tunnel injections was reduced when it became apparent during the testing that the estimated times would not allow sufficient time to complete the scheduled injections.

Twenty-four of the original 27 panels were tested at Mach 2.4, 2.6 and 3.0. Seventeen failed and 7 survived.

Many thermocouples failed to adhere to the surface of the specimens during tunnel exposure.

SECTION IV TEST ENVIRONMENT

Since the purpose of this test program was to determine the performance of various candidate windshield materials at simulated flight conditions, it was of paramount importance to produce a test environment that was similar to flight. The data presented here, to correlate the predicted test environment against the actual test environment, includes a summary of the tunnel conditions, shadowgraph photographs, and data from instrumented panel injections. Additional information concerning test correlation, data acquisition, data reduction and the uncertainty of measurements may be found in Reference 2.

TUNNEL CONDITIONS

Table 11, a summary of pertinent tunnel data, shows actual values compared to predicted values for the test environment.

The altitudes selected for this test were based on the limitations of the tunnel. Lower altitudes would have been simulated if possible. The actual altitudes were about 1 percent lower than predicted. These reductions were affected, in part, by the lower free stream Mach number of 5.95.

The wedge angles were slightly higher than planned. This variation resulted in a reduction of air flow across the specimen and, combined with the slight reduction in free stream tunnel flow, reduced the windshield Mach number by about 1 percent, as shown in Table 11.

Adiabatic wall temperature is dependent on free stream Mach number and stagnation temperature. It has a significant influence on the windshield heat-up rate and final temperature. The wall temperatures shown in Table 11 were calculated for the conditions that existed during the injections of the instrumented panel (Injections 9, 5 and 1) for the determination

TABLE 11. TEST ENVIRONMENT - ACTUAL VERSUS PREDICTED

	MACH 2.4		MACH 2.6		MACH 3.0	
	PLANNED	ACTUAL	PLANNED	ACTUAL	PLANNED	ACTUAL
ALTITUDE (FEET)	45,200	44,400(1)	52,900	51,800(2)	64,800	64,000(3)
WEDGE ANGLE (DEGREES)	33.2	33.3	31.5	31.6	28.3	28.4
MACH NUMBER - FREE STREAM	6	5.95	6	5.95	6	5.95
MACH NUMBER - WINDSHIELD	1.47	1.46	1.61	1.59	1.89	1.87
STAGNATION TEMPERATURE (°F)	380	380/390	458	450/460	632	630/640
STAGNATION PRESSURE (PSIA)	280	278/282	225	224/227	170	169/172
ADIABATIC WALL TEMPERATURE (°F)	357	353(4)	431	409(5)	597	586(6)
APPROACH PRESSURE (PSIA)	3.75	3.91(1)	2.73	2.87(2)	1.74	1.81(3)
CABIN TEMPERATURE (°F)	75	71/104	75	82/106	75	70/95
CABIN PRESSURE (PSIA)	7.12	7.00/7.44	6.47	6.46/6.68	5.83	5.84/5.91
EXPOSURE TIME (MINUTES)	5, 10, 15	5, 10	5, 10, 15	5, 10	1/2, 3	3

NOTES: (1) Based on Injection 8 ($P_0 = 277$ PSIA)(2) Based on Injection 6 ($P_0 = 225$ PSIA)(3) Based on Injection 3 ($P_0 = 171$ PSIA)(4) Based on Injection 9 ($T_0 = 390^\circ\text{F}$, $R = 0.95$)(5) Based on Injection 5 ($T_0 = 449^\circ\text{F}$, $R = 0.95$)(6) Based on Injection 1 ($T_0 = 634^\circ\text{F}$, $R = 0.95$)

(7) Injections 1 through 9 were instrumented panel injections.

of the heat transfer distributions. A recovery factor of 0.95 was used. The stagnation temperatures shown in Table 11 are for the specimen injections, and were slightly different than for the instrumented panel injections.

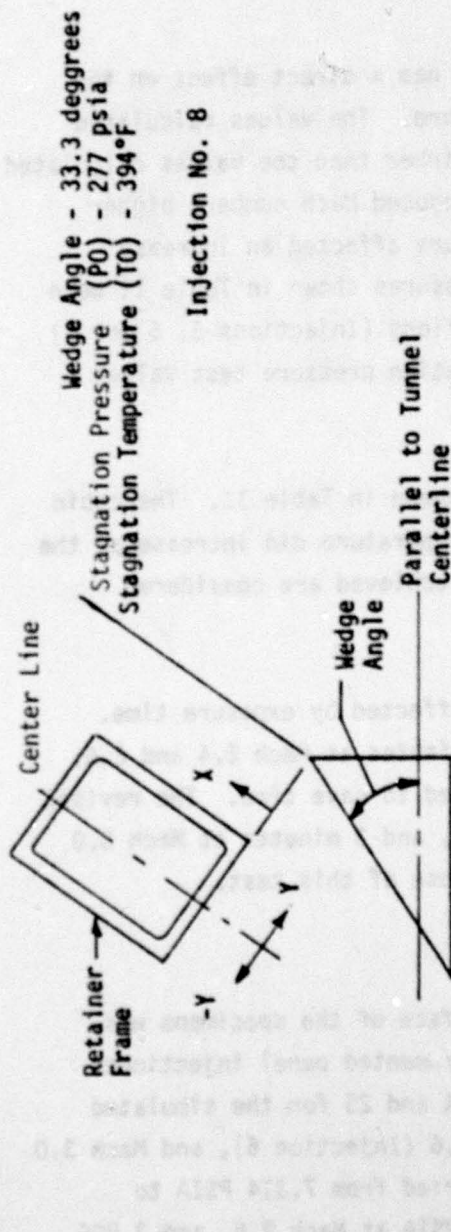
Approach pressure (see Figure 19), also has a direct effect on the wind-shield heat-up rate and final temperature. The values calculated from the test results were 4 to 5 percent higher than the values calculated for the predicted tunnel conditions. The reduced Mach number, higher wedge angle, and increased stagnation pressure affected an increase in the approach pressure. The approach pressures shown in Table 11 were calculated for the instrumented panel injections (Injections 8, 6 and 3) for pressure distribution. Since the stagnation pressure test values vary, the approach pressure would also vary.

Variations in the cabin conditions are shown in Table 11. The cabin pressure was fairly steady, but the cabin temperature did increase as the injection time increased. The temperatures achieved are considered acceptable for the purposes of this test.

Heat-up rate and final temperature are affected by exposure time. The planned exposure times of 5, 10 and 15 minutes at Mach 2.4 and 2.6, and 1/2 and 3 minutes at Mach 3.0 were revised to save time. The revised time of 5 and 10 minutes at Mach 2.4 and 2.6, and 3 minutes at Mach 3.0 are considered to be reasonable for the purpose of this test.

PRESSURE DISTRIBUTION

The pressure distribution across the surface of the specimens was provided by the data collected from the instrumented panel injections. These results are presented in Figures 23, 24 and 25 for the simulated conditions of Mach 2.4 (Injection 8), Mach 2.6 (Injection 6), and Mach 3.0 (Injections 2 and 4). The test pressures varied from 7.314 PSIA to 4.908 PSIA at Mach 2.4, 5.653 PSIA to 3.895 PSIA at Mach 2.6, and 3.890 PSIA to 2.723 PSIA at Mach 3.0. The test pressures were lower than the



Injection No. 8

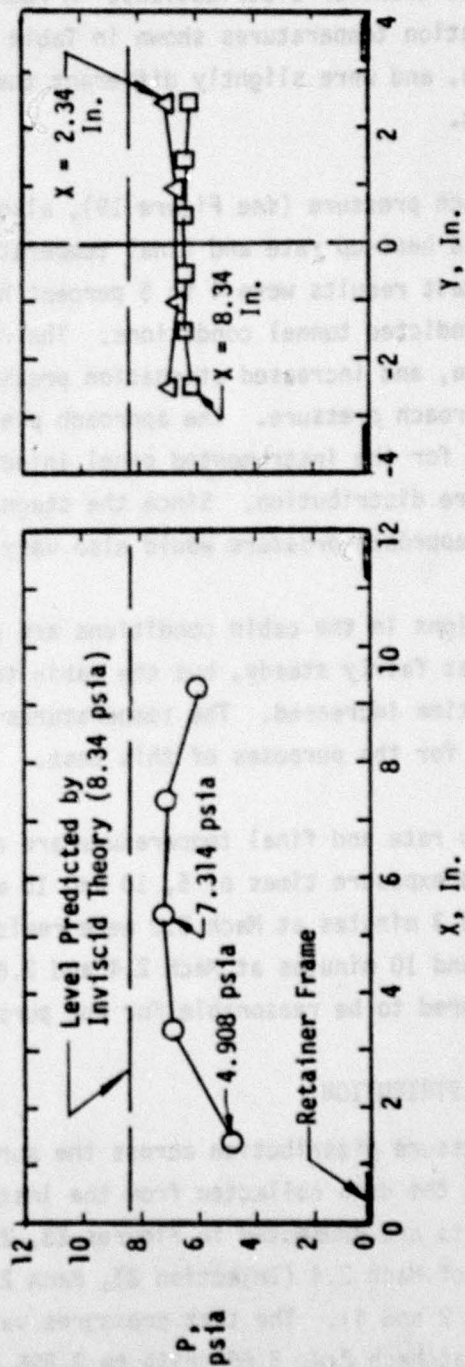


Figure 23. Pressure Distribution at Mach 2.4.

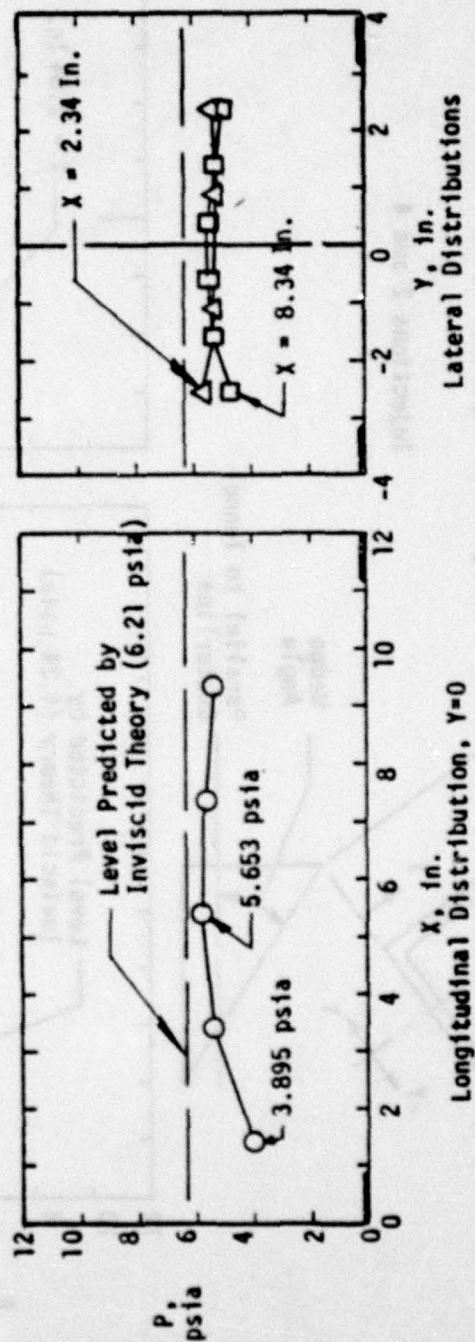
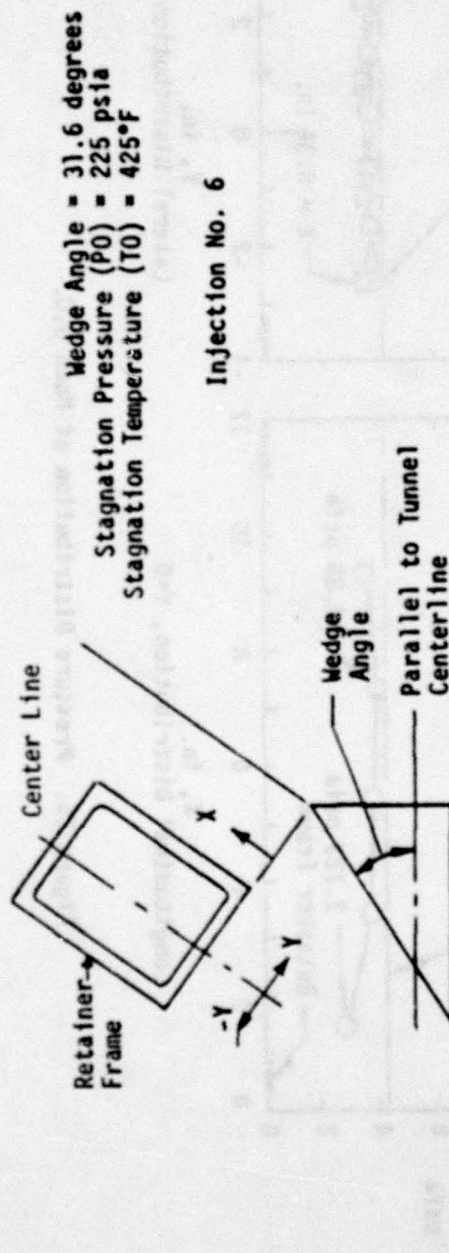


Figure 24. Pressure Distribution at Mach 2.6

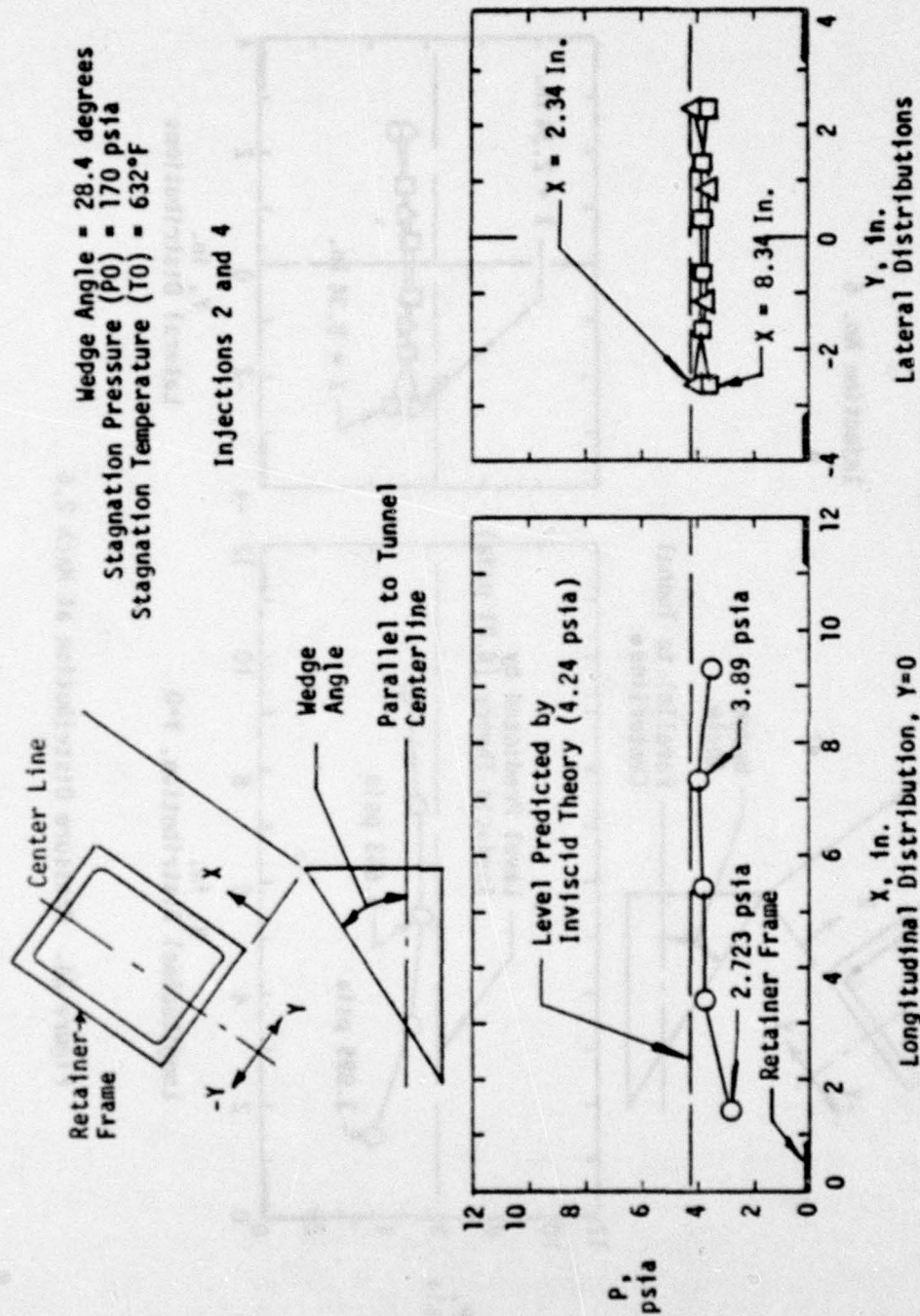


Figure 25. Pressure Distribution at Mach 3.0.

predicted pressure for all conditions: 12 percent lower at Mach 2.4, 9 percent lower at Mach 2.6 and 8 percent lower at Mach 3.0.

Figure 26 is presented to show the locations of the pressure orifices and the heat transfer rate gages located on the surface of the instrumented panel.

HEAT TRANSFER RATE DISTRIBUTION

The distribution of heat transfer rate across the surface of the specimens was provided by the data collected from the instrumented panel injections. These results are presented in Figures 27, 28 and 29 for the simulated conditions of Mach 2.4 (Injections 7 and 9), Mach 2.6 (Injection 5), and Mach 3.0 (Injections 1 and 3). The figures show that the heat transfer distributions were reasonably flat. The values varied from 69.5 to 91.1 BTU/ft²-hr-°R for the Mach 2.4 condition, 61.6 to 75.1 BTU/ft²-hr-°R for the Mach 2.6 condition, and 48.9 to 58.6 BTU/ft²-hr-°R for the Mach 3.0 condition. A detailed explanation of the method used to calculate these data is given in Reference 8. The values of the heat transfer distributions are higher than would be calculated for the flight conditions. This is due mainly to the shorter distance from the stagnation point to the windshield on the tunnel model than on an aircraft.

SHADOWGRAPH PHOTOS

Typical shadowgraph photos are presented in Figures 30 to illustrate the shock interactions and the flow field conditions that existed on the windshield specimens in the tunnel. A shock wave that emanated from the forward edge of the wedge is clearly visible, as are two waves that originated at the forward edge of the cabin simulator frame. The intersection of these waves produced an interference shock wave that impacted the test specimen and rebounded. The imprint of this shock wave on the specimen is clearly visible in the thermal paint photos shown later in Section VII. The interference shock was possibly the cause of the variation in pressure from front to back across the specimen surface. The longer nose to windshield distance on an aircraft would not produce such an interference shock.

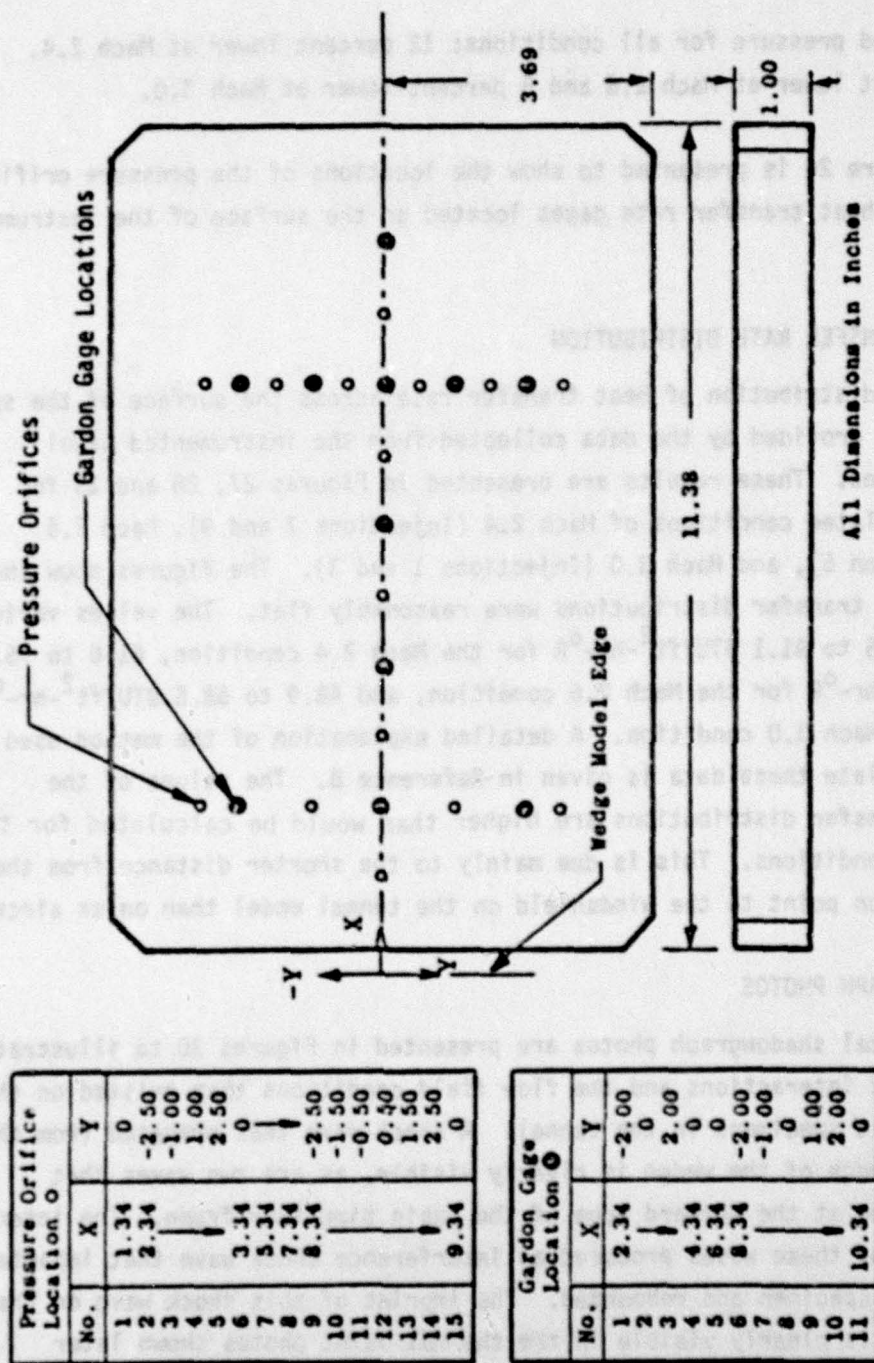
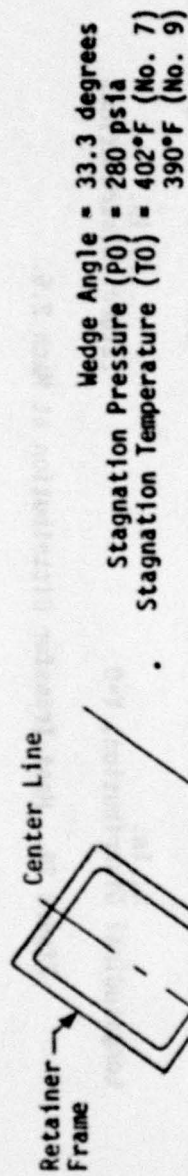


Figure 26. Instrumented Panel Showing Orifice and Gage Locations.



Injection 7 and 9

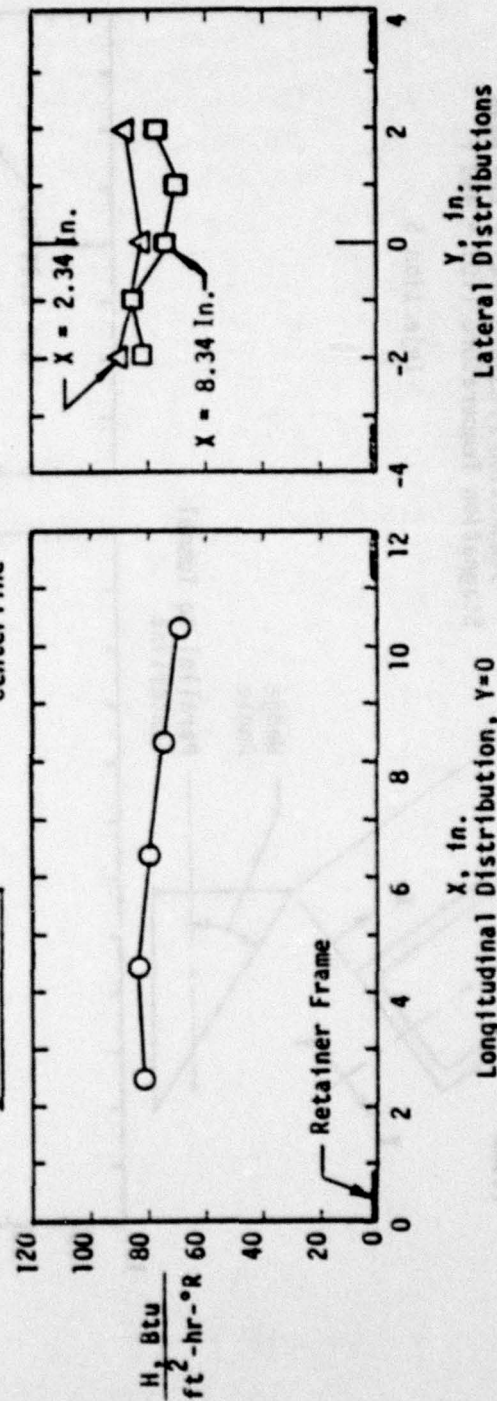


Figure 27. Heat Transfer Distribution at Mach 2.4.

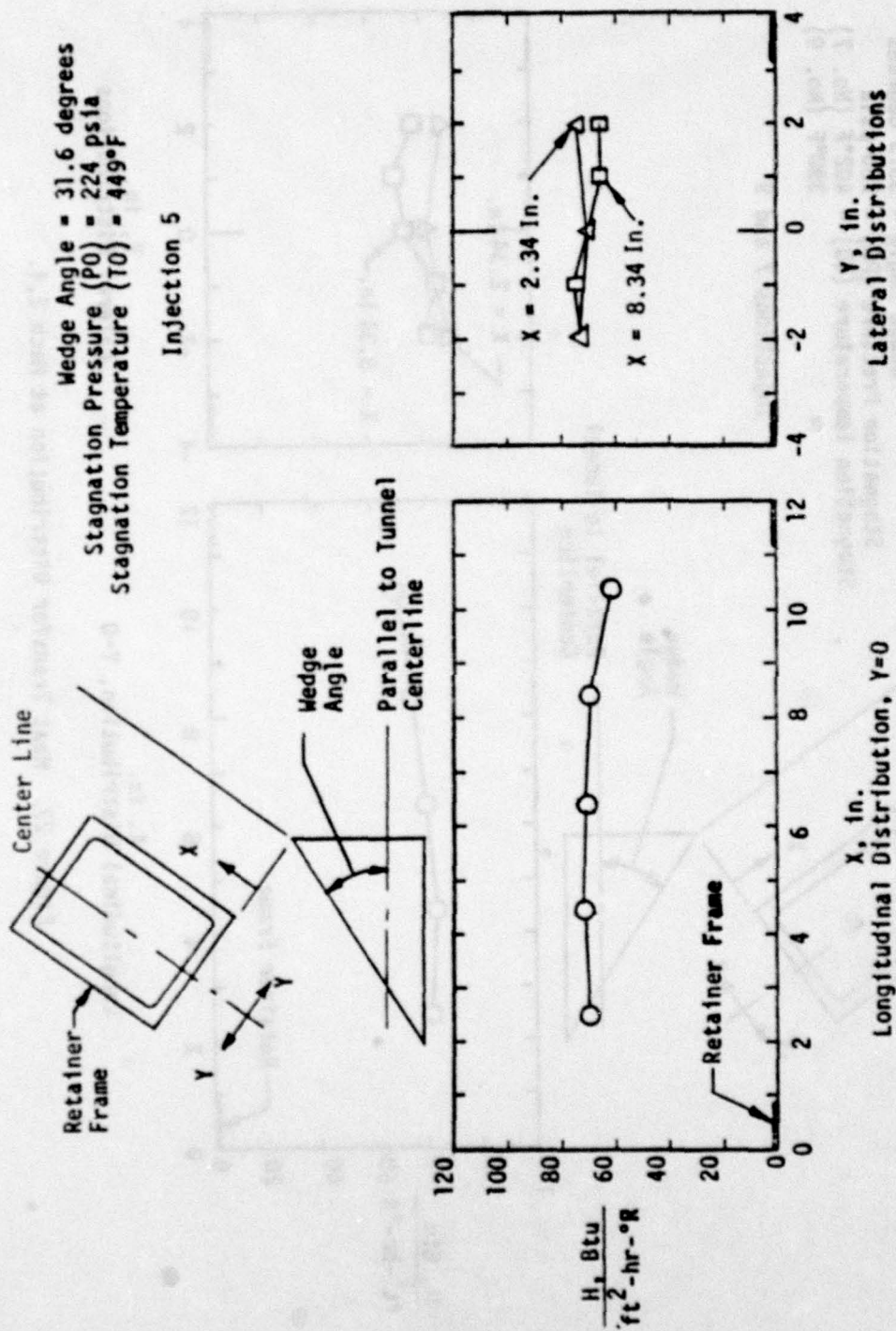


Figure 28. Heat Transfer Distribution at Mach 2.6.

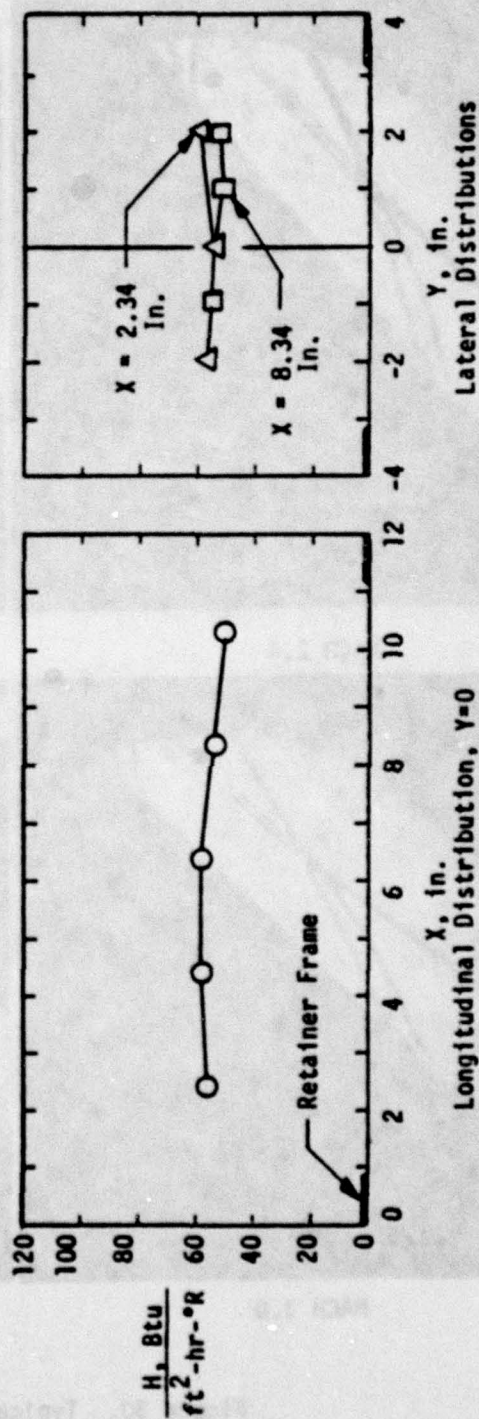
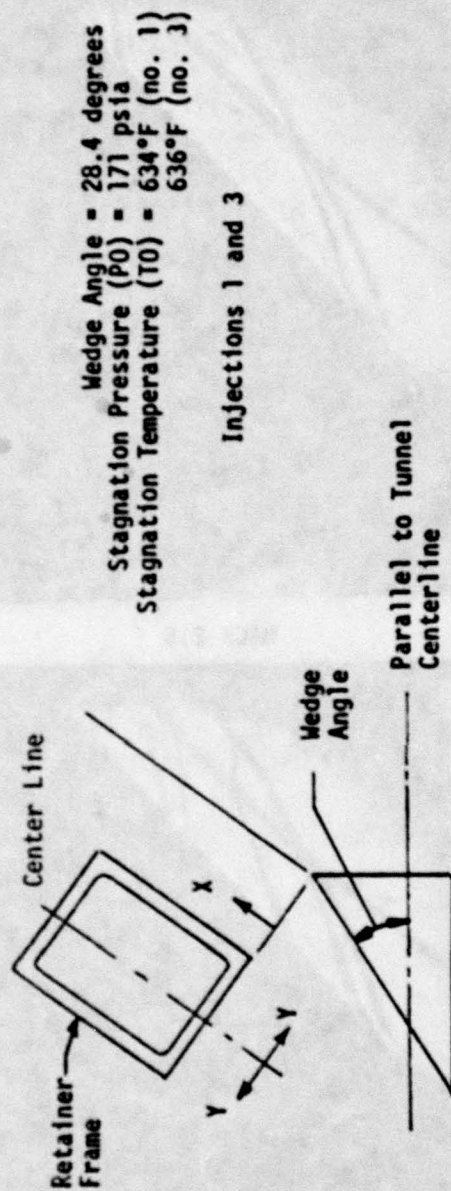


Figure 29. Heat Transfer Distribution at Mach 3.0.



MACH 2.4



MACH 2.6



MACH 3.0



MACH 2.6 (SWU22)

Figure 30. Typical Shadowgraphs.

SUMMARY

The altitudes selected for these tests were based on the limitations of the tunnel. Lower altitudes would have been simulated if possible. The actual test altitudes were less than planned by about one percent.

Tunnel test conditions are summarized as follows:

- a. Wedge angles were slightly higher than planned and resulted in reduced velocities.
- b. Stagnation temperatures varied by up to 10°F from planned temperatures.
- c. Stagnation pressures varied by 2 PSI maximum.
- d. Approach pressures were 4 to 5 percent higher than planned.
- e. Cabin temperatures climbed steadily as injection time increased.
- f. Specimen exposure times were less than planned due to a decrease in the number of injections per specimen.
- g. Pressure distribution across the instrumented panel was lower than planned and varied along the length of the panel.
- h. Heat transfer distribution, according to the instrumented panel data, was reasonably flat.
- i. The shadowgraph photos indicated the existence of an interference shock wave that impacted each test specimen near the aft edge, unlike real aircraft which have a longer nose to windshield dimension.

The overall results of this test indicated that the attempt to simulate a real flight environment was successful within the limits of the test facility and hardware.

SECTION V
MATERIALS EVALUATION

Windshield/canopy materials for supersonic aircraft must have the capability to survive the effect of a high-speed environment within the time frame of the aircraft operating conditions. A goal of this test program was to determine the survivability limits of materials selected for potential use as aircraft windshields. These limits would be established by subjecting the materials to simulated flight environments up to Mach 3.0. The effect of the test environment on these materials is described in this section.

Twenty-four of 27 specimens were tested for material survivability, three specimens were tested exclusively as thermal paint tests, and one specimen was tested for material and survivability and thermal paint data. Table 12 is a summary of the tested specimens. Fourteen specimens were tested at one Mach number simulation, eight were tested at two Mach number simulations, and two specimens (SK21 and SWU21) were tested at the three conditions of Mach 2.4, 2.6 and 3.0. Seven of 13 specimens survived the Mach 2.4 exposure, 6 of 12 specimens survived the Mach 2.6 exposure and 6 of 11 specimens survived the Mach 3.0 exposure. Seven specimens survived the entire test. The thermal paint tests are discussed in Section VII. A specimen was considered to have failed if it experienced delamination or interlayer bubbling.

To facilitate this evaluation the 24 specimens have been divided into four groups. The first three groups are laminated specimens and the fourth group is monolithic. The groups are as follows:

- Laminated - Acrylic Face Ply
 - No edge attachments
 - With edge attachments
 - Face ply cut back from edge
 - Face ply extended to edge

NOT
PRECEDING PAGE BLANK - FILMED

TABLE 12. SUMMARY OF TESTED SPECIMENS

	MACH 2.4	MACH 2.6	MACH 3.0
THERMAL PAINT TESTS	TEFLON PANEL SK21A SK22A SK23A SWU22	TEFLON PANEL SK21A SK22A SK23A SWU22	TEFLON PANEL
TOTAL	5	5	1
MATERIAL TESTS	SK05		SK05 F
	SK21	SK06 F SK21 SK22 SK23	SK21 S SK22 S SK23 S
	SWU21	SWU21 SWU22	SWU21 S SWU22 F
	PPG21 F PPG22 F		PPG21A F
		PPG22A F	
	GY03 GY04 GY05	GY01 F GY02 F GY03 S	GY04 S GY05 S
	GY21 F GY24 F GY25 F GY26 F	GY22 F	GY23 F
	TEX21	TEX21A F	TEX21 F
TOTAL	13 (6 Failed)	12 (6 Failed)	11 (5 Failed)

NOTE: F indicates specimen failed.
S indicates specimen survived entire test

- Laminated - Urethane Face Ply, No Edge Attachments
- Laminated - Glass Face Ply, With Edge Attachments
- Monolithic Polycarbonate, No Edge Attachments.

The specimens with the acrylic face ply are subdivided into specimens without edge attachments and those with edge attachments. The specimens with edge attachments are divided into three categories: those with the face ply cut back, therefore undrilled, those with the face ply extended to the edge of the part, rabbeted and drilled, and those with a face ply extended to the edge of the part and drilled. The specimens with the urethane face ply and the monolithic specimens do not have edge attachments. The specimens with the glass face ply have edge attachments, but the fasteners are through the edge frame and structural plies.

Each group of specimens is described by a table that summarizes the material damage, lists the face ply and interlayer thickness, notes the test conditions, and records edge deformation.

Edge deformation refers to a step in the face ply material around its perimeter caused by expansion of the unclamped material in the center of the specimen. The edges of the specimen are restrained by a cover that clamps the specimen against the pressure seal and holds the specimen in the cabin simulator. Slight edge deformation refers to a step less than 0.01-inch. A "Yes" notation refers to a step larger than 0.01-inch. The maximum step found on any specimen was approximately 0.06-inch.

LAMINATED - ACRYLIC FACE PLY, NO EDGE ATTACHMENTS

Three laminated specimens are included in this category, SK05, SK06 and GY01. These specimens had an acrylic face ply, silicone or urethane interlayer, and a polycarbonate structural ply (Figures 3 and 4). No edge attachments were simulated.

Table 13 presents a summary of the test results. As noted, these specimens were designed for a previous test (Reference 1), but only

GY01 was tested. SK06 and GY01 were previously subjected to a temperature of 250°F as part of an abrasion test (Reference 9). These three specimens sustained delamination of the face ply from the interlayer during the last seconds of tunnel injection and were considered to have failed. Specimen SK05 survived Mach 2.4 test but failed at Mach 3.0. Specimen SK06 and GY01 failed at Mach 2.6. The delamination of SK06 began in the area of the imbedded thermocouple at Mach 2.6. The delamination of SK05, Figure 31, and GY01, Figure 32, began near the aft edge and spread forward. The direction of air flow in these figures was left to right and aft edge is at the right side of the figure. The polycarbonate along the aft edge of both specimens bubbled and protruded about 0.10-inch. The material expanded until it contacted the forward face of the simulator cover (Figure 13, Page 19).

The three specimens sustained face ply deformation along the edges.

TABLE 13. POST-TEST SPECIMEN DESCRIPTION - ACRYLIC FACE PLY, NO EDGE ATTACHMENTS

SPECIMEN FACE PLY AND INTERLAYER	EXPOSURE TIME (MIN)			DESCRIPTION OF SPECIMEN DAMAGE	EDGE DEFOR- MATION
	MACH NO.				
	2.4	2.6	3.0		
SK05 0.030 A 0.100 S	5			No Change	Slight
	10			No Change	
	15			No Change	
			3	Face Ply Delaminated at End of Injection - 4 In. Dia x 1 In. High Bubble.	
SK06 0.080 A 0.100 S		5		No Change	Yes
		10		Face Ply Delaminated Under Thermocouple at End of Injection - 1 In. Diameter Bubble. Polycarbonate Bubbled and Deformed Along Aft Edge.	
GY01 0.100 A 0.040 U		5		No Change	Yes
		10		Severe Delamination of Face Ply Occurred at End of 10-Minute Injection - One 4 x 6 In. and two 1.5 In. Bubbles Aft End. Polycarbonate Bubbled and Deformed at Aft End.	

NOTES: (1) A = Acrylic face ply, S = Silicone interlayer, U = Urethane interlayer.

(2) GY01 was previously tested (Reference 1) for 20 minutes at Mach 2.0 and 10 minutes at Mach 2.2. No damage was reported.

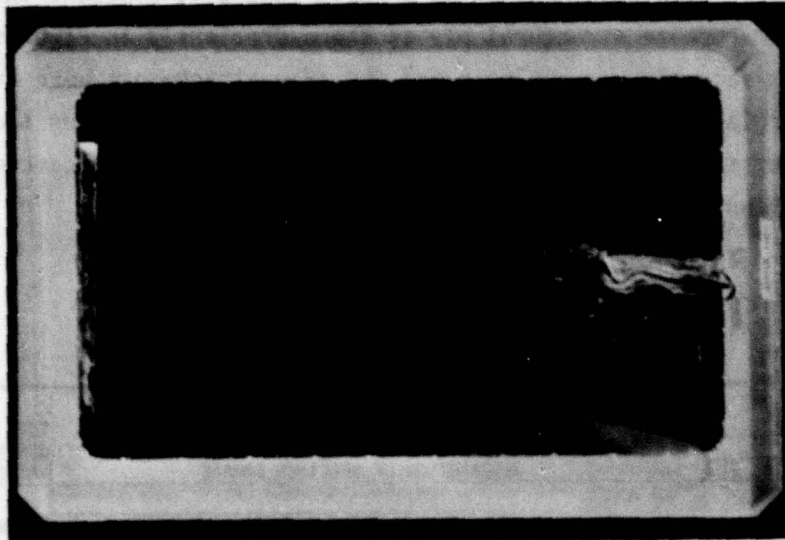


Figure 31. Post-Test Photo of Specimen SK05.



Figure 32. Post-Test Photo of Specimen GY01.

LAMINATED - ACRYLIC FACE PLY CUT BACK, EDGE ATTACHMENTS

Four laminated specimens are included in this category, SK21, SK22, SWU21, and SWU22. Each specimen has an acrylic face ply, silicone interlayer, and polycarbonate structural ply as shown previously in Figures 5 through 8. The face ply was cut back and the edge attachments were installed through a fiberglass spacer and the structural ply. Each specimen had a unique method of sealing the edge of the face ply. A post-test damage appraisal is shown in Table 14.

TABLE 14. POST-TEST SPECIMEN DESCRIPTION - ACRYLIC FACE PLY CUT BACK, EDGE ATTACHMENTS

SPECIMEN FACE PLY AND INTERLAYER	EXPOSURE TIME (MIN)			DESCRIPTION OF SPECIMEN DAMAGE	EDGE DEFOR- MATION
	PACH NO.				
	2.4	2.6	3.0		
SK21 0.188 A 0.120 S	5			No Change	Slight
	10			Discoloration of unstream surface of groove sealant	
		5		No Change	
		10		Further discoloration of groove sealant. Fiberglass adhesive melted along aft edge.	
			1/2	No Change	
			3	Separation of groove sealant from face ply along left side of aft edge.	
SK22 0.188 A 0.120 S		5		No Change	Yes
		10		Erosion under retainer, aft end.	
		15		Further erosion under retainer. Polycarbonate bubbled along aft edge. Fiberglass adhesive melted. Retainer pried up 0.05 inch.	
			1/2	No Change	
			3	Further erosion under retainer. Retainer pried up 0.10 inch.	
SWU21 0.188 A 0.120 S	5			Discoloration and erosion of groove sealant.	Slight
	10			Further discoloration.	
		5		No Change.	
		10		Further discoloration and erosion.	
			3	Further erosion of groove sealant.	
SWU22 0.188 A 0.120 S		5		No Change	Slight
		10		Delamination of face ply - 3 inch diameter spot	
			2	Face ply delamination - 3 inch diameter bubble along aft edge.	

NOTES: A = Acrylic Face Ply, S = Silicone Interlayer.

Specimen SK21, Figure 33, was tested at three Mach numbers. The groove sealant became discolored during the Mach 2.4 injection and the discoloring continued during subsequent injections. The reddish discoloration was removed easily from the sealant by lightly scraping and appears to be residue from the fiberglass spacer at the forward edge. The groove sealant separated from the face ply along the aft side during the final injection. The sealant remained pliable. Air flow was from left to right in the figure.

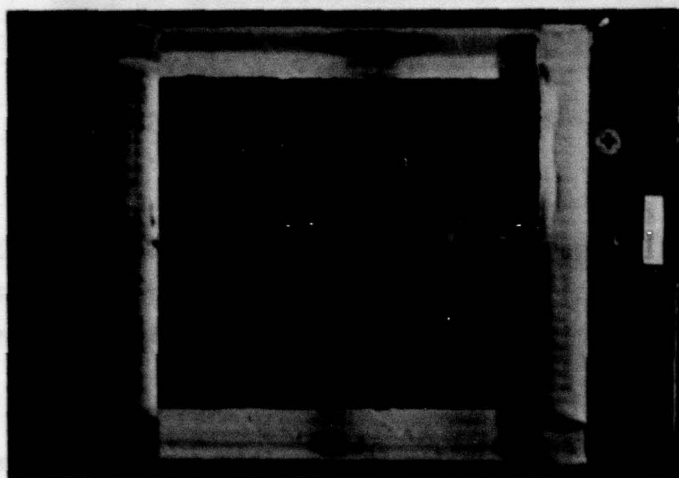


Figure 33. Post-Test Photo of Specimen SK21.

Specimen SK22, Figure 34, was tested at Mach 2.6 and Mach 3.0. This specimen was damaged by erosion of the adhesive under the aft steel retainer. The aft edge of the polycarbonate experienced severe bubbling and deformation.

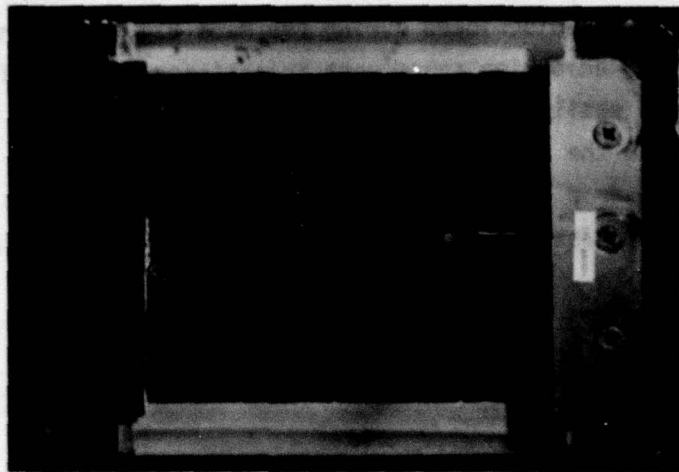


Figure 34. Post-Test Photo of Specimen SK22.

Specimen SWU21, Figure 35, was tested at Mach 2.4, 2.6 and 3.0. This specimen sustained erosion and discoloration of the groove sealant. The discoloration appeared to be residue from the fiberglass. The sealant remained pliable.

Specimen SWU22, is shown in Figure 36. This specimen suffered delamination during its second injection at Mach 2.6. The delamination began in the area of the imbedded thermocouple. No erosion occurred under the fiberglass retainer.

All four specimens experienced face ply deformation at the sides due to the restraining cover.

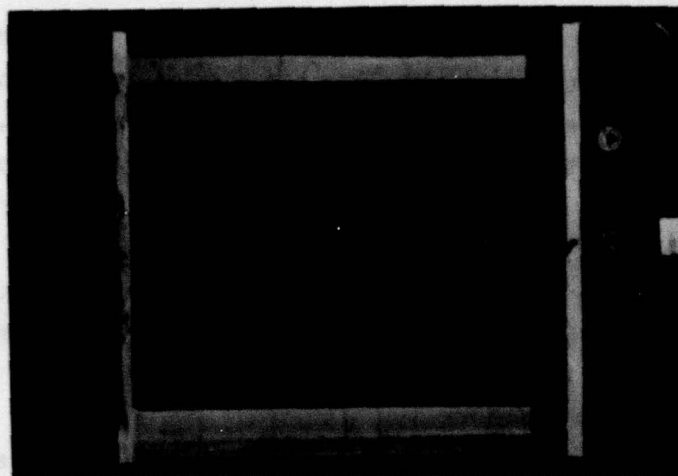


Figure 35. Post-Test Photo of Specimen SWU21.

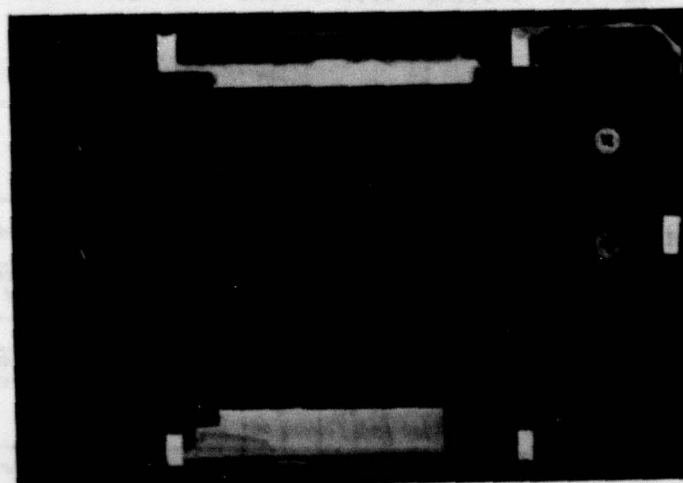


Figure 36. Post-Test Photo of Specimen SWU22.

LAMINATED - ACRYLIC FACE PLY, RABBETED AND DRILLED

This group of nine-ply specimens, GY21, GY22 and GY23 are described previously in Figures 11 and 12. They had acrylic face plies, silicone or urethane interlayer, three polycarbonate structural plies, and an inner acrylic ply. The exterior acrylic face ply extended to the end of the panel and was rabbeted to accept a fiberglass frame around the edges. Three screws and bushings were installed at each end through the face ply, and twelve aluminum spacers were installed around the perimeter to prevent compression of the interlayers. These spacers were filled with sealant.

An appraisal of the damage to these specimens is contained in Table 15.

TABLE 15. POST-TEST SPECIMEN DESCRIPTION - ACRYLIC FACE PLY RABBETED AND DRILLED

SPECIMEN FACE PLY AND INTERLAYER	EXPOSURE TIME (MIN)			DESCRIPTION OF SPECIMEN DAMAGE
	MACH NO.			
	2.4	2.6	3.0	
GY21 0.120 A 0.100 S	5			Face ply was cracked in two places during fabrication Cracks widened to about 0.05 in.
	10			Cracks widened to about 0.15 in. and progressed through interlayer. Face ply delamination across 80% of surface.
GY22 0.120 A 0.100 U		5		No Change
		6		Scalloped section of face ply ruptured along aft edge. Delamination of face ply started at crack and progressed swiftly across most of surface. Bushings melted and flowed out around screws.
GY23 0.180 A 0.100 S			3	Holes burnt through scalloped edges around perimeter. Bushings melted and flowed out around screws. Face ply surface very rough.

NOTES: A = Acrylic Face Ply
S = Silicone Interlayer
U = Urethane Interlayer

The acrylic face ply of GY21, shown in Figure 37, had been cracked in two places during fabrication. These cracks expanded during the Mach 2.4 tunnel injection and precipitated face ply delamination.

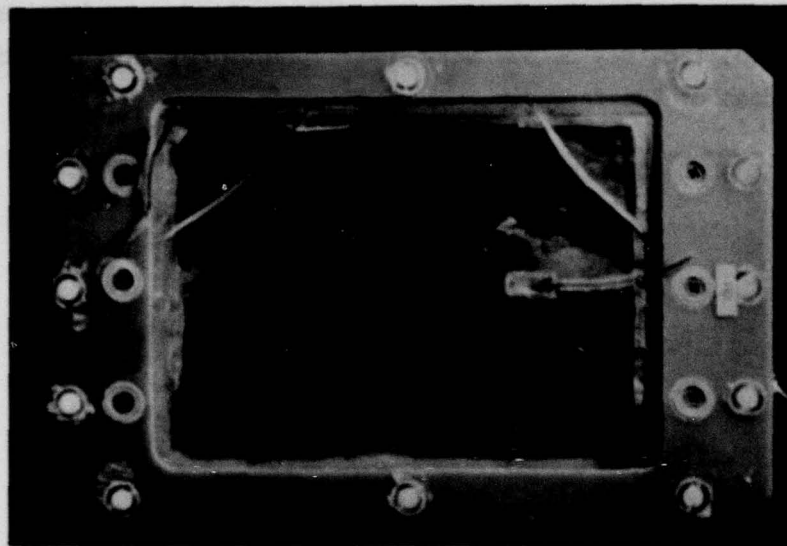


Figure 37. Post-Test Photo of Specimen GY21.

The rabbeted area of GY22, Figure 38, ruptured along the aft edge during the Mach 2.6 exposure and exposed the interlayer. Face ply delamination spread across most of the surface. The fiberglass filled polycarbonate bushings (part of the edge attachment system) melted and flowed around the screws.

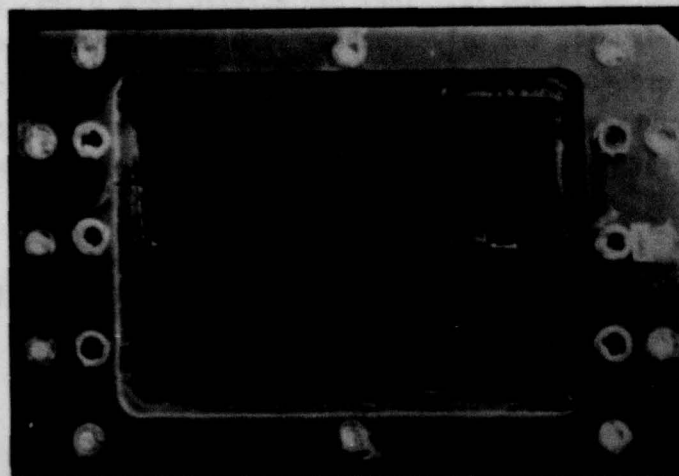


Figure 38. Post-Test Photo of Specimen GY22.

GY23, Figure 39, reacted similarly to GY22. Holes were burned in the rabbeted area of the face ply and the bushings melted during a Mach 3.0 exposure. This specimen also had a cracked face ply due to fabrication procedures. The face ply became very rough. Delamination occurred only around the edges of the face ply.

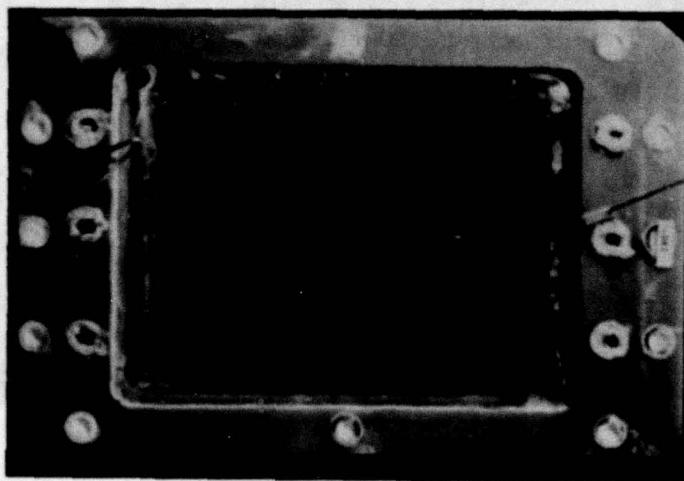


Figure 39. Post-Test Photo of Specimen GY23.

LAMINATED - ACRYLIC FACE PLY, DRILLED

This group of seven ply specimens, GY24, GY25 and GY26, are described previously in Figures 11 and 12. They had acrylic face plies, urethane or silicone interlayers, two polycarbonate structural plies, and an acrylic inner ply. The exterior acrylic face ply extended to the edge of the part. The edge attachment screws and bushings, as well as the peripheral spacers (to prevent interlayer crushing), were installed through the face ply.

An appraisal of these damaged specimens is presented in Table 16.

TABLE 16. POST-TEST DESCRIPTION - ACRYLIC FACE PLY DRILLED

SPECIMEN FACE PLY AND INTERLAYER	EXPOSURE TIME (MIN)			DESCRIPTION OF SPECIMEN DAMAGE	EDGE DEFOR- MATION
	MACH NO.				
	2.4	2.6	3.0		
GY24 0.120 A 0.040 U	5			Delamination rings around forward bolts.	Slight
	7			Face ply delaminated and 25% of the acrylic broke off and separated from the specimen. The face pulled in about 0.06 inch along the edges. The fastener c'sink expanded to about 0.80 inch.	
GY25 0.120 A 0.040 S	5			Slight delamination around thermocouple wires.	Yes
	10			Face ply delamination began at aft bolts and affected 25% of surface.	
GY26 0.180 A 0.040 U	5			No Change.	Slight
	10			Face ply delamination - 3 inch diameter bubble. Small delamination rings around fasteners and side spacers. Face ply pulled up slightly around fasteners.	

NOTES: A = Acrylic Face Ply
 U = Urethane Interlayer
 S = Silicone Interlayer

Specimen GY24 is shown in Figure 40. After the first Mach 2.4 injection slight delamination was visible in the area of the bolts. During the second

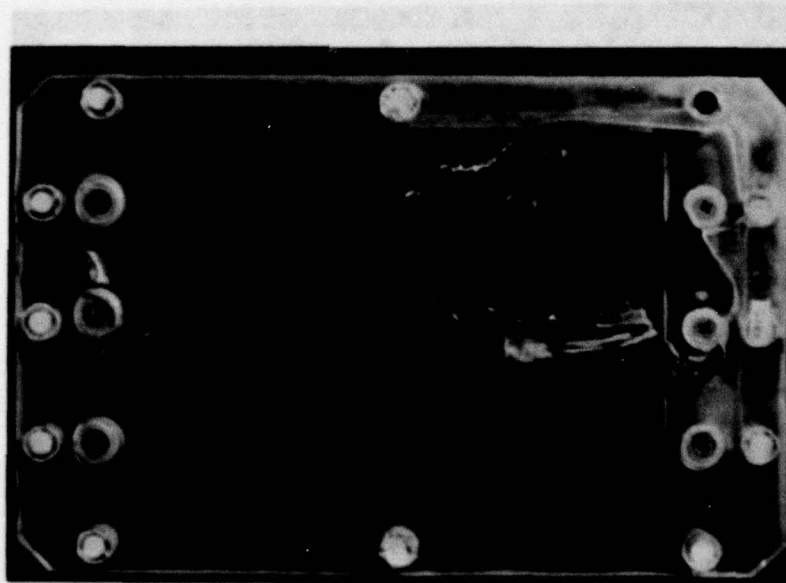


Figure 40. Post-Test Photo of Specimen GY24.

injection the delamination spread. The face ply ruptured and a large segment separated from the specimen. The face ply was pulled in along the edges and the countersink for the screws had expanded.

An examination of GY25, Figure 41, revealed slight face ply/interlayer delamination in the area of the imbedded thermocouples after the first injection at Mach 2.4. Severe delamination occurred during the second injection.

Specimen GY26 delaminated during its second injection at Mach 2.4. Small areas of delamination were also visible near the attachments and spacers.

These specimens were all affected by edge deformation due to expansion of the material in the area not clamped by the cabin simulator cover.

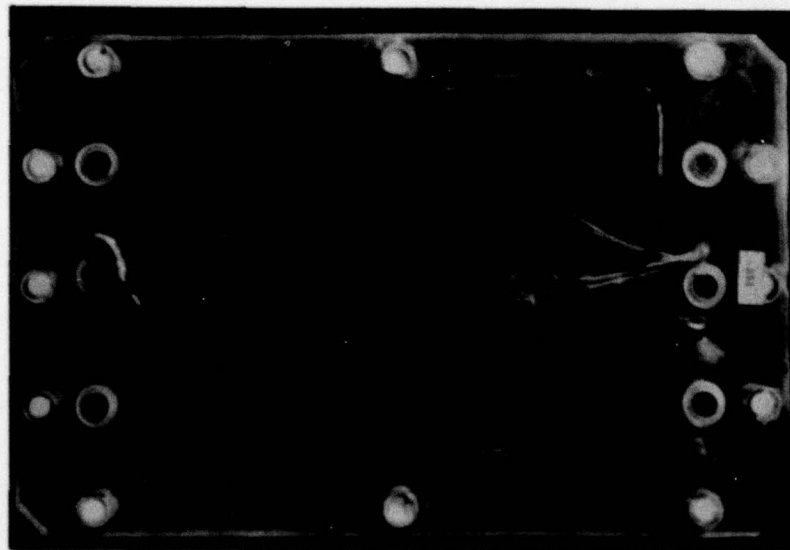


Figure 41. Post-Test Photo of Specimen GY25.

LAMINATED - URETHANE FACE PLY, NO EDGE ATTACHMENTS

This group of five-ply specimens, GY02, GY03, GY04 and GY05, are previously described in Figure 4. They had urethane face plies which extended to the edges, urethane or silicone interlayer, and polycarbonate structural plies. These specimens did not have edge attachments. They were tested previously in a Mach 1.6, Mach 3.0 and Mach 2.2 wind tunnel environment (Reference 1), and did not sustain damage.

An appraisal of the damage to three specimens is given in Table 17.

TABLE 17. POST-TEST SPECIMEN DESCRIPTION - URETHANE FACE PLY, NO EDGE ATTACHMENTS

SPECIMEN FACE PLY AND INTERLAYER	EXPOSURE TIME (MIN)			DESCRIPTION OF SPECIMEN DAMAGE	EDGE DEFOR- MATION
	MACH NO.				
	2.4	2.6	3.0		
GY02 0.100 U 0.040 U	5			No Damage	Yes
	10			Face Ply Delaminated and Ruptured Under Thermocouple at End of 10-Minute Injection - 1 In. Diameter Bubble. Small Bubbles in Interlayer Throughout. Polycarbonate Bubbled and Melted Along Entire Aft Edge and Forward Edge at Both Corners. (Outer Ply Only.)	
GY03 0.100 U 0.040 U	5			Salt Abrasion Ring Disappeared (Reference 9)	Slight
	10			No Change	
		5		No Change	
		10		Polycarbonate Bubbles and Flowed Along Aft Edge. (Outer Ply Only) One small delamination spot.	
GY04 0.100 U 0.100 S	5		4	No Change	Slight
	10			No Change	
			3	No Change	
GY05 0.100 U 0.100 U	5			No Change	Slight
	10			No Change	
			3	No Change	

NOTES: (1) U = Urethane, S = Silicone

(2) Specimens were previously tested (Reference 1). No damage was reported.

GY02: 30 min. at Mach 1.6

GY03: 10 min. at Mach 1.6, 40 min. at Mach 2.0, 10 min. at Mach 2.2.

GY04: 40 min. at Mach 2.2

GY05: 40 min. at Mach 2.0

The urethane face ply of GY02, Figure 42, delaminated at the imbedded thermocouple and formed a 1.0-inch diameter bubble in the face ply. It is not clear whether the separation occurred between the face ply and interlayer, or interlayer and polycarbonate. The delamination occurred at the end of the second injection at Mach 2.4. Post-test examination revealed bubbles and deformation of the outer polycarbonate ply along its aft edge. The polycarbonate bubbled and expanded aft about 0.10-inch until it contacted the surface of the simulator cover as evidenced by its flat shape. The intensity of the bubbles gave the polycarbonate a frothy appearance, as shown in Figure 43. Similar bubbling occurred at each corner of the forward edge. Minute bubbles are visible throughout the urethane interlayer.

GY03, tested at Mach 2.4 and 2.6, sustained the same type of polycarbonate bubbling as did GY02. A small area of delamination was visible along the forward edge. The separation occurred between the interlayer and the outer surface of the outboard polycarbonate ply. The abraded spot on the face ply, caused by a salt impact test (Reference 8), disappeared.

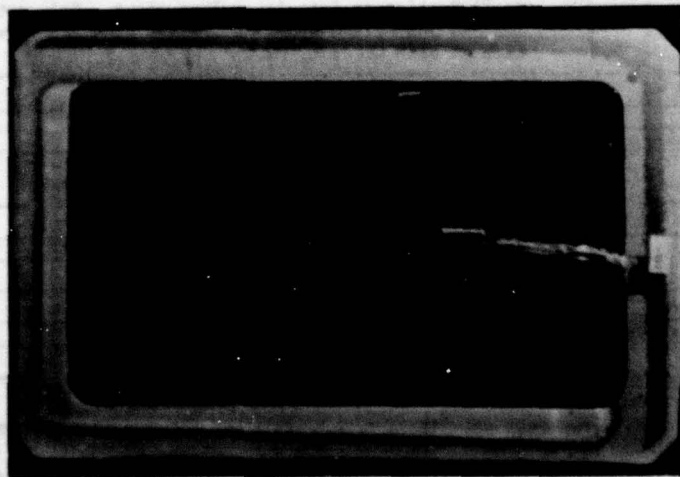


Figure 42. Post-Test Photo of Specimen GY02.

GY04 and GY05, tested at Mach 2.4 and 3.0, sustained slight edge deformation from the simulator cover.

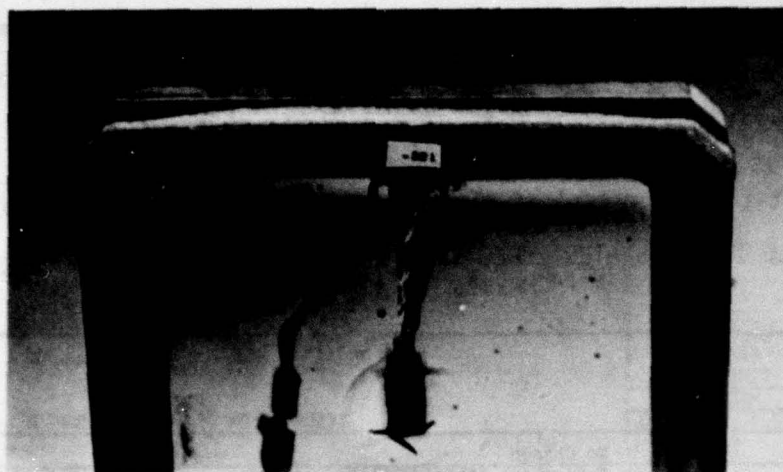


Figure 43. Post-Test Photo of Specimen GY02, Aft Edge.

LAMINATED - GLASS FACE PLY, EDGE ATTACHMENTS

There are six specimens with glass face plies, SK23, SK23A, PPG22, PPG22A, PPG21 and PPG21A. These specimens had edge attachments and fiberglass frames. Specimens SK23 and SK23A are described previously in Figures 5 and 6. They had a glass face ply, silicone interlayer, and polycarbonate structural ply. The glass and interlayer were cut back at the forward and aft edge. The fasteners went through the fiberglass spacer and polycarbonate.

Specimen PPG22 and PPG22A (Figures 9 and 10) consisted of a glass face ply, urethane interlayer, and glass structural ply. The edges were completely enclosed by a fiberglass frame. The edge fasteners were through the frame.

Specimen PPG21 and PPG21A (Figures 9 and 10) consisted of five plies: a glass face ply, two polycarbonate structural plies, and urethane interlayer.

AD-A078 673

DOUGLAS AIRCRAFT CO LONG BEACH CA

F/6 1/3

EVALUATION OF AIRCRAFT WINDSHIELD MATERIALS IN A SIMULATED SUPE--ETC(U)

JUN 79 J B HOFFMAN

F33615-75-C-3105

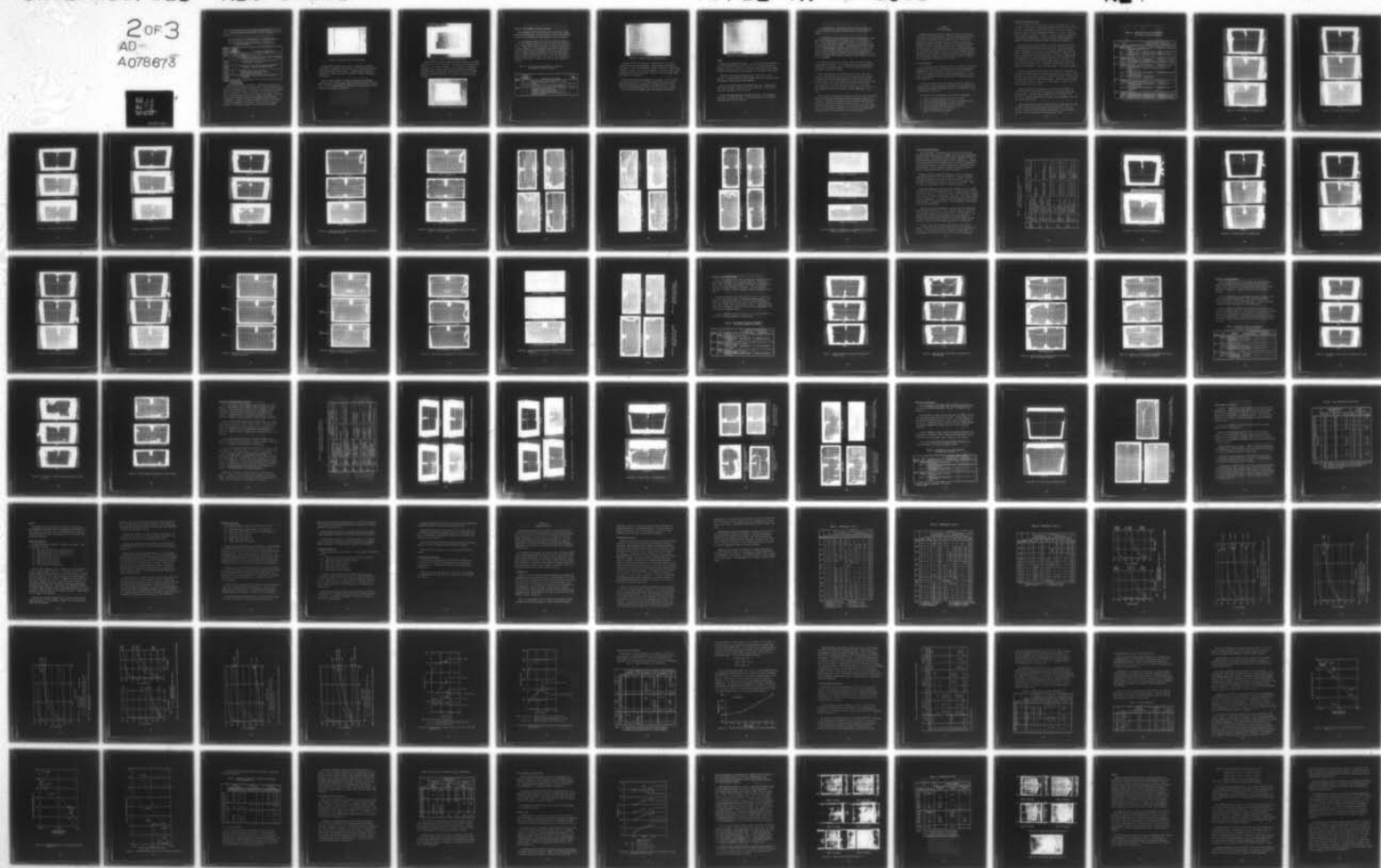
UNCLASSIFIED

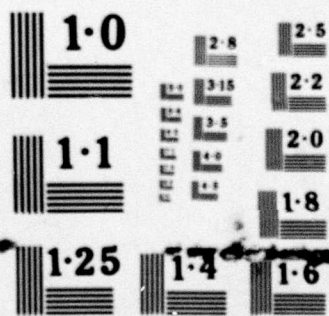
MDC-J7186

AFFDL-TR-79-3058

NL

2 OF 3
AD-A078673





NATIONAL BUREAU OF STANDARDS
MICROCOPY RESOLUTION TEST CHART

The glass was cut back from the four edges and replaced with a fiberglass frame. The edge attachments were through the frame, interlayer and polycarbonate.

A post-test appraisal of these specimens is contained in Table 18.

TABLE 18. POST-TEST SPECIMEN DESCRIPTION - GLASS FACE PLY, EDGE ATTACHMENTS

SPECIMEN FACE PLY AND INTERLAYER	EXPOSURE TIME (MIN)			DESCRIPTION OF SPECIMEN DAMAGE
	MACH NO.			
	2.4	2.6	3.0	
SK23 0.110 G 0.270 S		5		No Change
		10		Fiberglass adhesive melted at edge.
			1/2	No Change
			3	Discoloration of upstream surface of groove sealant. Polycarbonate bubbled and deformed along aft edge.
PPG22 0.120 G 0.320 P	5			Small round bubbles in interlayer. Separation of face ply from interlayer around perimeter.
PPG22A 0.120 G 0.320 P		2		Severe bubbling. Flat bubbles at interface of face ply and interlayer. Groove sealant degraded at one spot.
PPG21 0.120 G 0.350 P	5 10			Interlayer bubbled slightly around edges. Severe interlayer bubbling at end of injection. Interlayer melted along all edges.
PPG21A 0.120 G 0.350 P			1.5	Severe bubbling. Flat bubbles at interface of face ply and interlayer.

NOTES: G = Glass face ply
S = Silicone interlayer
P = PPG112 interlayer

Specimen SK23 is shown in Figure 44. This specimen, tested at Mach 2.6 and 3.0, sustained bubbling and deformation of the polycarbonate structural ply along the aft edge. The flatness of the deformed area indicates that this surface was in direct contact with the simulator cover's aft edge. The adhesive that bonds the aft fiberglass edge members, consisting of two sheets, melted and oozed out from between the two pieces of fiberglass. The sealant in the groove between the edge of the glass and fiberglass edge member was discolored. The discoloration was easily removed and is apparently residue from the fiberglass edge member.

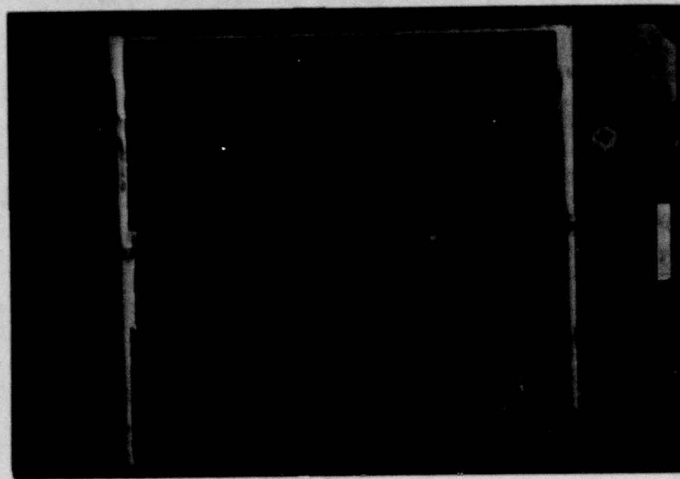


Figure 44. Post-Test Photo of Specimen SK23.

Specimen PPG22 developed small bubbles in the PPG112 interlayer (about 0.06 inch diameter in size) during its first injection at Mach 2.4. It was withdrawn from further testing. The edges showed evidence of delamination. Neither the glass nor interlayer extends to the edge of this specimen.

Specimen PPG22A (identical to PPG22) sustained severe interlayer bubbling during its initial tunnel injection at Mach 2.6 and was retracted early. The flat shaped bubbles are apparently at the face ply/interlayer interface, and are shown in Figure 45.

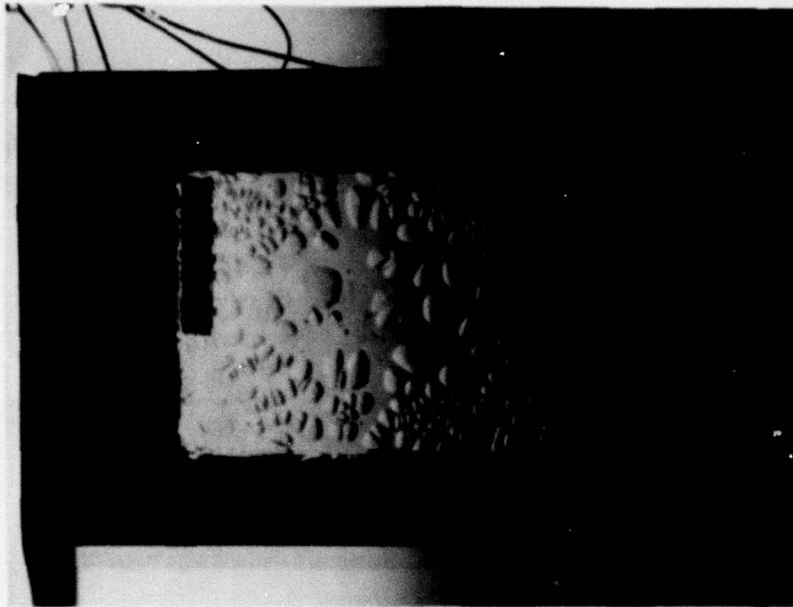


Figure 45. Post-Test Photo of Specimen PPG22A.

Specimen PPG21 (Figure 46) displayed interlayer bubbles at the edges after its initial Mach 2.4 injection. The entire surface bubbled at the termination of its second injection. The interlayer, which extends to the edges of this specimen, melted on all four edges, and especially along the forward and aft edges. Specimen PPG21A (identical to PPG21) suffered interlayer bubbling early in its Mach 3.0 injection and was retracted.

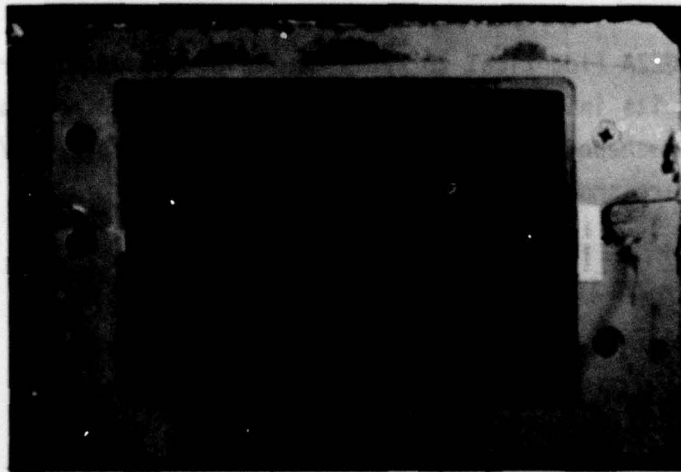


Figure 46. Post-Test Photo of Specimen PPG21.

MONOLITHIC POLYCARBONATE, NO EDGE ATTACHMENTS

These specimens, TEX21 and TEX21A, were 1.00 inch thick, coated, monolithic polycarbonate. They did not have a frame or edge fasteners. An appraisal of the damage to these specimens is given in Table 19.

TEX21 was tested at Mach 2.4 for 5 and 10 minutes and at Mach 3.0 for 1 minute. Hazing occurred at 1 minute of its initial injection but did not increase after about 1.5 minutes. No change occurred during its second injection. It was injected at Mach 3.0 but bubbled and was removed at about 1 minute. The bubbles are on the extreme exterior surface but under the protective coating. Figure 47, shown below, is a post-test photo of Specimen TEX21. The surface of the specimen had a series of random cracks in the coating, which gave the appearance of "dry mud".

TABLE 19. POST-TEST SPECIMEN DESCRIPTION - MONOLITHIC POLYCARBONATE, NO EDGE ATTACHMENTS

SPECIMEN	EXPOSURE TIME (MIN.) MACH NO.			DESCRIPTION OF SPECIMEN DAMAGE	EDGE DEFORMATION
	2.4	2.6	3.0		
TEX21	5			Hazing occurred at 1 minute on right hand side (looking forward). No change after 1.5 minutes.	Slight
	10			No Change.	
			1	Severe bubbling of outer surface occurred immediately.	
TEX21A		5		Slight bubbling occurred on outer surface. Aft corner deformed and bubbles in polycarbonate. Approximately 5 cracks appeared in outer surface, 3 to 4 inches long, resembling "dry mud" cracks. Very fine ripples occurred on surface along forward and aft edge where frame ended.	Yes

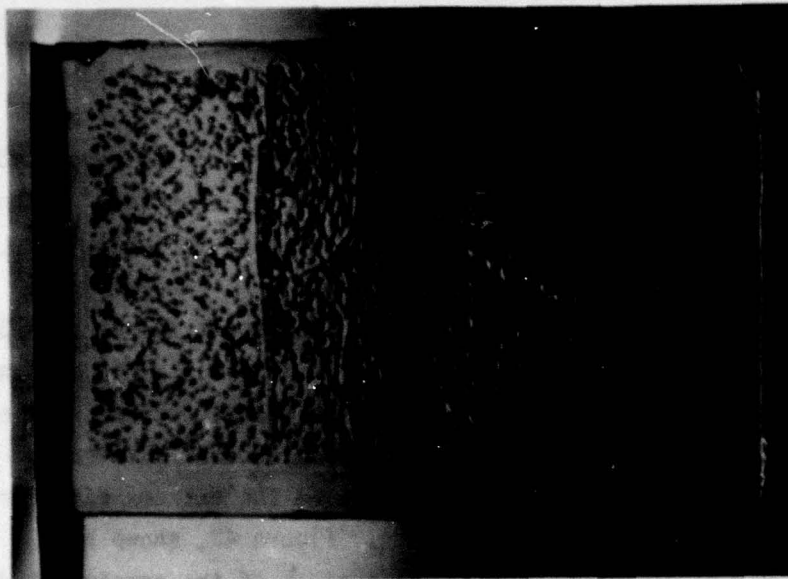


Figure 47. Post-Test Photo of Specimen TEX21.

Specimen TEX21A was injected for 5 minutes at Mach 2.6. Slight surface bubbling occurred throughout. Severe bubbling occurred at the aft corner. Surface cracks appeared as shown in Figure 48. These cracks, as noted previously, had a "dry mud" appearance. Very fine surface ripples occurred at each end of the specimen, adjacent to the frame, where there was movement of the material.

TEX21 and TEX21A were examined under a microscope. It was verified that the bubbles did occur in the outer surface of the polycarbonate. Many of the bubbles were covered with the protective surface coating, while others had ruptured the coating. The coating cracks were about 1 to 4 mils wide and did appear to penetrate into the polycarbonate.

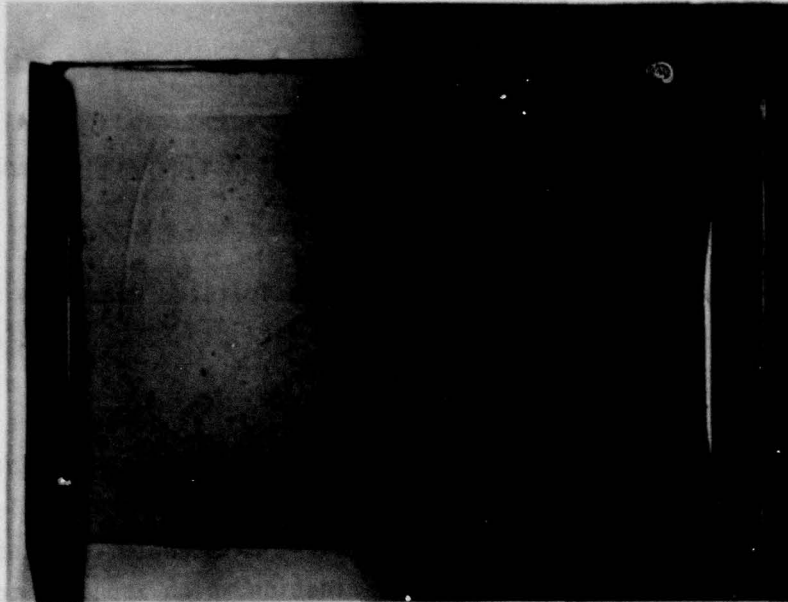


Figure 48. Post-Test Photo of Specimen TEX21A.

SUMMARY

Twenty-four specimens were tested: 7 of 13 survived exposure at Mach 2.4, 6 of 12 survived exposure at Mach 2.6, and 6 of 11 survived at Mach 3.0. Subsequent testing of a specimen at more than one Mach number led to further failures but seven specimens were undamaged at the completion of the tests.

Thirteen of the tested specimens had acrylic face plies. Three survived. The survivors (SK21, SK22 and SWU21) were of the acrylic/silicone/polycarbonate construction with edge fasteners.

Four of the tested specimens had urethane face plies. Three survived (GY03, GY04 and GY05). These specimens had urethane and silicone interlayers and polycarbonate structural plies.

Five of the tested specimens had glass face plies. The one survivor (SK23) had a silicone interlayer. The failed specimens (all PPG panels) sustained severe interlayer bubbling.

Two coated monolithic polycarbonate panels (TEX21 and TEX21A) were tested and failed at the higher velocities, after surviving a Mach 2.4 exposure.

The edge designs of certain specimens precipitated premature failures, specifically the specimen with the rabbeted face ply (GY21, GY22 and GY23), and the specimen which extended the face ply to the edge without an edge frame (GY24, GY25 and GY26). The rabbeted specimens were damaged by holes burned through the rabbeted area of the face ply. Two of these specimens (GY22 and GY23), tested at Mach 2.6 and 3.0, had the plastic bushings melt. The remaining specimens (GY24, GY25 and GY26), tested at Mach 2.4, sustained severe face ply delamination which appeared to originate at the attachments.

The design utilizing a metal retainer (SK22) failed due to sealant erosion under the retainer. The "V" groove edge (SK21) sustained partial delamination of the groove sealant. The square grooved specimen (SK23 and SWU21) survived without damage.

Many of the specimens with polycarbonate plies (SK05, GY01, SK22, GY03, and SK23) sustained bubbling of the polycarbonate along the panel aft edge, indicating higher edge temperatures than at the mid section or forward edge. This is attributed to the rebound shock mentioned in the previous chapter which caused higher heating rates at the aft edge (see Chapter VII). Also, the aft edge of the simulator cover (Figure 13), was an apparent heat sink and resulted in higher temperatures in that area.

Prior to this test program the aerodynamic effects of a Mach 2.4 through Mach 3.0 environment on transparent plastic and interlayer materials was not known. It had been anticipated that the selected materials might not survive high temperatures generated at these velocities. The tests have shown that plastic face ply materials, such as as-cast acrylic and urethane and silicone and urethane interlayers will survive the high temperatures experienced at Mach 2.4 through Mach 3.0 for short exposures.

SECTION VI

OPTICS EVALUATION

Windshield/canopy materials for supersonic aircraft must have the capability to survive the effect of a high-speed environment within the time frame of the potential aircraft operating conditions, and still provide a relatively undistorted view for the pilot. A goal of this program was to define the optical distortion that might be sustained by a series of laminated windshield configurations for potential use in Mach 3.0 aircraft. This evaluation was achieved by testing 23 specimens in a wind tunnel environment of Mach 2.4, 2.6 and 3.0 and measuring the resultant in-tunnel optical distortion, the permanent optical distortion, the loss of light transmission, and the increase in haze. The results of this evaluation are presented in this section.

OPTICAL DISTORTION

Five in-tunnel photos were taken through each specimen of a lined grid painted on the tunnel wall. After testing, first and last photos were superimposed to show the apparent line distortion and loss of line clarity. The apparent grid size in these included photos is 0.17 inch. Loss of light transmission and/or severe distortion thwarted the use of some of the photos.

Pre-test and post-test photos were taken through each specimen of a lined grid board. These photos were superimposed to show apparent line distortion as a measure of permanent distortion. The apparent grid size in these photos is 0.25 inch.

Evaluation of the 23 specimens is divided into six categories:

- Three Ply Laminated Specimens with Acrylic Face Ply
- Five Ply Laminated Specimens with Acrylic or Urethane Face Ply
- Seven Ply Laminated Specimens with Acrylic Face Ply
- Nine Ply Laminated Specimens with Acrylic Face Ply
- Laminated Specimens with Glass Face Ply
- Monolithic Polycarbonate Specimens.

Three-Ply Laminated Specimens

Five specimens are included in this group: SK05, SK06, SK21, SK22 and SWU21. These three-ply specimens were fabricated with an acrylic face ply and a polycarbonate structural ply joined by a silicone interlayer. Specimens SK05 and SK06 were described previously in Figure 3, SK21 and SK22 in Figure 5, and SWU21 in Figure 7. SK05 and SK06 were designed for a previous test (Reference 1). Table 20 presents a photo evaluation summary. The grid line photos are shown in Figures 49 through 59.

Figure 49 shows grid board photos of Specimen SK05 before and after tunnel testing, and an overlay of the two photos. Similar photos are shown in Figures 50, 51, 52, and 53 for Specimens SK06, SK21, SK22 and SWU21. The delamination suffered by SK05 is evident in Figure 49. Haze-ness is visible in all the pre-test photos and is seen by comparing the specimen surface with the lines beyond the frame of the specimen. The oval shaped hazy spot visible in SK06 (lower, center) was caused by an abrasion test (Reference 9). All specimens suffered distortion at the edges of the specimens. Slight line displacement is seen in the overlays.

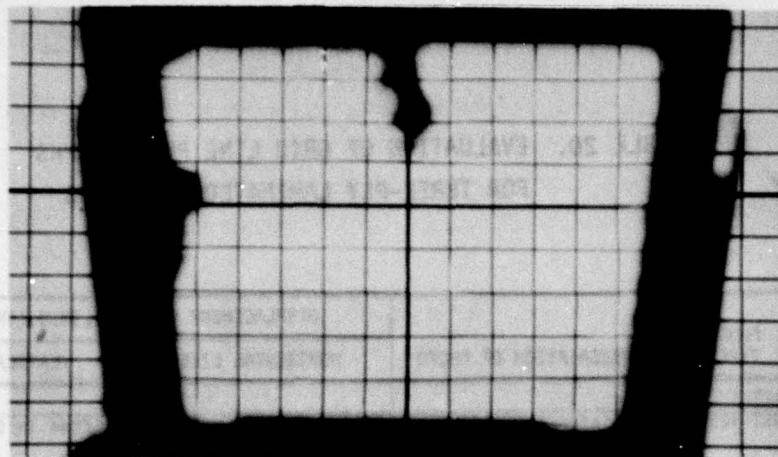
The final tunnel photos and overlays for the Mach 2.4 injections are presented in Figures 54 and 55 for Specimens SK05, SK21 and SWU21. These were the last photos taken during the 10-minute injections. Specimen SK21 sustained more distortion than SK05 and SWU21. The cross section of SK21 and SWU21 were identical. Maximum line displacement is about 0.18 inch for the horizontal lines of SK21.

Photos and overlays for the Mach 2.6 injections are exhibited in Figures 56 and 57 for the 10-minute injection of Specimens SK06, SK21, SK22 and SWU21. Specimen SK06 and SWU21 display the clearest line definition. Specimen SK06 shows the largest line displacement, 0.25 inch for its horizontal lines.

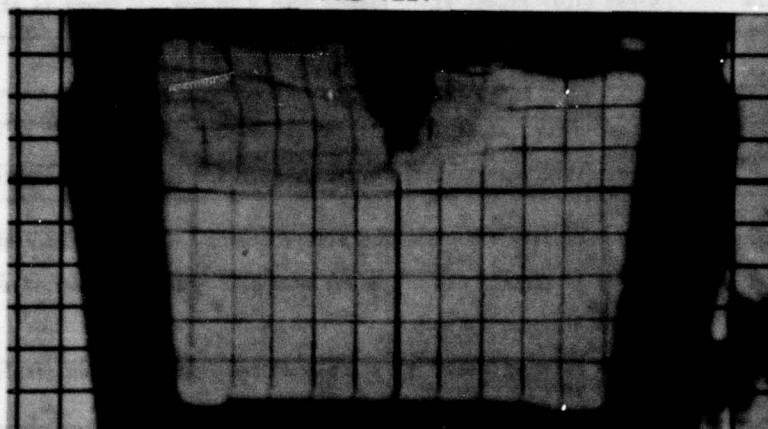
Photos and overlays for the 3-minute injection of Specimen SK05, SK22 and SWU21 at Mach 3.0 are exhibited in Figures 58 and 59. The line quality is better for SK05 and SWU21 than for SK22. Line displacement for SK05 is 0.25-inch maximum for the horizontal lines.

TABLE 20. EVALUATION OF GRID LINE PHOTOGRAPHS
FOR THREE-PLY LAMINATED SPECIMENS

SPECIMEN	PHOTO TYPE	DESCRIPTION OF PHOTO	DISPLACEMENT OF GRID LINES (INCHES)	
			HORIZONTAL LINES	VERTICAL LINES
SK05	PRETEST	Clear		
	POST-TEST	Line intensity diminished Delamination upper left corner	Shifted up 0.05	Shifted in 0.07 at sides
	M2.4	Lines clear except at edges	Bowed down 0.18 max.	Bowed in at sides 0.12 max.
	M3.0	Lines clear except at left side	Bowed down 0.25 max.	Rotated in at sides 0.07
SK06	PRETEST	Hazy spots		
	POST-TEST	Lines obscure at sides and lower edge	Displacement at lower edge	Shifted in 0.07 at sides
	M2.6	Lines distorted at sides	Bowed down 0.25 max.	Sides rotated in 0.18 max.
SK21	PRETEST	Hazy spots		
	POST-TEST	Line intensity diminished Lines blank at sides	No displacement	Shifted right 0.12 max.
	M2.4	Severe distortion at sides Some horizontal lines blank.	Bowed down 0.12 max.	Distorted at sides
	M2.6	Severe distortion and loss of line clarity especially at sides	Bowed downward	Sides displaced and rotated
	M3.0	Severe distortion and loss of line clarity	Photo too dark to measure lines	
SK22	PRETEST	Clear		
	POST-TEST	Line intensity diminished Lines blank at sides.	Shifted down 0.06	Shifted in 0.06
	M2.6	Lines irregular. Severe distortion and loss of clarity at sides	Shifted down 0.12	Shifted at sides
	M3.0	Lines irregular. Severe distortion at sides	Shifted down	Bowed out at sides
SWU21	PRETEST	Some haziness		
	POST-TEST	Lines obscure at sides	Shifted up 0.06	Shifted in 0.06
	M2.4	Lines obscure at edges	Bowed down 0.10 max.	Rotated in at sides 0.06
	M2.6	Lines distorted at edges	Bowed down 0.12	Rotated at sides 0.06
	M3.0	Distortion at sides	Shifted down 0.06	Shifted out at sides 0.12



PRE-TEST

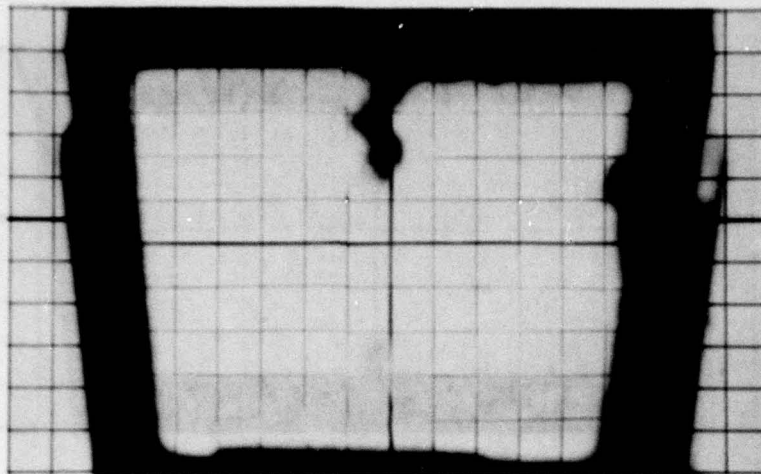


POST-TEST

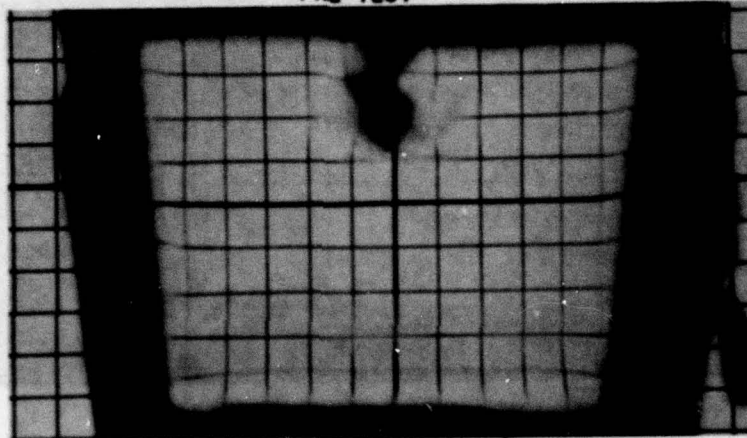


OVERLAY

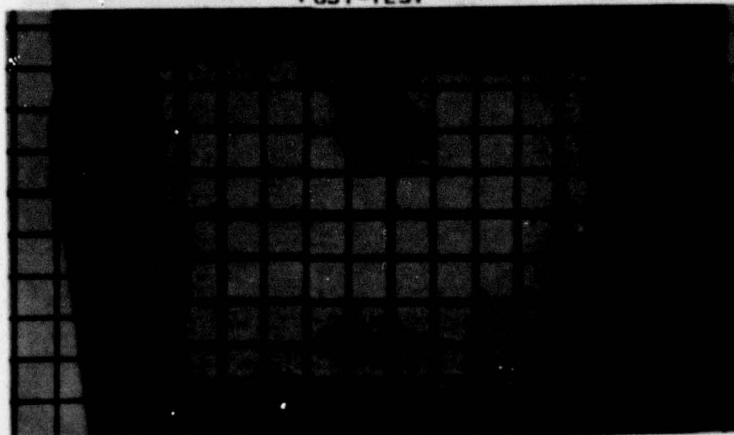
Figure 49. Grid Board Photos for Specimen SK05.



PRE-TEST

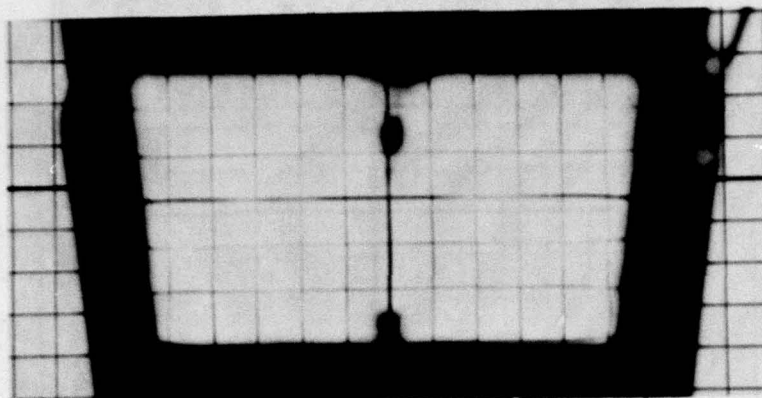


POST-TEST

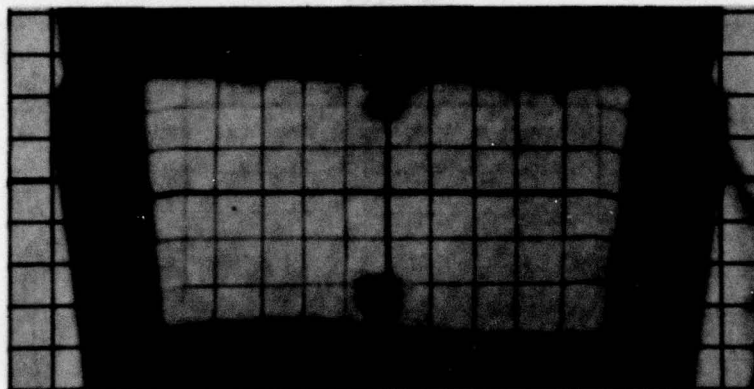


OVERLAY

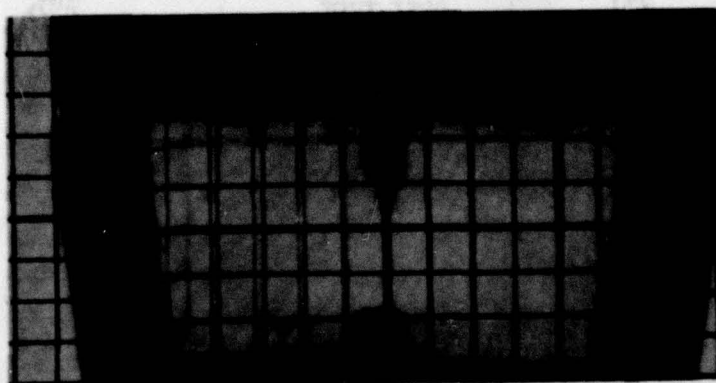
Figure 50. Grid Board Photos for Specimen SK06.



PRE-TEST

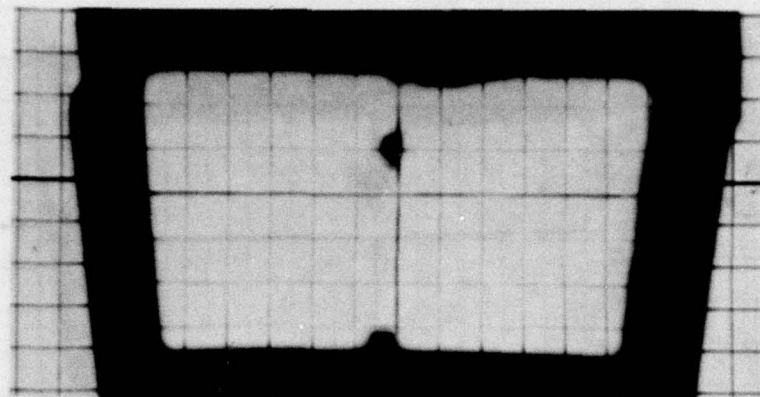


POST-TEST

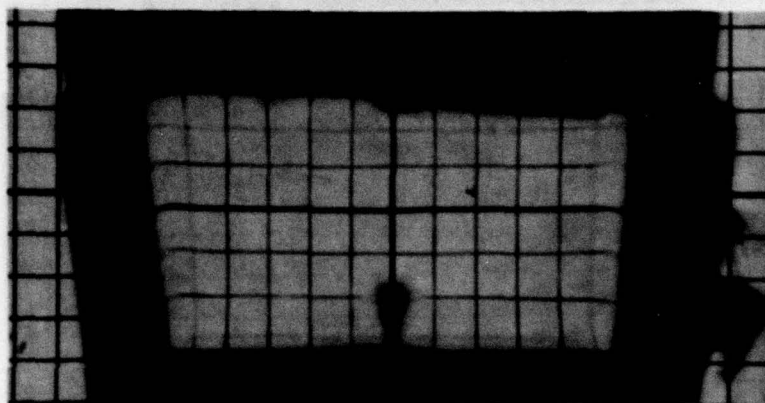


OVERLAY

Figure 51. Grid Board Photos for Specimen SK21.



PRE-TEST

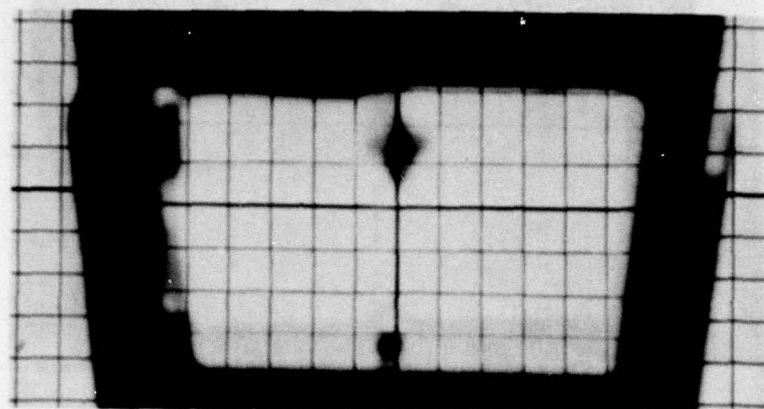


POST-TEST

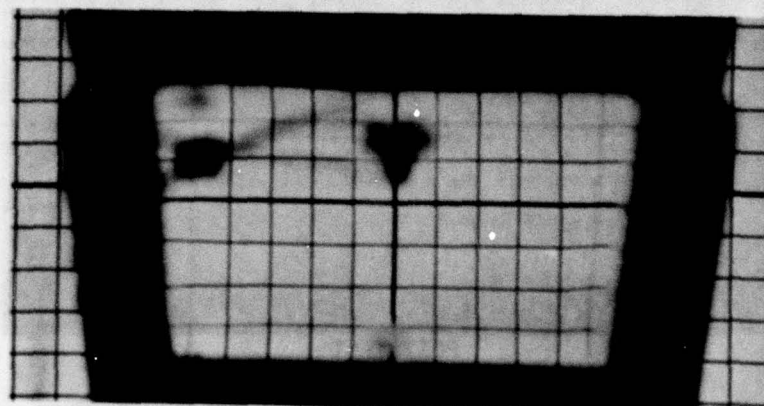


OVERLAY

Figure 52. Grid Board Photos for Specimen SK22.



PRE-TEST

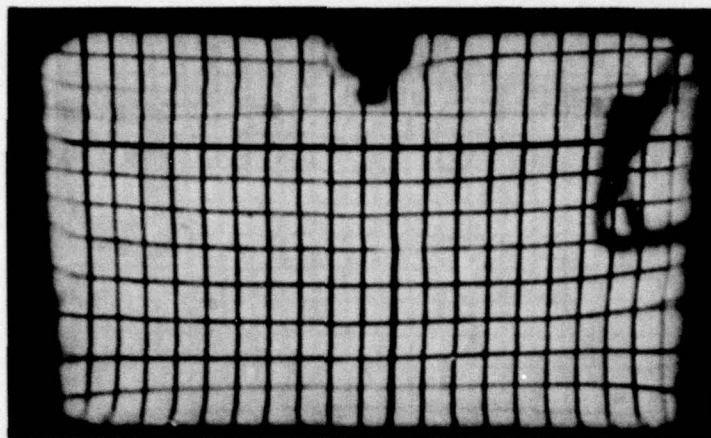


POST-TEST

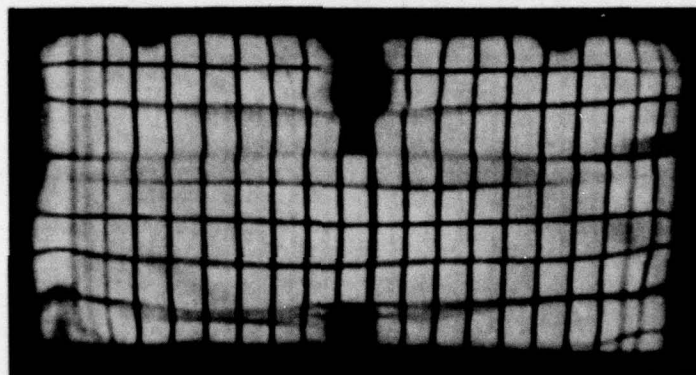


OVERLAY

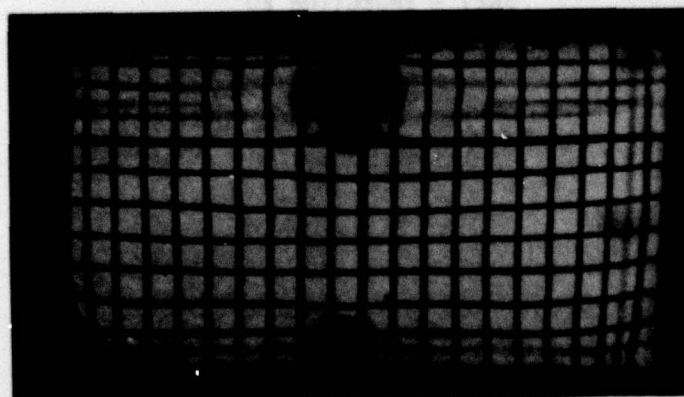
Figure 53. Grid Board Photos for Specimen SMU21.



SK05 - INJECTION 17

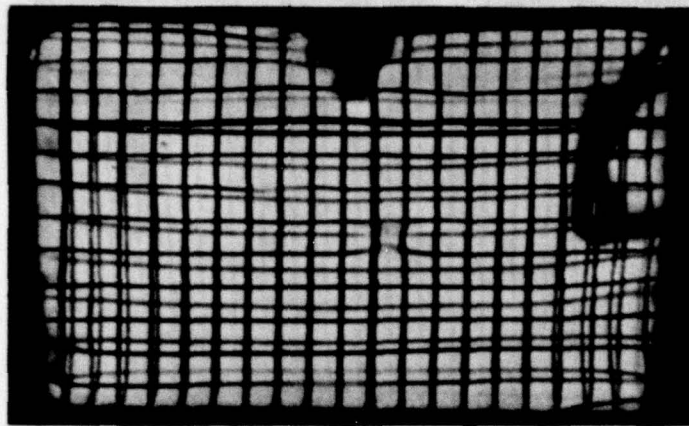


SK21 - INJECTION 20

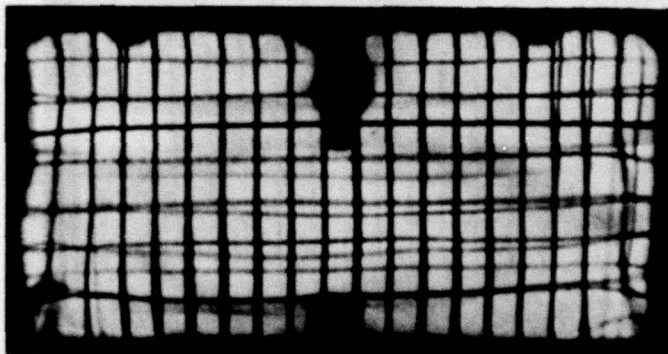


SHU21 - INJECTION 22

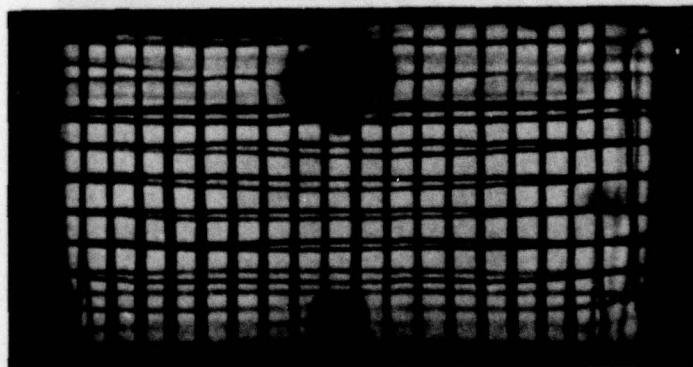
Figure 54. Tunnel Photos for Specimens SK05, SK21 and SHU21 at Mach 2.4 (10-Minute Injection).



SK05 - INJECTION 17



SK21 - INJECTION 20

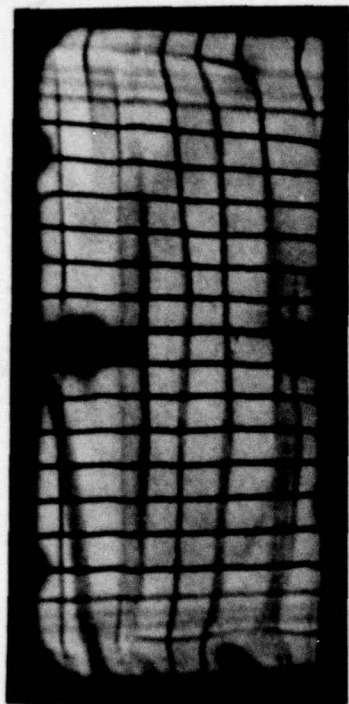


SWU21 - INJECTION 22

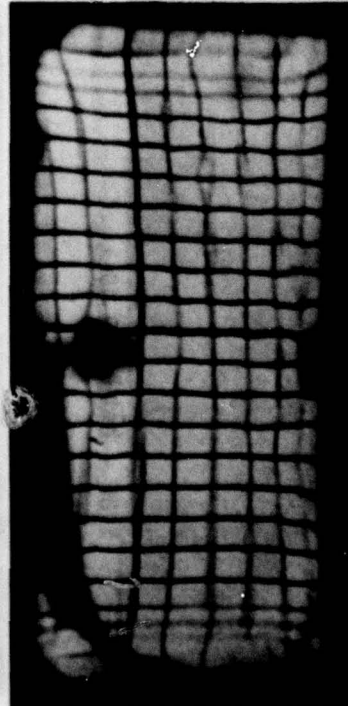
Figure 55. Overlays of Tunnel Photos for Specimens SK05, SK21 and SWU21 at Mach 2.4 (10-Minute Injection).



SK06 - INJECTION 49



SK21 - INJECTION 51



SK22 - INJECTION 53

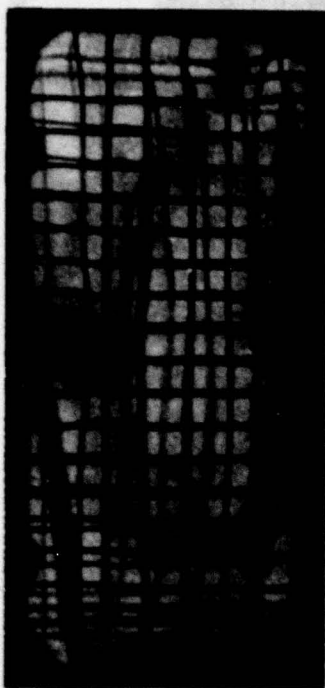


SMU21 - INJECTION 60

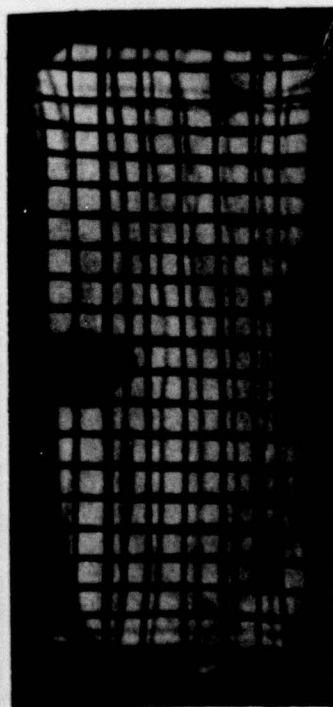
Figure 56. Tunnel Photos for Specimens SK06, SK21, SK22 and SMU21 at Mach 2.6 (10-Minute Injection).



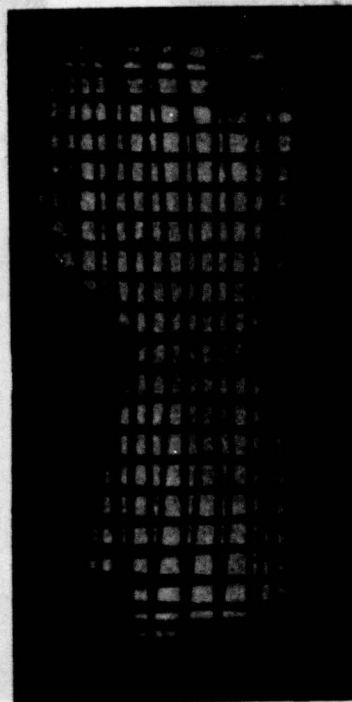
SK06 - INJECTION 49



SK21 - INJECTION 51

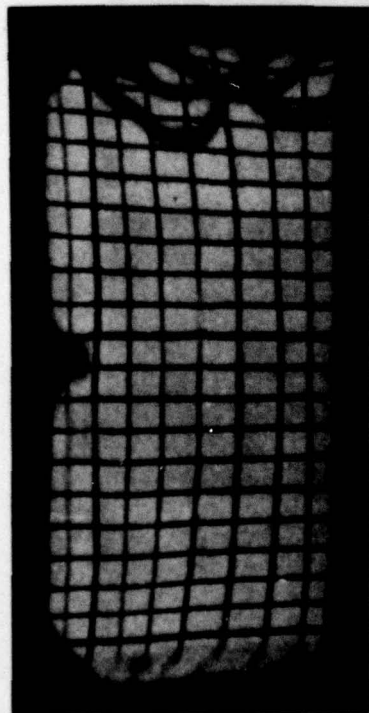


SK22 - INJECTION 53

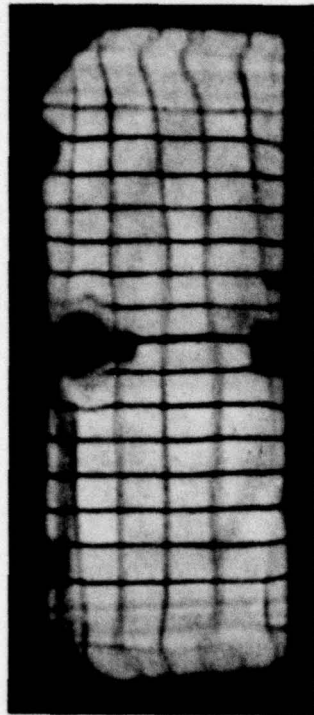


SMU21 - INJECTION 60

Figure 57. Overlays of Tunnel Photos for Specimens SK06, SK21, SK22 and SMU21 at Mach 2.6 (10-Minute Injection).



SK05 - INJECTION 85



SK21 - INJECTION 74

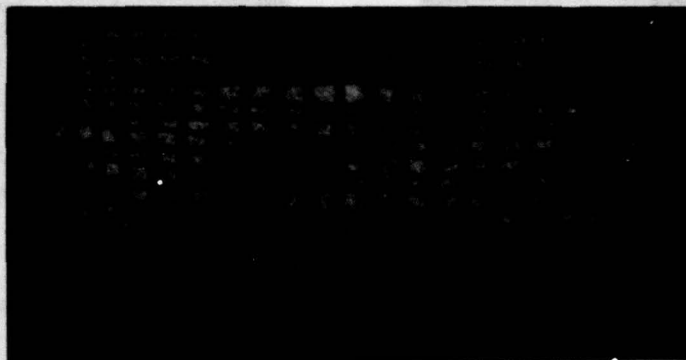


SK22 - INJECTION 76

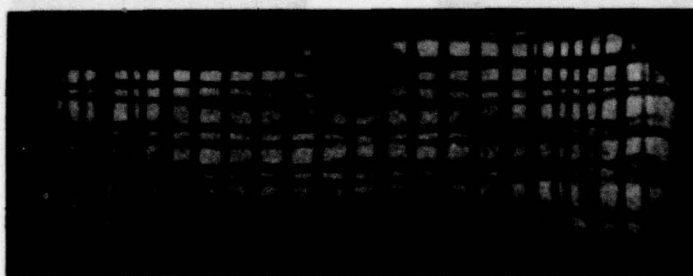


SMU21 - INJECTION 79

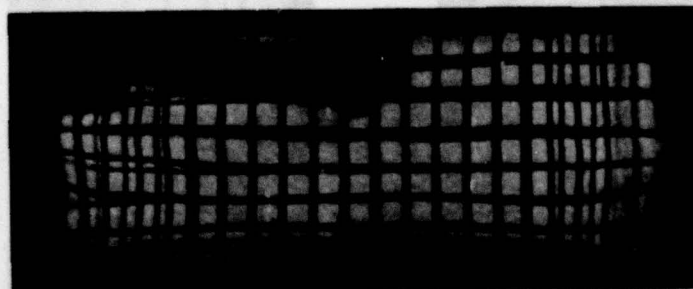
Figure 58. Tunnel Photos for Specimens SK05, SK21, SK22 and SMU21 at Mach 3.0 (3-Minute Injection).



SK05 - INJECTION 85



SK22 - INJECTION 76



SWU21 - INJECTION 79

Figure 59. Overlay of Tunnel Photos for Specimens SK05, SK22 and SWU21 at Mach 3.0 (3-Minute Injection).

Five-Ply Laminated Specimens

The five specimens in this group, GY01, GY02, GY03, GY04 and GY05 were fabricated with an acrylic or urethane face ply and two polycarbonate structural plies. These specimens were previously described in Figure 4 and were designed and previously tested as noted in Reference 1. Specimen GY01, GY02 and GY03 were also tested for face ply abrasion per Reference 8, and the resultant hazy spot is visible on the lower center area of these three specimens. Table 21 presents a summary of the photo evaluation. The grid line photos are shown in Figures 60 through 70.

Figures 60 through 64 show grid board photos of the five specimens taken before testing and at the test completion. Overlays of pre-test and post-test photos are also shown for GY02 through GY05. All five specimens show distortion and loss of line clarity at the edges. There is slight line displacement visible in the photo overlays.

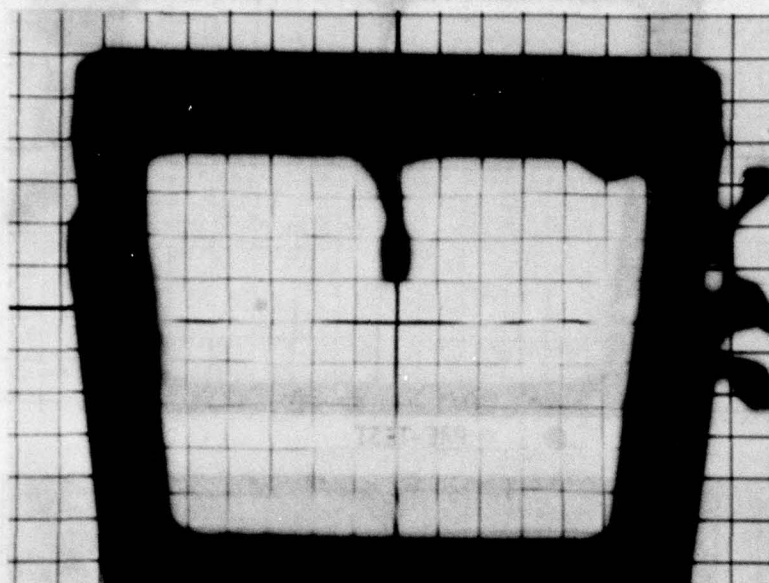
Figure 65 presents the final tunnel grid line photos for the 10-minute injections of GY03, GY04 and GY05 at Mach 2.4. Figure 66 displays overlays for the same injections. The dark oval spots in the GY03 overlay (Figure 66) is not visible in the final tunnel photo (Figure 65). This area was abraded with salt (Reference 9). The photos indicate consistent distortion for the three specimens. The maximum horizontal line displacement is approximately 0.20 inch for each specimen.

Photos and overlays are presented in Figures 67 and 68 for Specimens GY01, GY02 and GY03 at Mach 2.6. These injections were five minutes for Specimens GY01 and GY02, and 10 minutes for GY03. The oval spots in the photos for GY01 and GY02 resulted from salt abrasion (Reference 9). Specimen GY02 displays the least severe line distortion among the three specimens. Maximum line displacement approaches 0.25 inch for GY03.

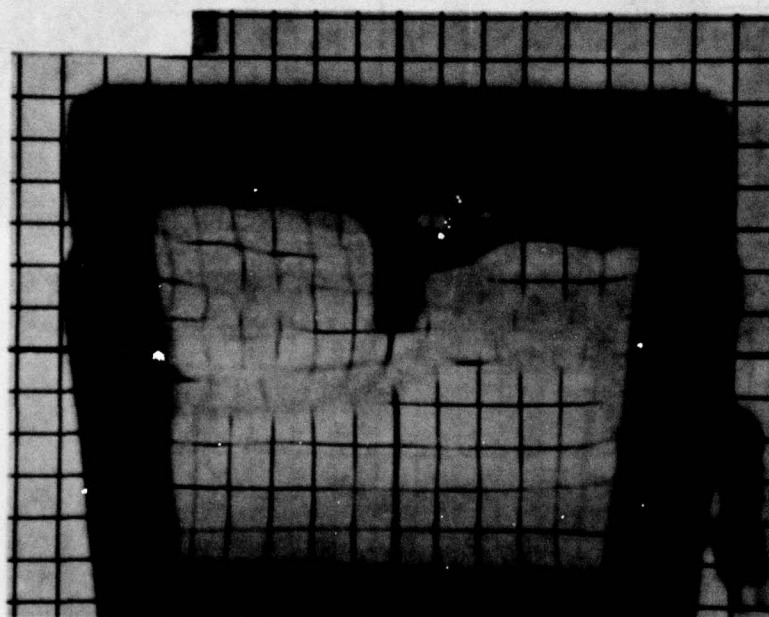
The final tunnel grid line photos and overlays for the 3-minute Mach 3.0 injections are exhibited in Figures 69 and 70 for Specimens GY04 and GY05. The most severe distortion occurred in Specimen GY04. The displacement of the horizontal lines is 0.25 inch for both specimens.

TABLE 21. EVALUATION OF GRID LINE PHOTOGRAPHS FOR
FIVE-PLY LAMINATED SPECIMENS

SPECIMEN	PHOTO TYPE	DESCRIPTION OF PHOTOS	DISPLACEMENT OF GRID LINES (INCHES)	
			HORIZONTAL LINES	VERTICAL LINES
GY01	PRETEST	Hazy spots. Abrasion spot in center (Ref 9)		
	POST-TEST M2.6	Delamination upper half Lines wavy and distorted	No overlay Shifted down	Shifted in.
GY02	PRETEST	Good clarity. Abrasion spot in center (Ref 9)		
	POST-TEST M2.6	Distortion at edges Lines clear	Shifted up slightly Bowed down 0.18 max.	No displacement Bowed in at sides 0.06
GY03	PRETEST	Hazy spots. Abrasion spot in center (Ref 9)		
	POST-TEST M2.4	Lines obscure at edges Lines clear	Shifted up 0.06 max. Bowed down 0.12 max.	Slight displacement Rotated out at top, in at bottom.
	M2.6	Lines distorted at sides	Bowed down 0.25 max.	Rotated out at top, in at bottom.
GY04	PRETEST	Good clarity		
	POST-TEST M2.4	Lines obscure at edges Lines distorted at sides	Shifted up 0.06 Bowed down 0.25 max.	Rotated out at sides 0.06 Rotated out at top, in at bottom
	M3.0	Lines bowed. Severe distortion at sides	Bowed down 0.25 max.	Rotated out at top, in at bottom.
GY05	PRETEST	Good clarity		
	POST-TEST	Lines blank at lower edge	Shifted up 0.12 max.	No displacement.
	M2.4	Lines clear and continuous	Bowed down 0.18 max.	Rotated out at top, in at bottom.
	M3.0	Lines clear but bowed	Bowed down 0.25 max.	Rotated out at top, in at bottom.

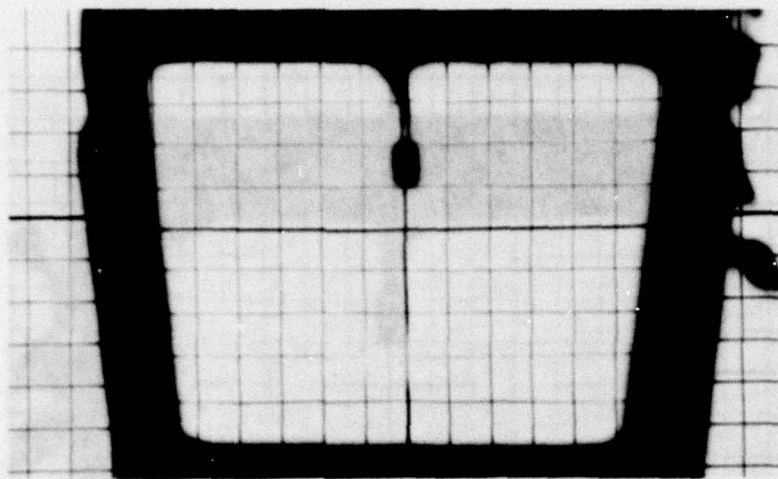


PRE-TEST

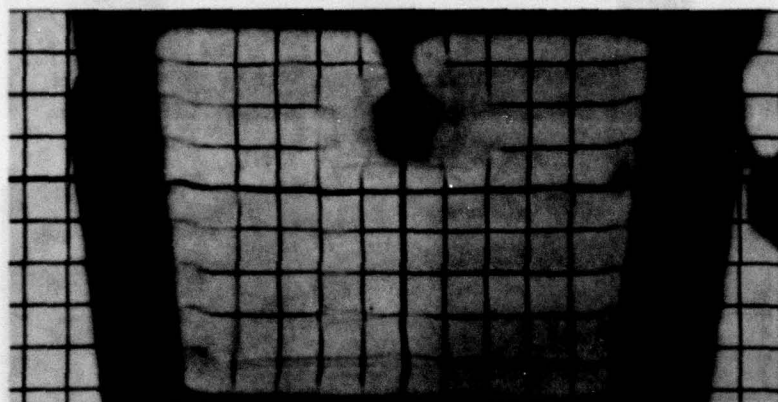


POST-TEST

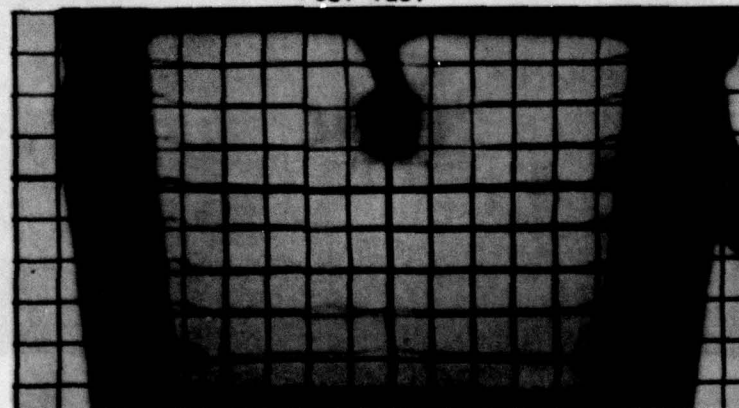
Figure 60. Grid Board Photos for Specimen GY01.



PRE-TEST

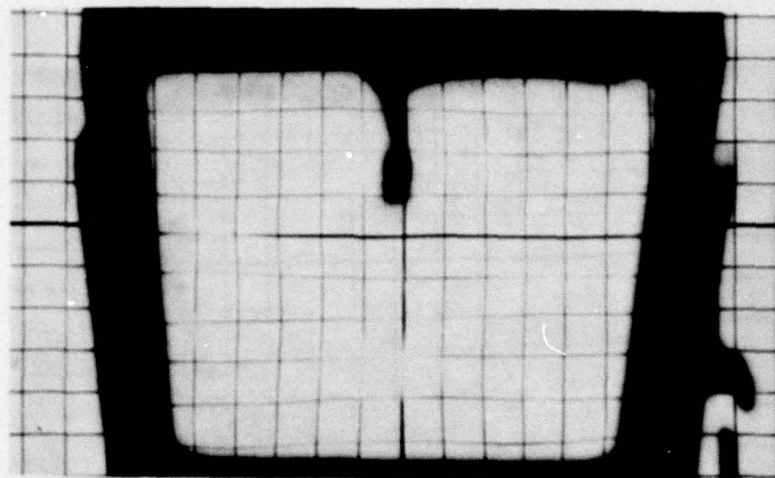


POST-TEST

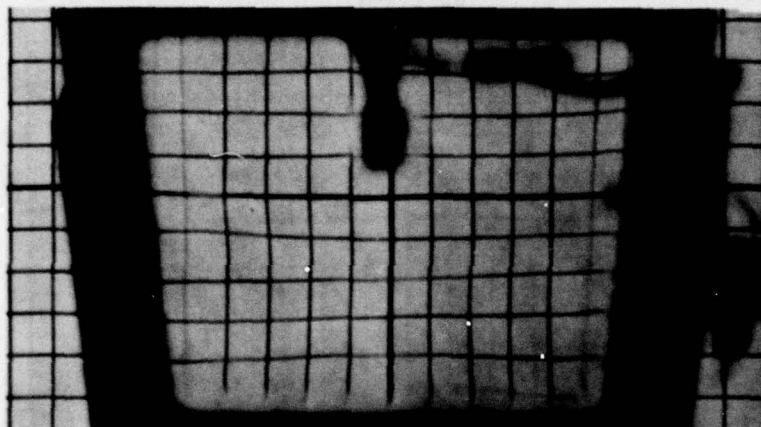


OVERLAY

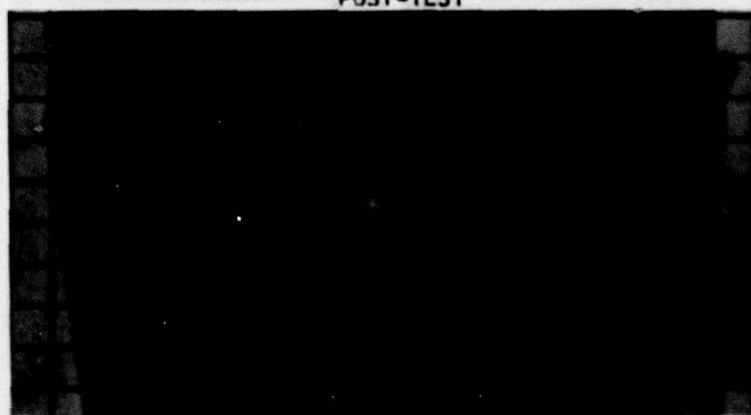
Figure 61. Grid Board Photos for Specimen GY02.



PRE-TEST

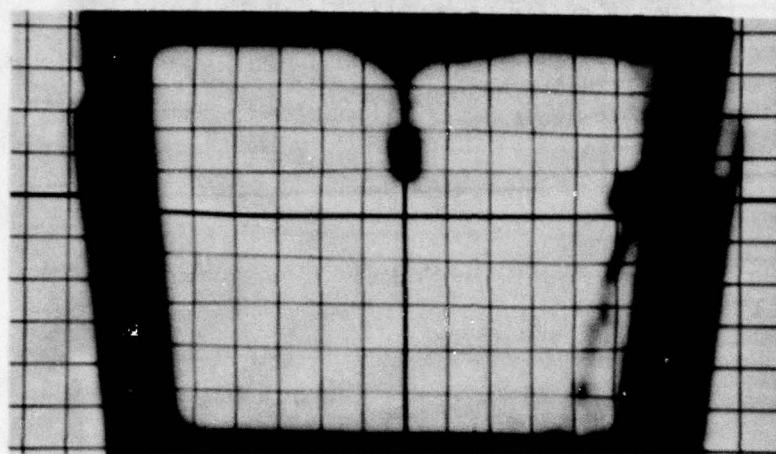


POST-TEST

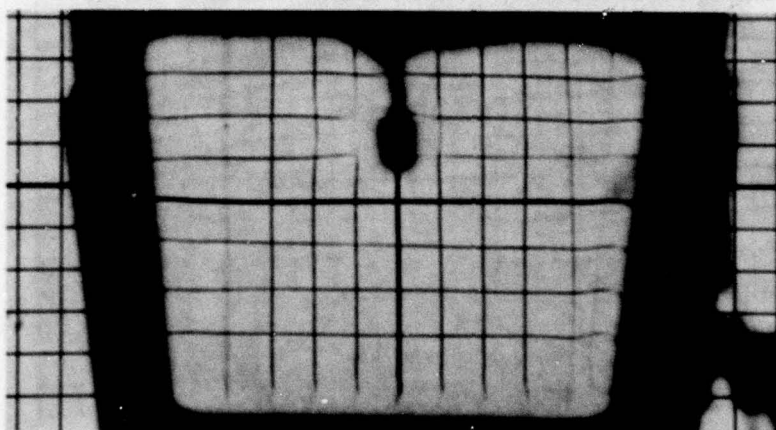


OVERLAY

Figure 62. Grid Board Photos for Specimen GY03.



PRE-TEST

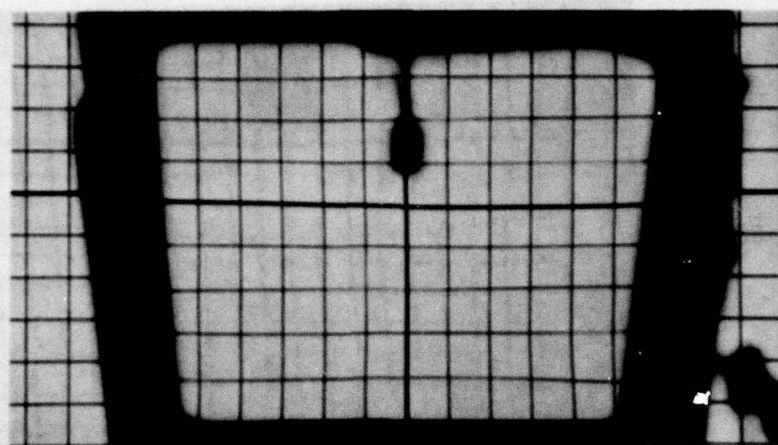


POST-TEST

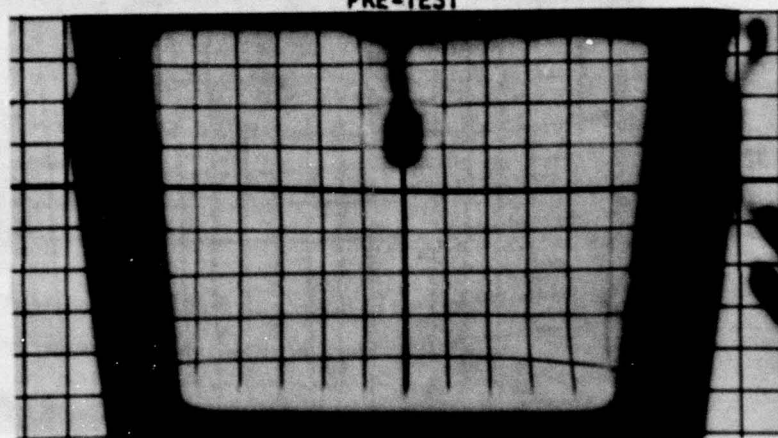


OVERLAY

Figure 63. Grid Board Photos for Specimen GY04.



PRE-TEST



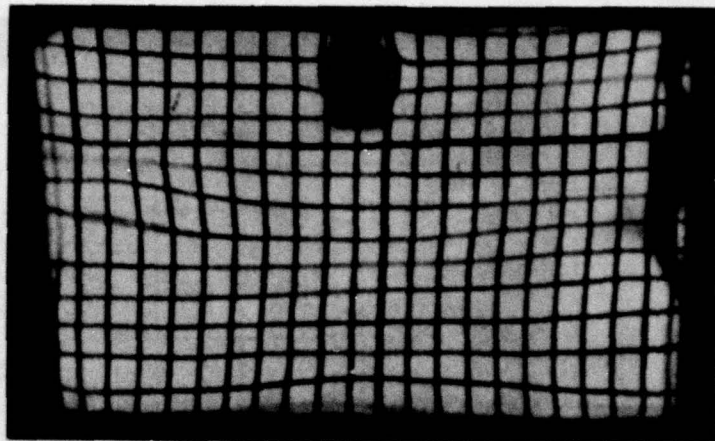
POST-TEST



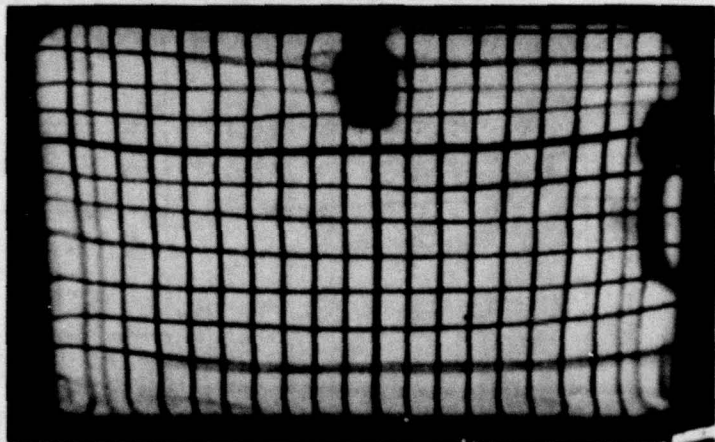
OVERLAY

Figure 64. Grid Board Photos for Specimen GY05.

GY03
INJECTION 30



GY04
INJECTION 32



GY05
INJECTION 34

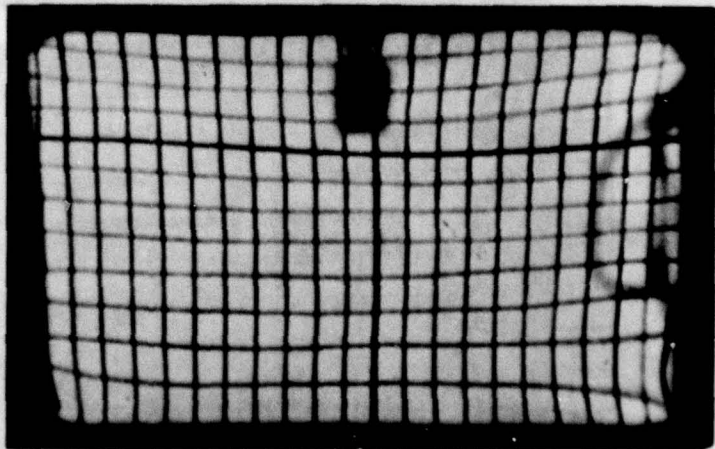
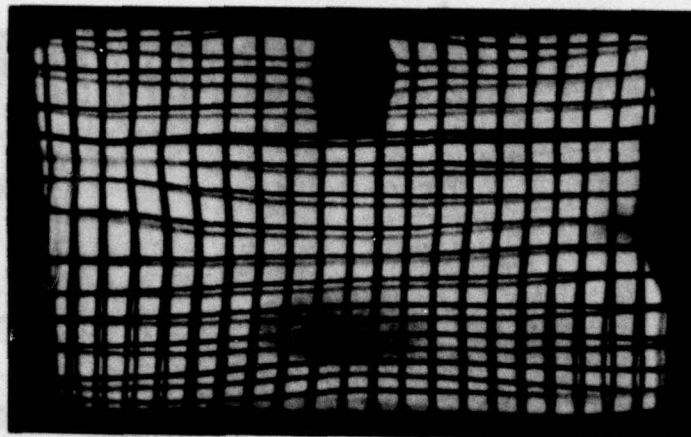
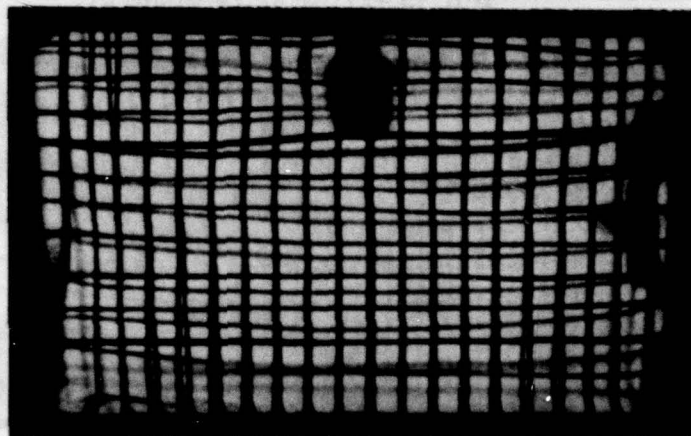


Figure 65. Tunnel Photos for Specimens GY03, GY04 and GY05 at Mach 2.4 (10-Minute Injection).

GY03
INJECTION 30



GY04
INJECTION 32



GY05
INJECTION 34

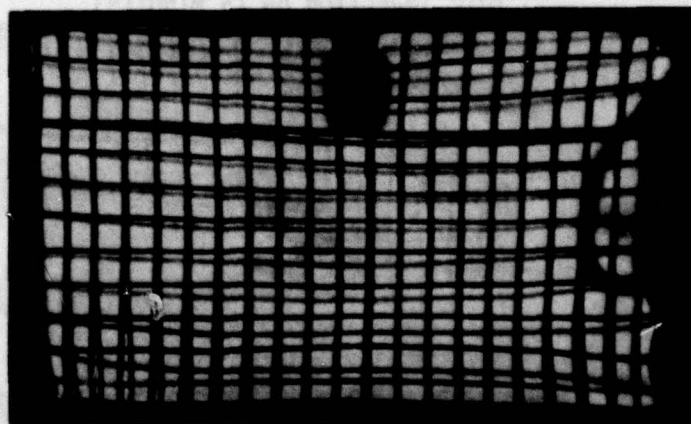
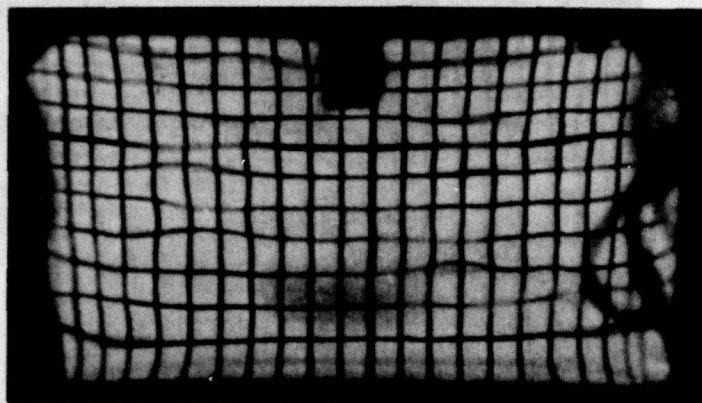
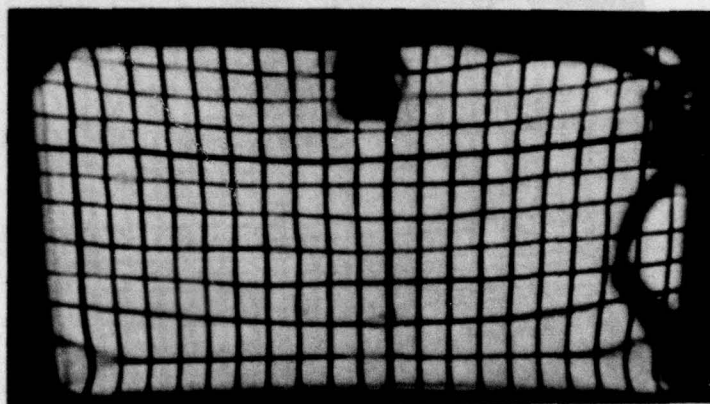


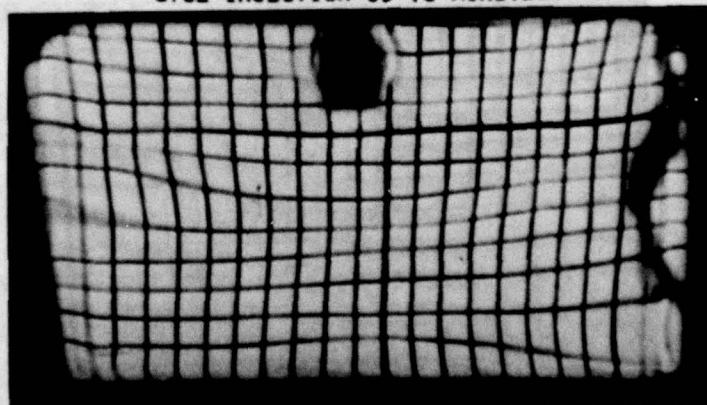
Figure 66. Overlays of Tunnel Photos for Specimens GY03, GY04 and GY05 at Mach 2.4 (10-Minute Injection).



GY01 INJECTION 67 (5 MINUTES)

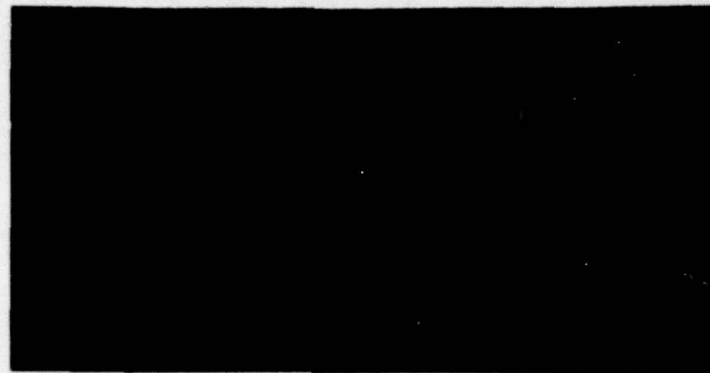


GY02 INJECTION 69 (5 MINUTES)



GY03 INJECTION 72 (5 MINUTES)

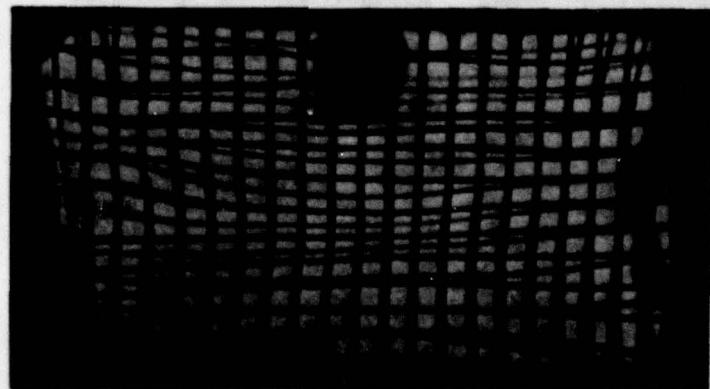
Figure 67. Tunnel Photos for Specimens GY01, GY02 and GY03 at Mach 2.6.



GY01 INJECTION 67 (5 MINUTES)

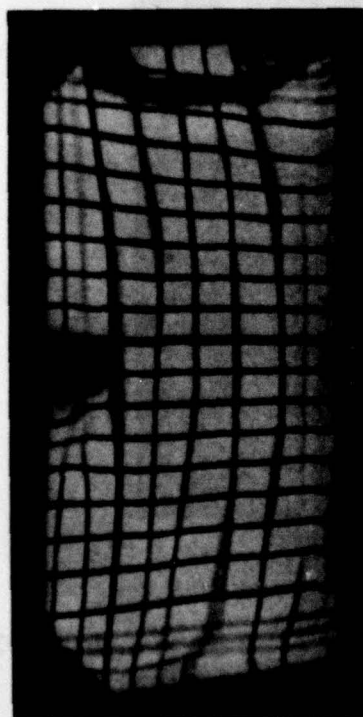


GY02 INJECTION 69 (5 MINUTES)

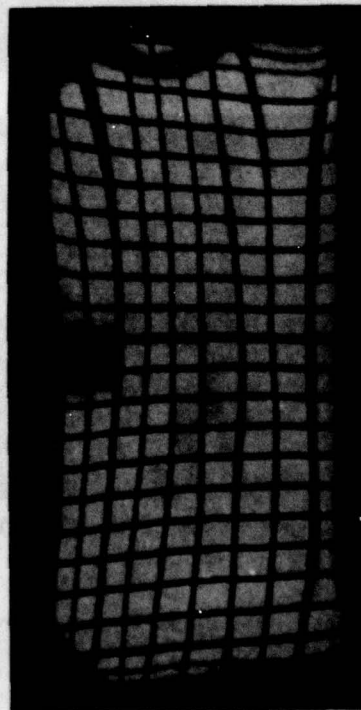


GY03 INJECTION 72 (10 MINUTES)

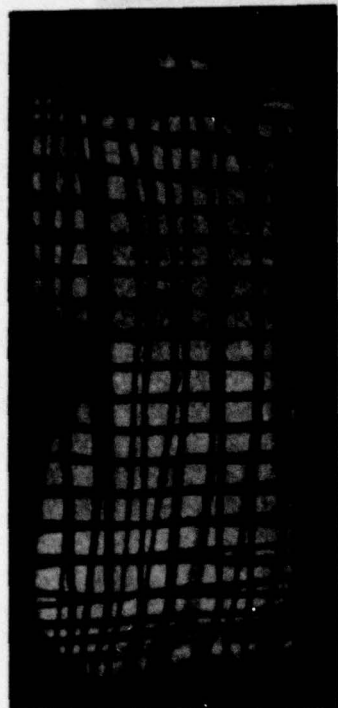
Figure 68. Overlay of Tunnel Photos for Specimen GY01, GY02 and GY03 at Mach 2.6.



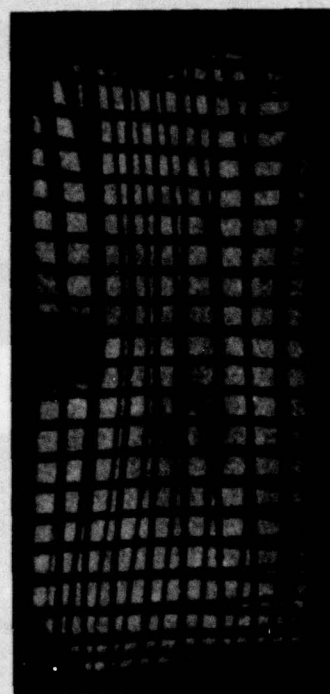
GY04 INJECTION 82



GY05 INJECTION 83



GY04 INJECTION 82



GY05 INJECTION 83

Figure 69. Tunnel Photos for Specimens GY04 and GY05 at Mach 3.0 (3-Minute Injection).

Figure 70. Tunnel Photo Overlays for Specimens GY04 and GY05 at Mach 3.0 (3-Minute Injection).

Seven-Ply Laminated Specimens

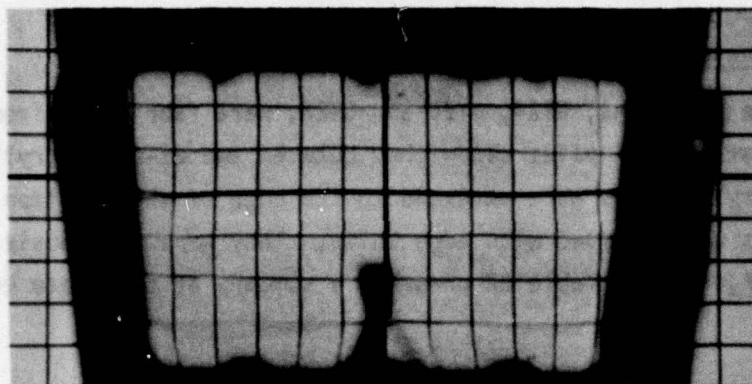
These three specimens, GY24, GY25 and GY26, were fabricated from two polycarbonate structural plies sandwiched between two as-cast acrylic plies. The acrylic plies were extended to the edge of the specimen and the seven plies were clamped with edge bolts. They were previously described in Figure 12. Table 22 presents a summary of the photo evaluation.

Pre-test and post-test grid board photos are shown in Figures 71 and 72 for Specimens GY24 and GY26. Overlays were not made because of the severity of damage to the specimens. Figure 73 shows tunnel photos for GY24, GY25 and GY26. Overlays are shown in Figure 74. These photos were taken during the 5-minute injection since the specimens delaminated during the subsequent 10-minute injection.

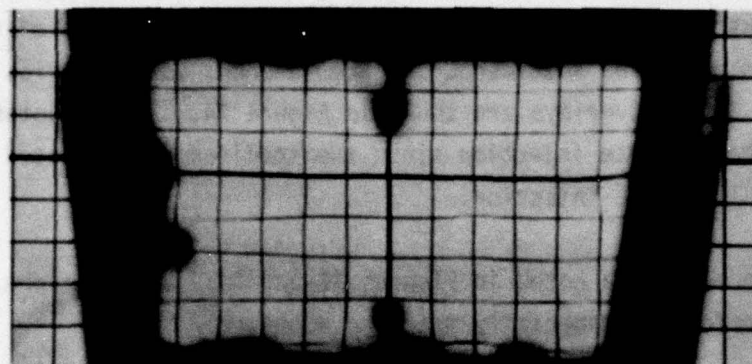
Line displacement, as noted in Figures 73 and 74, is not severe, but the lines are deformed, especially near the edges.

TABLE 22. EVALUATION OF GRID LINE PHOTOGRAPHS
FOR SEVEN-PLY LAMINATED SPECIMENS

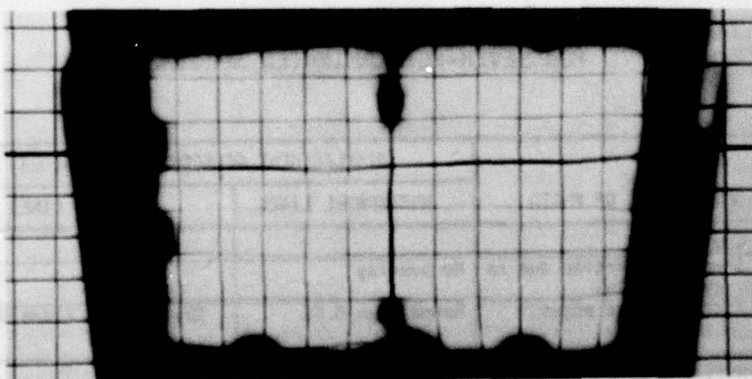
SPECIMEN	PHOTO TYPE	DESCRIPTION OF PHOTO	DISPLACEMENT OF GRID LINES (INCHES)	
			HORIZONTAL LINES	VERTICAL LINES
GY24	PRETEST	Hazy spots		
	POST-TEST	Severe distortion due to delamination	No overlay	
	M2.4	Distortion at edges. Lines wavy.	Bowed down 0.06	Bowed in at sides 0.06
GY25	PRETEST	Hazy spots		
	POST-TEST	Delamination lower half Distortion at edges	No overlay	
	M2.4	Distortion at edges Lines wavy.	Bowed down 0.06	Bowed in at sides 0.06
GY26	PRETEST	Hazy spots		
	POST-TEST	Delamination lower half Distortion at edges.	No overlay	
	M2.4	Distortion at edges and in center.	Bowed down 0.06	Bowed in at sides 0.06



GY24

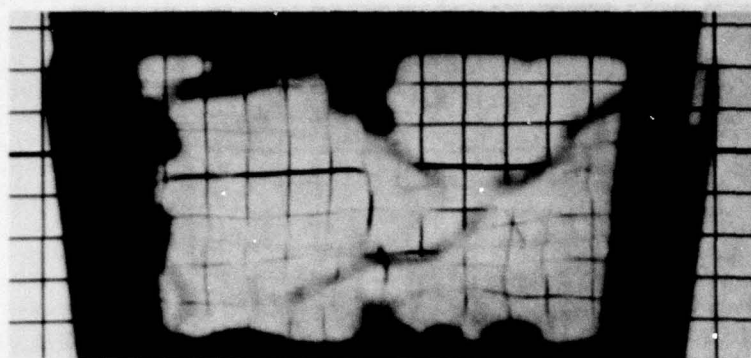


GY25

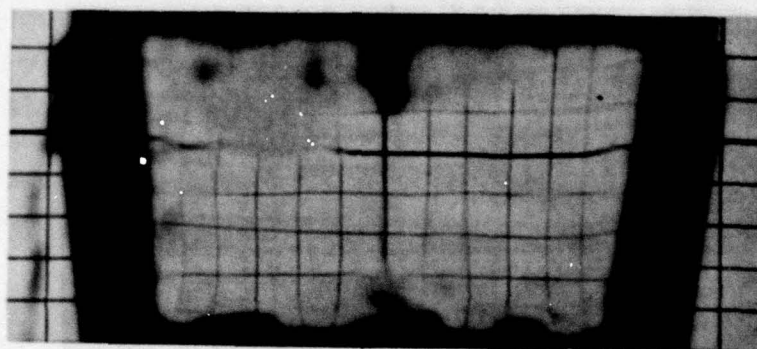


GY26

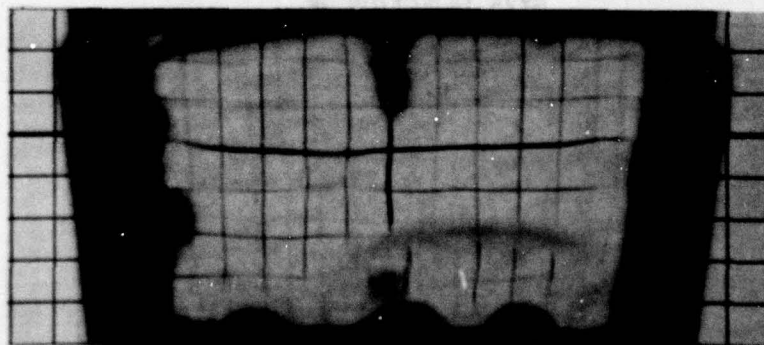
Figure 71. Pre-Test Grid Board Photos for Specimens GY24, GY25 and GY26.



GY24

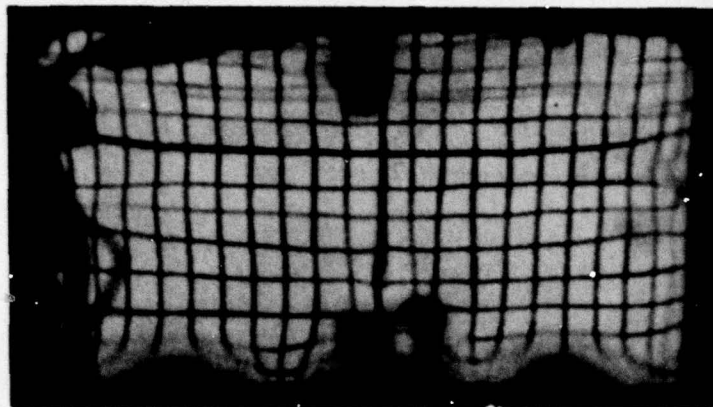


GY25

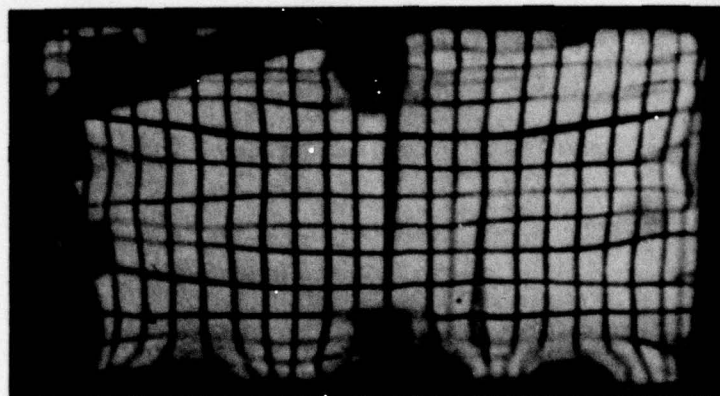


GY26

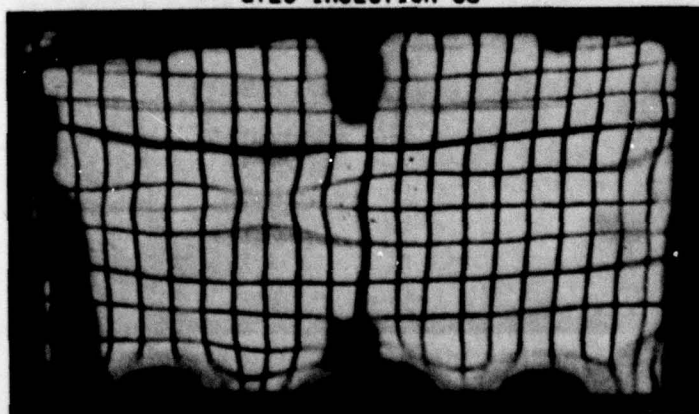
Figure 72. Post-Test Grid Board Photos for Specimens GY24, GY25 and GY26.



GY24 INJECTION 36

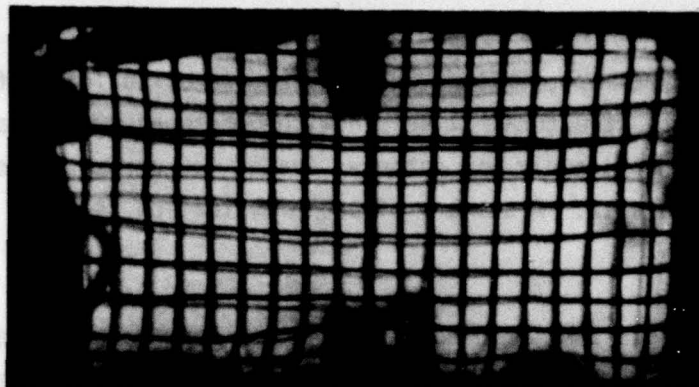


GY25 INJECTION 38

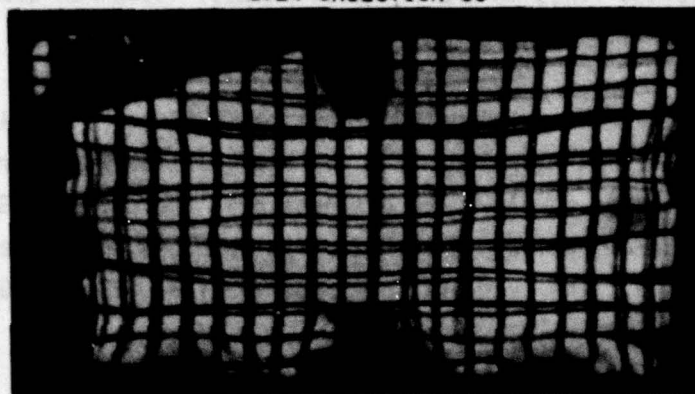


GY26 INJECTION 40

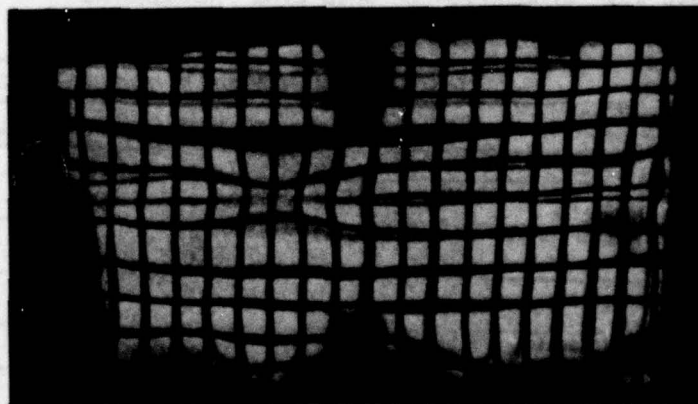
Figure 73. Tunnel Photos for Specimens GY24, GY25 and GY26 at Mach 2.4 (5-Minute Injection).



GY24 INJECTION 36



GY25 INJECTION 38



GY26 INJECTION 40

Figure 74. Overlays of Tunnel Photos for Specimens GY24, GY25 and GY26 at Mach 2.4 (5-Minute Injection).

Nine-Ply Laminated Specimens

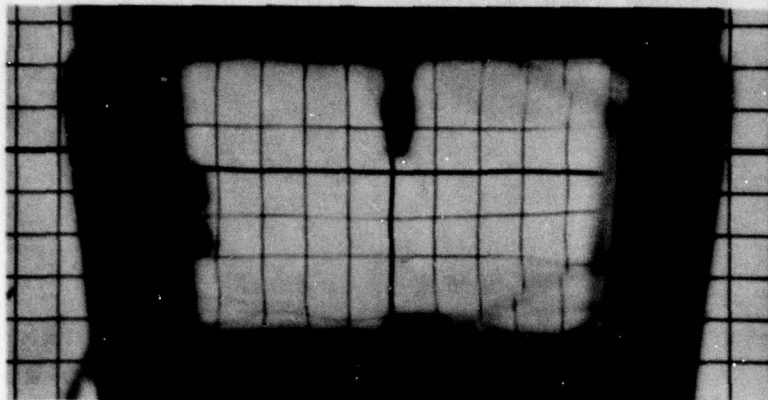
These three specimens, GY21, GY22 and GY23, were fabricated from three polycarbonate structural plies sandwiched between two as-cast acrylic plies. The face ply was rabbeted around the perimeter as shown previously in Figure 12. A summary of photo evaluation is given in Table 23.

Pre-test and post-test grid board photos are shown in Figures 75 and 76 for Specimen GY21, GY22 and GY23. These specimens exhibit hazy spots and indistinct lines on the pre-test photos. Specimen GY23 shows a definite loss of line clarity in its post-test photo.

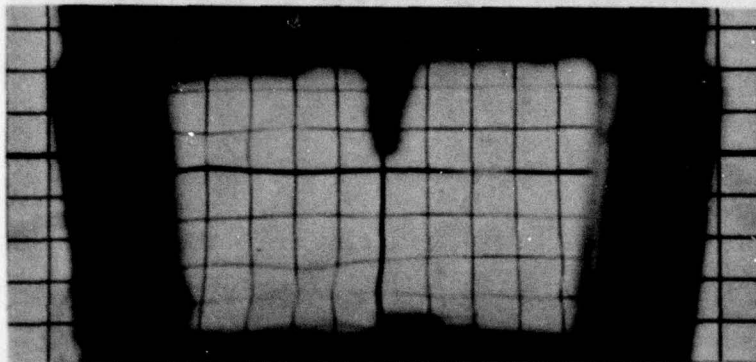
Figure 77 shows a tunnel photo for Specimen GY21 at Mach 2.4, GY22 at Mach 2.6 and GY23 at Mach 3.0. The photo of GY21 shows severe distortion due to cracks in the face ply. The distortion in the photo of GY22 is due to face ply delamination. The photo of GY23 shows poor line intensity and line distortion. The overlays for Specimen GY21, GY22 and GY23 were not clear.

TABLE 23. EVALUATION OF GRID LINE PHOTOGRAPHS
FOR NINE-PLY LAMINATED SPECIMENS

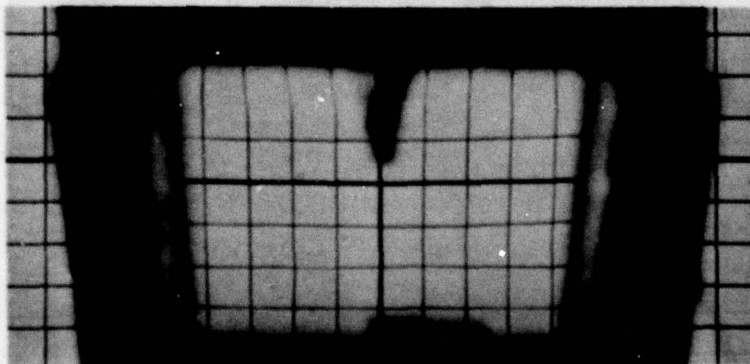
SPECIMEN	PHOTO TYPE	DESCRIPTION OF PHOTO	DISPLACEMENT OF GRID LINES (INCHES)	
			HORIZONTAL LINES	VERTICAL LINES
GY21	PRETEST	Hazy spots		
	POST-TEST	Severe distortion due to delamination	No overlay	
	M2.4	Lines distorted due to cracks	No overlay	
GY22	PRETEST	Hazy spots and wavy lines		
	POST-TEST	Severe distortion due to delamination	No overlay	
	M2.6	Distortion due to delamination	No overlay	
GY23	PRETEST	Hazy spots		
	POST-TEST	Lines obscure. Poor light transmission	No overlay	
	M3.0	Line distortion and poor line intensity	No overlay	



GY21

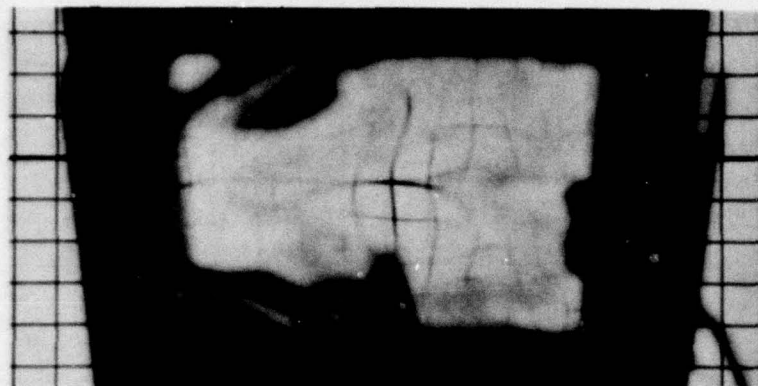


GY22

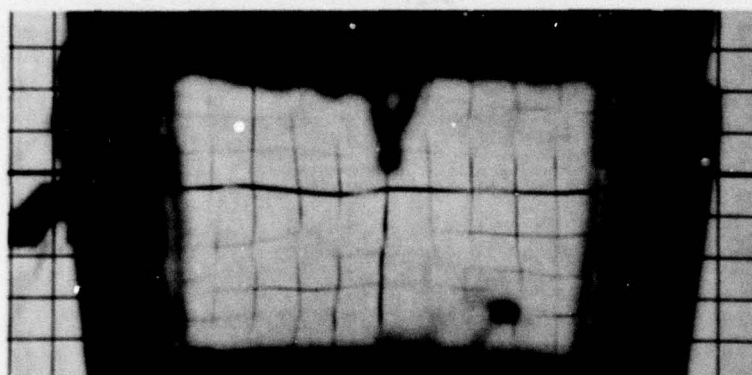


GY23

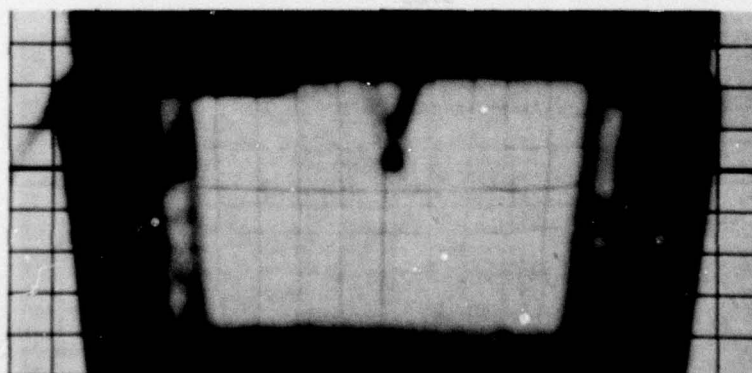
Figure 75. Pre-Test Grid Board Photos for Specimens GY21, GY22 and GY23.



GY21

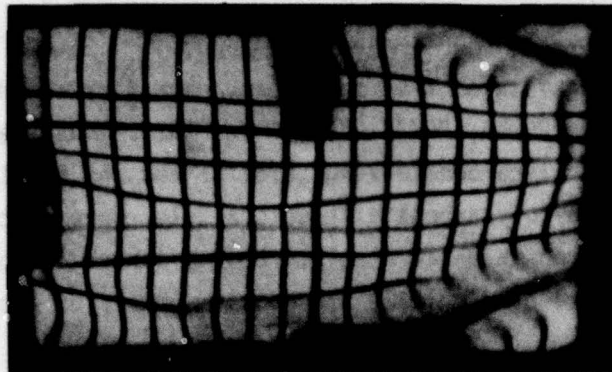


GY22

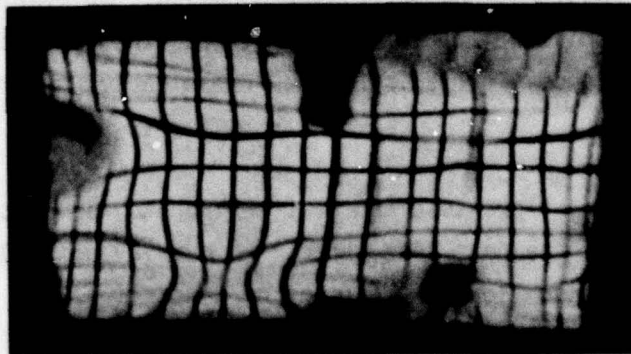


GY23

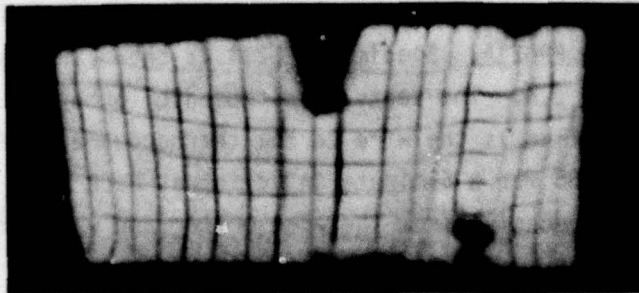
Figure 76. Post-Test Grid Board Photos for Specimens GY21, GY22 and GY23.



GY21, MACH 2.4, INJECTION 25 (5 MINUTES)



GY22, MACH 2.6, INJECTION 64 (10 MINUTES)



GY23, MACH 3.0, INJECTION 84 (3 MINUTES)

Figure 77. Tunnel Photos for Specimens GY21, GY22 and GY23.

Laminated Specimens with Glass Face Ply

This group consists of five specimens, each fabricated with a glass face ply: PPG21, PPG21A, PPG22, PPG22A and SK23. Specimens PPG21 and PPG21A, with two polycarbonate structural plies, and Specimens PPG22 and PPG22A, with a polycarbonate structural ply, were described in Figure 10. Specimen SK23 had a polycarbonate structural ply and was described in Figure 6. Table 24 presents a summary of photo evaluation.

Figure 78, 79, 80 and 81 show pre-test grid board photos and overlay photos for Specimens PPG21, PPG21A, PPG22 and PPG22A. The spots in the overlay photos resulted from interlayer bubbling. An overlay photo of PPG22 is not shown since it did not experience line displacement or distortion. The spot visible in Figure 78 was caused by a defect in the interlayer.

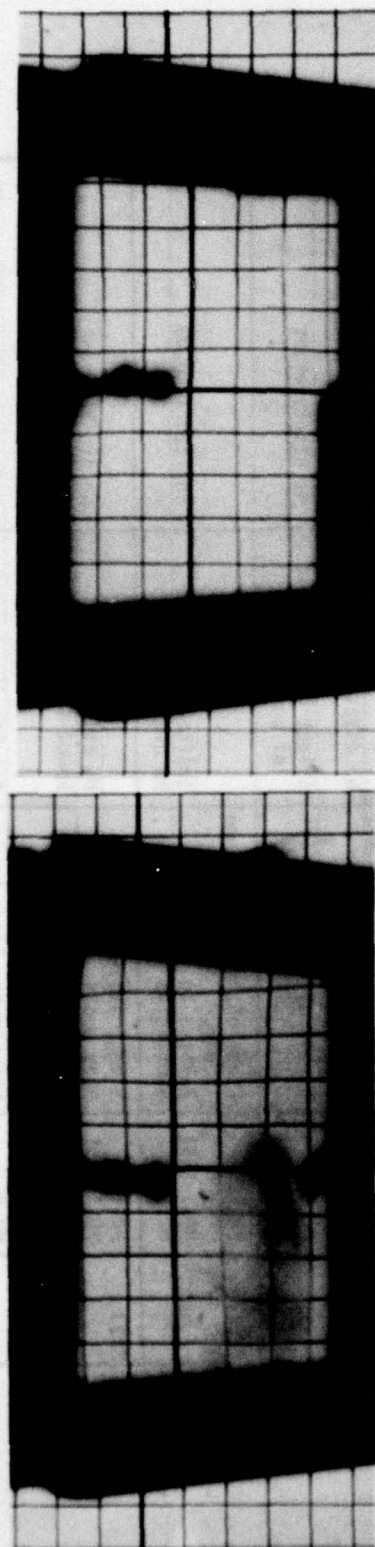
Figure 82 shows a pre-test and post-test photo for Specimen SK23. Haze is visible in the post-test photo. No overlay of SK23 is shown since it did not experience line displacement or distortion.

Figure 83 shows Specimen PPG21 at the completion of a 10-minute injection at Mach 2.4. Interlayer bubbling is visible at the perimeter. Loss of light transmission caused by interlayer bubbles prevented tunnel photos for Specimen PPG21A. Specimen PPG22A is shown in Figure 84 after 2.5 minutes at Mach 2.6. The spots were caused by bubbles in the interlayer. The curved line is the wire to the thermocouple. Specimen PPG22 is shown in Figure 85 for a 5-minute injection at Mach 2.4. The vertical line was caused by adhesive from the edge member and was removed with cleaning. PPG22 experienced slight line displacement.

Specimen SK23 is shown in Figure 86 at Mach 2.6 and Figure 87 at Mach 3.0. The spots in Figure 86 were caused by adhesive from the edge member. SK23 displays less line distortion at Mach 2.6 than at Mach 3.0. The haze visible in Figure 87 is also present in Figure 82.

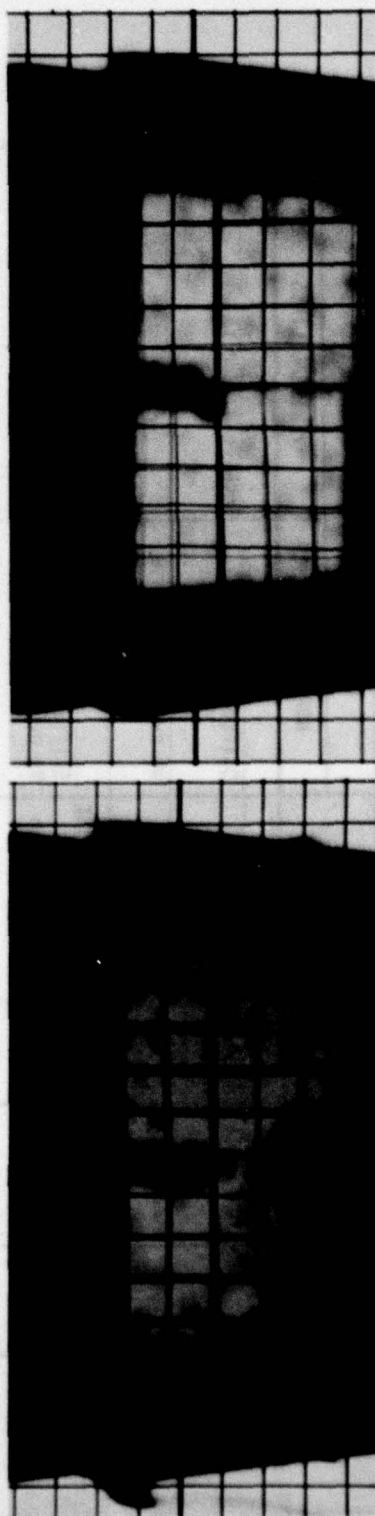
TABLE 24. EVALUATION OF GRID LINE PHOTOGRAPHS FOR
LAMINATED SPECIMENS WITH GLASS FACE PLY

SPECIMEN	PHOTO TYPE	DESCRIPTION OF PHOTO	DISPLACEMENT OF GRID LINES (INCHES)	
			HORIZONTAL LINES	VERTICAL LINES
PPG21	PRETEST POST-TEST	Hazy spot Lines straight. Spots due to bubbles in interlayer.	Shifted up 0.12 max.	Shifted in 0.12 max.
	M2.4	Bubbles in interlayer. Hazy spot	No overlay.	
PPG21A	PRETEST POST-TEST	Lines clear and straight Bubbles in interlayer Complete loss of vision due to bubbles in interlayer	Shifted up 0.06 No overlay	Shifted in 0.12 max.
	M3.0			
PPG22	PRETEST POST-TEST	Lines clear and straight Streak of adhesive on outer surface	No displacement	No displacement
	M2.4	Streak of adhesive	Slight displacement of one line.	No displacement
PPG22A	PRETEST POST-TEST	Lines obscure at extreme edge. Bubbles in interlayer	Shifted down 0.10 No overlay	Shifted in 0.03
	M2.6	Bubbles in interlayer		
SK23	PRETEST POST-TEST	Slight haziness Hazy spots Spots due to adhesive from edge spacer.	No displacement Bowed down 0.12 max.	No displacement Sides rotated out 0.18 max.
	M2.6	Lines bowed Hazy spots, lines bowed	One line bowed down	Sides rotated out 0.12
	M3.0			



PRE-TEST

POST-TEST



PRE-TEST

POST-TEST

Figure 78. Grid Board Photos for Specimen PG21. Figure 79. Grid Board Photos for Specimen PG21A.

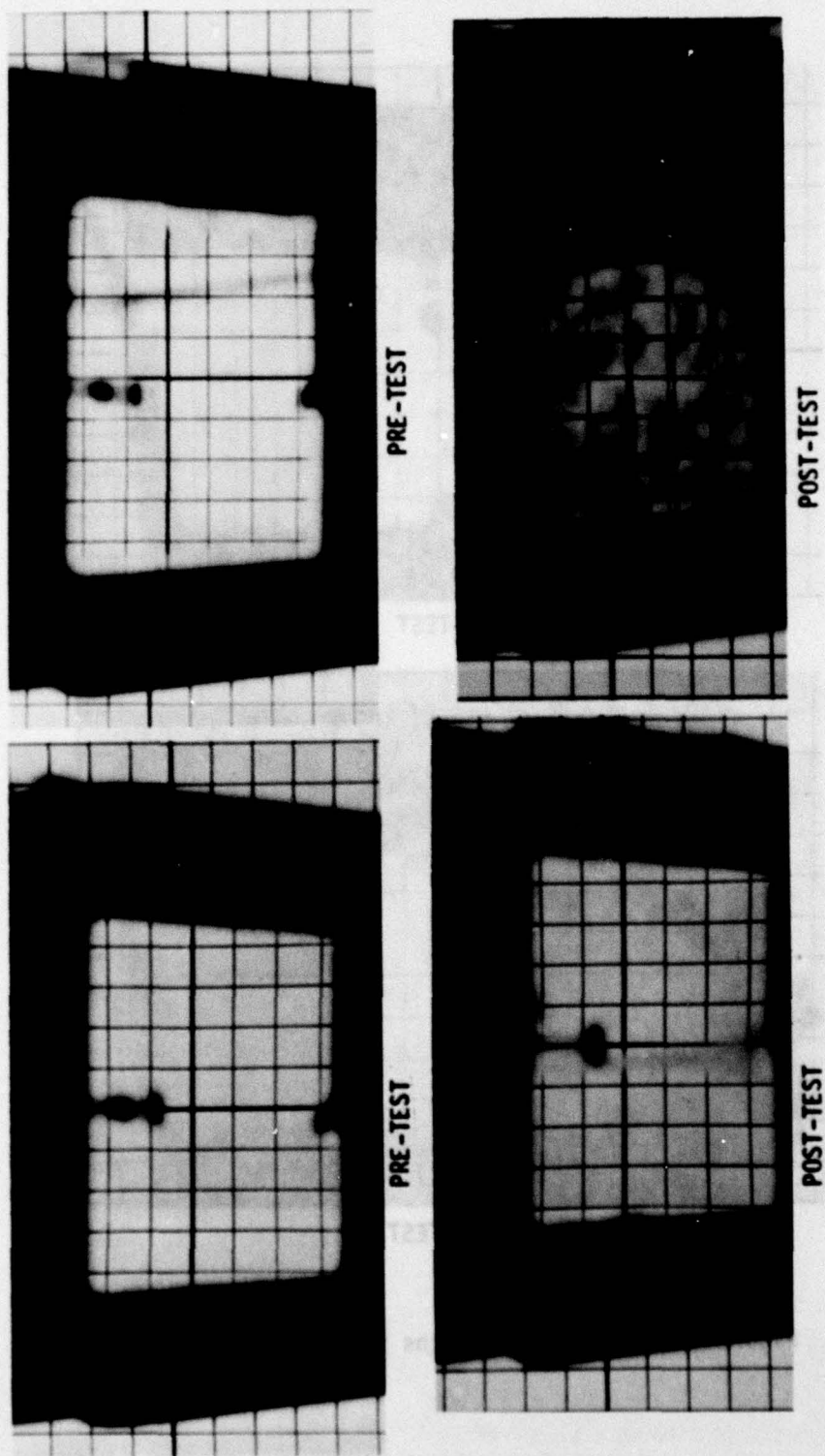
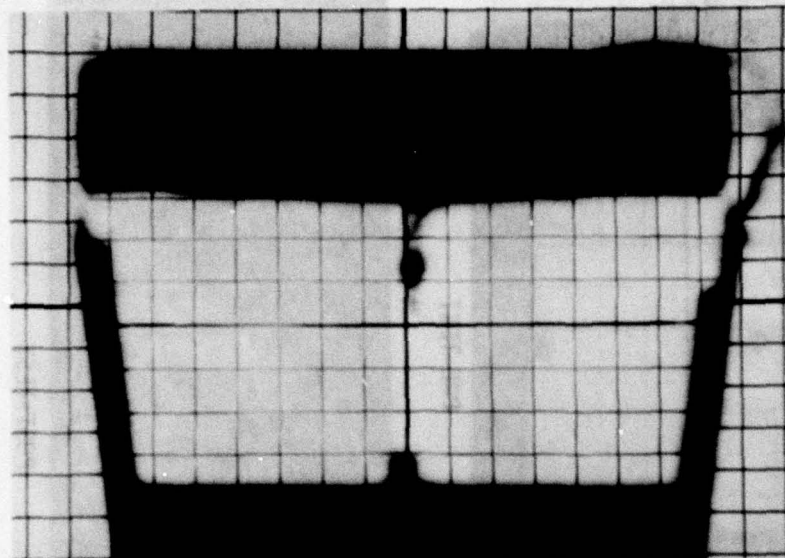


Figure 80. Grid Board Photos for Specimen PPG22. Figure 81. Grid Board Photos for Specimen PPG22A.



PRE-TEST



POST-TEST

Figure 82. Grid Board Photos for Specimen SK23.

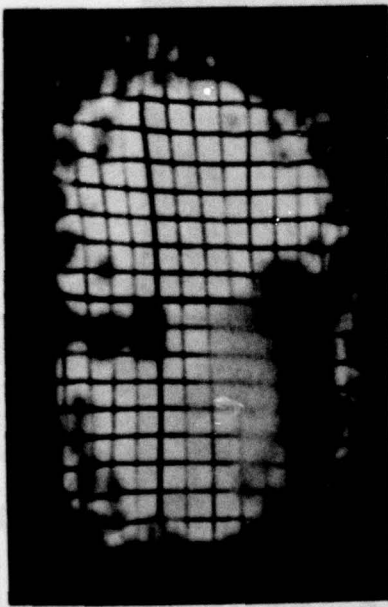
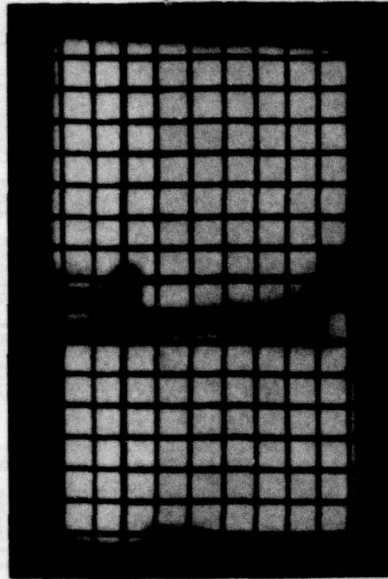


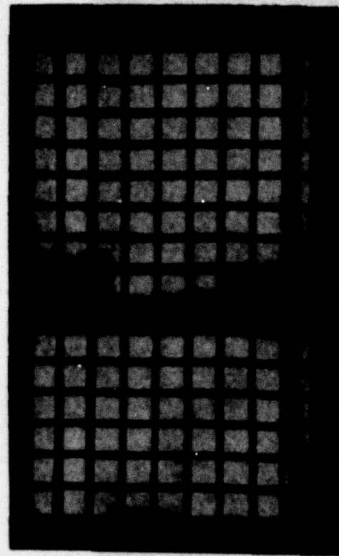
Figure 83. Tunnel Photo for Specimen PPG21 at Mach 2.4 (Injection 24, 10 Minutes).



Figure 84. Tunnel Photo for Specimen PPG22A at Mach 2.6 (Injection 66, 2.5 Minutes).

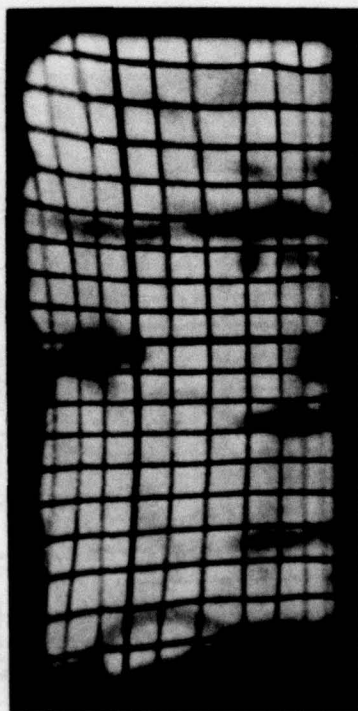


Tunnel Photo



Overlay

Figure 85. Tunnel Photo and Overlay for Specimen PPG22 at Mach 2.4 Injection 35 (5 minutes)

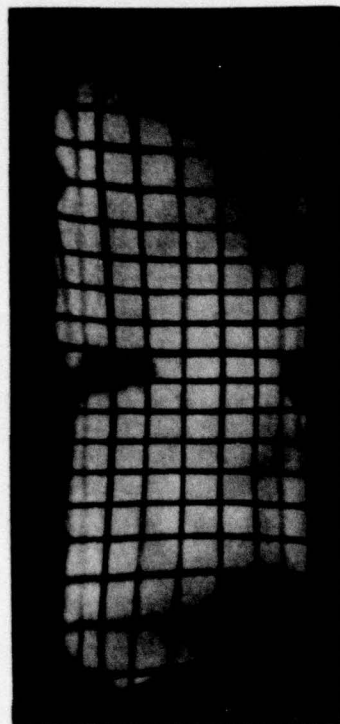


TUNNEL PHOTO

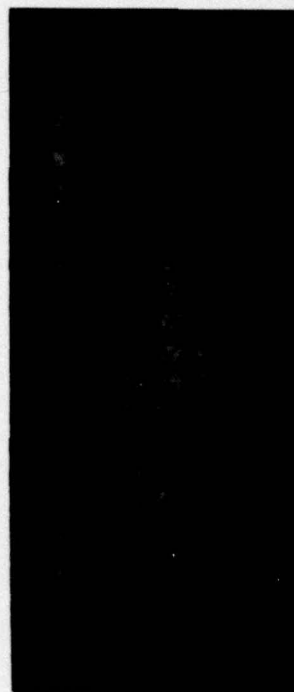


OVERLAY

Figure 86. Tunnel Photo and Overlay for Specimens SK23 at Mach 2.6 (Injection 56, 10 Minutes).



TUNNEL PHOTO



OVERLAY

Figure 87. Tunnel Photo and Overlay for SK23 at Mach 3.0 (Injection 78, 3 Minutes).

Monolithic Polycarbonate

The two specimens in this group, TEX21 and TEX21A, were fabricated from 1.00 inch coated polycarbonate. Table 25 is a summary of photo evaluation.

Figure 88 shows a pre-test and post-test photo for TEX21A. The pre-test appearance of TEX21 was similar to TEX21A. The hazy spots in the post-test photo of TEX21A are due to cracks in the exterior coating on the specimen. A post-test photo of Specimen TEX21 is not shown because the specimen sustained severe bubbling during its Mach 3.0 tunnel injection.

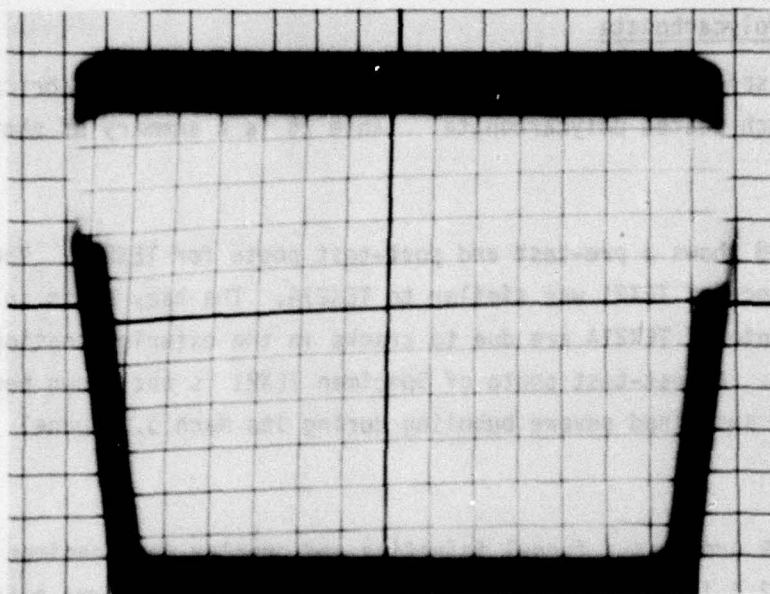
Figure 89 presents a tunnel injection and overlay for Specimen TEX21 at the Mach 2.4 injection. Haze is obvious in the right lower quadrant. Displacement of the horizontal lines is about 0.25 inch maximum.

Figure 90 is a tunnel photo of Specimen TEX21A at Mach 2.6. The lines are cracks in the exterior protective coating.

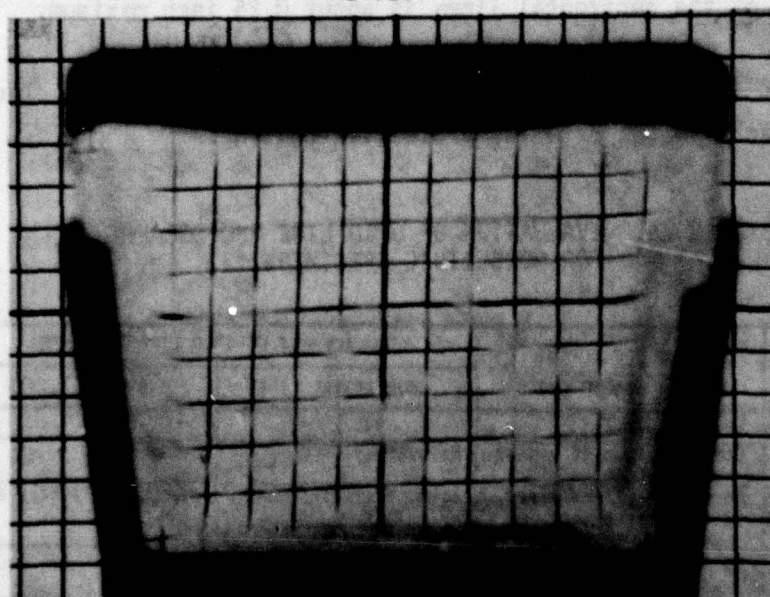
TABLE 25. EVALUATION OF GRID LINE PHOTOGRAPHS
FOR MONOLITHIC SPECIMENS (1)

SPECIMEN	PHOTO TYPE	DESCRIPTION OF PHOTO	DISPLACEMENT OF GRID LINES (INCHES)	
			HORIZONTAL LINES	VERTICAL LINES
TEX21	PRETEST	Slight haze (2)		
	POST-TEST	Complete loss of vision due to bubbles	No overlay	
	M2.4	Horizontal lines bowed. Lines clear except for two hazy spots	Bowed down 0.25 max.	Bowed in slightly at sides
	M3.0	Complete loss of vision due to bubbles	No overlay	
TEX21A	PRETEST	Slight haze		
	POST-TEST	Discontinuity in lines due to cracks in coating	No overlay	
	M2.6	Discontinuity in lines due to coating cracks	No overlay	

- (1) Specimen is monolithic polycarbonate, 1.00 inch thick.
(2) Photo not shown.

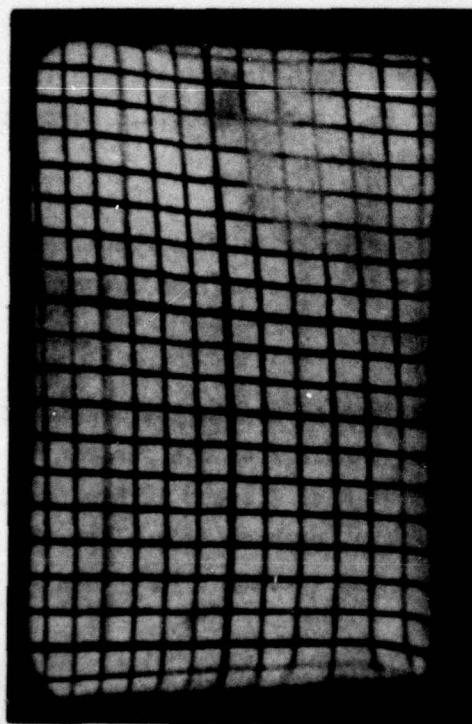


PRE-TEST



POST-TEST

Figure 88. Grid Board Photos for Specimen TEX21A.



TUNNEL PHOTO



Figure 89. Tunnel Photo and Overlay for Specimen TEX21 at Mach 2.4 (Injection 28, 10 Minutes).



Figure 90. Tunnel Photo for Specimen TEX21A at Mach 2.6 (Injection 65, 5 Minutes).

LIGHT TRANSMISSION AND HAZE

Table 26 is a compilation of light transmission and haze data for the test specimens. These values were measured by the participating vendors at the spots shown previously in Figure 20. Fifteen of the specimens were returned to the vendors for post-test readings. The values are the average of five readings. The angle of incidence for these measurements was zero degrees.

Five of the specimens (GY01, GY02, GY03, GY04 and GY05) had been tested previously per Reference 1.

Specimens PPG21 and PPG21A transmitted a significantly smaller amount of light than the other specimens. The pre-test readings were 49.8 percent and 54.5 percent. Specimens PPG22 and PPG22A had pre-test readings of 77.5 percent and 78.1 percent. No post-test readings were made for these specimens.

Specimen SWU22 was the only panel to show a significant decrease in light transmission, from a pre-test value of 85.1 percent to 73.3 percent. This loss is attributed to the use of thermal paint.

No specimen had a pre-test haze reading greater than 10 percent. Five specimens exceeded 10 percent after testing. The maximum change in haze was plus 6.9 percent for Specimen SWU22.

The average haze reading for the acrylic face plies was 10.75 percent for the two specimens (GY25 and GY26) tested at Mach 2.4, 6.5 percent for the two specimens (SK06 and GY01) tested at Mach 2.6 and 10.6 percent for seven specimens tested at Mach 3.0. For the urethane face plies the average haze reading was 5.85 percent for the two specimens (GY04 and GY05) tested at Mach 3.0.

TABLE 26. LIGHT TRANSMISSION AND HAZE DATA

	LIGHT TRANSMISSION (PERCENT) (1)			HAZE (PERCENT) (1)		
	PRE-TEST	POST-TEST	CHANGE	PRE-TEST	POST-TEST	CHANGE
SK05	87.6	85.2	-2.4	3.4	9.3	+5.9
SK06	87.9	86.8	-1.1	5.7	7.4	+1.7
SK21	87.0	84.3	-2.7	(3)	13.8	-
SK22	86.5	85.5	-1.0	(3)	11.1	-
SK23	85.1	85.5	+0.4	(3)	9.1	-
SWU21	85.7	84.9	-0.6	4.4	8.1	+3.7
SWU22	85.1	73.3	-11.8	4.8	11.7	+6.9
PPG21	49.8	(3)	-	5.5	(3)	-
PPG21A	54.5	(3)	-	2.6	(3)	-
PPG22	77.5	(3)	-	1.6	(3)	-
PPG22A	78.1	(3)	-	1.8	(3)	-
GY01 (2)	82.2	80.1	-2.1	6.2	5.6	-0.6
GY02 (2)	80.9	78.5	-2.4	6.3	5.1	-1.2
GY03 (2)	80.9	77.3	-3.6	6.4	5.4	-1.0
GY04 (2)	80.6	80.4	-0.2	5.9	6.3	+0.4
GY05 (2)	80.9	80.4	-0.5	4.0	5.4	+1.4
GY21	83.9	(3)	-	6.4	(3)	-
GY22	85.6	(3)	-	6.8	(3)	-
GY23	85.5	83.5	-2.0	9.8	11.2	+1.4
GY24	87.7	(3)	-	4.0	(3)	-
GY25	87.9	85.0	-2.9	6.0	12.5	+6.5
GY26	88.0	86.7	-1.3	4.7	9.0	+4.3
TEX21	82.22	(3)	-	2.1	(3)	-
TEX21A	82.22	(3)	-	2.1	(3)	-

- NOTES: (1) These values are the average of 5 readings made by each vendor.
 (2) These specimens were tested previously per Reference 1.
 These readings were made after the previous test.
 (3) No measurements were made.

SUMMARY

This summary of the specimen optical distortion is based on grid line photographs taken before the tests, during the tunnel exposure, and after the tests. A separate summary is presented for each of the test simulations of Mach 2.4, Mach 2.6 and Mach 3.0, and for the light transmission and haze data.

Distortion at Mach 2.4

Thirteen specimens were exposed to the Mach 2.4 environment. They are described as follows:

- (1) SK05, SK21 and SWU21 (3-ply, acrylic face ply).
- (2) GY03, GY04 and GY05 (5-ply, urethane face ply).
- (3) GY24, GY25 and GY26 (7-ply, acrylic face ply).
- (4) GY21 (9-ply, acrylic face ply).
- (5) PPG21 (5-ply, glass face ply).
- (6) PPG22 (3-ply, glass face ply).
- (7) TEX21 (monolithic polycarbonate).

Specimen PPG22 displayed the least distortion and line displacement of the 13 tested specimens (Figure 85). It was tested for only five minutes, however, since bubbles began to form in the interlayer. Specimen PPG21 was injected for five and ten minute exposures and was damaged by severe interlayer bubbling (Figure 83). Permanent distortion occurred as indicated by movement of the lines in the overlay photo (Figure 78). A heat resistant interlayer would be required to make these configurations acceptable for use at Mach 2.4. The pre-test light transmission reading for Specimen PPG21, 50 percent, makes it unacceptable for use as an aircraft windshield. PPG22 was better with a reading of 78 percent. These readings were the lowest of all specimens.

Specimen SK05 and SWU21 displayed good line clarity at Mach 2.4 and moderate horizontal line displacement. Specimen SK21 was distorted and some lines were obscured.

Specimens GY03, GY04 and GY05 withstood the Mach 2.4 environment very well. The lines were clear and dark (Figure 65). GY04 displayed some distortion along the sides. Generally, the horizontal line displacement (Figure 66) did not exceed 0.12 inch.

Specimen TEX21 survived a 10-minute injection in good shape. The lines were clear and dark except for a spot of haze (Figure 89). The displacement of the horizontal lines approaches 0.25 inch.

Specimen GY21 experienced severe delamination (Figures 86 and 77) which was precipitated by cracks in the face ply that occurred during fabrication.

Specimens GY24, GY25 and GY26 experienced small line displacement after their initial 5-minute injections, but the lines became irregular and distorted (Figures 73 and 74). The distortion along the lower edge of each specimen was due to the projection of the edge bolts into the field of vision at the 60 degree angle of incidence. The distortion would be less severe if these fasteners were removed. These three specimens failed by delamination of the exterior ply during this subsequent 10-minute injection. These specimens sustained comparatively large increases in haze.

Based on the optical photography results, Specimen SK05, SWU21, GY03, GY04, GY05 and TEX21 are viable candidates for Mach 2.4 windshields. Specimen SK21 had the same cross section as SWU21 and therefore should be considered, despite its poor performance. Specimens GY24, GY25 and GY26 could be windshield candidates if they had a different edge design. Specimen GY21 could not be evaluated because of cracks in the exterior ply. Specimen PPG21 and PPG22 cannot be considered as potential windshield candidates with the present interlayer and poor light transmission.

Distortion at Mach 2.6

The 12 specimens tested at Mach 2.6 are described as follows:

- (1) SK06, SK21, SWU21 and SWU22 (3-ply, acrylic face ply)
- (2) GY01, GY02 and GY03 (5-ply, acrylic or urethane face ply)
- (3) GY22 (9-ply acrylic face ply)
- (4) SK23 (3-ply, glass face ply)
- (5) PPG22A (3-ply, glass/glass ply)
- (6) TEX21A (monolithic polycarbonate).

The acrylic/silicone/polycarbonate configuration is a viable candidate for aircraft windshields that will operate at the Mach 2.6 level, as evidenced by the clarity of the tunnel photos for Specimen SK06 and SWU21 (Figures 56 and 57). Some distortion did occur along each side. Line displacement was about 0.25 inch maximum for the horizontal lines. Specimen SK21 and SK22 did not fare well. The photos showed irregular lines, distortion and loss of clarity. Specimen SWU22 could not be evaluated because the application of thermal paint prevented light transmission.

Specimens GY01 and GY02 and GY03 are potential windshield candidates for a Mach 2.6 environment. The tunnel photos (Figures 67 and 68) are for 5-minute injections since Specimen GY01 and GY02 delaminated at the termination of their 10-minute injections. GY03 survived. It sustained some distortion and the displacement of the horizontal lines was 0.25 inch maximum.

The poor optics for Specimen GY22 was caused by face ply delamination (Figure 77). The delamination was precipitated by a rupture in the rabbeted section of the face ply. This configuration would require a redesigned edge to be considered as a potential Mach 2.6 windshields.

Specimen SK23 sustained severe rotation of the vertical lines at the upper corners (Figure 86). The spots in the photo were caused by

adhesive flowing from the forward edge retainer. The lines in the center of the panel were clear and straight and this configuration is a potential candidate for Mach 2.6 aircraft.

Specimen PPG22A was affected by interlayer bubbling and would require a higher temperature interlayer to be considered for Mach 2.6 aircraft.

Specimen TEX21A was tested for 5 minutes at Mach 2.6. It sustained loss of vision due to the effect of the high temperature on the external protective coating. This effect occurred at the end of the injection.

Distortion at Mach 3.0

Eleven specimens were tested at Mach 3.0. These specimens are described as follows:

- (1) SK05, SK21, SK22, SWU21 and SWU22 (3-ply, acrylic face ply)
- (2) GY04 and GY05 (5-ply, urethane face ply)
- (3) GY23 (9-ply, acrylic face ply)
- (4) SK23 (3-ply, glass face ply)
- (5) PPG21A (5-ply, glass face ply)
- (6) TEX21 (Monolithic polycarbonate).

The optical clarity of Specimen SK05 and SWU21 make the acrylic/silicone/polycarbonate configuration a potential candidate for Mach 3.0 aircraft (Figures 58 and 59). Further studies are needed to define the cause of optical degradation experienced by similar specimens, SK21 and SK22. Specimen SWU22 could not be evaluated due to the application of thermal paint.

Specimen GY05 displayed acceptable optics at the Mach 3.0 condition (Figures 69 and 70). Specimen GY04 was distorted at the edges but clear in the center. The maximum displacement of the horizontal lines was 0.25 inch for both specimens.

Specimen GY23 became very cloudy and vision through this configuration was severely degraded. The face ply material became rough.

Specimen SK23 became hazy along both sides of the panel (Figure 87). Line distortion was severe at the edges but minimal in the center of the panel. The cloudiness eliminates this specimen from consideration as a potential Mach 3.0 windshield.

Vision through Specimen PPG21A was completely obscured by interlayer bubbling. It is not a potential Mach 3.0 windshield candidate.

Specimen TEX21 was completely ruined by bubbling on the exterior surface.

Light Transmission and Haze

The configuration represented by Specimen PPG21 and PPG21A is not considered to be a windshield candidate due to its relatively poor light transmission. The remaining configurations are acceptable for consideration.

Based on the limited haze data (12 of the 24 panels were measured), the urethane material is more resistant to haze than acrylic when used as a face ply.

SECTION VII

THERMAL EVALUATION

Windshield/canopy materials for supersonic aircraft must have the capability to survive the high temperatures experienced during the operation of the aircraft. A goal of this test program was to define the thermal environment for aircraft operating up to Mach 3.0. This goal was achieved by exposing 27 windshield test specimens to a Mach 2.4 through Mach 3.0 wind tunnel environment and recording the appropriate temperatures. An evaluation of the resultant thermal data is presented in this section.

This investigation addresses the following areas: specimen instrumentation, specimen temperature/time histories, exterior and interior transparency surface temperatures, the thermal insulating capability of the face ply/interlayer combinations, the effect of edge structure on temperature distribution, the potential heat conduction through a fastener, the heat conduction of a plastic insert compared to an aluminum insert, and the use of a thermal paint method to locate "hot spots".

INSTRUMENTATION

Twenty-five of the 27 potential test specimens were instrumented with thermocouples (the TEX specimens were not). Seven specimens (the SK0 and GY0 series) were instrumented with three thermocouples apiece, one external, one internal and one imbedded against the outer polycarbonate surface (Figures 3 and 4). Six specimens (the SK2 series) were instrumented with five thermocouples, one on the exterior surface and four imbedded (Figures 5 and 6). Twelve specimens (the SWU2, PPG2 and GY2 series) were instrumented with five thermocouples, two external, one internal and two imbedded (Figures 7 through 12).

Many of the thermocouples failed to adhere to the specimen surface and others did not function properly. The data that was collected is

presented in Tables 27, 28 and 29. Some values were extrapolated from temperature/time data. The specimen identifier, injection number, and length of exposure are listed. The temperatures are given in degrees Fahrenheit and are the first and last recorded temperature.

TEMPERATURE/TIME HISTORY

Temperature versus time was plotted for the 5 and 10 minute injections at Mach 2.4, 2.6 and 3.0 and the results are presented in Figures 91 through 99. These temperatures were recorded on the exterior surface, the interior surface, and the outer surface of the structural ply. The thermocouples were located 3.7 to 4.0 inches forward of the aft edge of each specimen. The exterior surfaces approached 90 percent of their peak temperature within the first minute of exposure and increased slowly thereafter. Generally, the exterior surfaces reached steady state in about 7 to 8 minutes. The interior and interface temperatures were steadily increasing at the termination of the 10-minute injections. Two 15-minute exposures (Injection 18 at Mach 2.4 and Injection 54 at Mach 2.6) showed that the interior and interface temperatures were increasing slowly at the end of the 15-minute exposures. The temperatures at the termination of Injection 18 was 148°F (Table 27), 15 degrees higher than at 10 minutes. The rate of change, 15 degrees in 5 minutes, indicated that the temperature was approaching steady state. The rate of change for the interface temperature was 9 degrees in 5 minutes, also indicating the approach of a steady state region.

Figures 91, 92, 93 and 94 represent the temperature/time histories for the 5 and 10-minute injections at Mach 2.4. The 15-minute injection of SK05 is shown because the external thermocouple did not function for the 5 and 10-minute injections. The exterior temperature rose quickly and surpassed 300°F within one minute. Generally, the exterior surface temperatures and the interior surface temperatures were similar for all specimens. The exception was the interior temperature for SK05. The interface temperatures varied with the thickness of face ply and inter-layer and with the material properties. The interior and interface

temperatures for the 10-minute injections were consistently higher than for the 5-minute injections because the initial temperature at time of injection was hotter. The specimens were cooled to 160°F between injections.

Temperature/time curves are presented in Figures 95, 96 and 97 for the 5 and 10-minute injections at Mach 2.6. The exterior surfaces heated rapidly and peaked at about 385°F. The interior surface and interface surface temperatures were increasing at the end of the injections. There was a variation in the interface temperature curves and the interior temperature curves for certain specimens.

Temperature/time curves are presented in Figures 98 and 99 for 3-minute injections at Mach 3.0. The exterior surfaces heated rapidly and approached or passed 500°F. The temperatures were rising at retraction of the specimen. The temperature of the interior surface reacted slowly.

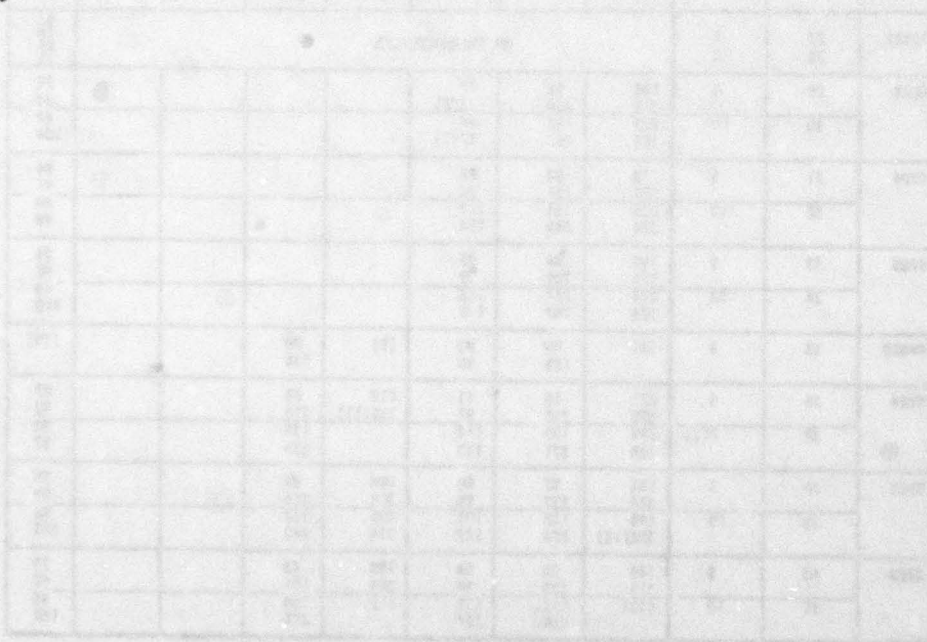


TABLE 27. TEMPERATURES AT MACH 2.4

SPECIMEN	INJECTION NUMBER	EXPOSURE TIME (MINUTES)	TEMPERATURE (°F)									
			AFT THERMOCOUPLES			FORWARD THERMOCOUPLES				CABIN		
			EXTERIOR	IMBEDDED	INTERIOR	EXTERIOR	IMM. CTR	IMM. LEFT	IMM. RIGHT			
			FIRST LAST	FIRST LAST	FIRST LAST	FIRST LAST	FIRST LAST	FIRST LAST	FIRST LAST			
SK05	16	5	101 (2)	104 247	80 96						71 71	
	17	10	(3)	136 276	111 133						79 79	
	18	15	132 329	143 285	118 148						80 97	
SK21	19	5		82 146	(2) 96	81 (1)	80 155	81 146	118 157		74 84	
	20	10		140 207			138 213	136 201	142 218		78 93	
SMU21	21	5	(1)	85 164	81 90	(3)	82 209				78 90	
	22	10		141 216	94 112	(3)	135 247				79 99	
PPG21	23	5	139 267(4)	78 113	83 88	163 316(5)	77 112				80 89	
	24	10		144 186	96 114		141 181				85 96	
GY21	25	5	206 336	(3) 193	86 193	210 323	81 193				80 89	
	26	10	(1)		102 119	225 337(6)	143 233				86 98	
TEX21	27	5	NO THERMOCOUPLES									87
	28	10										
GY03	29	5	198 319	82 224	77 77(7)						75 89	
	30	10	235 324	142 267	64 67(7)						87 104	
GY04	31	5	170 320	83 191	86 96						84 91	
	32	10	225 324	151 243	119 133						88 99	
GY05	33	5	190 319	84 209	86 99						85 92	
	34	10	214 323	167 260	122 138						89 100	
PPG22	35	5	(8)	80 125	80 95	(9)	80 135				(10)	
GY24	36	5	221 328	86 238	85 97	210 335(11)	85 218				87 92	
	37	7(2)	249 328	139 271	110 133		134 238				80 97	
GY25	38	5	192 316	87 237	80 96	209 324	84 215				75 97	
	39	10	249 322(12)	139 270	107 129	205 324	132 247				84 103	
GY26	40	5	189 316	85 205	84 94	196 319	83 191				79 92	
	41	10	(13)	147 254	111 127	(1)	130 225				85 102	

NOTES: (1) Lost Thermocouple immediately. (7) Apparent error
 (2) Withdrew at 7 minutes. Temperatures are extrapolated for 10-minute exposure. (8) Lost Thermocouple at 90 seconds
 (3) Inoperative Thermocouple. (9) Lost Thermocouple at 120 seconds
 (4) Lost Thermocouple at 27 seconds. (10) No data
 (5) Lost Thermocouple at 200 seconds. (11) Lost Thermocouple at 170 seconds
 (6) Lost Thermocouple at 243 seconds. (12) Lost Thermocouple at 380 seconds
 (13) Lost Thermocouple on previous retraction.

TABLE 28. TEMPERATURES AT MACH 2.6

SPECIMEN	INJECTION NUMBER	EXPOSURE TIME (MINUTES)	TEMPERATURE (°F)								CABIN
			AFT THERMOCOUPLES			FORWARD THERMOCOUPLES					
			EXTERIOR	IMBEDDED	INTERIOR	EXTERIOR	IMR-CTR	IMB-LEFT	IMR-RIGHT		
			FIRST LAST	FIRST LAST	FIRST LAST	FIRST LAST	FIRST LAST	FIRST LAST	FIRST LAST		
SK06	48	5	179 386	85 227	79 93					73 82	
	49	10	229 394	159 287	113 141					82 106	
SK21	50	5		85 164			84 178	84 167	83 180	76 92	
	51	10		168 239			168 252	165 240	171 256	83 106	
SK22	52	5		89 180		169 372	86 213	86 213	85 207	71 90	
	53	10		154 247		241 277	165 277	168 278	166 273	77 102	
	54	15		150 266		241 383	154 294	156 293	155 292	76 105	
SK23	55	5		90 186		163 333(2)	86 228	(3)	86 207	81 100	
	56	10		168 261			160 289	(3)	164 276	75 98	
SMU21	57	5	(4)	89 184	91 101	(4)	86 241			86 99	
	60	10		160 248	96 117		157 291			77 101	
SMU22	61	5	(4)	89 187	85 97	173 278	85 176			82 96	
	62	10		164 258	97 119	275 384	149 235			82 108	
GY22	63	5	227 382(5)	87 263	80 94	227 382(6)	85 259			71 91	
	64	6(1)		168 302	104 133		159 293			83 100	
TEX21A	65	5	NO THERMOCOUPLES								84 96
PPG22A	66	2(1)	155 343(7)	87 103	86 88	158 360(8)	84 108			84 88	
GY01	67	5	199 375	77 265	73 100					66 86	
	68	10	253 386	147 310	117 151					78 87	
GY02	69	5	200 381	79 226	81 108					79 94	
	70	10	250 385	157 334	127 161					85 94	
GY03	71	5	218 381	77 254	96 (3)					79 93	
	72	10	250 388	156 308	(3) (3)					82 105	

NOTES: (1) Withdrew early. Values extrapolated.
 (2) Lost Thermocouple at 19 seconds.
 (3) Inoperative Thermocouple.
 (4) Lost Thermocouple immediately.

(5) Lost Thermocouple at 44 seconds, extrapolated.
 (6) Lost Thermocouple at 64 seconds, extrapolated
 (7) Lost Thermocouple at 54 seconds.
 (8) Lost Thermocouple at 99 seconds.

TABLE 29. TEMPERATURES AT MACH 3.0

SPECIMEN	INJECTION NUMBER	EXPOSURE TIME (MINUTES)	TEMPERATURE (°F)							
			AFT THERMOCOUPLES			FORWARD THERMOCOUPLES				FIRST LAST
			EXTERIOR	IMBEDDED	INTERIOR	EXTERIOR	IMB-CTR	IMB-LEFT	IMB-RIGHT	
			FIRST LAST	FIRST LAST	FIRST LAST	FIRST LAST	FIRST LAST	FIRST LAST	FIRST LAST	
SK21	73	0.5		85 85			88 89	88 89	87 88	68 70
	74	3.0		117 163			121 181	116 167	122 186	71 86
SK22	75	0.5		76 78		238 437	83 90	82 87	83 90	69 72
	76	3.0		118 173		264 496	137 229	136 220	135 223	70 86
SK23	77	0.5		76 80			81 95	(2) (2)	(2) (2)	76 79
	78	3.0		127 203			140 250	(2) (2)	(2) (2)	79 94
SWJ21	79	3.0		77 159	82 89		81 242			81 94
SWJ22	80	2.0 (1)		74 194	84 92	280 500	81 158			82 91
PPG21A	81	1.5	153 333(3)	76 79	78 79	169 386	80 86			73 80
GY04	82	3.0	205 498	80 209	84 90					79 92
GY05	83	3.0	204 499	78 235	94 90					84 95
GY23	84	3.0	246 424(4)	77 202	81 85	(5) 245	83 245			79 91
SK05	85	3.0	276 510	77 306	81 86					79 91
TEX21	86	1.0	NO THERMOCOUPLES							81 82

NOTES: (1) Withdrew early. Temperatures are extrapolated for 3 minute injection.
 (2) Inoperative Thermocouple.
 (3) Lost Thermocouple at 29 seconds.
 (4) Lost Thermocouple at 9 seconds.
 (5) Lost Thermocouple immediately.

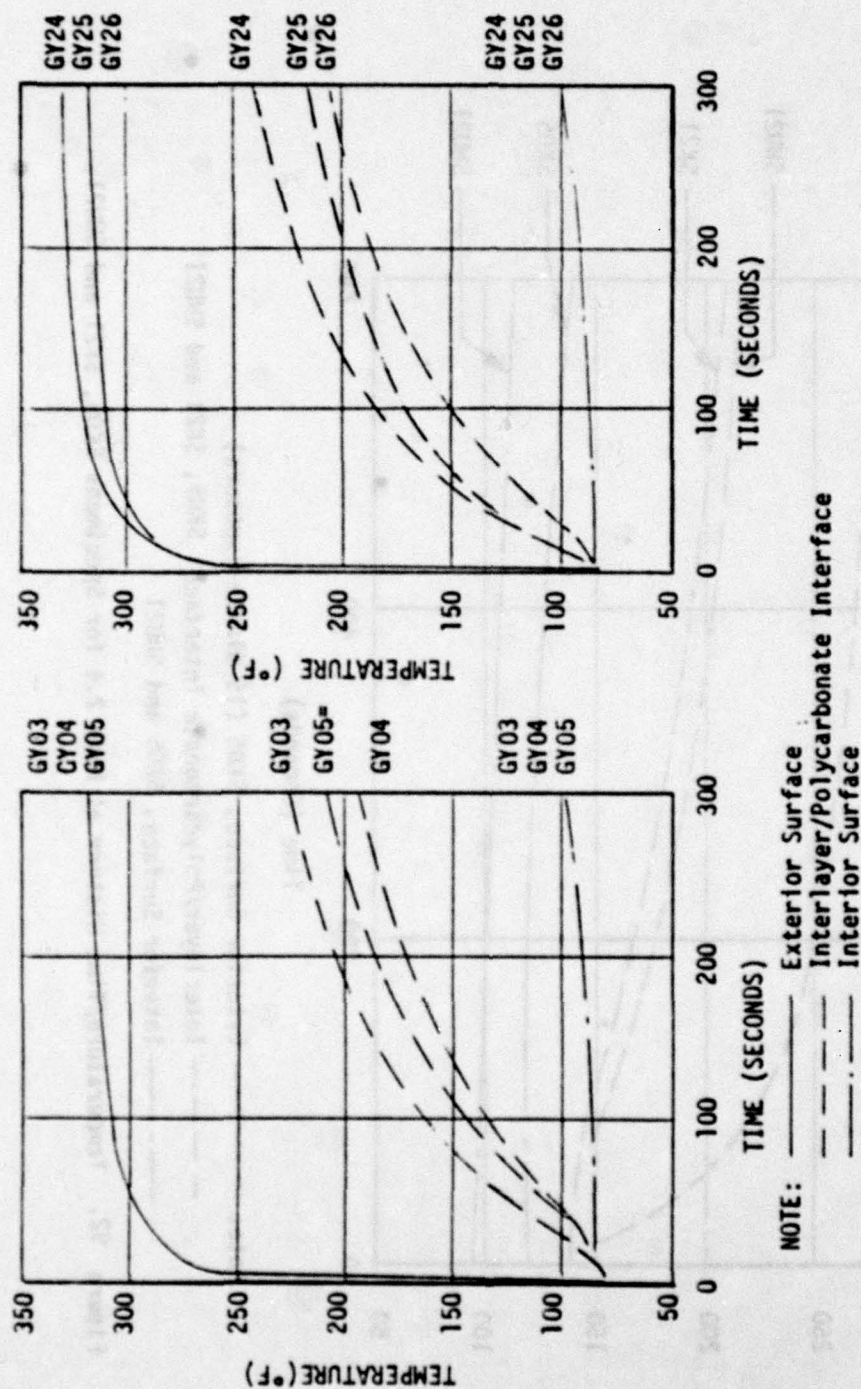
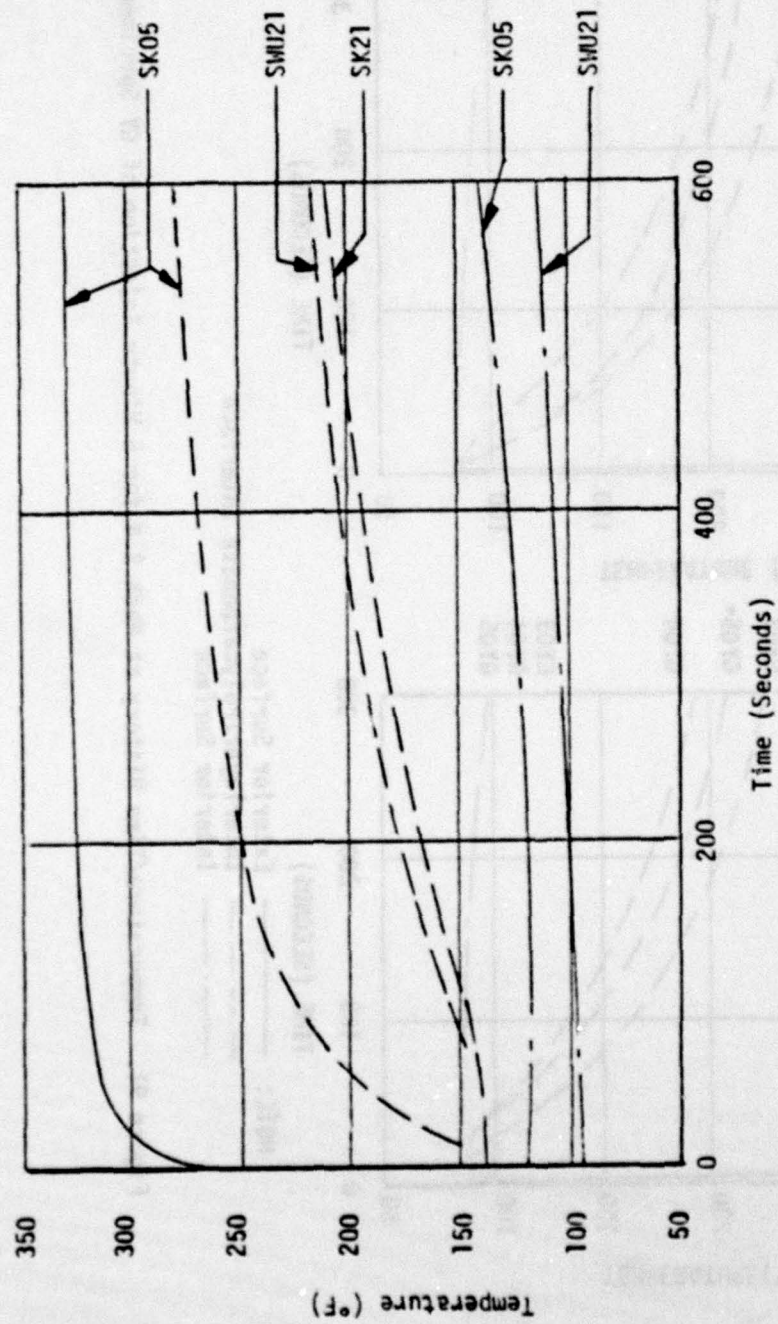
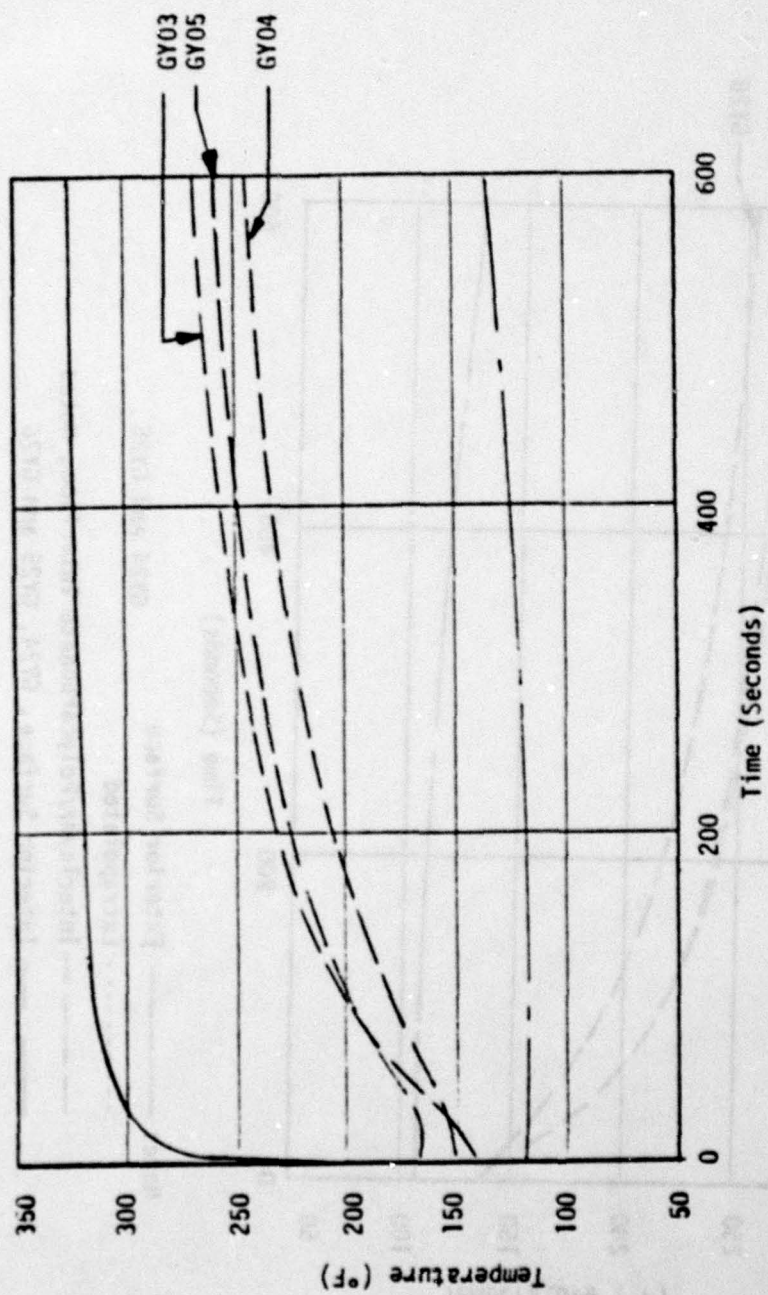


Figure 91. Temperature/Time History at Mach 2.4 for 5 Minute Injection of GY Specimens.



Note: — Exterior Surface, SK05 (15 minute exposure)
 - - - Interlayer/Polycarbonate Interface, SK05, SK21 and SHU21
 - . - Interior Surface, SK05 and SHU21

Figure 92. Temperature/Time History at Mach 2.4 for Specimens SK05, SK21 and SHU21.



Note: — Exterior Surface, GY03, GY04 and GY05
 - - - Interlayer/Polycarbonate Interface, Noted
 - . - Interior Surface, GY03, GY04 and GY05

Figure 93. Temperature/Time History at Mach 2.4 for 10-Minute Injections of Specimens GY03, GY04 and GY05.

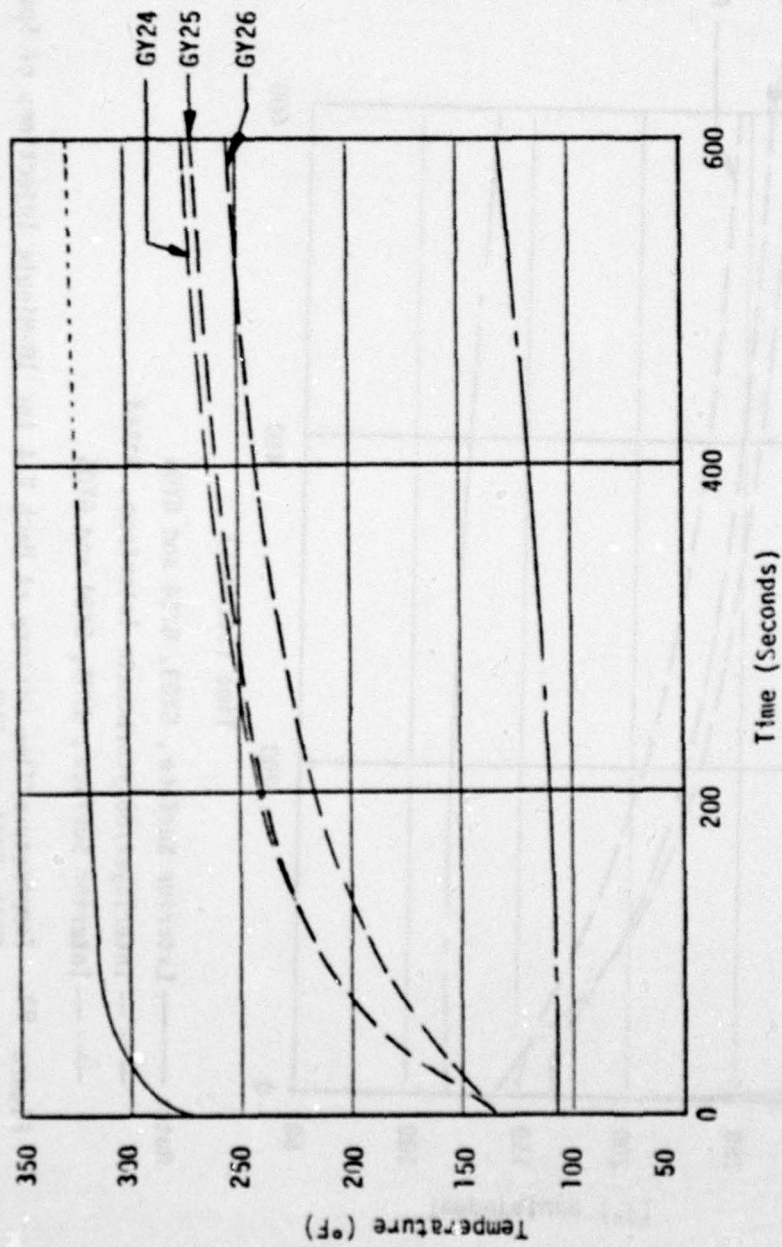


Figure 94. Temperature/Time History at Mach 2.4 for 10-Minute Injections of Specimens GY24, GY25 and GY26.

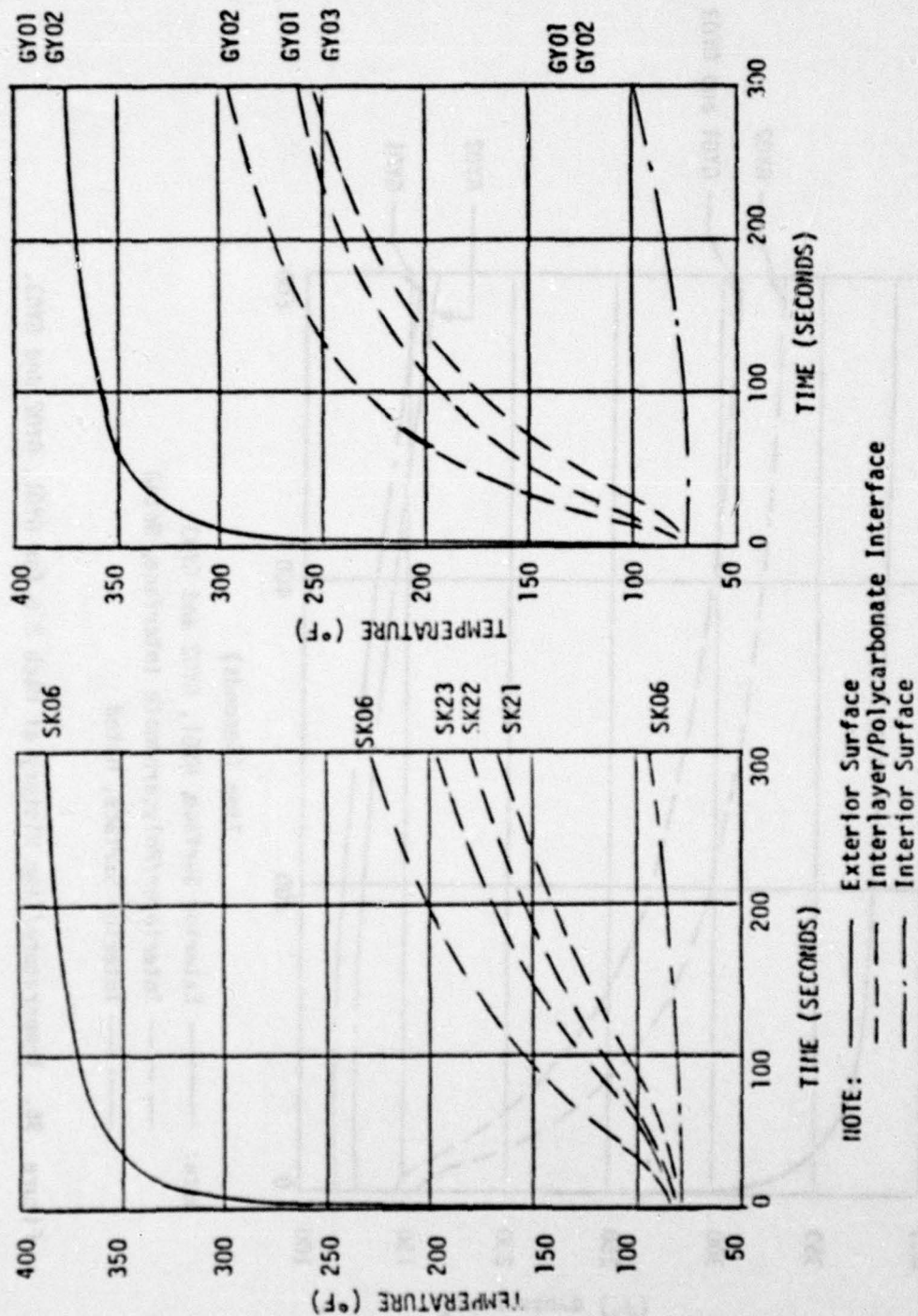


Figure 95. Temperature Time History at Mach 2.6 for 5 Minute Injections of SK and GY Specimens

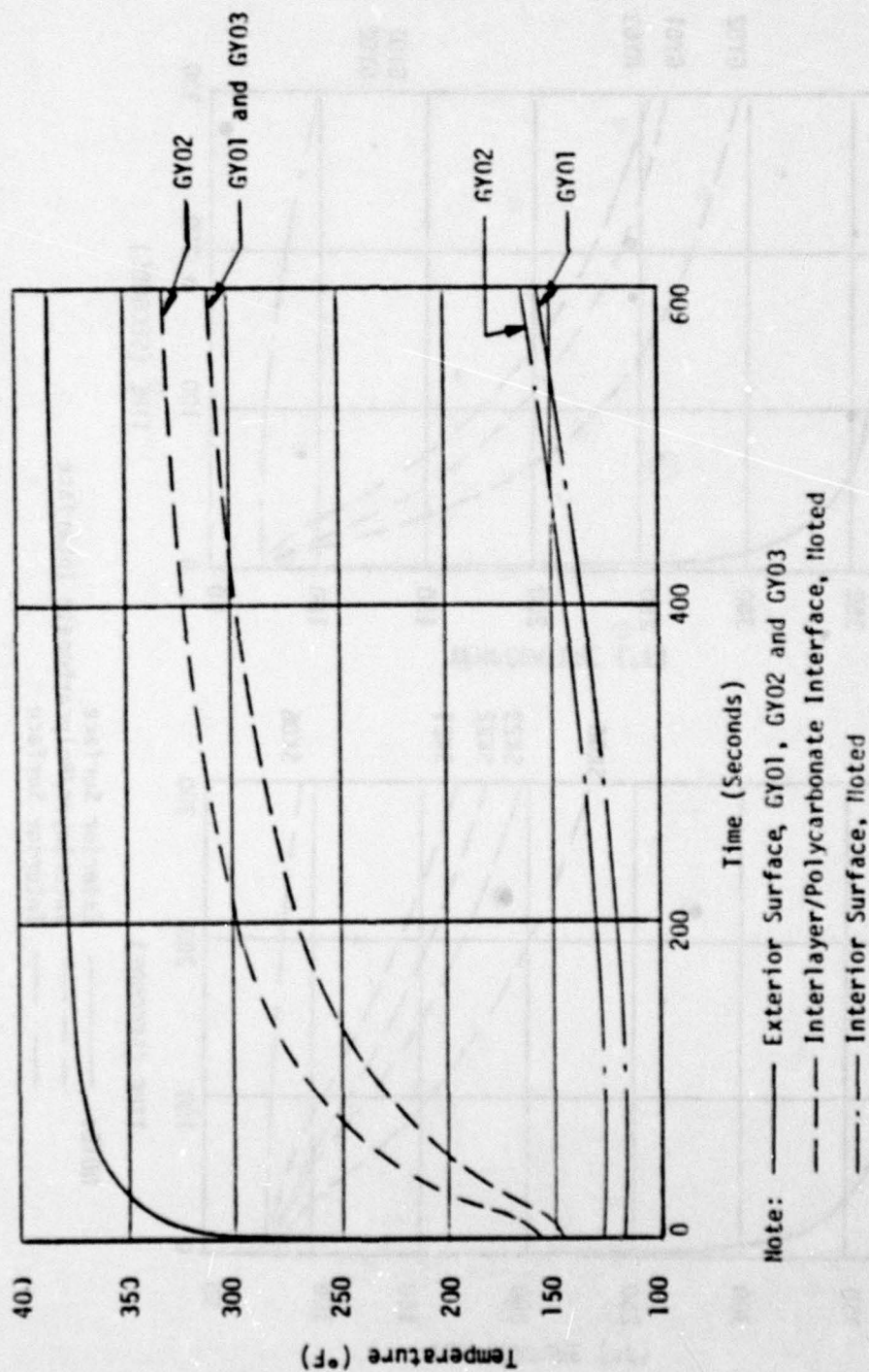


Figure 96. Temperature/Time History at Mach 2.6 for GY01, GY02 and GY03.

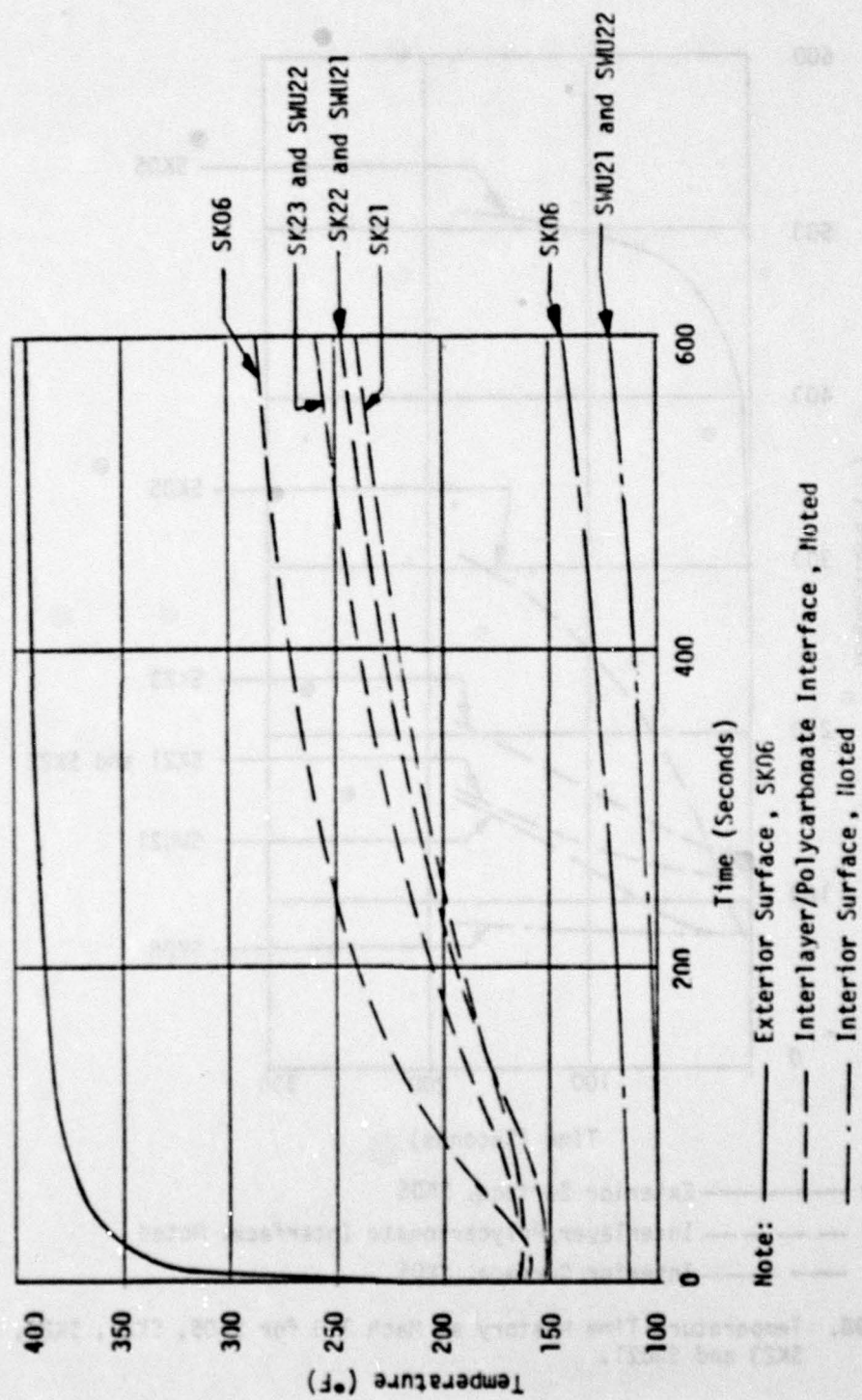
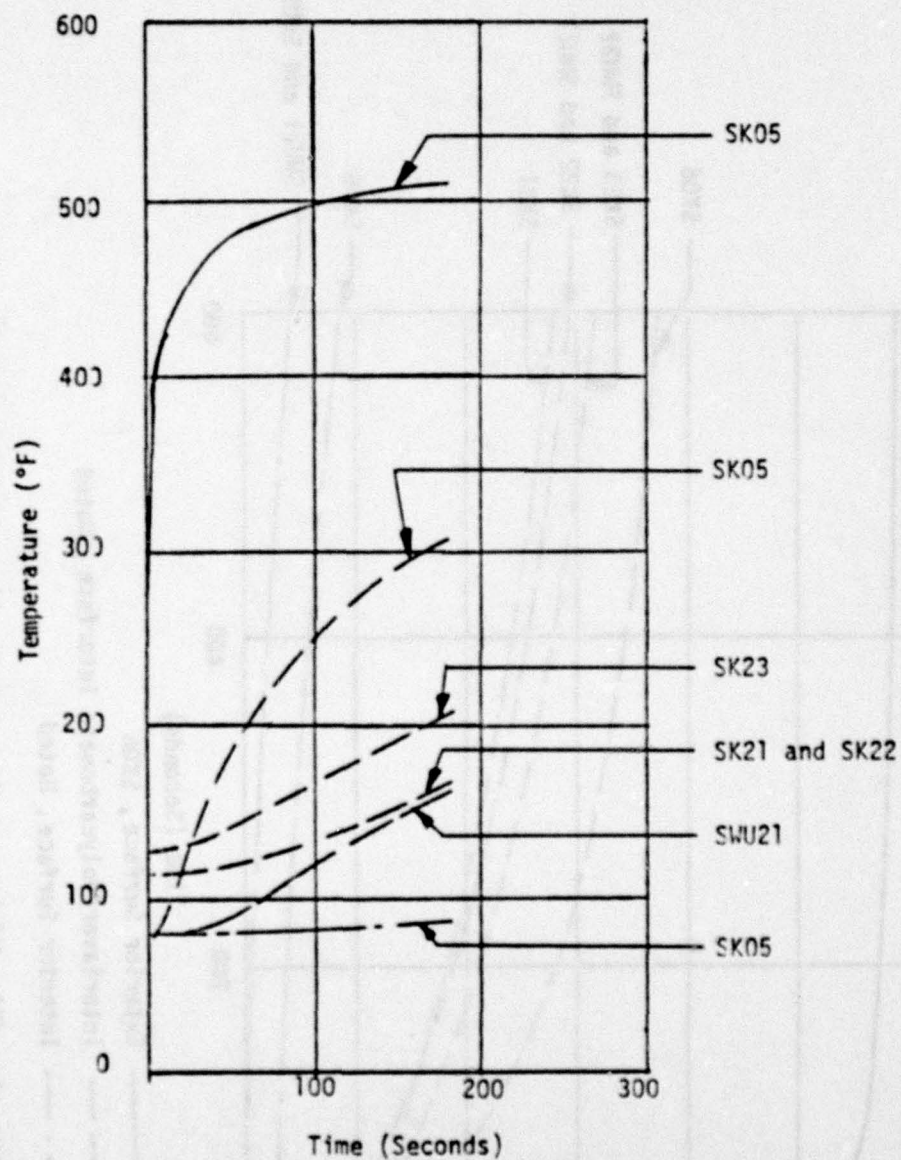
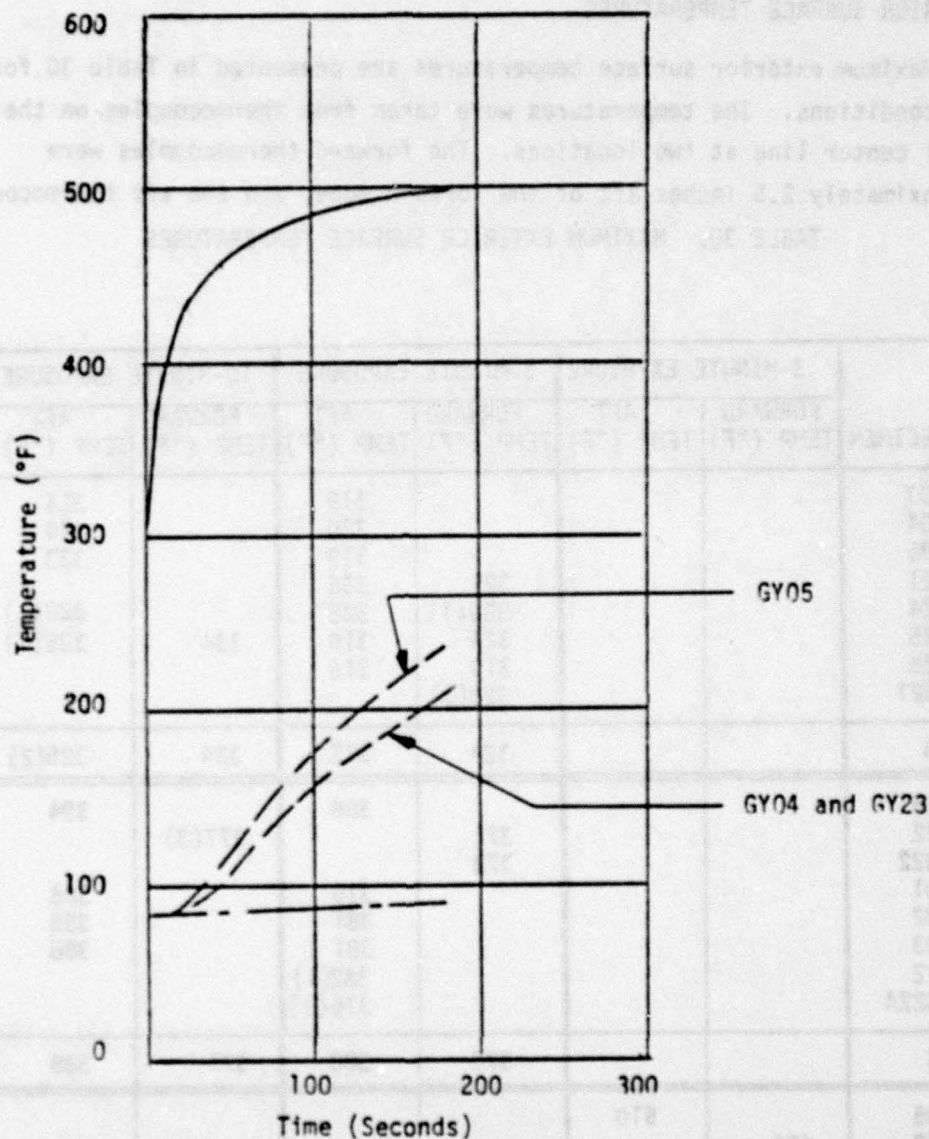


Figure 97. Temperature/Time History at Mach 2.6 for SK and SMU Specimens



Note: ——— Exterior Surface, SK05
 - - - - - Interlayer/Polycarbonate Interface, Noted
 — . — Interior Surface, SK05

Figure 98. Temperature Time History at Mach 3.0 for SK05, SK21, SK22, SK23 and SWU21.



Note: ——— Exterior Surface, GY04, GY05 and GY23
 - - - Interlayer/Polycarbonate Interface, Noted
 - . - Interior Surface, GY04, GY05 and GY23

Figure 99. Temperature/Time History at Mach 3.0 for Specimens GY04, GY05 and GY23.

EXTERIOR SURFACE TEMPERATURES

Maximum exterior surface temperatures are presented in Table 30 for all conditions. The temperatures were taken from thermocouples on the panel center line at two locations. The forward thermocouples were approximately 2.5 inches aft of the forward edge, and the aft thermocouples

TABLE 30. MAXIMUM EXTERIOR SURFACE TEMPERATURES

SPECIMEN		3-MINUTE EXPOSURE		5-MINUTE EXPOSURE		10-MINUTE EXPOSURE	
		FORWARD TEMP (°F)	AFT TEMP (°F)	FORWARD TEMP (°F)	AFT TEMP (°F)	FORWARD TEMP (°F)	AFT TEMP (°F)
MACH 2.4	GY03				319		324
	GY04				320		324
	GY05				319		323
	GY21			321	336		
	GY24			339(1)	328		323(1)
	GY25			324	316	334	325(1)
	GY26			319	316		
	PPG21			320(1)			
	AVG			324	322	334	325(2)
MACH 2.6	SK06				386		394
	SK22			372		377(3)	
	SWU22			378			
	GY01				376		386
	GY02				381		385
	GY03				381		388
	GY22				382(1)		
	PPG22A				376(1)		
	AVG			375	380	377	388
MACH 3.0	SK05		510				
	SK22	496					
	SWU22		500(1)				
	GY04		498				
	GY05		499				
	AVG	496	502				

- NOTES: (1) Temperature extrapolated from temperature/time curves.
 (2) Specimen SK05 registered 329°F at 15 minute exposure.
 (3) Specimen SK22 registered 383°F at 15 minute exposure.

were approximately 4 inches forward of the aft edge. For the Mach 2.6 and 3.0 conditions, the average aft temperatures were slightly higher than the forward temperatures. In all cases the test temperatures were less than the pre-test calculated temperatures which were computed by a proprietary heat transfer program using a nodal, transient, one-dimensional model. The calculated temperatures were:

349°F at Mach 2.4,

419°F at Mach 2.6, and

554°F at Mach 3.0.

These calculated temperatures are 7, 8 and 11 percent higher than the test temperatures recorded at Mach 2.4, 2.6 and 3.0 and the differences are attributed to discrepancies in the material properties used in the analysis. These results are consistent with the data presented in Reference 1 which reported higher calculated temperatures than test temperatures. The average test temperatures are plotted in Figure 100, together with the temperatures from Reference 1 for Mach 1.6, 2.0 and 2.2. The curve indicates an increase in the temperature/velocity ratio as the Mach number rises and is consistent with the theory.

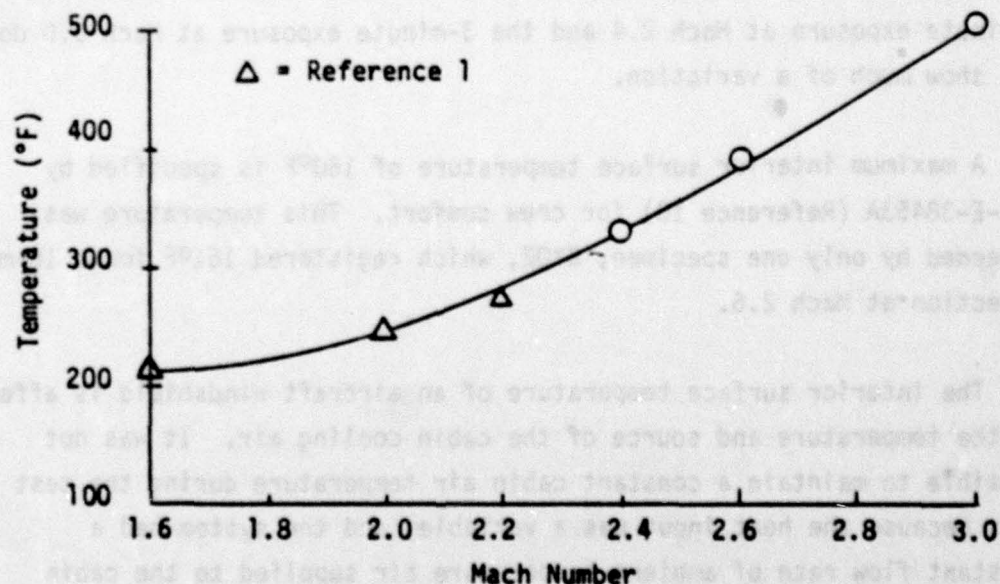


Figure 100. Average Maximum Surface Temperature Versus Mach Number.

Table 31 presents the exterior surface heat-up rate (in °F/second) for the initial injection of selected specimens. These values were calculated by dividing the change in temperature by the time increment for the first 5 seconds of exposure, for 5 to 50 seconds, and for 50 to 300 seconds. Face ply material is noted. As shown here and previously in Figures 91 through 99, the maximum surface heating occurred during the first few seconds of exposure and the rate of change rapidly dwindled after about 50 seconds. There does not appear to be a significant difference in heat-up rate for the two plastic materials, but the glass specimen (PPG22A) did heat up more slowly at Mach 2.6 than did the specimens with plastic face plies. This is consistent with the capability of the materials since the thermal conductivity of glass is approximately six times that of the plastic materials.

INTERIOR SURFACE TEMPERATURES

Maximum interior surface temperatures (cabin side) are listed in Table 32. The specimens are listed according to total thickness and indicate that the interior temperature did vary inversely with material thickness for the 10-minute exposures at Mach 2.4 and Mach 2.6. The 5-minute exposure at Mach 2.4 and the 3-minute exposure at Mach 3.0 do not show much of a variation.

A maximum interior surface temperature of 160°F is specified by MIL-E-38453A (Reference 10) for crew comfort. This temperature was exceeded by only one specimen, GY02, which registered 161°F for a 10-minute injection at Mach 2.6.

The interior surface temperature of an aircraft windshield is affected by the temperature and source of the cabin cooling air. It was not possible to maintain a constant cabin air temperature during the test runs because the heat input was a variable, and the system had a constant flow rate of ambient temperature air supplied to the cabin

TABLE 31. EXTERIOR SURFACE HEAT-UP RATE, INITIAL INJECTIONS ($^{\circ}\text{F}/\text{SECOND}$)

SPECIMEN	FACE PLY MATERIAL	MACH 2.4			MACH 2.6			MACH 3.0		
		0 to 50 Seconds	5 to 50 Seconds	50 to 300 Seconds	0 to 5 Seconds	5 to 50 Seconds	50 to 300 Seconds	0 to 5 Seconds	5 to 50 Seconds	50 to 180 Seconds
SK05	Acrylic									
SK06										
GY21		33.2	1.14	0.130	38.8	1.77	0.108	61.2	2.1	0.25
GY22						(1)				
GY24		35.9	1.02	0.071						
GY25		33.4	1.11	0.048						
GY26		32.7	1.11	0.068						
GY01	Urethane				39.7	1.53	0.120			
GY02					39.5	1.71	0.112			
GY03		33.0	1.13	0.080	41.2	1.56	0.112	50.6	2.8	0.31
GY04		31.5	1.31	0.084				51.1	2.8	0.29
GY05		32.0	1.24	0.076						
PPG22A	Glass				28.8	2.35	(1)			

NOTE: (1) Lost Thermocouple.

simulator and then discharged into the tunnel free stream. The result was that the measured cabin air temperature typically varied from about 75 to 108°F during a 10-minute test cycle. In an aircraft it would be possible to control the temperature of the cabin air supply, although the source of cooling air would not be located as close to the transparency as for this test model.

The temperature at the beginning of each 10-minute injection was higher than at the beginning of the 5-minute injection since the specimens had cooled to approximately 160°F between injections as measured by the imbedded thermocouples. In all cases the interior surface temperature was climbing at the completion of each injection. Specimen SK05 was injected for 15 minutes and registered 148°F at retraction. This is 15°F higher than at the termination of the 10-minute run. The rate of change, 15 degrees in 5 minutes, indicates that the temperature was approaching steady state.

TABLE 32. MAXIMUM INTERIOR SURFACE TEMPERATURES (°F)

SPECIMEN	TOTAL THICKNESS (INCHES)	MACH 2.4		MACH 2.6		MACH 3.0
		INJECTION TIME		INJECTION TIME		INJECTION TIME
		5 MIN	10 MIN	5 MIN	10 MIN	3 MIN
GY01	0.68			100	151	
GY02	0.68			108	161	
GY04	0.74	96	133			90
GY05	0.74	99	138			90
GY24	0.74	97	133			
GY25	0.74	95	129			
GY26	0.808	94	127			
SK05	0.825	96	133			86
SK06	0.825			93	141	
SWU21	0.933	90	112	101	117	89
SWU22	0.933			97	119	92
PPG22	0.94	95				
PPG22A	0.94					
GY21	1.03	93	119			
GY22	1.03			94	133	
GY23	1.10					35
PPG21	1.25	88	114			

THERMAL RESISTANCE OF FACE PLY/INTERLAYER MATERIAL

Most of the test specimens were fabricated with a structural ply of polycarbonate material. The strength of polycarbonate diminishes as the temperature increases. Hence, it was desirable to measure the heat resistance of the face ply/interlayer combinations and their ability to protect the polycarbonate ply.

Thermocouples were imbedded in the specimens (all except TEX21 and TEX21A) adjacent to the outer surface of the polycarbonate structural ply to provide the appropriate temperature data. The thermocouples were located about 4 inches from the aft edge on the center line. The material thermal conductivity was used to calculate thermal resistance, defined as the thickness of the material divided by its thermal conductivity ($\text{HR-FT}^2\text{-}^\circ\text{F/BTU}$).

Table 33 lists the nominal properties that determine the insulating qualities of the face ply and interlayer materials. Specific heat and density were not a factor in calculating thermal resistance, since the specimens were near steady state conditions.

TABLE 33. MATERIAL PROPERTIES

	MATERIAL	THERMAL CONDUCTIVITY (BTU IN./HR FT ² °F)	SPECIFIC HEAT (BTU/LB °F)	DENSITY (LB/FT ³)
Face Ply	Acrylic	1.26	0.35	74
	Urethane	1.00	0.29	70.6
	Glass	6.70	0.20	148
Interlayer	Silicone	1.15	0.37	65.5
	Urethane	1.44	0.40	70.25
	PPG112	2.00	0.44	69.12

The ratio of temperature to thermal resistance (face ply plus interlayer) is shown in Figures 101, 102 and 103 for Mach 2.4, 2.6 and 3.0. The range of temperatures broadens as the Mach numbers increase.

Specimen PPG21 falls well below the curve at Mach 2.4; the thermal conductivity value for the PPG112 interlayer material is suspect. A lower value would increase thermal resistance and bring the point more in line with the curve.

Variations in temperatures are apparent for similar specimens. For Specimens SK21, SK22, SWU21 and SWU22 (which have identical cross sections but different edge designs) there is a difference in the internal temperatures of 190°F at Mach 2.6 and 360°F at Mach 3.0. These discrepancies are attributed to the effect of the different edge configurations as well as the use of values for thermal conductivity that do not represent the true material properties. Inconsistencies inherent in the testing and instrumentation do effect small differences in the test results.

A comparison of pre-test calculated temperatures and test temperatures is presented in Table 34. Close correlation is shown for Specimen GY22 at Mach 2.6. For specimen PPG21 the calculated temperature at Mach 2.4 is 6 percent higher than the test temperature. The remaining calculated temperatures are low; 15 to 34 percent at Mach 2.4, 24 percent at Mach 2.6 and 54 to 88 percent at Mach 3.0. A similar discrepancy between calculated and test temperatures was reported in Reference 1.

As noted earlier the thermal conductivity value for the PPG112 interlayer is suspect. A lower value than shown in Table 33 would decrease the calculated temperature for Mach 2.4 conditions, thereby reducing its disparity with the test temperature. The PPG112 interlayer was operating at its thermal limit where the thermal conductivity value may not be a linear function. A higher thermal conductivity value would be required for the other specimens to increase the pre-test calculated temperatures and reduce the discrepancy between calculated and test temperature. This procedure was followed for the previous test program as reported in Reference 1.

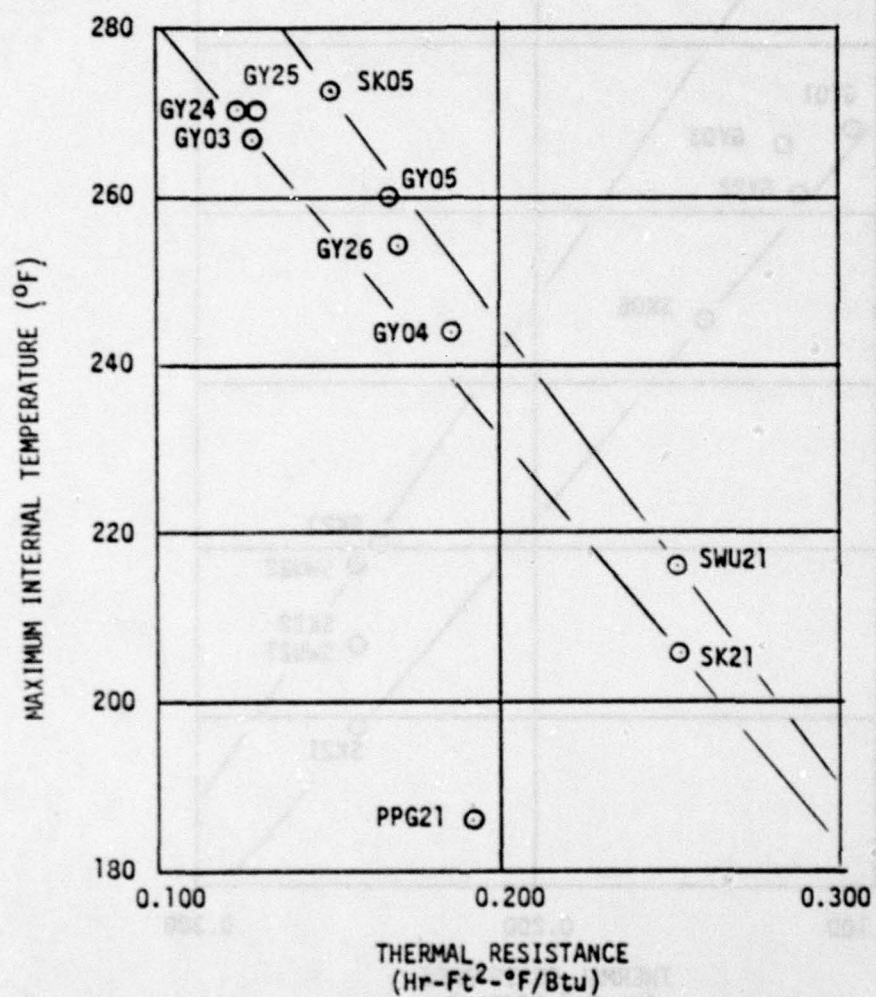


Figure 101. Thermal Resistance of Face Ply Plus Interlayer at Mach 2.4.

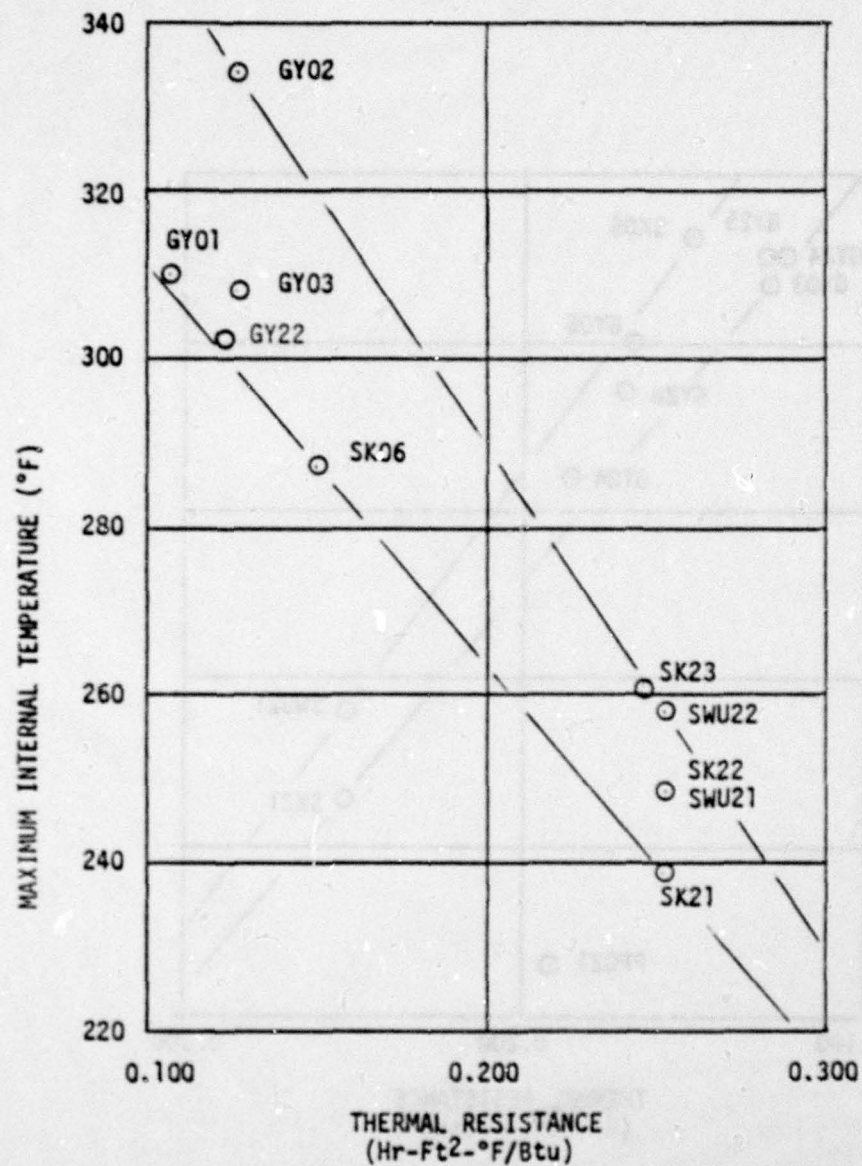


Figure 102. Thermal Resistance of Face Ply Plus Interlayer at Mach 2.6.

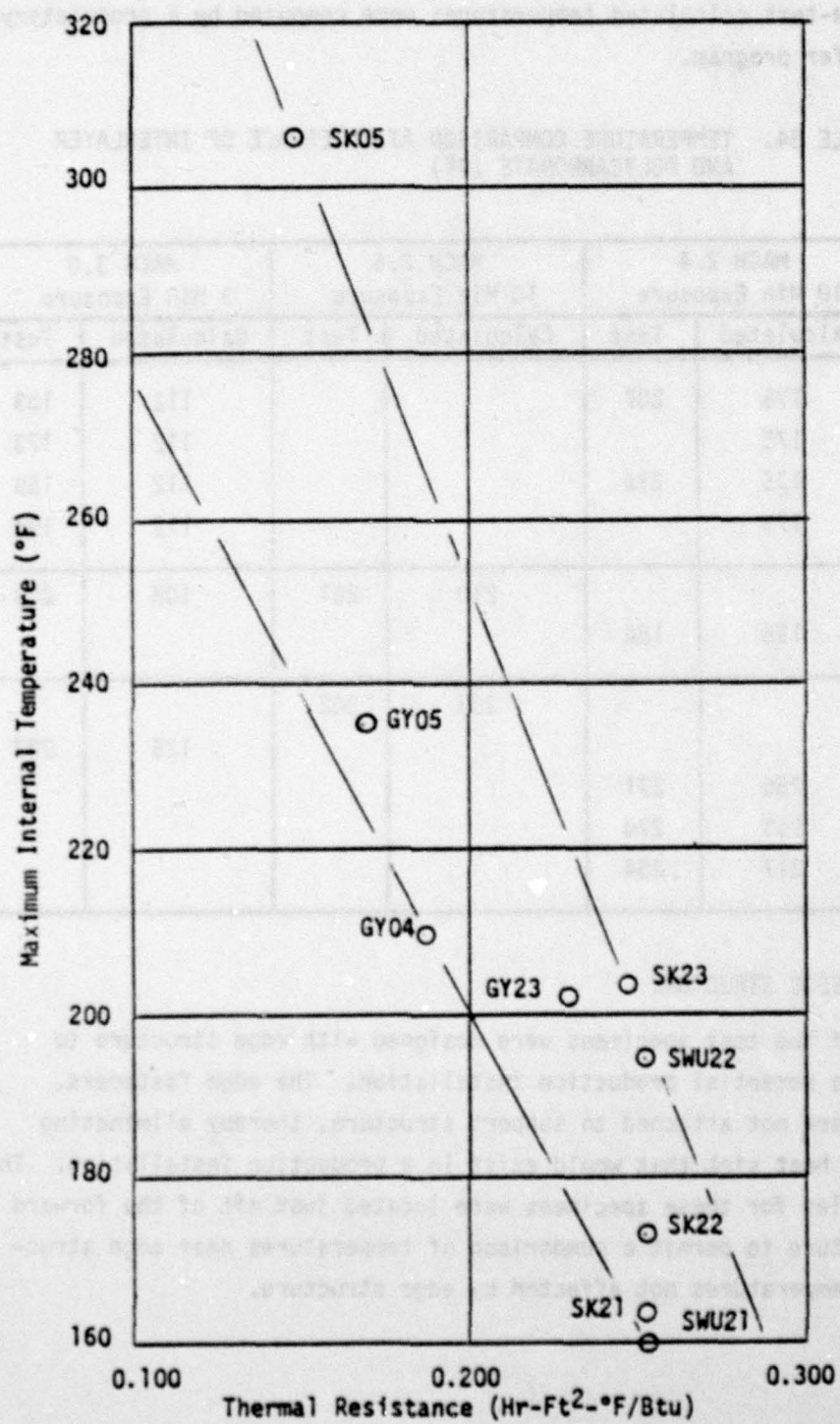


Figure 103. Thermal Resistance of Face Ply Plus Interlayer at Mach 3.0.

The pre-test calculated temperatures were computed by a proprietary heat transfer program.

TABLE 34. TEMPERATURE COMPARISON AT INTERFACE OF INTERLAYER AND POLYCARBONATE (OF)

	MACH 2.4 10 Min Exposure		MACH 2.6 10 Min Exposure		MACH 3.0 3 Min Exposure	
	Calculated	Test	Calculated	Test	Calculated	Test
SK21	175	207			112	163
SK22	175				112	173
SWU21	175	216			112	159
SWU22	175				112	194
SK23			210	261	108	203
PPG21	198	186				
GY22			303	302		
GY23					125	202
GY24	256	271				
GY25	253	270				
GY26	217	254				

EFFECT OF EDGE STRUCTURE

Many of the test specimens were designed with edge structure to represent a potential production installation. The edge fasteners, however, were not attached to support structure, thereby eliminating the normal heat sink that would exist in a production installation. The thermocouples for these specimens were located just aft of the forward edge structure to permit a comparison of temperatures near edge structure and temperatures not affected by edge structure.

The exterior thermocouple temperatures were shown previously in Table 30. For the 10-minute injections, only the thermocouples on Specimen GY25 survived, and they recorded a higher temperature near the edge structure. For the 5-minute injections, Specimens GY24, GY25 and GY26 registered higher temperatures near the edge structure. Specimen GY21 registered higher temperatures at the center of the panel, away from the edge structure. The results from the thermocouples do not provide enough data to make a significant judgment concerning edge effects. However, additional edge effects are discussed later under the thermal paint subsection.

HEAT CONDUCTION BY EDGE FASTENERS

Many of the test specimens were designed with edge structure to represent a potential production installation. The edge fasteners, however, were not attached to support structure and therefore could not conduct heat away from the outer structure as in a production installation. The thermocouples for these specimens were imbedded under the face ply interlayer, adjacent to the fastener on the center line. The Sierracin specimen had additional thermocouples imbedded adjacent to the fasteners on either side of the center line.

A comparison of temperatures from the aft imbedded thermocouples (away from the edge fasteners) and the temperatures near the forward fasteners is presented in Table 35. The results of the Mach 2.4 condition show slight temperature differences for SK21 and PPG21. For Specimens GY24, GY25 and GY26 the temperatures were cooler near the fastener; for Specimen SWU21 the temperature was hotter near the fastener. The face ply for GY24, GY25 and GY26 extended to the edge of the part and the thermocouples were directly under the face ply. On SWU21 the thermocouple was imbedded under the edge sealant.

FIGURE 35. EFFECT OF EDGE FASTENERS ON INTERNAL TEMPERATURES

SPECIMEN	TEMPERATURE (°F)					
	MACH 2.4		MACH 2.6		MACH 3.0	
	NEAR FASTENER	AFT	NEAR FASTENER	AFT	NEAR FASTENER	AFT
SK21	213	207	252	239	181	163
SK22			277	247	229	173
SWU21	247	216	291	248	242	159
SWU22			235	258	158	194
GY22			293	302		
GY23					245	202
GY24	238	271				
GY25	247	270				
GY26	225	254				
PPG21	181	186				
SK23			289	261	250	203

At Mach 2.6 all the thermocouples near the edge fasteners registered higher temperatures than those aft except for SWU22, where the thermocouple area was shielded by an internal fiberglass retainer. Specimen SK23 registered 27 degrees hotter near the fastener. SK22, fabricated with a steel retainer, was 30 degrees hotter near the fastener.

The temperatures at the Mach 3.0 condition followed the same trend as at Mach 2.6. SWU22 shows a cooler reading, SK21, moderate, and SK22 and SK23 a large differential. GY23 shows a high temperature difference but this temperature reading was affected by the reduced face ply thickness at the rabbeted edge.

PLASTIC VERSUS ALUMINUM BUSHINGS

Certain specimens fabricated by Sierracin were assembled with a plastic bushing and an aluminum bushing as part of the edge structure to permit a comparison of heat conducted to the area of the structural ply. Thermocouples were imbedded adjacent to the edge fasteners to record temperatures. The results are shown in Figure 104.

The results for SK21 were consistent at the three conditions. The temperatures were predictably hotter near the aluminum bushings, and was 8.5 percent higher at Mach 2.4, 6.7 percent higher at Mach 2.6, and 11 percent higher at Mach 3.0. The area near the left plastic bushing was cooler than the center line plastic bushings.

The temperatures for SK22 at Mach 2.6 and Mach 3.0 were consistent but do not agree with SK21.

THERMAL PAINT

A phase-change paint technique was used to locate "hot spots" on selected specimens, to correlate surface heating time with the thermocouple data, and to correlate heat patterns with the instrumented panel data. Five panels were tested with phase-change paint as indicated in Table 12.

The phase-change paint technique of obtaining heat transfer data uses a fusible coating which changes from an opaque solid to a transparent liquid (i.e., it melts) at a specified temperature (Reference 2). The demarcations between melted and unmelted paint (melt lines) are model surface isotherms. The progress of the melt lines was photographed with a 70-mm sequence camera at the rate of one frame per second. A 300°F paint was used for the Mach 2.4 conditions, 350°F for Mach 2.6, and 400°F for Mach 3.0.

The phase-change paint data gave the same qualitative heating pattern as the heat transfer distributions. However, the levels were approximately 30 percent lower than the gage data. The paint data are not shown

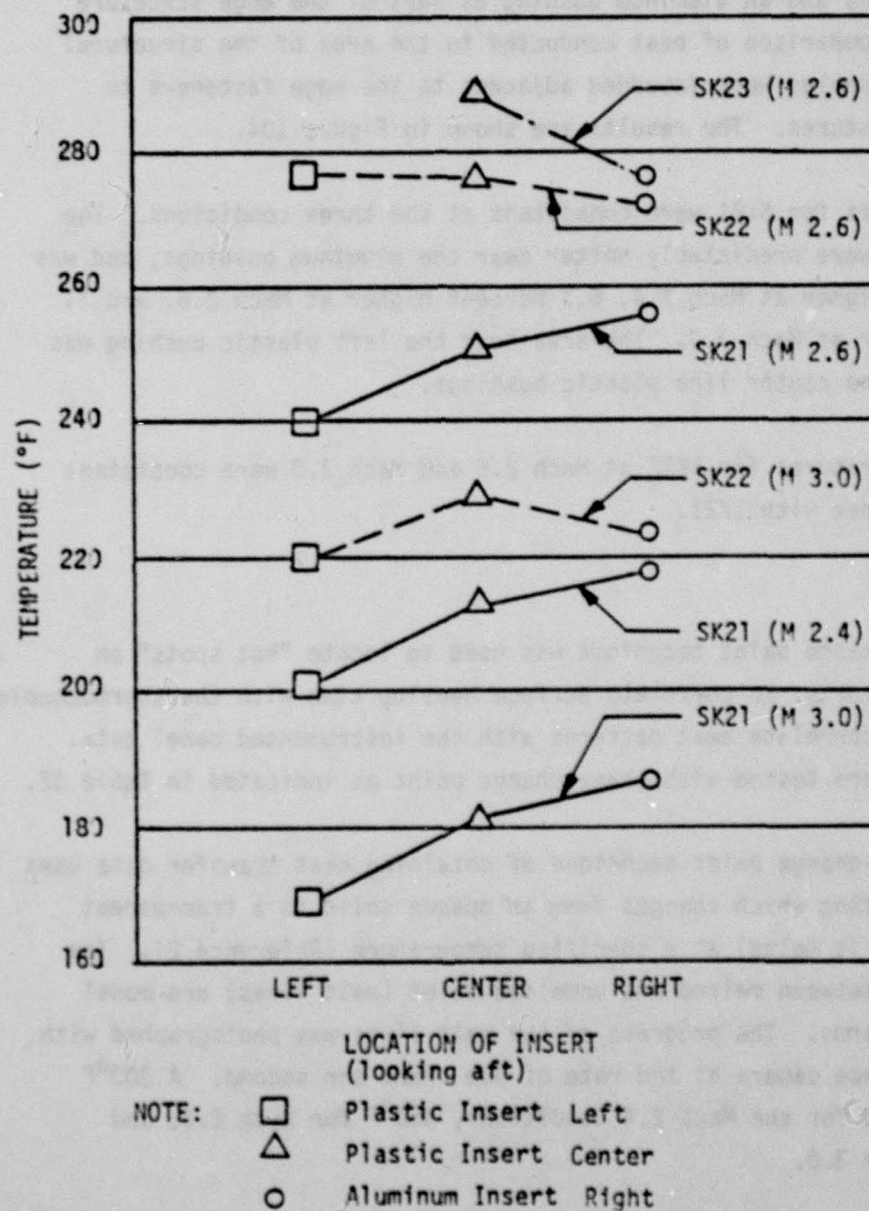


Figure 104. Maximum Temperature at Interlayer/Polycarbonate Interface Adjacent to Forward Inserts.

since the uncertainty in the technique is inherently high. The paint photos do indicate "hot spots" and uneven heating patterns which resulted primarily from the edge structure and also from a shock wave striking the specimen surface.

Phase-change paint photos are shown in Figure 105 for Specimens SK21A, SK22A and SWU22 for the Mach 2.4 condition at 25 and 30 seconds. The dark areas show where the paint had melted at 300°F. The air flow was left to right. The arc (hot spot) visible on the right side of each photo was caused by the interference shock visible in the shadowgraph photos shown previously in Figure 30. The shock impacted the panels at the aft thermocouple location. Another hot spot is visible on Specimen SK22A and SWU22 along the forward (up-wind) edge of the aft retainer. Figure 30 shows a shock wave emanating from this spot. The photos shown (at 25 and 30 seconds) indicate the difference in heat patterns for a five second interval. At 40 seconds all the paint had been dissipated except for slight traces near the forward (up-wind) end of the panels. These results indicate a faster heat-up time than shown in Table 36 for the thermocouple data where the specimens with an acrylic face ply did not reach 300 degrees for 23 to 58.8 seconds for the initial injection.

Figure 106 shows specimens SK21A and SK22A for the Mach 2.6 condition at 35 and 40 seconds. These specimens had been coated with a paint that would melt at 350°F. Shock wave patterns are visible, as well as a hot spot along the retainer on Specimen SK22A. The paint was completely gone after 45 seconds of exposure. The dark area in the center of the specimens indicates a high temperature area. Table 36 shows a faster heat-up time for the acrylic material than for the urethane material, indicating that urethane dissipates heat quicker than acrylic.

A teflon panel was coated with 400°F paint and injected at Mach 3.0. This specimen is shown in Figure 107 at 15 seconds. The paint dissipated rapidly and was completely gone in 20 seconds. The heat-up time was consistent with the data shown in Table 36.



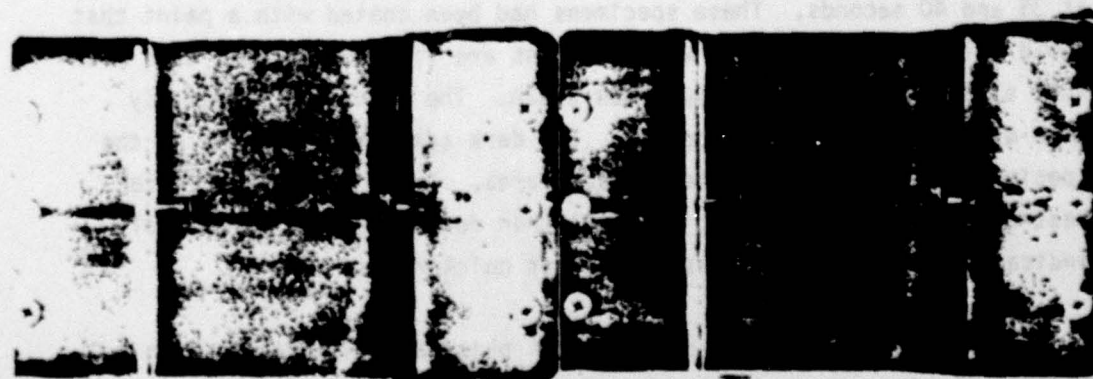
SK21A, 25 Seconds

SK21A, 30 Seconds



SK22A, 25 Seconds

SK22A, 30 Seconds



SWU22, 25 Seconds

SWU22, 30 Seconds

Figure 105. Thermal Paint Injections at Mach 2.4.

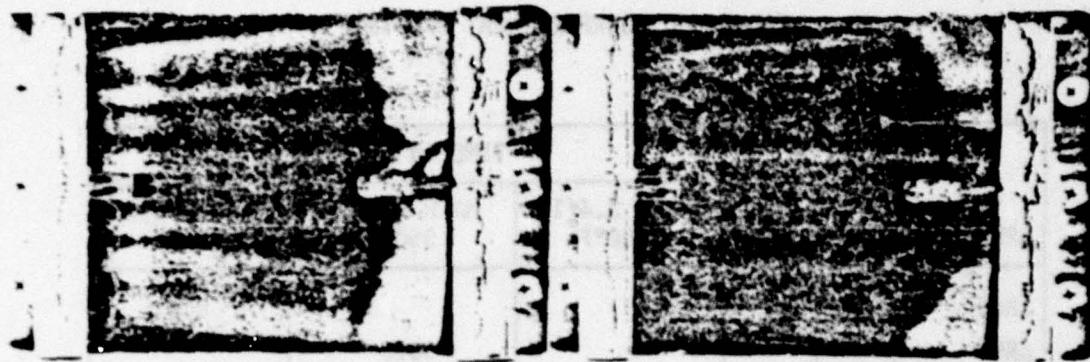
TABLE 36. SURFACE HEAT UP TIME

SPECIMEN	FACE PLY	TIME IN SECONDS		
		MACH 2.4(1) 300°F	MACH 2.6(1) 350°F	MACH 3.0(2) 400°F
SK05	Acrylic ↓			8.8
SK06			33.8	
GY21		38.8		
GY22			21.3	
GY24		23.0		
GY25		43.8		
GY26		58.8		
GY01	Urethane ↓		63.9	
GY02			48.8	
GY03		53.8	43.8	
GY04		53.8		14.8
GY05		53.9		13.9
PPG22A	Glass		54.8	

NOTE: (1) For 5-minute injection (first exposure)

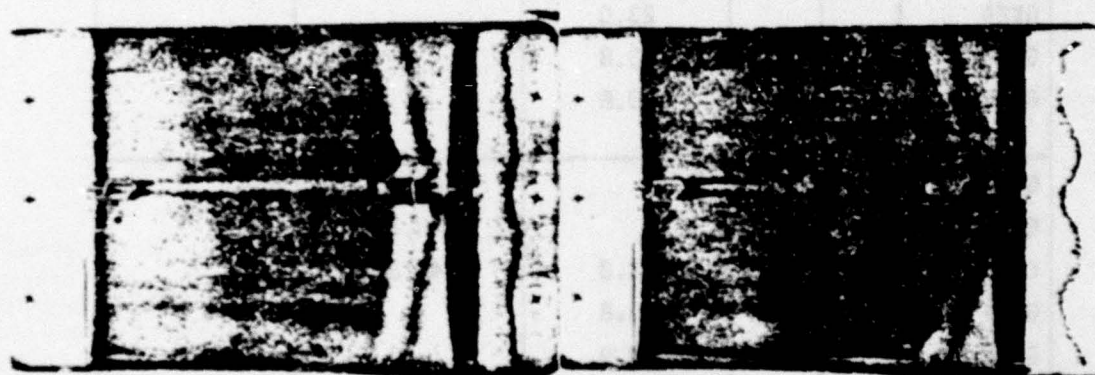
(2) For 3-minute injection (first exposure)

(3) Temperatures are from aft thermocouples.



SK21A, 35 Seconds

SK21A, 40 Seconds



SK22A, 35 Seconds

SK22A, 40 Seconds

Figure 106. Thermal Paint Injections at Mach 2.6.



Figure 107. Teflon Panel Injection at Mach 3.0.

SUMMARY

Thermal data was collected to provide a windshield designer with guidelines for the selection of material and thicknesses for use in aircraft that will operate in the Mach 2.4 to Mach 3.0 regime. The data from this series of tests provides temperature/time histories for specific materials, exterior and interior surface temperatures for selected laminated configurations, the insulating characteristics for face ply/interlayer combinations, the effect of edge structure and fasteners on transparency temperatures, and the heat conduction for plastic versus aluminum inserts. Hot spots were defined on some specimens by use of phase-change paint. The temperatures were monitored by thermocouples installed on the exterior and interior surfaces, and at the interface of the interlayer and structural ply. In many cases the thermocouples failed to adhere to the specimen surface or did not function properly.

The temperature/time curves show that the temperature of the exterior surfaces rose rapidly and reached steady state in about 7 to 8 minutes. The internal temperature (at the interface of the structural ply and face ply/interlayer combination) lagged behind the exterior temperature. The interior temperature (cabin surface) had a lower rate of change than the internal temperature and was affected by the cabin cooling as well as by the material thickness and thermal conductivity. Internal and interior temperatures did not reach steady state until after 15 minutes of heat exposure.

The maximum internal temperature and interior temperature were affected by the temperature of the specimen at injection. Consequently, the second injection of each specimen resulted in the maximum temperature. As was expected the maximum exterior surface temperature was not affected by the specimen initial temperature.

The average maximum exterior surface temperatures were:

325°F at Mach 2.4 for a 10-minute injection.

388°F at Mach 2.6 for a 10-minute injection.

502°F at Mach 3.0 for a 3-minute injection.

The values varied by less than 2 percent between specimens.

The interior surface temperatures did not exceed the 160°F specified by MIL-E-38453A (Reference 10) for crew comfort, with one exception (the exception was 161°F). The temperatures varied with injection time, initial temperature, material properties, and material thicknesses. The higher temperatures occurred at the longer injections and for the thinner specimens.

The temperature at the interface of the face ply/interlayer and structural ply was monitored and plotted to show the insulating capability of the face ply and interlayer combination. The temperatures were plotted against specimen thermal resistance (material thickness divided by thermal conductivity). Variations in temperature did occur for similar materials. These variations are attributed to differences in edge configurations and to the use of values for calculating thermal conductivity that do not represent the true material properties.

Thermocouples were installed on the exterior surfaces adjacent to the forward edge structure to provide data that could be used to study the effect of edge structure on temperature distribution. Most of the exterior thermocouples peeled off during the test. These results indicated that PS-18 (an acrylic based cement) is not an acceptable bonding agent for acrylic when subjected to elevated temperatures. M-Bond 600 is acceptable for acrylic materials but is not usable for bonding to glass.

Imbedded thermocouples were installed to study possible heat conduction to the internal areas via the edge fasteners. The results of the Mach 2.6 and Mach 3.0 tests were consistent. They show higher temperatures

near the fasteners than in the center of the panel. The data from the Mach 2.4 tests did not agree with these results. A variation in the hot spots from shock wave interactions was a possible cause but could not be proved with the available data.

Data was recorded to permit a comparison of heat conduction by plastic inserts versus aluminum inserts. The results for one specimen were consistent at the three Mach numbers and verified higher heat conduction through the aluminum inserts.

Test temperatures were compared to pre-test calculated temperatures. The calculated exterior surface temperatures were 7 to 11 percent higher than the test temperatures for the three test conditions of Mach 2.4, 2.6 and 3.0. The discrepancy between pre-test calculated temperatures and test temperatures at the internal interface varied from zero to 82 degrees. These deviations were due to the effect of the edge configuration on temperature distribution as well as the use of values for calculating thermal resistance that did not represent the true material properties. The results were consistent with a previous test program reported in Reference 1.

A phase-change paint method was used on selected panels to locate hot spots to correlate heat-up time with thermocouple data, and to correlate heat patterns with the instrumented panel data. The paint data gave the same qualitative heating pattern as the instrumented panel but the levels were approximately 30 percent lower than the gage data. The paint data showed a faster heat-up time than did the thermocouple data. The paint dissipation pattern indicates that the aft center portion of the panel heats up faster than the perimeter. This is the result of a shock wave which strikes the panel in this area. The shock wave is stronger at the center line of the panel, decreasing in intensity toward the edge of the panel. For the specimens with steel edge retainers, hot spots were evident in the transparent material near the retainers.

AD-A078 673

DOUGLAS AIRCRAFT CO LONG BEACH CA
EVALUATION OF AIRCRAFT WINDSHEILD MATERIALS IN A SIMULATED SUPE--ETC(U)
JUN 79 J B HOFFMAN
MDC-J7186

F/6 1/3

F33615-75-C-3105

NL

AFFDL-TR-79-3058

UNCLASSIFIED

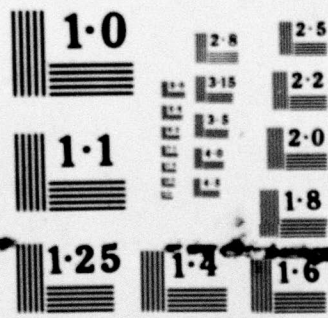
3 OF 3

AD-
4078673



END
DATE
FILMED

1-80
DDC



NATIONAL BUREAU OF STANDARDS
MICROCOPY RESOLUTION TEST CHART

Further tunnel testing to acquire temperature data with thermocouples would require a more reliable bonding agent (such as M-Bond 600) for the installation of the thermocouples on exterior surfaces. Other methods of thermal data acquisition have been developed by the ARO/AEDC. One such technique, infrared scanning, would provide heat patterns in color and digital analysis, but was rejected for these tests because the infrared scanning equipment could not be installed concurrently with the photographic equipment, resulting in a delay. An additional penalty was the requirement to coat the different face ply materials in order to obtain emissivity data. It is recommended that potential tunnel users consult with the ARO/AEDC for possible use of other test techniques.

SECTION VIII

CONCLUSIONS AND RECOMMENDATIONS

This report addresses the results of a wind tunnel test program that was conducted to evaluate the limits and capabilities of materials and laminated configurations for potential use in the design of windshields for Mach 3.0 aircraft. The goals of this test program were to determine material survivability in a Mach 2.4 through Mach 3.0 flight environment, evaluate the resultant effect of the environment on the materials' optics, delineate the ensuing thermal gradients, investigate potential edge designs, and determine the effect of edge structure on temperature distribution. These goals were achieved.

Prior to this program, the aerodynamic effect of a Mach 2.4 to Mach 3.0 flight environment on transparent plastic and interlayer materials was unknown. These tests demonstrated that laminated configuration of acrylic/silicone/polycarbonate or urethane/urethane/polycarbonate, as well as glass/silicone/polycarbonate, are viable candidates for Mach 3.0 aircraft windshields. The limits for these materials are still unknown and further testing is recommended at higher velocities and longer exposures to define their maximum capabilities.

Conclusions and recommendations are presented for each phase of the test program.

TEST PLAN

It is recommended that potential tunnel users utilize the normal pre-test conference provided by the test facility to assure that the responsibilities and limits of participation of the involved personnel be well defined in the test plan, and to assure that all participants understand the test goals and the limits of the test facility.

TEST OPERATION

It is recommended that tunnel dates be scheduled well in advance due to heavy usage, and that the potential tunnel user delineate his test schedule carefully to avoid changes and costly delays. Close attention must be given to such details as time to install and replace a specimen since successful completion of a test program depends on maximum utilization of available time.

TEST ENVIRONMENT

It is recommended that the simulation of a real flight environment would be improved if the test were conducted in a tunnel where the free stream conditions were similar to the flight conditions; i.e., use a Mach 3.0 tunnel to simulate a Mach 3.0 environment.

It is also recommended that further Mach 3.0 tests be conducted at lower altitudes (high pressure conditions) on similar materials. The original altitudes selected for the potential aircraft operating envelope were not possible to simulate because of the limits of the tunnel capability. Hence, higher altitudes were simulated than originally planned.

An undesirable interference shock wave impinged on the specimen surfaces. It is recommended that the interference shock be eliminated so as to provide an environment more compatible with flight conditions. The wedge that was used as a flow generator was not designed for this type of test. The interference shock could be eliminated with a wedge designed specifically for this type of application.

It is recommended that a more realistic test would be achieved with larger test specimens since specimen size has an effect on heat distribution and heat dissipation. This revision would, of course, necessitate a tunnel of larger diameter because of potential air blockage.

It is recommended that future tests at higher velocities use a different flow generator and camera arrangement since the present system has

reached its maximum utilization. Further reductions in the wedge angle would rotate the cabin simulator window out of the camera's line of sight.

MATERIAL EVALUATION

Prior to this test program the aerodynamic effect of a Mach 2.4 through Mach 3.0 flight environment on plastic materials was not known. It had been anticipated that the selected materials might not survive the high temperatures generated at these velocities. Based on these tests, it is concluded that plastic face ply materials such as as-cast acrylic and urethane, will survive the high temperature experienced at Mach 2.4 through Mach 3.0 for short exposures.

These tests have further demonstrated the potential value of laminated aircraft windshields in the Mach 3.0 environment, specifically, those configurations consisting of as-cast acrylic/silicone/polycarbonate, urethane/urethane/polycarbonate, and glass/silicone/polycarbonate, are recommended as potential windshield candidates for aircraft that will operate in the Mach 3.0 regime for short periods of time.

The limits for these materials and laminated configurations are still unknown and further testing is recommended to define the maximum velocity environment and exposure time limits for as-cast acrylic and urethane face ply material, as well as for silicone and urethane inter-layers.

Additional testing is recommended at Mach 2.4 and above to establish the effects of repeated exposure to high temperatures and pressures for these materials and laminated configurations. It is suggested that larger specimens be tested since thermal expansion and heat dissipation are affected by panel size.

It is concluded that the limit for effective use of coated polycarbonate for short term exposure is in the region of Mach 2.4.

It is concluded that PPG112 interlayer is not an acceptable material for the temperatures experienced at Mach 2.4 because of heat induced bubbling.

These tests have verified the importance of correct edge designs for the survivability of a laminated windshield configuration. One type of edge design utilizing a steel retainer (SK22) sustained erosion of the sealant under the retainer and is considered unacceptable. A similar fiberglass retainer (SWU22) survived without erosion and is recommended as a potential edge design.

Two types of face-ply to edge-structure transition methods, a "V" groove edge (SK21) and a straight edged groove (SK23 and SWU21), were tested and are recommended for laminated configurations. Further testing is recommended to fully validate these edge designs when subjected to cyclic expansion in the Mach 3.0 regime.

It is concluded that a rabbeted type acrylic face ply represented by Specimen GY21, GY22 and GY23, is not an acceptable edge design for high temperature environments because holes were burned through the material. It is recommended that a thicker face ply or some method of protection be used for this type of edge. It is further recommended that a high temperature bushing be developed for the edge attachments since the polycarbonate bushings employed in these specimens melted.

It is concluded that the type of design represented by Specimens GY24, GY25 and GY26 is not an acceptable edge design. These specimens, with the acrylic face ply extended to the edge and drilled, sustained severe face ply delamination which originated at the fasteners.

Many of the specimens sustained bubbling of the polycarbonate along the aft panel edge. The high temperature in this area was generated by a rebound shock wave which struck the panels near the aft edge and

was intensified by a heat sink that existed as part of the left edge of the cabin simulator cover. It is recommended that these problems be eliminated if further tests are to be conducted with this equipment.

OPTICS EVALUATION

Based on an interpretation of the grid line photographs, the 3-ply laminates (SK05 and SWU21), the 5-ply laminates (GY03, GY04 and GY05), and the monolithic polycarbonate (TEX21) are recommended candidates for Mach 2.4 aircraft windshields. The 7-ply laminates would be candidates if the edge design was revised to preclude premature failure. Laminates with a glass face ply (PPG21) would be acceptable with an interlayer that could survive the temperature environment.

Based on an interpretation of the grid line photographs, the 3-ply laminates (SK06 and SWU21), and the 5-ply laminates (GY01, GY02 and GY03) are recommended candidates for Mach 2.6 aircraft windshields. The results for the glass face ply laminates were positive when the interlayer was silicone (SK23) but negative when PPG112 was used (PPG22A). Coated polycarbonate (TEX21A) sustained loss of vision at this test condition and is not recommended for use at Mach 2.6.

Based on the optical clarity of the photographs taken at Mach 3.0, the 3-ply laminates (SK05 and SWU21) are candidates for Mach 3.0 aircraft windshields. The 5-ply laminates (GY04 and GY05) are recommended, although the optics were not as clear as for the 3-ply specimens.

The PPG specimens are the only configurations not recommended for potential aircraft windshields due to poor light transmission.

Based on limited test data, it is concluded that urethane material is more resistant to haze than acrylic when used as a face ply material and tested at the conditions of Mach 2.4 through 3.0.

It is recommended that further tests of this nature be performed on larger specimens since deflection and optical distortion would be affected by panel size.

THERMAL EVALUATION

The following conclusions were derived from an analysis of the thermal data for the tested specimens.

- a. The maximum exterior surface temperature climbed rapidly, reached steady state in 7 to 8 minutes, was unaffected by initial temperature, and did not vary with face ply material.
- b. The interior surface temperatures were consistent with the requirements of MIL-E-38453A (Reference 10) for crew comfort.
- c. Although the results were scattered, the thermal resistance of the face ply plus interlayer, i.e., its ability to protect the structural ply, did vary directly with thickness and inversely with material thermal conductivity.
- d. Internal material temperatures were influenced by the heat conducted through the fasteners and bushings.
- e. Hot spots did exist adjacent to the metal edge retainers.

Further tests are recommended to obtain more accurate data that could be used for predicting the temperatures at the outer surface of the structural plies.

The use of phase-change paint is recommended as a useful tool for defining hot spots on the surface of a test specimen.

It is recommended that further wind tunnel tests of this type use a more reliable bonding agent (such as M-Bond 600) for the exterior thermocouples and that other methods of thermal data acquisition be investigated for potential use by consulting with the test facility personnel.

REFERENCES

1. Hoffman, J. B., Evaluation of Windshield Materials Subjected to Simulated Supersonic Flight Environments, AFFDL-TR-77-92, (AD-A049981), September 1977.
2. Carver, D. B., Aerothermodynamic Evaluation of Windshield Materials in a Simulated Supersonic Flight Environment, AEDC-TR-77-68, June 1977.
3. Test Facilities Handbook (Tenth Edition), Von Karman Gas Dynamics Facility, Volume 3, Arnold Engineering Development Center, May 1974.
4. Equations, Tables and Charts for Compressible Flow, Report 1135, Ames Research Staff, Ames Aeronautical Laboratory, Moffett Field.
5. Matthews, R. K., Experimental Investigation of Water Ejection from a Wedge Model at Mach Number 6, AEDC-TR-71-26 (AD 72 1448), April 1971.
6. Federal Test Method Standards Manual 406, Method 3011 and Method 3022, 5 October 1961, General Services Administration, Washington, D.C.
7. American Society for Testing and Materials, Standard Method of Test for Haze and Luminous Transmittance of Transparent Plastics, ASTM-STD-D1003-61.
8. Carver, D. B., Aerothermodynamic Evaluation of Windshield Materials at Simulated Flight Speeds of Mach 2.4 to 3.0, AEDC-TR-78-V33, September 1978.
9. Coker, M. J., Hoffman, J. B., Lawrence, J. H., Windshield Technology Demonstrator Program - Canopy Detail Design Options Study, AFFDL-TR-78-114, June 1978.
10. Military Specification, General Specification for Aircraft Environmental Control, Environmental Protection and Engine Bleed Air Systems, MIL-E-38453A (USAF), 2 December 1971.